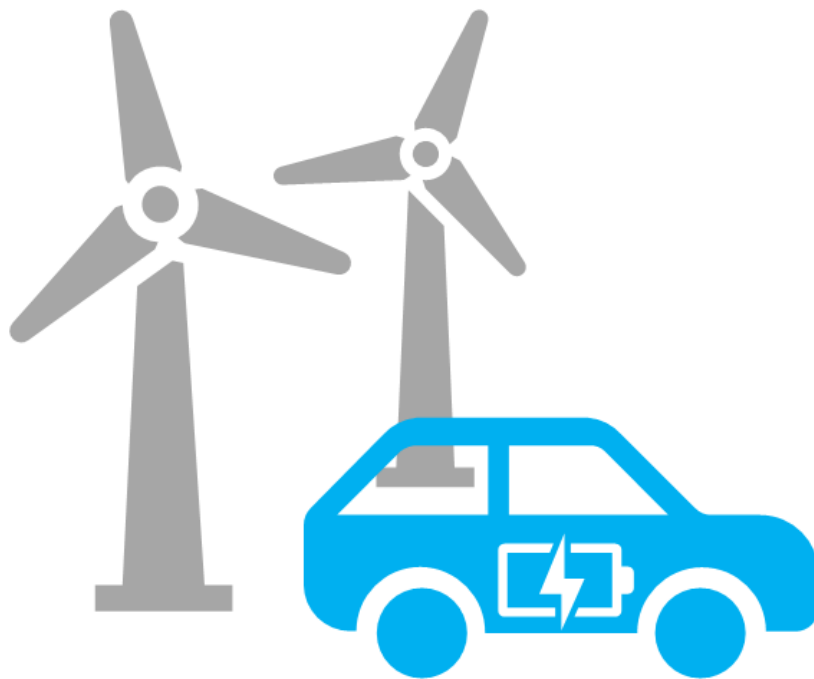


The Future of Nickel in a Transitioning World

Exploratory System Dynamics Modelling and Analysis of the Global
Nickel Supply Chain and its Nexus with the Energy System



Universiteit
Leiden

Jessie Bradley
2156164; 4908244
Supervisor 1: Benjamin Sprecher
Supervisor 2: Willem Auping
MSc. Industrial Ecology
Leiden University & TU Delft
18/3/2021

Table of Contents

| | |
|--|-----------|
| Abstract | 3 |
| Acknowledgements | 4 |
| List of figures and tables | 5 |
| List of abbreviations | 8 |
| 1. Introduction | 11 |
| 2. Methods | 13 |
| 2.1 Resilience framework | 13 |
| 2.2 Exploratory System Dynamics Modelling and Analysis | 14 |
| 2.3 Model structure and data sources | 15 |
| 2.3.1 Demand sub-model | 17 |
| 2.3.2 Supply sub-model | 22 |
| 2.3.3 Price sub-model | 27 |
| 2.3.4 Impacts sub-model | 33 |
| 2.4 Model verification and validation | 33 |
| 2.5 Experimental set-up | 35 |
| 3 Results | 37 |
| 3.1 Demand projections | 37 |
| 3.2 Disruption scenarios | 39 |
| 3.2.1 Business as usual | 39 |
| 3.2.2 Energy transition | 40 |
| 3.2.3 Radical innovation | 45 |
| 3.2.4 Resource depletion | 45 |
| 3.2.5 Supply disruption | 46 |
| 3.3 Sustainability policies | 47 |
| 3.3.2 EoL waste management | 47 |
| 3.3.2 Supply chain loss reduction | 48 |
| 3.3.3 EV battery lifetime increase | 49 |
| 3.4 Structural validation | 49 |
| 3.4.1 Structural uncertainties | 49 |
| 3.4.2 Parametric uncertainties | 51 |

| | |
|---|-----------|
| 3.5 Replicative validation | 54 |
| 3.5.1 Comparison with historic developments | 54 |
| 3.5.2 Comparison with literature | 56 |
| 3.5.3 Summary of new insights | 57 |
| 3.6 The resilience of the nickel supply chain | 63 |
| 4 Conclusion and discussion | 66 |
| 4.1 General conclusion | 66 |
| 4.2 Societal relevance | 67 |
| 4.2.1 Implications for the energy transition | 67 |
| 4.2.2 Usefulness for the mining industry | 68 |
| 4.2.3 Externalities of nickel production | 68 |
| 4.3 Academic relevance | 69 |
| 4.3.1 Energy-material nexus | 70 |
| 4.3.2 Supply chain resilience | 70 |
| 4.3.3 System dynamics research | 70 |
| 4.4 Limitations and recommendations for future research | 71 |
| 4.4.1 Demand system | 71 |
| 4.4.2 Supply system | 73 |
| 4.4.3 Price system | 75 |
| 4.4.4 Sustainability impacts | 76 |
| References | 78 |
| Appendices | 84 |

(See appendices for a table of contents of the appendices)

Abstract

Acceleration of the energy transition requires increased mining of materials. An important material for the energy transition is nickel, used in the stainless steel required for all energy infrastructure and an important component for both stationary batteries and batteries used in electric vehicles. Previous research has been done on the global nickel requirements for the energy transition at a high level of aggregation. In this thesis, exploratory system dynamics modelling and analysis was used to assess the resilience of the nickel supply chain and its nexus with the energy system at the level of individual mines.

The development of the global nickel supply chain, and its energy requirements and greenhouse gas emissions, was modelled and explored between 2015 and 2060 under different disruption scenarios, sustainability policies and uncertainties. A nickel demand of 6 - 18 million tonnes per year is projected by 2060 for the BAU scenario, with projections up to 38 million tonnes per year in the scenarios that aim to limit global temperature increase to 1.5 °C. The main contributors to this large demand are electric vehicle batteries. The nickel system is conditionally resilient to the energy transition, given sufficient exploration and annual capacity increase. To increase the resilience of the nickel system, policies that support innovation in battery material composition and lifetime and good end of life waste management of batteries can play an important role.

Modelling the nickel supply chain at mine level leads to different behaviour compared to previous research where mines were aggregated. Insights obtained from the detailed modelling in this thesis include a higher demand than previously projected; the possibility of the average ore grade increasing over time as mines with lower ore grades are decommissioned; average final energy requirements that can decrease, increase or increase rapidly depending on a varying average ore grade, a varying composition of processing methods and a varying composition of by-products; average energy costs that differ depending on the projected electricity mix in the countries containing deposits; and a reduction in end of life nickel recycling rate for most scenarios due to an increasing share of batteries.

The most important contribution of this thesis is not in the data and assumptions, but in the model itself, which can be adapted and refined in further research, where more stakeholder input is included, to make the outcomes more robust and useful for decision making. Other important avenues for further research include determining how much exploration is possible and how quickly mining capacity can be increased.

Acknowledgements

The writing of this thesis has been an arduous yet enjoyable journey that would not have been possible without the support and assistance of many amazing people.

First, I would like to express my profound gratitude to my supervisors Benjamin Sprecher and Willem Auping, not only for giving me constructive advice and feedback on the contents of my thesis, but also for supporting and understanding me on an emotional level. Without your guidance, it would have taken me much longer to successfully complete my thesis.

I also wish to thank Kiki Boomgaard and Lucienne Willems for supporting me along the way and for giving me helpful tips for managing my time and balancing my thesis with other activities. I greatly appreciate the compassion you both showed and the time you invested in me.

My gratitude goes out to Lisette van Hulst for her wonderful course on academic writing, her engaging and personal approach to teaching and her extensive feedback on the text of my drafts. In addition, I am grateful to Erika van der Linden for providing her cobalt model, which served as a basis for the nickel model in this thesis, and for kindly walking me through it.

Many thanks to Gavin Mudd, for providing his database on nickel mines, without which a model at mine level would not have been possible, and for giving me a better understanding of the mining world. Thanks also to Tim Werner and Rene Kleijn for listening to my updates and for giving me useful tips to improve my model.

Thanks to Kornelis Blok and Andrea Ramirez for answering some of my energy system related questions and thanks to Claude Friehe and Mark Mistry of the Nickel Institute for sending me their nickel LCA report and for giving me useful advice on allocation.

Finally, I would like to thank my grandfather, John Bradley, for sharing his knowledge on nickel mining, my parents, Adam and Fiona Bradley, for helping me where they could and my other family and friends for their continued support and motivation.

List of figures and tables

Figures

| | | |
|-------------|---|----|
| Figure 2.1 | <i>Types of system disturbances, important aspects of resilience and mechanisms that can increase resilience</i> | 13 |
| Figure 2.2 | <i>The XLRM framework applied to the nickel system</i> | 15 |
| Figure 2.3 | <i>CLD of the energy-material nexus</i> | 16 |
| Figure 2.4 | <i>Overall model structure and data sources</i> | 17 |
| Figure 2.5 | <i>Components considered in the bottom-up modelling of the energy system and the scenarios used to determine their input data</i> | 18 |
| Figure 2.6 | <i>Structure for determining electricity generation capacity</i> | 18 |
| Figure 2.7 | <i>Structure for determining storage</i> | 19 |
| Figure 2.8 | <i>Structure for determining vehicles</i> | 20 |
| Figure 2.9 | <i>Structure for determining nickel intensity and demand of components</i> | 20 |
| Figure 2.10 | <i>Structure for determining nickel demand for the RoE (top down) and total nickel demand before the influence of price effects</i> | 21 |
| Figure 2.11 | <i>CLD of price related mechanisms with a balancing effect on the system, thereby increasing resilience</i> | 21 |
| Figure 2.12 | <i>Structure for price effects</i> | 22 |
| Figure 2.13 | <i>Supply components considered in the model</i> | 23 |
| Figure 2.14 | <i>Structure for exploration and further discovery</i> | 23 |
| Figure 2.15 | <i>Structure for the conversion from measured and indicated resources to reserves</i> | 24 |
| Figure 2.16 | <i>Structure for creating new brownfield or greenfield capacity</i> | 24 |
| Figure 2.17 | <i>Structure for operating and mothballed capacity</i> | 25 |
| Figure 2.18 | <i>Structure for the forward nickel supply chain</i> | 25 |
| Figure 2.19 | <i>Nickel sources, important primary production routes, products and the applications of these products</i> | 26 |
| Figure 2.20 | <i>Structure of the reverse nickel supply chain</i> | 27 |
| Figure 2.21 | <i>Economics included in the nickel model</i> | 28 |
| Figure 2.22 | <i>Structure for nickel costs</i> | 28 |
| Figure 2.23 | <i>Structure for nickel and by-product ore grades</i> | 29 |
| Figure 2.24 | <i>Structure for by-product allocation</i> | 30 |
| Figure 2.25 | <i>Structure for determining price</i> | 30 |

| | | |
|-------------|---|----|
| Figure 2.26 | <i>Structure for calculating current and current potential profit</i> | 31 |
| Figure 2.27 | <i>Structure for calculating future potential profit</i> | 32 |
| Figure 2.28 | <i>Structure for exploration increase</i> | 32 |
| Figure 2.29 | <i>Structure for investment attractiveness</i> | 33 |
| Figure 2.30 | <i>Structure for determining GHG emissions</i> | 33 |
| Figure 2.31 | <i>Uncertainties included in the model</i> | 35 |
| Figure 3.1 | <i>Final nickel demand and cumulative final demand per assessed SSP</i> | 37 |
| Figure 3.2 | <i>Total functional nickel demand and total substitution per assessed SSP</i> | 38 |
| Figure 3.3 | <i>Nickel demand for vehicle batteries and the RoE</i> | 38 |
| Figure 3.4 | <i>Price change vs production change for a single BAU run with base settings</i> | 39 |
| Figure 3.5 | <i>Nickel mining and cumulative mined nickel per SSP</i> | 40 |
| Figure 3.6 | <i>Cumulative cobalt and palladium production from nickel mines per SSP</i> | 40 |
| Figure 3.7 | <i>Average periodic nickel price, degree of nickel scarcity and average marginal costs</i> | 41 |
| Figure 3.8 | <i>Average final energy use and average energy costs</i> | 42 |
| Figure 3.9 | <i>Overall average nickel ore grade of existing mines and of all deposits in the database by Mudd (2020)</i> | 43 |
| Figure 3.10 | <i>Average electricity price per fuel price scenario and per SSP</i> | 43 |
| Figure 3.11 | <i>Cumulative GHG emissions over time and average carbon costs per tonne of nickel</i> | 44 |
| Figure 3.12 | <i>Results for the impact of radical innovation that halves battery substitution threshold in 2035 and in 2050</i> | 45 |
| Figure 3.13 | <i>Scarcity and nickel price in the FSP</i> | 46 |
| Figure 3.14 | <i>Depletion of original resources for the FSP and the OCP</i> | 46 |
| Figure 3.15 | <i>Results for the influence of a 1-year supply disruption in 2030 and 2045 where mining stopped in the country with the largest share of supply at those times</i> | 47 |
| Figure 3.16 | <i>EoL RR for the four waste management strategies and per SSP</i> | 47 |
| Figure 3.17 | <i>Cumulative mined nickel and average periodic nickel price based on EoL waste management strategy</i> | 48 |
| Figure 3.18 | <i>Cumulative mined nickel and cumulative GHG emissions based on the inclusion of loss reduction</i> | 48 |
| Figure 3.19 | <i>The impact of EV battery lifetime increase on various key performance metrics</i> | 49 |
| Figure 3.20 | <i>Some key performance metrics categorized based on processing energy allocation method</i> | 50 |
| Figure 3.21 | <i>Some key performance metrics categorized based on the inclusion of by-products</i> | 51 |
| Figure 3.22 | <i>Average final energy use and average ore grade of existing mines for lower values for power for ore grade (≤ 0.3) and higher values (> 0.3).</i> | 52 |

| | | |
|-------------|--|----|
| Figure 3.23 | <i>Average periodic nickel price and cumulative mined nickel for lower values for administration of postponed demand (≤ 1 year) and higher values (> 1 year)</i> | 53 |
| Figure 3.24 | <i>Average periodic nickel price, cumulative mined nickel, degree of nickel scarcity and exploration for lower values for power for price-based exploration (≤ 0.7) and higher values (> 0.7)</i> | 53 |
| Figure 3.25 | <i>Average periodic nickel price for a global maximum capacity increase percentage between 1% and 30% per SSP and for high (>0.10) and low (≤ 0.10) values for global maximum capacity increase percentage</i> | 54 |
| Figure 3.26 | <i>Historic nickel price adjusted for inflation based on Trading Economics (2020) and model results for nickel price for runs for SSP2-baseline (BAU) and SSP5-19 (the most extreme ET scenario) with base settings</i> | 55 |
| Figure 3.27 | <i>Historic annual change in mining vs values for SSP2-baseline and SSP5-19 with base settings</i> | 55 |
| Figure 3.28 | <i>Nickel demand projections in literature</i> | 56 |
| Figure 3.29 | <i>Cumulative nickel demand comparison</i> | 59 |
| Figure 3.30 | <i>Average nickel ore grade in the model by Van der Linden (2020) compared to the average nickel ore grade of existing mines in the current model</i> | 60 |
| Figure 3.31 | <i>Average final energy use in the model by Van der Linden (2020) compared to average final energy use in the current model</i> | 61 |
| Figure 3.32 | <i>Average energy costs in the model by Van der Linden (2020) compared to average energy costs in the current model</i> | 61 |
| Figure 3.33 | <i>EoL RR for nickel in the model by Van der Linden (2020) compared to EoL RR for nickel in the current model</i> | 62 |

Tables

| | | |
|-----------|--|----|
| Table 2.1 | <i>Disruption scenarios included in the model</i> | 36 |
| Table 3.1 | <i>The energy-nickel nexus in numbers</i> | 42 |
| Table 3.2 | <i>GHG emissions due to nickel production.</i> | 44 |
| Table 3.3 | <i>Summary of the differences in input and behaviour between previous research and this thesis</i> | 48 |
| Table 3.4 | <i>Resilience of the nickel system in the model to the disruptions assessed in this thesis</i> | 65 |

List of abbreviations

| | |
|---------|---|
| 2DS | 2 °C Scenario |
| ABM | Agent-Based Modelling |
| ATL | Atmospheric Leaching |
| B2DS | Beyond 2 °C Scenario |
| BAU | Business As Usual |
| BECCS | Bio Energy with Carbon Capture and Storage |
| BEV | Battery Electric Vehicle |
| BF | Blast Furnace |
| BP | British Petroleum |
| BNEF | Bloomberg New Energy Finance |
| CCS | Carbon Capture and Storage |
| CF | Capacity factor |
| CLD | Causal Loop Diagram |
| CRIRSCO | Combined Reserves International Reporting Standards Committee |
| CSP | Concentrated Solar Power |
| C&M | Care and Maintenance |
| DNI | Direct Nickel |
| DSM | Deep Sea Mining |
| DSO | Direct Shipping Ore |
| EAF | Electric Arc Furnace |
| EIA | Energy Information Administration |
| EMA | Exploratory Modelling and Analysis |
| EoL | End of Life |
| EoL CR | End of Life Collection Rate |
| EoL PR | End of Life Processing Rate |
| EoL RR | End of Life Recycling Rate |
| ERC | Exergy Replacement Costs |
| ESDMA | Exploratory System Dynamics Modelling and Analysis |
| ET | Energy Transition |

| | |
|--------|--|
| EuRIC | European Recycling Industries' Confederation |
| EV | Electric Vehicle |
| FC(E)V | Fuel Cell (Electric) Vehicle |
| FSP | Fixed Stock Paradigm |
| GDP | Gross Domestic Product |
| GHG | Greenhouse Gas |
| GWP | Global Warming Potential |
| HC | Hydrogen Council |
| HEV | Hybrid Electric Vehicle |
| HL | Heap Leaching |
| HM | Hydrometallurgical |
| HPAL | High Pressure Acid Leaching |
| IAM | Integrated Assessment Model |
| ICE | Internal Combustion Engine |
| IE | Industrial Ecology |
| IEA | International Energy Agency |
| IIASA | International Institute for Applied Systems Analysis |
| IRENA | International Renewable Energy Agency |
| LCA | Life Cycle Assessment |
| MFA | Material Flow Analysis |
| NCA | Nickel Cobalt Aluminium |
| NMC | Nickel Manganese Cobalt |
| OC | Open Cut |
| OCP | Opportunity Cost Paradigm |
| PED | Primary Energy Demand |
| PHEV | Plug-in Hybrid Electric Vehicle |
| PHS | Pumped Hydro Storage |
| PM | Pyrometallurgical |
| PV | Photovoltaics |
| RCP | Representative Concentration Pathway |
| REN21 | Renewable Energy Network 21 |

| | |
|--------|--|
| RKEF | Rotary Kiln Electric arc Furnace |
| RoE | Rest of the Economy |
| RTS | Reference Technology Scenario |
| SBS | Stationary Battery Storage |
| SD | System Dynamics |
| SMM | Sumitomo Metal Mining |
| SSP | Shared Socioeconomic Pathway |
| STRADE | Strategic Dialogue on Sustainable Raw Materials for Europe |
| TES | Thermal Energy Storage |
| TFC | Total Final Consumption |
| TPES | Total Primary Energy Supply |
| UG | Underground |
| UNEP | United Nations Environment Programme |
| USGS | United States Geological Survey |
| V2G | Vehicle to Grid |
| VRE | Variable Renewable Energy |
| WEC | World Energy Council |
| XIDZ | X If Divided by Zero |
| XLRM | Exogenous uncertainties, levers, relationships and metrics |
| ZIDZ | Zero If Divided by Zero |

1. Introduction

To prevent irreversible environmental damage, one of the most important challenges of this century is the mitigation of climate change. To limit global temperature increase to 1.5 °C above pre-industrial levels, annual CO₂ emissions should be reduced to zero by 2050 (Rogelj et al., 2015). This can be realised through acceleration of the energy transition (ET); a transition from conventional energy sources, mainly fossil fuels, to a low-carbon system. However, the ET requires radical changes that can have far reaching impacts due to the interconnectivity of the energy system with other systems.

One aspect of the ET that is often underestimated is the interconnection between the energy system and the material sector, the so-called energy-material nexus (Watari et al., 2019). The material sector is very energy-intensive, but at the same time many (scarce) materials are required for (renewable) energy infrastructure. It is important to consider whether supply can meet demand, especially in a fast-paced ET.

This can be understood in the context of supply chain resilience, which is defined as ‘the capacity to supply enough of a given material to satisfy the demands of society, and to provide suitable alternatives if insufficient supply is available’ (Sprecher et al., 2015, p.2). The ET is a disruption that can potentially impact the resilience of material supply chains, thereby negatively impacting society. In addition, mining and processing of materials can lead to undesired externalities in the form of social and environmental impacts. These impacts should be considered and minimised for the ET to be as sustainable as possible.

Recently, an increasing number of authors have assessed material requirements of the ET, covering different locations, time scales, materials, system components and energy scenarios. 29 of these papers, with a global scope covering multiple materials and components, are summarised in appendix A. Most papers provide an estimate of future material demand based on expected energy demand and changes in energy mix outlined in various scenarios. The general conclusion of the papers is that the ET can be hampered by material availability and that it is important to increase recycling to meet growing demand.

There is also research that focuses on specific materials needed for the ET. This includes research on copper (Auping, 2011; Auping et al., 2012; Harmsen, 2013), lithium (Grosjean et al., 2012; Kushnir & Sandén, 2012), platinum (Elshkaki, 2013), dysprosium (Hoenderdaal et al., 2013), neodymium (Gloeser-Chahoud et al., 2016), tellurium (Houari et al., 2014; Bustamante & Gaustad, 2016), indium (Stamp et al., 2014; Choi et al., 2016) and cobalt (Van der Linden, 2020). A benefit of focusing on a single (or a limited number of) material(s) is that more in-depth research can be done, leading to a more detailed representation of market behaviour. A drawback of such a narrow focus is that certain system information can be lost. To reduce information loss, it is important to consider by-products and potential substitutes.

A material for which not much in-depth research was found is nickel, even though it is important for the energy system. It is used in the stainless steel required for all energy infrastructure and it forms a large share of many battery types, both stationary and in Electric Vehicles (EVs) (Nickel Institute, n.d.; BNEF, 2019). Nickel was also identified as a potential bottleneck for the ET by multiple papers in appendix A.

Past research on nickel stocks and flows includes the following: Schmidt et al. (2016) conducted a static Material Flow Analysis (MFA) of nickel and cobalt in lithium-ion batteries; Elshkaki et al. (2017) developed scenarios for future global nickel supply and demand and the associated energy and water use, but did not focus specifically on demand for the energy system; Amit & Venugopal (2018) and Golroudbary et al. (2019) used System Dynamics (SD) modelling to assess lithium-ion batteries; and Van der Linden (2020) included nickel in her SD model on cobalt in which she focused on EVs and battery storage.

However, previous dynamic models assessed global nickel stocks and flows at a high level of aggregation, in which a single 'global mine' was included. In this thesis, the nickel supply chain is modelled at a more detailed level in which regions, countries and individual mines and their characteristics are considered. A new database on nickel resources (Mudd, 2020) that includes i.a. location, principal processing method, ore grade and by-product composition of (potential) projects, makes it possible to create a detailed nickel model that is geographically and technologically specific.

There is a large heterogeneity across mines, which can lead to situations where the aggregated system behaves differently than the disaggregated system. These dynamics are interesting to capture, to obtain a better picture of potential future developments of nickel demand and supply, related sustainability impacts and the overall resilience of the system, as well as the implications for the ET. Furthermore, although impacts are visible at a global level, decisions are generally made at a regional level or lower. A clearer picture of regional differences can therefore better facilitate decision making, increasing the usefulness of the model for stakeholders.

The goal of this thesis is to explore the development of the nickel supply chain and its externalities (in terms of energy use, greenhouse gas (GHG) emissions and by-product production), as well as its resilience under various disruption scenarios, including the ET, between 2015 and 2060. The impacts of certain sustainability policies and other key uncertainties, are also considered. The nickel supply chain is explored with the following research question and sub questions:

How may the global nickel supply chain and its externalities develop between 2015 and 2060 under different disruption scenarios, sustainability policies and key uncertainties?

- What is the range of possible nickel demand between 2015 and 2060 based on various energy system scenarios for electricity generation, road transport and electricity storage?
- How resilient is the nickel system to changes in demand due to the ET and substitution and changes in supply due to resource depletion and disruptions in dominant supplying countries?
- What are the impacts of end of life (EoL) waste management strategies and policies to reduce forward supply chain losses and increase EV battery lifetime?
- What are other key uncertainties influencing the development and resilience of the nickel system?
- How do the results compare to historic developments and other model results in literature?

The outcomes of the model and findings of this thesis are the results of a first attempt of SD modelling of global material flows at mine level and a contribution to the growing literature on material impacts of the ET with a focus on resilience. The model and the findings can be useful for governments and companies interested in accelerating the ET in a sustainable way, as well as for actors in the mining industry, especially the nickel industry.

In the following chapters, first, the research methods are described, including the theoretical framework, the type of modelling, the model structure and data sources, verification and validation, and the experimental set-up. Then, the results are presented, structured according to the research questions. Next, the research questions are answered in a conclusion and the findings are discussed, including the societal and academic relevance and limitations and avenues for future research.

2. Methods

In this chapter, first some theoretical background information is provided on the resilience framework used in this thesis. Then, the main method, Exploratory System Dynamics Modelling and Analysis (ESDMA), with elements from Agent Based Modelling (ABM), is described. This is followed by a description of the model structure and data sources and a section on model verification and validation. Finally, the experimental set-up is described.

2.1 Resilience framework

For assessing supply chain resilience, a framework by Sprecher et al. (2015) was used. As stated in the introduction, resilience refers to the capacity of a supply chain to meet the demand for a certain material. A system with high resilience undergoes minimal disturbance or is able to recover from large changes in demand or potential supply disruptions in a reasonable time frame.

Sprecher et al. (2015) describe different types of disturbances, distinguishing between supply disturbances and demand disturbances that can be either slow or fast. They also discuss three important aspects of resilience; resistance, rapidity and flexibility, as well as mechanisms that can increase resilience. These are shown in figure 2.1.

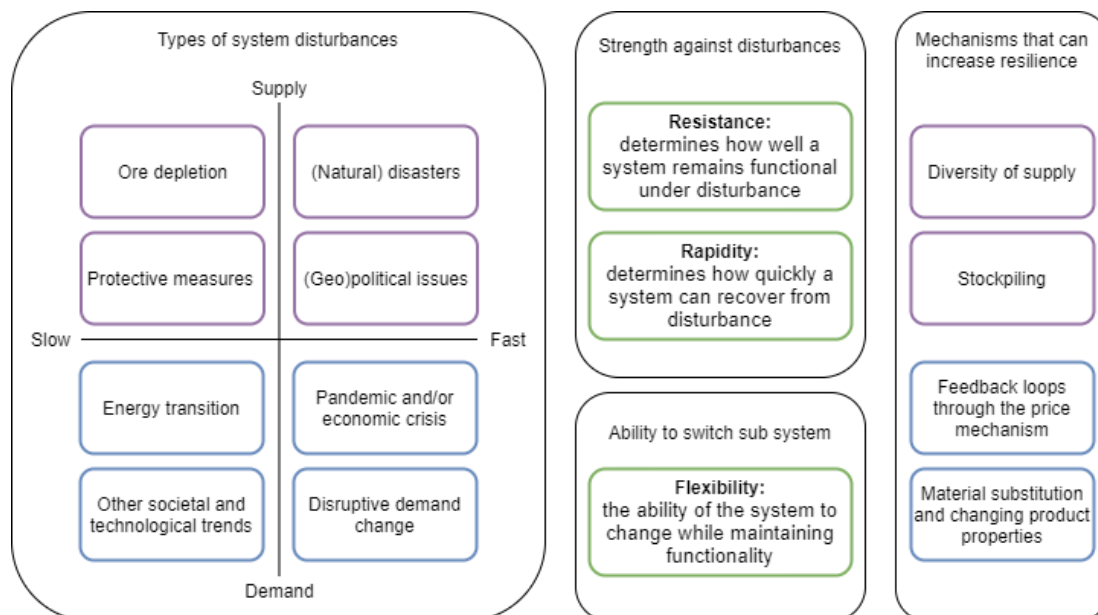


Figure 2.1: Types of system disturbances, important aspects of resilience and mechanisms that can increase resilience, both near the start of the supply chain (purple) and near the end of the supply chain (blue). Created with information from Sprecher et al. (2015).

On the left-hand side of figure 2.1, possible disturbances are categorised based on speed of impact (whether it occurs in the long term or in the short term) and the part of the supply chain where the impact takes place (supply or demand). On the supply side, slow disturbances include the gradual depletion of high-grade ores and protective policies, such as taxes and export quotas. Fast disturbances include natural or anthropogenic disasters, such as floods or explosions, and (geo)political issues, such as armed conflicts, miner strikes or export bans (Sprecher et al., 2015).

On the demand side, fast disturbances include disruptive changes such as the introduction of a new popular product or a novel way of making a certain product. An economic crisis and/or a pandemic, such as the recent Corona crisis, can also lead to relatively fast changes in demand. Slow disturbances are often the result of long-term socio-technical trends, such as the ET (Sprecher et al., 2015).

The ET is a gradual process; however, the pace of this transition determines the level of disturbance in material supply chains and in turn, the resilience of the supply chains determines how well supply can keep up with the increasing demand and to what degree the speed of the transition may be hampered. An important issue is whether mining activities, which usually have long time horizons, and recycling activities, can be scaled up fast enough to match increasing demand (Vesborg & Jaramillo, 2012). This makes material aspects one of the key risks for the pace of the ET.

The middle of figure 2.1 shows the three important aspects of resilience and the right-hand side shows the mechanisms that can increase resilience. Diversity of supply and stockpiling are supply side mechanisms and they are explained in more detail in section 2.3.2. Feedback loops through the price mechanism, material substitution and changing product properties occur later on in the supply chain, and they are described further in section 2.3.1.

Often the supply chains of bulk materials, like nickel, are more resilient than those of minor metals. This is because minor metals are often mined as a by-product and thus their supply is driven less by demand dynamics (Sprecher et al., 2017). However, the sheer size of the ET means there may also be a risk for bulk materials (Kleijn & van der Voet, 2010).

2.2 Exploratory System Dynamics Modelling and Analysis

The main method used in this thesis is ESDMA, with the addition of ABM elements. ESDMA combines SD and Exploratory Modelling and Analysis (EMA). SD is a modelling approach used to describe and simulate complex systems over time. SD models consist of variables connected by differential and integral equations, and often include multiple positive or negative feedback loops and delay structures, allowing the simulation of complex behaviour (Forrester, 1958; Forrester, 1961; Forrester, 1995; Pruyt, 2013).

Other papers that used SD to model material stocks and flows include Auping (2011), Auping et al. (2012), Houari et al. (2014), Choi et al. (2016), Gloeser-Chahoud et al. (2016) and van der Linden (2020). However, these papers all used SD in its traditional sense, where the system is approached mostly in a highly aggregated, top-down, continuous manner (Borshchev & Filippov, 2004).

In this thesis, material stocks and flows were assessed at the level of individual mines, thereby using SD in a more hybrid form, by including aspects from Agent-Based Modelling (ABM). ABM is a methodology where complex systems are approached in a disaggregated, bottom-up, more discrete manner, where global behaviour emerges from the different behaviour of individual entities (Borshchev & Filippov, 2004).

The choice was made to add ABM elements to SD instead of only using ABM, because creating a pure ABM would make it more difficult to model supply chains and to incorporate the feedback loops that characterise both the development of the energy system and the development of resource flows. In the hybrid model used in this thesis, both individual mines and other detailed elements were included, as well as more aggregated system processes.

Adding very discrete elements to an SD model can be seen as a limitation, but it can also lead to new insights by generating behaviour that could not be generated from a model with a high level of aggregation. Other limitations of the approach are inherent to modelling exercises: it includes many assumptions, leading to uncertain results.

EMA is an approach that works with the uncertain nature of models. No single model is correct and to get a better picture of possible futures, inherent uncertainties should be explored. This can be done using the XLRM framework, in which X represents exogenous uncertainties that cannot be easily controlled, L refers to policy levers that can be controlled, R represents relationships within the system and M refers to performance metrics (Bankes, 1993; Lempert et al., 2003; van der Linden, 2020). This framework is shown in figure 2.2.

With EMA, many different model runs are done, all with varying structures, levers and uncertainties. Each run leads to different values for the performance metrics over time, creating a vast output space that shows the deep uncertainty of the model (Auping, 2018; Van der Linden, 2020).

Adding EMA to SD allows explicit inclusion of deep uncertainty, leading to more realistic results (Auping, 2018). Many assumptions will still have to be made and the results will not lead to any predictions of the future, but they will allow for exploration of multiple possible futures, and especially system behaviours, which could lead to useful insights for stakeholders.

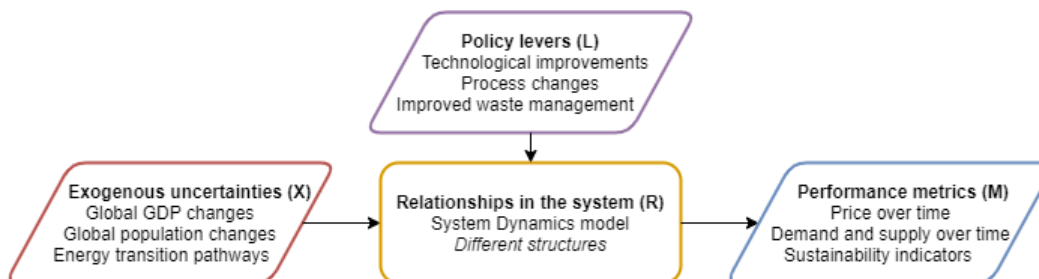


Figure 2.2: the XLRM framework applied to the nickel system (adapted from van der Linden, 2020). For a more elaborate version of this framework applied to the nickel system, see figure B1 (appendix B).

2.3 Model structure and data sources

The models on copper by Auping (2011) and cobalt by van der Linden (2020) were used as a basis for the model in this thesis. Their models were adapted to include demand sectors in the energy system that are especially relevant for nickel, a geographically and technologically specific supply structure at mine level, and a more detailed price structure suitable for determining the economics of multiple mines.

Two important parts of the nickel system are the demand and the supply system. These sub-systems are connected through price dynamics and together this leads to certain sustainability impacts. Figure 2.3 shows the complex relationships between energy, materials and the economy through multiple feedback loops in a Causal Loop Diagram (CLD). These are the main relationships included in the nickel model.

In figure 2.3, the impact of more renewables in the energy mix on the energy price is shown with a dashed line and a question mark because it is highly uncertain and the sign can change over time. In the model various scenarios are assumed. This is described in more detail in section 2.3.3. A carbon tax is included because this is part of the ET scenarios included in this thesis.

In the model, demand dynamics, supply dynamics, price dynamics and impacts are split into four sub-models. The structure of these sub-models and data sources are described below and summarised in figure 2.4. The complete structures of each sub-model are shown in appendix B.

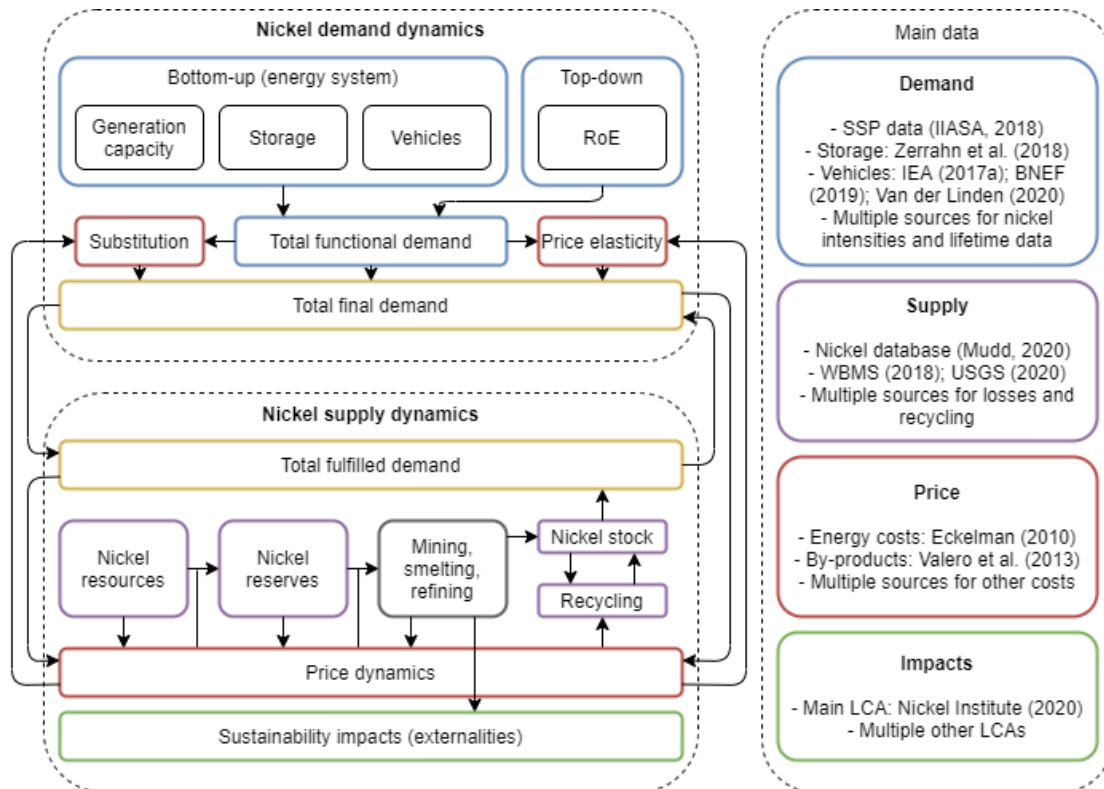


Figure 2.4: overall model structure and data sources. Demand, supply, price and impacts are each a sub-model of the total model. RoE = Rest of the Economy. Further details are shown in figures 2.5, 2.13 and 2.20. Note: not all data sources are shown in this figure, only the largest contributing sources. Other sources are described in the text.

2.3.1 Demand sub-model

Nickel is an important metal for society. It is used in stainless steel (70%), various other alloys (16%), plating (8%) and batteries (5%) (Nickel Institute, n.d.). Nickel is used in many different end-use sectors, including the energy system which is expected to undergo significant change in the ET.

Material demand can be modelled in two ways: top-down and bottom-up. Top-down models are based on general GDP developments. Bottom-up models are based on specific end-use sector developments (Auping, 2011; Van der Linden, 2020). In this thesis, the focus is on nickel demand for the ET, so various parts of the energy system (specifically, electricity generation, storage and vehicles) were modelled in a bottom-up way and the RoE was modelled in a top-down way.

The exact bottom-up demand components included in the model are shown in figure 2.5, as well as the scenarios used to determine their input data. Only components in the power sector, storage and road transport were considered, because of data availability and because these are the sectors that are expected to change most in the ET through increased electrification of the energy system (Blok & Nieuwlaar, 2021). The selected components, including data on nickel intensity and lifetime and the position of components and their relationships in the energy system, are described in appendix C. Input values for the demand sub-model are described in appendix F.

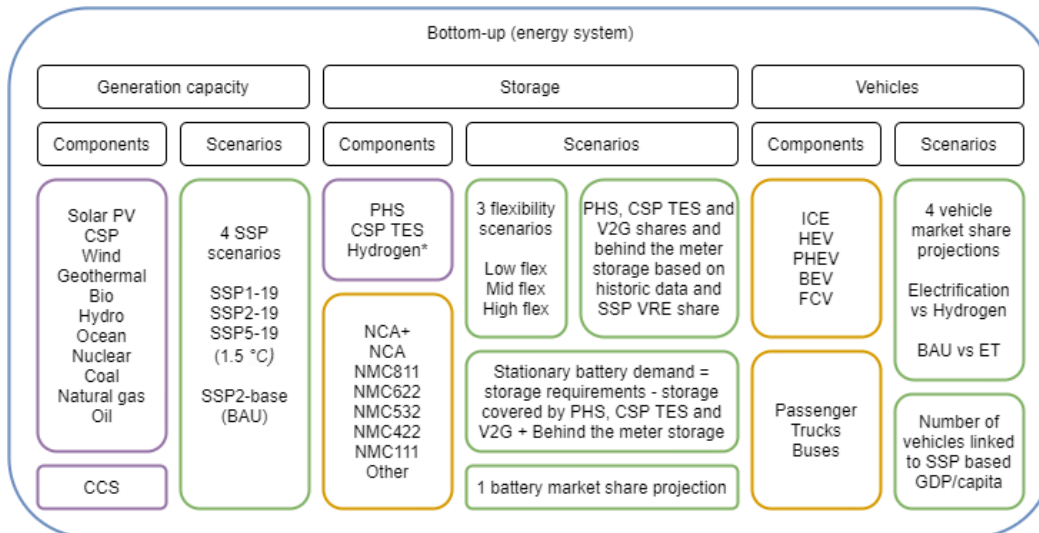


Figure 2.5: components considered in the bottom-up modelling of the energy system and the scenarios used to determine their input data. For the components in the purple boxes, only nickel in stainless steel was assessed. For the components in the orange boxes, only nickel in batteries was assessed. For the RoE, nickel in stainless steel and an 'other' category were assessed. PV = photovoltaics, CCS = Carbon Capture and Storage, PHS = pumped hydro storage, CSP (TES) = Concentrated Solar Power (Thermal Energy Storage), V2G = Vehicle to Grid, VRE = Variable Renewable Energy, NCA = Nickel Cobalt Aluminium battery, NMC = Nickel Manganese Cobalt battery (the numbers indicate the relative shares of the three components), HEV = Hybrid Electric Vehicle, PHEV = Plug-in Hybrid Electric Vehicle, BEV = Battery Electric Vehicle, FCV = Fuel Cell Vehicle, GDP = Gross Domestic Product.
 *Hydrogen is only considered in relation to its use in road transportation.

The main data source for the demand scenarios is the database for Shared Socioeconomic Pathways (SSPs). SSPs were created by the climate change research community for use in Integrated Assessment Models (IAMs) to analyse the impacts of climate change. The different SSPs describe alternative future socio-economic developments up to 2100, including changes in population, GDP and energy demand (Riahi et al., 2017; IIASA, 2018). In this thesis, three SSP pathways that conform to the 1.5 °C temperature increase target (SSP1-19, SSP2-19 and SSP5-19) were selected, as well as a Business as Usual (BAU) pathway (SSP2-baseline). These scenarios are described in appendix D1.

The SSPs were used to model changes in electricity generation and generation capacity for each of the components in figure 2.5. CCS was also included for fossil fuel and biomass-based generation. The structure for determining generation capacity is shown in figure 2.6.

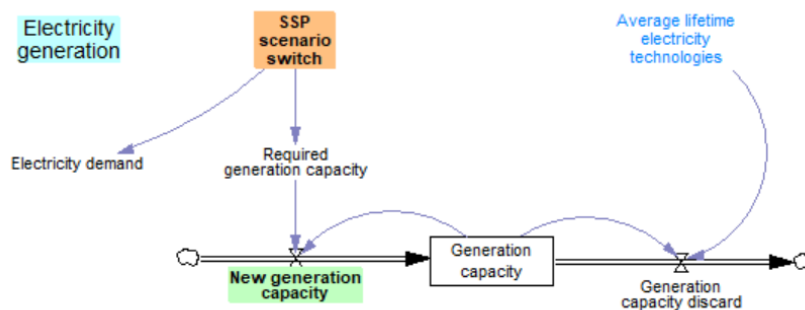


Figure 2.6: structure for determining electricity generation capacity. Blue = constant, orange = switch, green = output.

To model changes in storage and vehicles, additional scenarios were used. Storage requirements were based on the share of VRE derived from the SSPs and the relationship between VRE share and storage as a fraction of energy demand adapted from Zerrahn et al. (2018). The amount of storage required also depends on the implementation of other flexibility measures, such as grid expansion, demand response, flexible dispatch and curtailment (Brown et al., 2018), so three flexibility scenarios were created. These scenarios and further details on storage are described in appendix D2.

The types of storage included in the model are PHS, CSP TES, V2G storage, where EVs are used for storage, and stationary battery storage (SBS). It is assumed that most storage requirements are covered by PHS, CSP TES and V2G (IRENA, 2017) and that the remaining requirements are covered by SBS. Additional SBS demand from behind the meter applications is also included. Some of the SBS is assumed to come from the production of new batteries and some is assumed to come from the repurposing of old EV batteries. Battery market shares were based on BNEF (2019). The structure for determining energy storage is shown in figure 2.7.

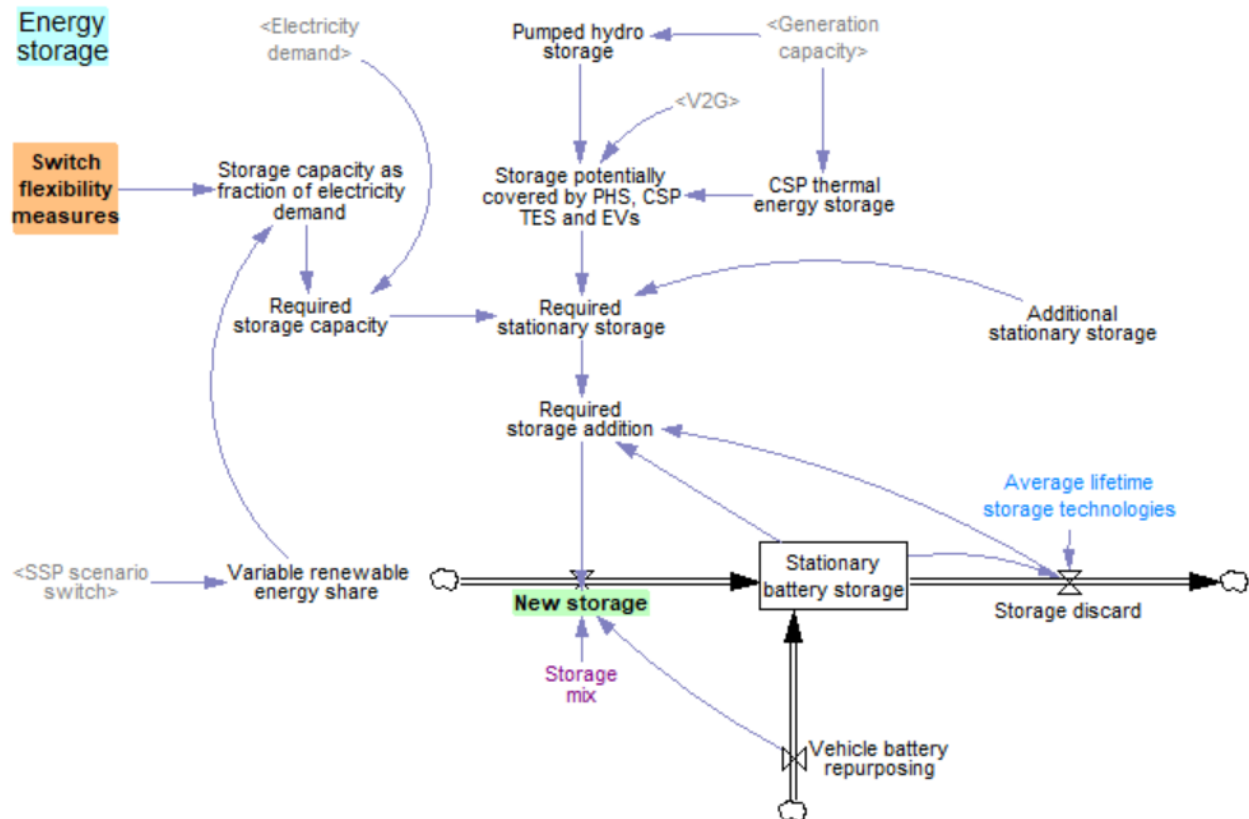


Figure 2.7: structure for determining storage. Blue = constant, purple = lookup, orange = switch, green = output.

For vehicles, two scenarios were created, an electrification scenario, considering a transition to predominantly BEVs, based on BNEF (2019) and Van der Linden (2020), and a hydrogen scenario, considering a transition where a significant number of FCVs are also created, based on HC (2017). These are quite ambitious scenarios, so for the BAU pathway, vehicle shares were based on the Reference Technology Scenario (RTS) from the IEA (2017a) and the number of FCVs was reduced based on IRENA (2018). The scenarios are described in appendix D3. The structure for determining vehicle battery demand is shown in figure 2.8.

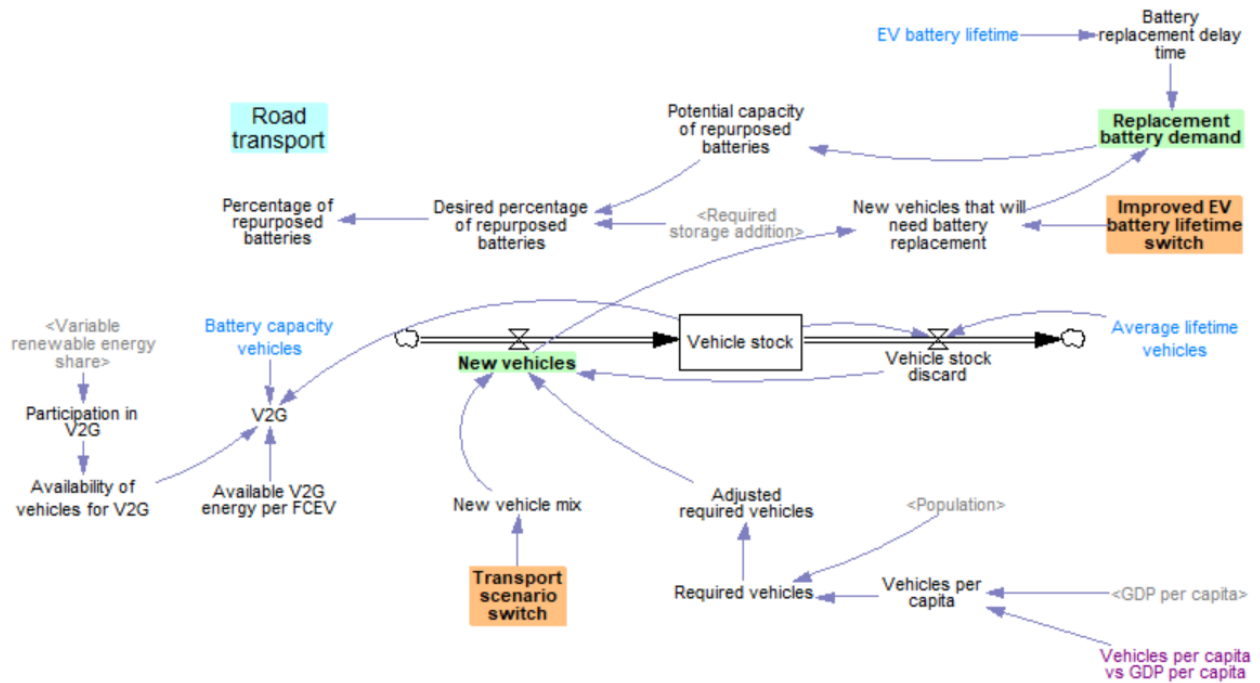


Figure 2.8: structure for determining vehicles. Blue = constant, purple = lookup, orange = switch, green = output. In addition to the transport scenario switch, an improved battery lifetime switch is included (see section 2.5)

Nickel demand for each of the sectors was determined by multiplying the required generation capacity, storage and vehicles by their respective nickel intensities. The nickel intensity was assumed to change over time in the opportunity cost paradigm (OCP; described below) due to material efficiency changes. The structure for determining nickel demand is shown in figure 2.9 for the energy system and in figure 2.10 for the RoE.

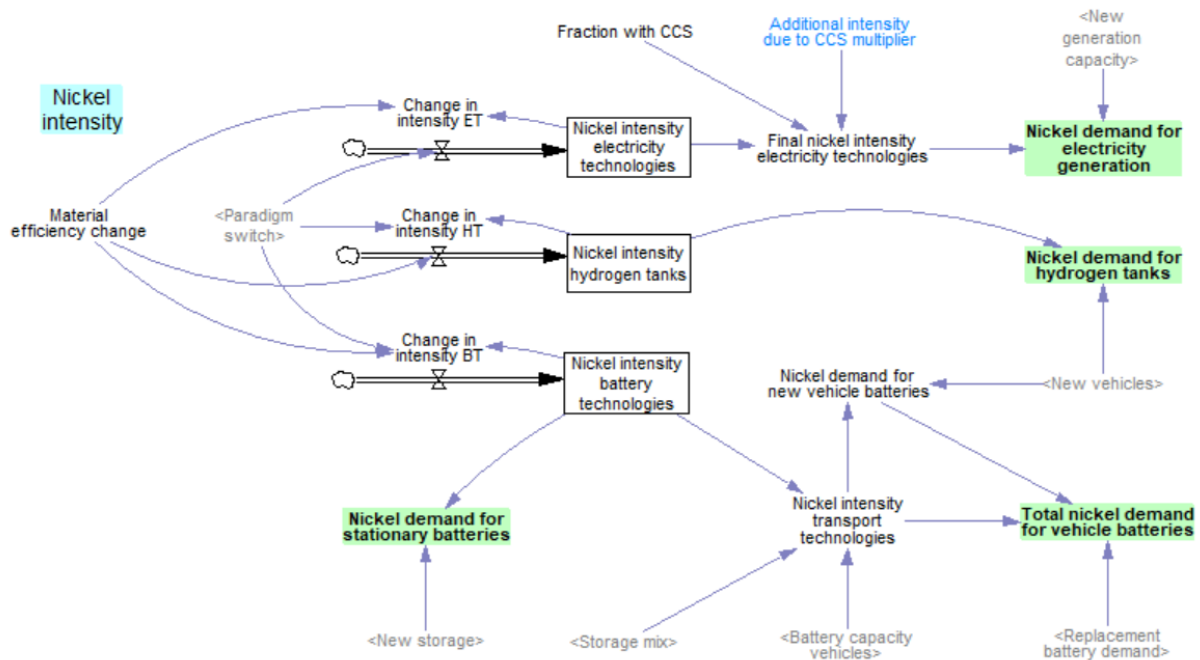


Figure 2.9: structure for determining nickel intensity and demand of components. Blue = constant, green = output.

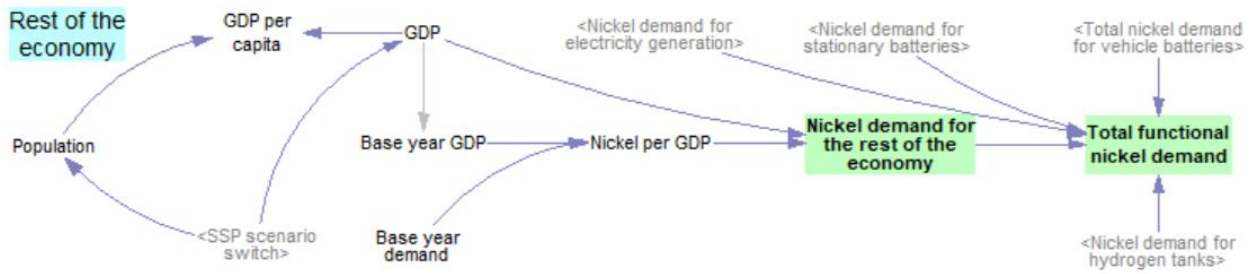


Figure 2.10: structure for determining nickel demand for the RoE (top down) and total nickel demand before the influence of price effects. Green = output.

Adding the nickel requirements for electricity generation, storage, vehicles and the RoE together leads to the total functional nickel demand. However, this is not the final demand because price dynamics can still influence it. Two different paradigms are included in the model, the Fixed Stock Paradigm (FSP), in which no exploration occurs and nickel demand is not influenced by price dynamics and the OCP, where exploration does occur and nickel demand is influenced by price dynamics. These paradigms are described in more detail in appendix E1.

The following three price effects were included in the model: price elasticity, substitution and intensity changes. These three effects are similar but there are also some distinct differences. Price elasticity leads to the discontinuation of a certain portion of demand, whereas substitution leads to the replacement of a certain option and intensity reduction reflects savings within a certain option. What all price effects have in common is the balancing effect they have on the system, thereby increasing resilience. This is illustrated in the CLD in figure 2.11. The structure for the price effects is shown in figure 2.12. More details on these price effects are described in appendix E.

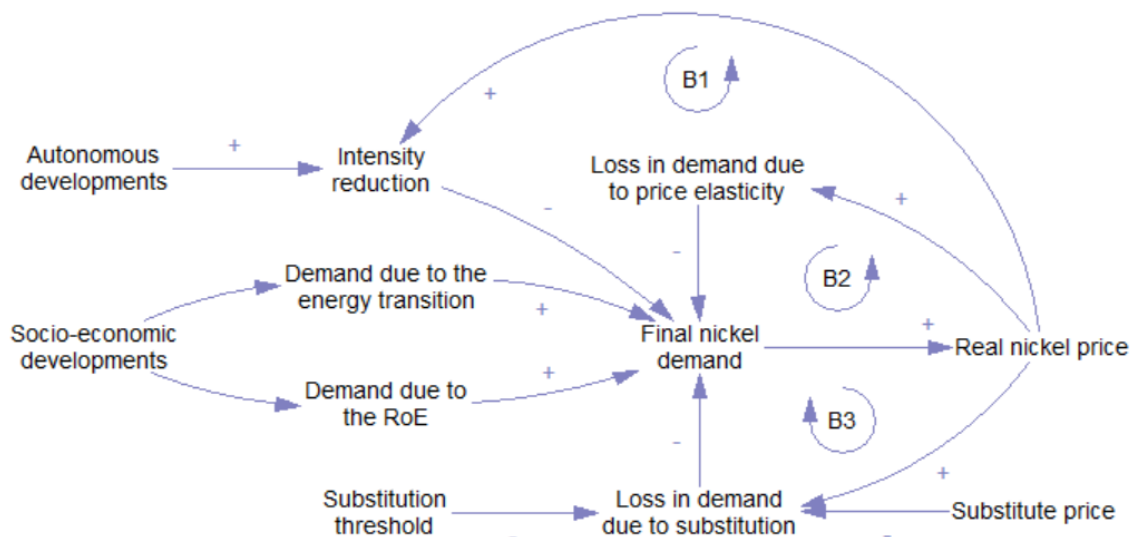


Figure 2.11: CLD of price related mechanisms with a balancing effect on the system, thereby increasing resilience. B1 = nickel intensity improvement balancing loop; B2 = price elasticity of demand balancing loop; B3 = substitution balancing loop.

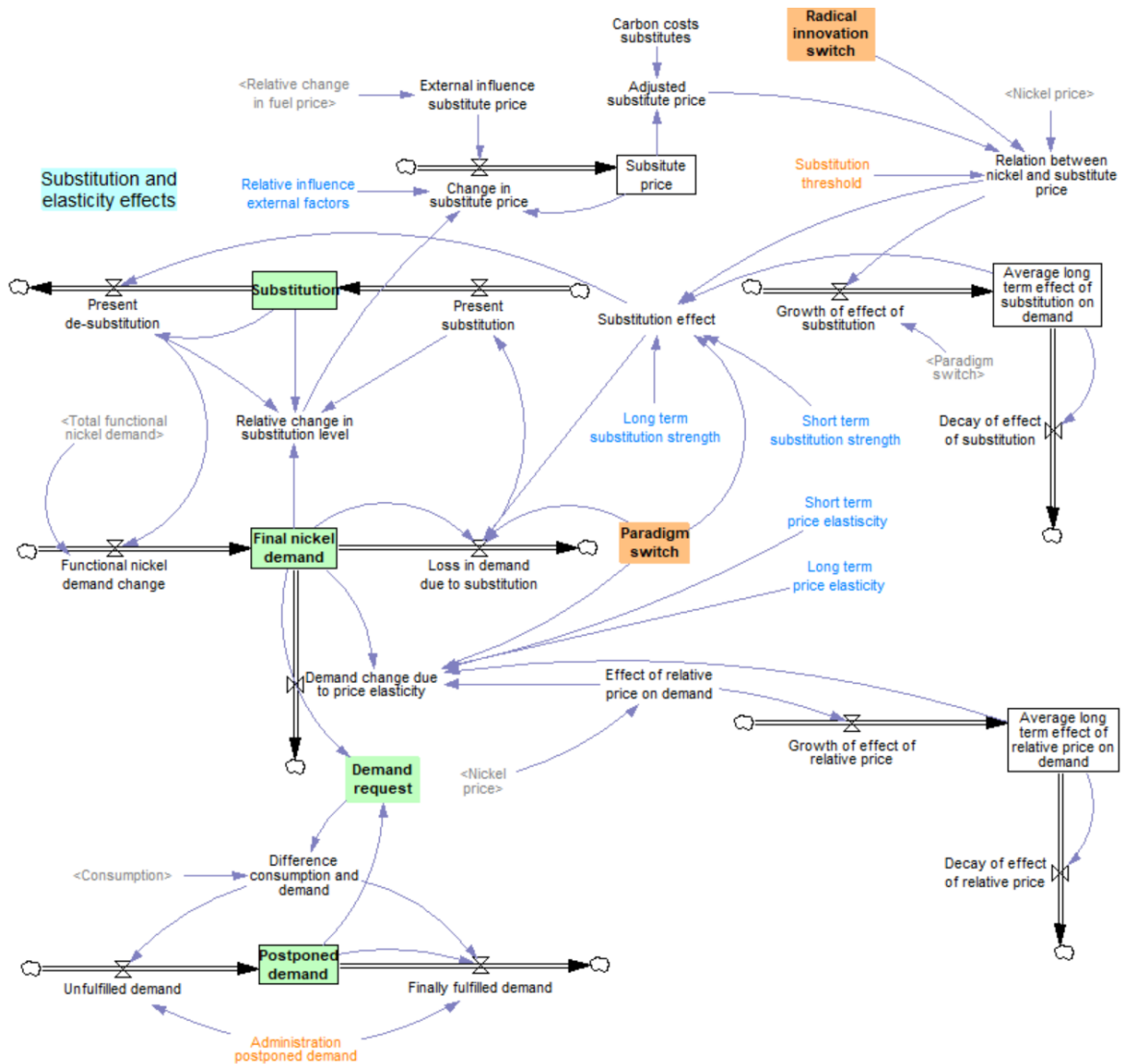


Figure 2.12: price effect structure. Blue = constant, orange box = switch, orange = key uncertainty, green = output. In addition to the paradigm switch, a radical innovation switch is included (see section 2.5).

2.3.2 Supply sub-model

Current measured, indicated and inferred nickel resources are estimated to be about 334 million tonnes (Mudd, 2020). For the definitions of the different types of resources, see CRIRSCO (2019). Deposits and operating mines are located in 45 different countries and there are also deep-sea deposits in international waters (Mudd, 2020). Figure G1 in appendix G shows the global distribution of nickel resources and reserves, as well as the ore type. Nickel is a major metal that functions primarily as host metal. This means it is usually the main product of a certain mine, with only ~5% produced as a by-product from platinum mining, a figure that has remained quite stable over the years (Nassar et al., 2015).

There are two main ore types from which nickel can be extracted, sulfides and laterites. Sulfides require less energy to process and have therefore been preferred historically, but they are less abundant, leading to a relative increase of laterite mining over time. Laterites are mainly found in tropical regions and mined from Open Cut (OC) mines, while sulfides are mainly found in colder areas and mined from Underground (UG) mines (Mudd, 2010; Crundwell et al., 2011).

The main data source for the supply system is a database created by Mudd (2020), which gives a detailed description of global nickel resources and reserves and mentions various attributes of different deposits, including ore type, location, mine type, operating status and principal processing method. The supply components included in the model are shown in figure 2.13. Input values for the supply sub-model are described in appendix H.

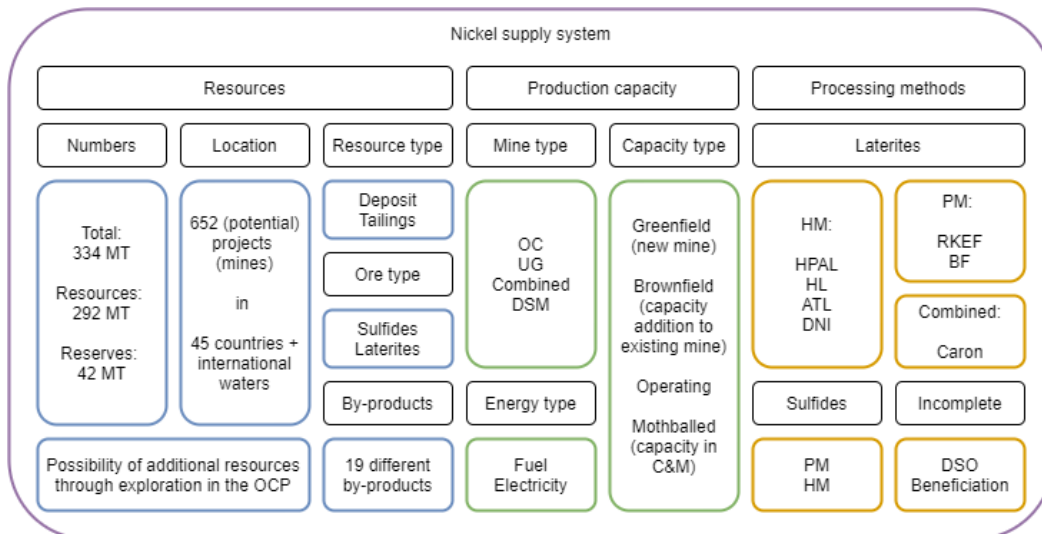


Figure 2.13: supply components considered in the model. Based on Mudd (2020). DSM = Deep Sea Mining, C&M = Care & Maintenance, HM = Hydrometallurgical, PM = Pyrometallurgical, HPAL = High Pressure Acid Leaching, HL = Heap Leaching, ATL= Atmospheric Leaching, DNI = Direct Nickel, RKEF = Rotary Kiln Electric arc Furnace, BF = Blast Furnace, DSO = Direct Shipping Ore.

Important parts of the supply model include the resources, the production capacity and the supply chain, including different processing methods. If the OCP is used, exploration occurs. In the model, exploration is based on a historic element, a price-based element and an element based on expectations of the ET. Once resources have been discovered, they can be turned into probable or proved reserves when they become economically extractable. The structures for exploration and the conversion of resources to reserves are shown in figure 2.14 and 2.15 respectively and they are described in further detail in appendix G1.1 and appendix G1.2 respectively.

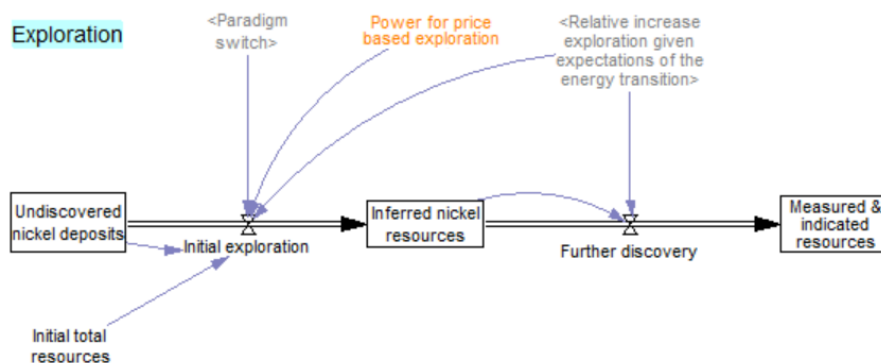


Figure 2.14: structure for exploration. See appendix G1.1 for the formula. Orange = key uncertainty

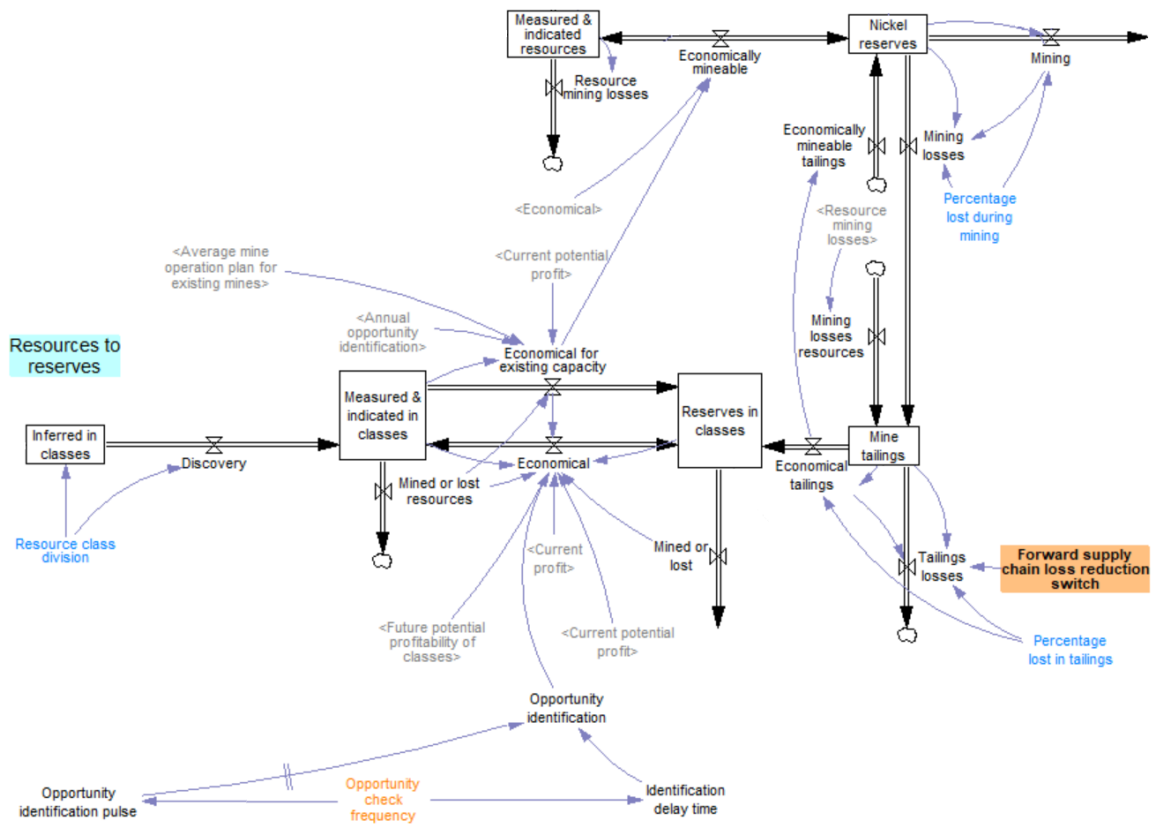


Figure 2.15: structure for resource to reserve conversion. The reason for this extended structure with resources and reserves split into classes is explained in appendix G1.2. Blue = constant, orange box = switch, orange = key uncertainty. The forward supply chain loss reduction switch is explained in section 2.5.

Based on the reserves, a certain mining capacity is built. If this is in a new area, it is referred to as greenfield capacity. If it is an addition to an existing mine, it is referred to as brownfield capacity. After a certain development or upgrading time, a mine becomes operational if it is still profitable. Production capacity increase is described in further detail in appendix G2.2 and its structure is shown in figure 2.16.

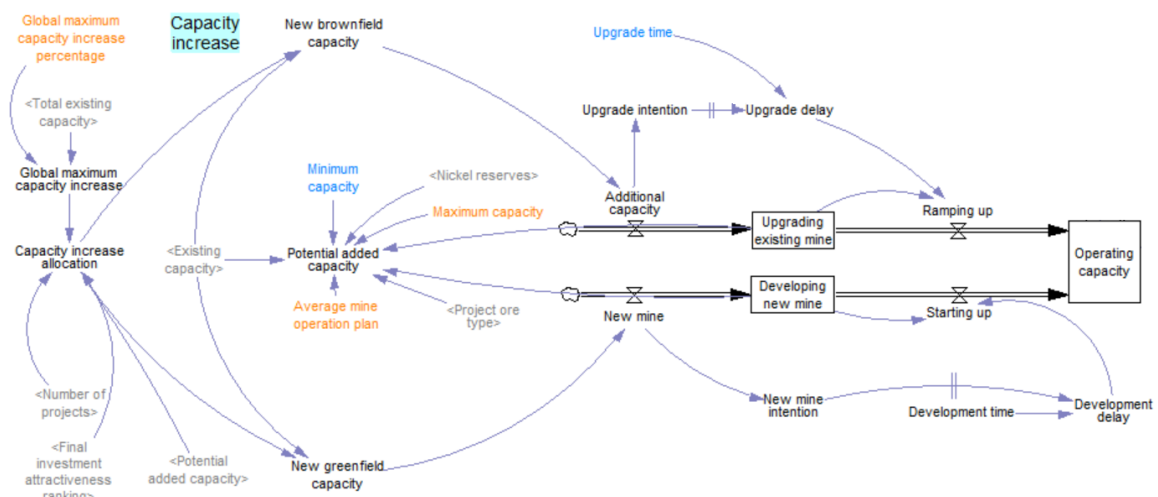


Figure 2.16: structure for creating new brownfield or greenfield capacity. Blue = constant, orange = key uncertainty. The global maximum capacity increase percentage limits total annual capacity increase and leads to selection of projects with the highest investment attractiveness.

If a certain mine is no longer profitable it is mothballed, which means it goes into C&M where operation is ceased, until it becomes profitable again or is decommissioned. A mine doesn't go in and out of C&M immediately when profitability changes. This depends on the degree and length of time of the (un)profitability. The mechanism for mothballing is described in further detail in appendix G2.1 and its structure is shown in figure 2.17.

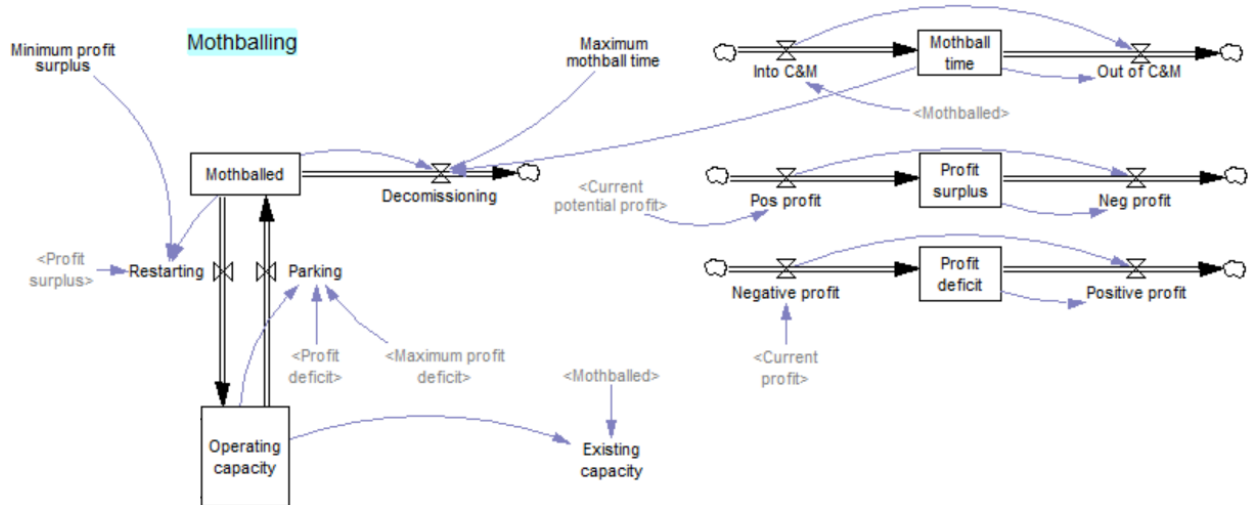


Figure 2.17: structure for operating and mothballed capacity. Three key uncertainties relevant for mothballing are not visible in this representation. These are the average maximum profit deficit as percentage of investment, average minimum profit surplus as percentage of investment and average maximum mothball time (See appendix H for a description of these variables).

Operating capacity is used to mine nickel. The structure for mining and the rest of the forward nickel supply chain is shown in figure 2.18. A switch was included in the model with the option to mine resources in the period when a mine is unprofitable but not mothballed yet. Once nickel has been mined, it is processed using different processing methods.

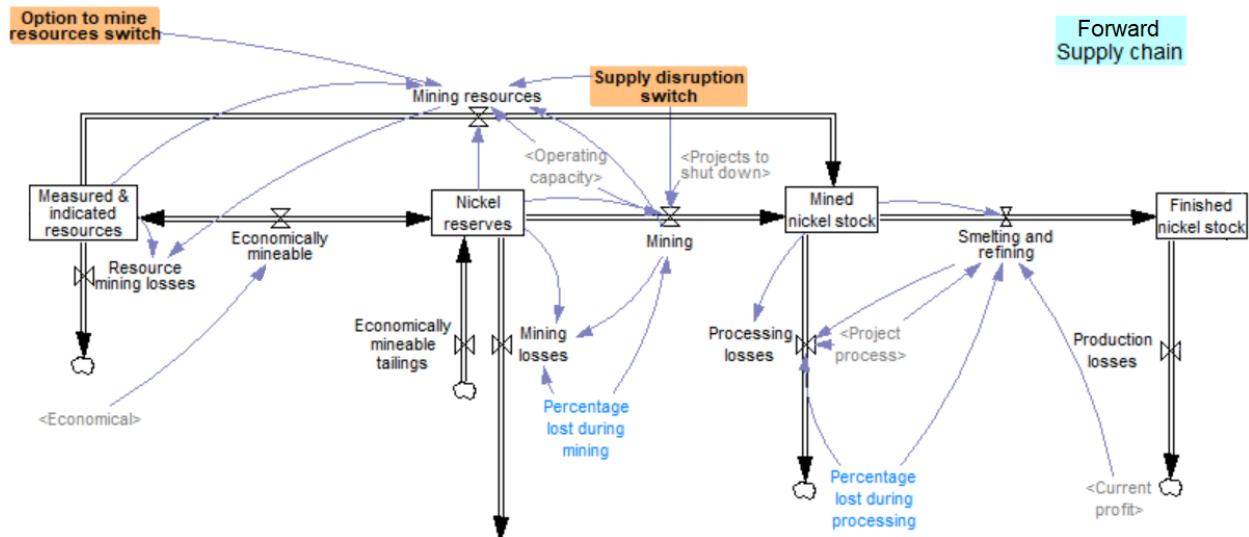


Figure 2.18: structure for the forward nickel supply chain. This includes mining and processing of reserves, as well as the mining of resources when the option to mine resources switch is turned on. Blue = constant, orange = switch. In addition to the option to mine resources switch, a supply disruption switch is included (see section 2.5).

Processing capacity differs from mining capacity, but this is not included in the model. For further details, see appendix G2. The selection of a suitable processing method is based i.a. on deposit characteristics, such as ore type (Kyle, 2010). Figure 2.19 shows different processing routes for different ore types, which leads to different products, including class I products (> 99% nickel) required for batteries and class II products (<99% nickel) used mostly in stainless steel (Schmidt et al., 2016). The processing methods are described in more detail in appendix G3.1.

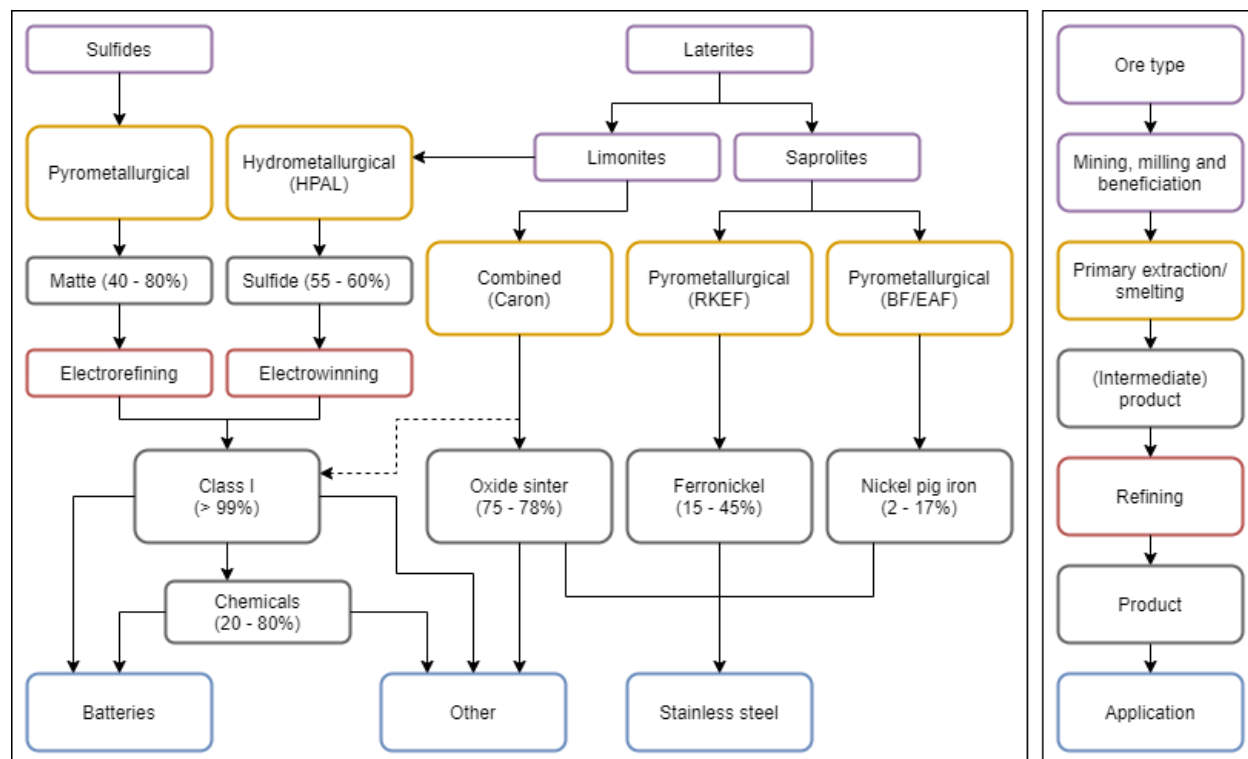


Figure 2.19: nickel sources (purple), important primary production routes (orange), products (grey) and the applications of these products (blue). Nickel content of the products is added in brackets. Adapted from Schmidt et al. (2016) with additional information from SMM (n.d.), Eckelman (2010) and Nickel Institute (2020). EAF = Electric Arc Furnace.

After processing, nickel ends up in the finished nickel stock. Here nickel can be stockpiled, however, this was not included in the current version of the model. Stockpiling can improve resistance by acting as a buffer for sudden price and/or supply changes (Sprecher et al., 2015).

When it comes out of stock, the nickel is used to manufacture final products, where some of the nickel is lost, some becomes primary scrap and the rest ends up in final products in use. Once a product's lifetime has been reached, it is discarded and the nickel is lost or becomes secondary scrap. Nickel scrap can be recycled back to the refined stock in a circular process. More details on losses and recycling are described in appendix G3.2.

Recycling increases the diversity of supply and thereby the resilience of the system. Diversity of supply also increases with a larger number of mines in different countries and alternative ways of mining, such as DSM and illegal mining operations (Sprecher et al., 2015). If supply comes from multiple sources, the impact of one source being disrupted is less. The structure for the reverse nickel supply chain is shown in figure 2.20.

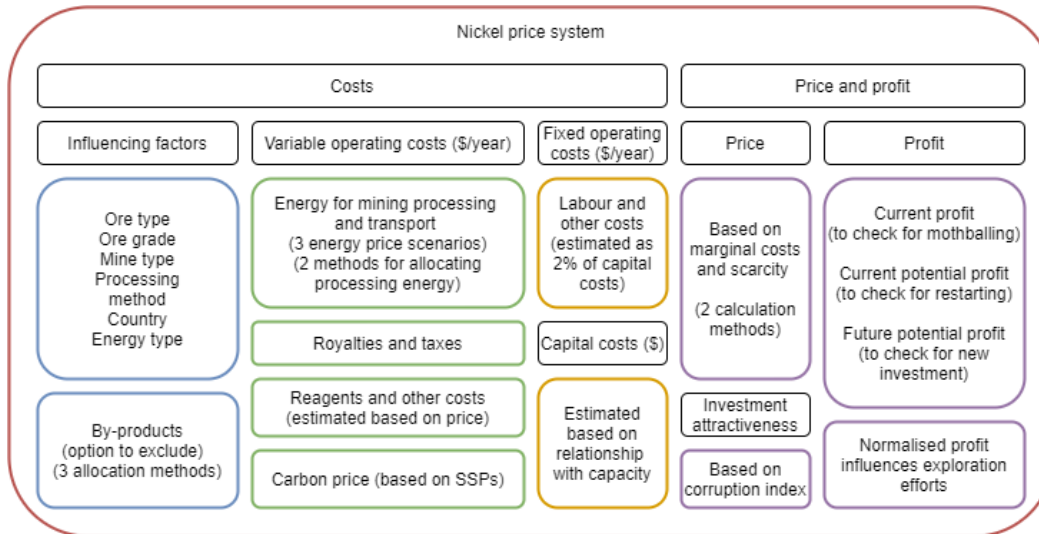


Figure 2.21: Economics included in the nickel model. Created with information from Bleiwas (1984), Eckelman (2010), Dry (2013) and STRADE (2016).

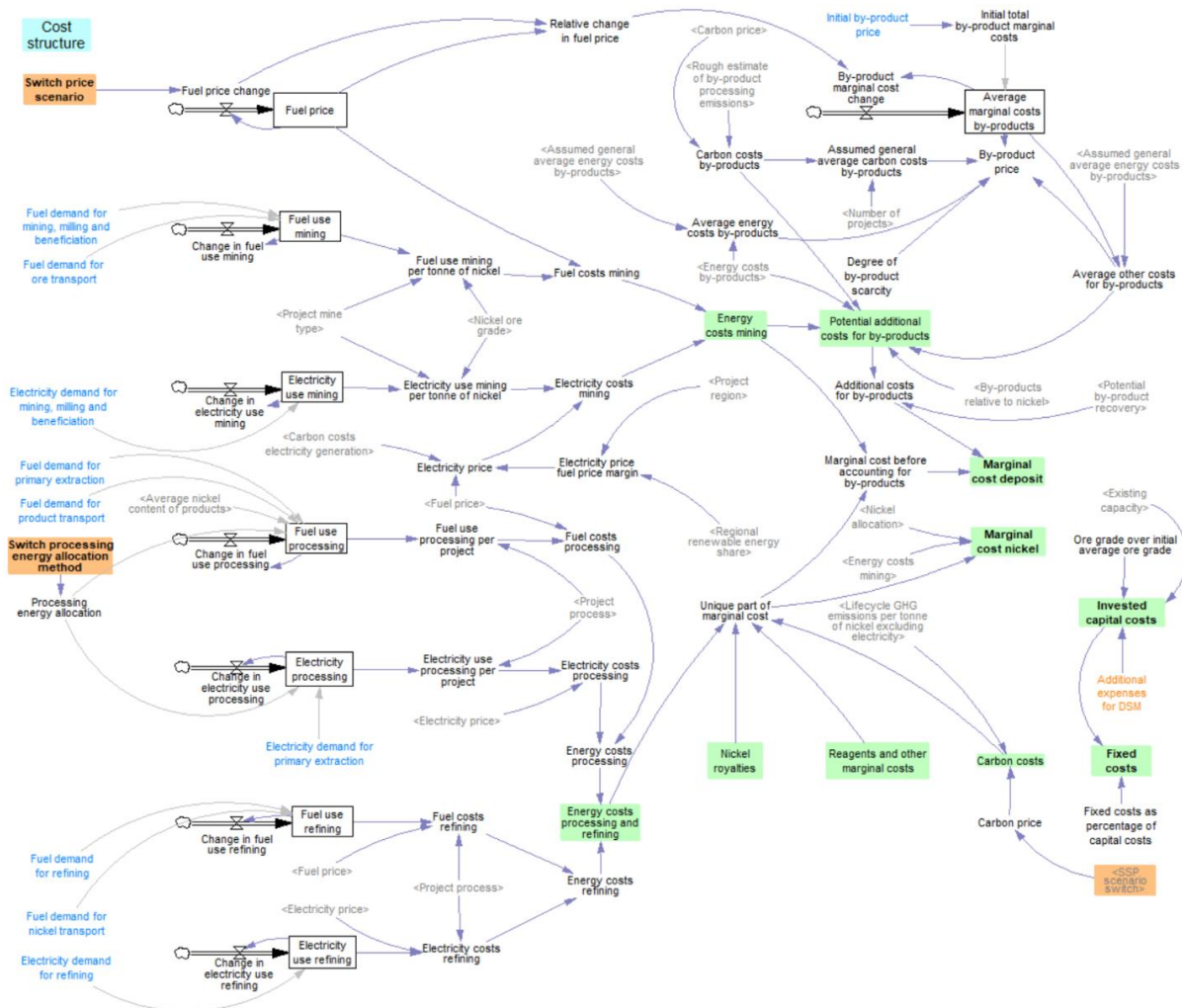


Figure 2.22: cost structure for nickel. Blue = constant, orange box = switch, orange = key uncertainty, green = output. The switch for price scenario and the switch for processing energy allocation method are described below.

A variable that has an important influence on energy use is ore grade. Data on average ore grades was provided by Mudd (2020) for current known resources. For future resources, ore grade was assumed to decay exponentially based on van der Linden (2020). This is explained in more detail in appendix I1.1. The structure for determining ore grade is shown in figure 2.22.

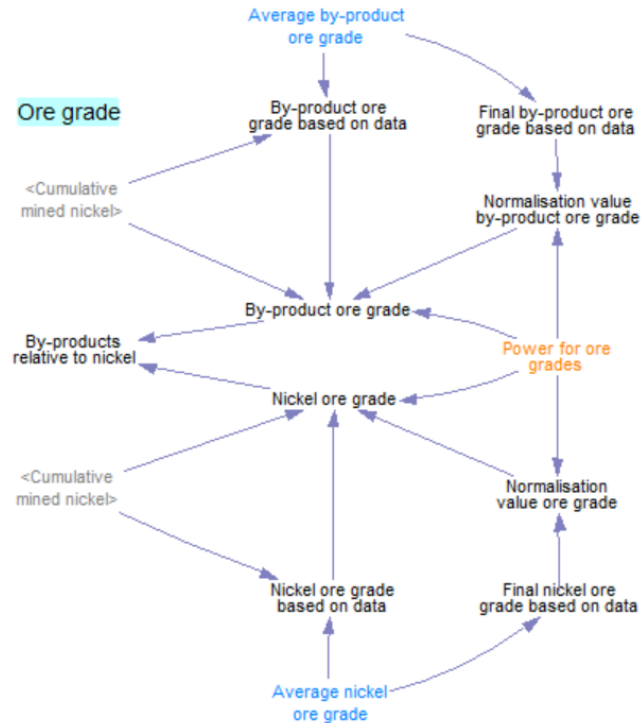


Figure 2.23: structure for nickel and by-product ore grades. Blue = constant, orange = key uncertainty

Energy use for processing was determined based on the principal processing method of a certain mine. Two methods for processing energy allocation, one based on mass and one on full allocation to nickel, were used to determine energy use for class II nickel products. For more details, see appendix I1.3.

In addition to energy use, an energy price is needed to determine energy costs. In the model, a distinction was made between fuel and electricity price. The fuel price is highly uncertain and is estimated based on three different fuel price scenarios, one with an increasing price, one with a decreasing price and one that fluctuates between the others. These scenarios are shown in figure I4 in appendix I1.4.

The electricity price was based on the fuel price and the renewable share of the energy mix in the region where a specific mine is located. It was assumed that as the renewable share increased, the margin between electricity price and fuel price would become increasingly smaller, with the electricity price becoming cheaper at high penetrations of renewables. For more details, see appendix I1.4.

Many nickel mines can also produce by-products. If a by-product leads to a higher potential additional revenue than it leads to potential additional costs, it is recovered from the deposit and increases the profitability of a certain mine. The mining costs are then allocated between nickel and the by-products based on one of three allocation methods: mass-based allocation, price-based allocation or allocation based on Exergy Replacement Costs (ERC).

Details on the by-products, how they are included in the model and the allocation methods are described in appendix I2. Because there is a lot of uncertainty surrounding the inclusion of by-products, an additional switch was included in the model with the choice to exclude by-products. The structure for by-product allocation is shown in figure 2.24.

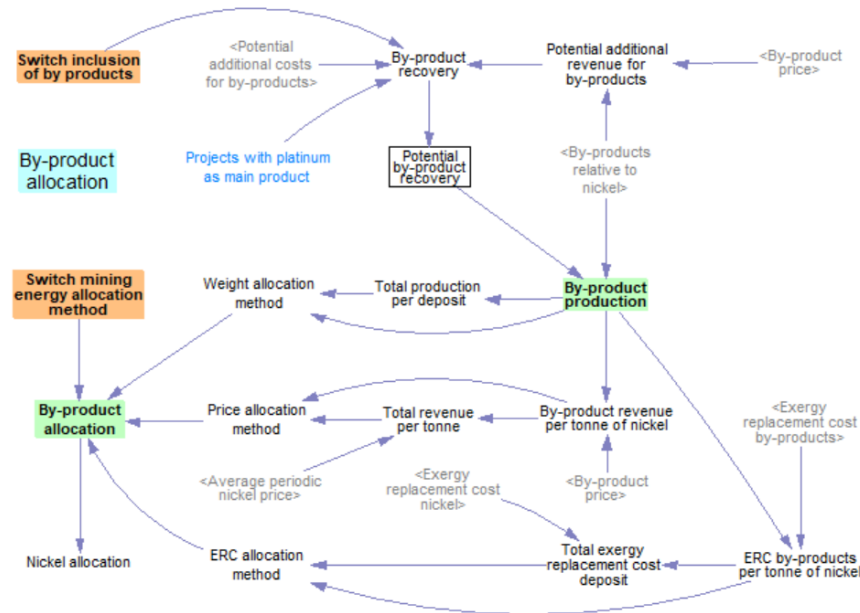


Figure 2.24: structure for by-product allocation. Blue = constant, orange = switch, green = output.

Once the marginal costs for a certain deposit are determined, the average marginal costs of all existing mines (operating and mothballed) are used together with the degree of nickel scarcity to determine price. Two price calculation methods were included in the model, one based on days of demand in stock and one based on availability and consumption. These price calculation methods are described in more detail in appendix I3.2. The structure for determining price is shown in figure 2.25.

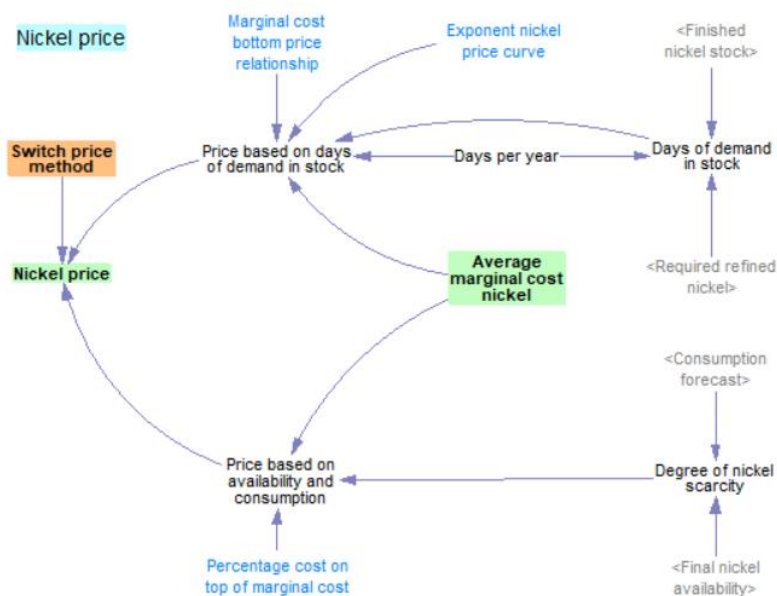


Figure 2.25: structure for determining price. Blue = constant, orange = switch, green = output.

A distinction was made between three different types of profit; current profit, current potential profit and future potential profit, to determine different processes in the model. Current profit is based on actual mining based on operating capacity and reserves, the marginal cost of a certain deposit and the average periodic nickel price at a certain time step. It is used to determine profit deficit, which determines whether a certain project should be put into C&M.

Current potential profit is based on potential mining, based on existing capacity (which includes operating capacity and mothballed capacity) and reserves, the marginal cost of a certain deposit and the average periodic nickel price at a certain time step. It is used to determine profit surplus, which determines whether a certain project should come out of C&M. It is also used to determine whether certain reserves should be turned back into resources. The structure for current profit and current potential profit is shown in figure 2.26.

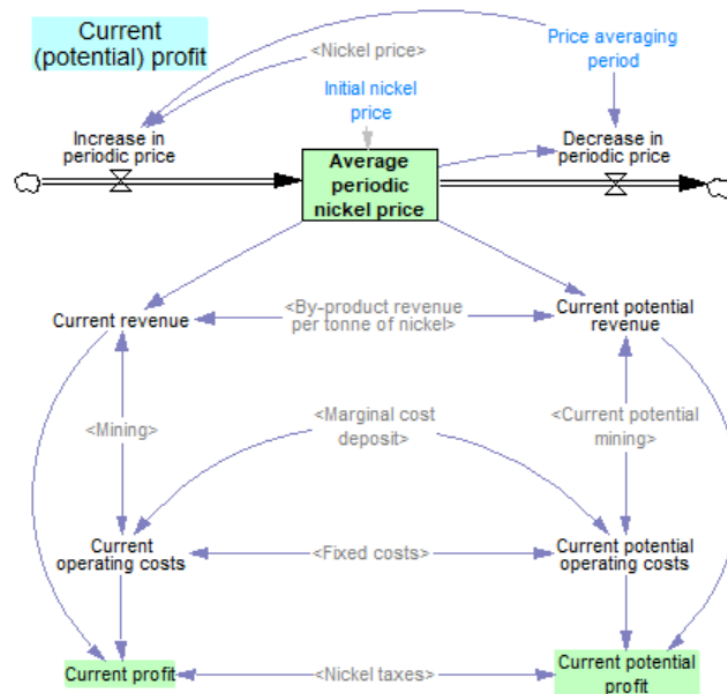


Figure 2.26: structure for calculating current and current potential profit. Blue = constant, green = output.

Future potential profit is based on future potential new capacity, which is based on measured and indicated resources and the average mine operation plan (the time a mine wishes to operate at a certain capacity), the forecasted marginal cost of a certain deposit and an investment price premise. It is used to determine future potential profitability of different resource segments (see appendix G1.2), which will change into reserves if the profit is higher than the minimum profit over investment. It is also used to determine profit over investment ranking, which plays a role in determining which projects are invested in first to create new brownfield or greenfield capacity.

Finally, it is used to determine normalised future potential profit, which is used to increase exploration efforts in a certain area where money is expected to be made. The structure for future potential profit is shown in figure 2.27 and the structure for exploration increase, which also includes the impact of the expectations of the ET, is shown in figure 2.28. Further details on profit are described in appendix I3.3.

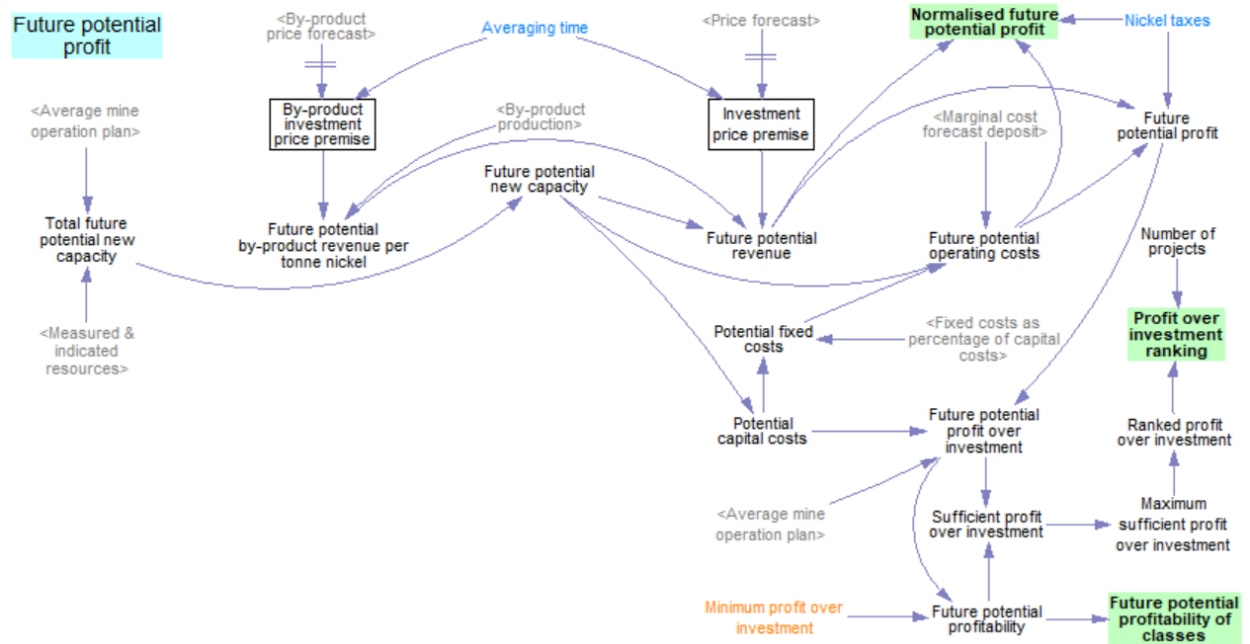


Figure 2.27: structure for calculating future potential profit. Blue = constant, green = output, orange = key uncertainty.

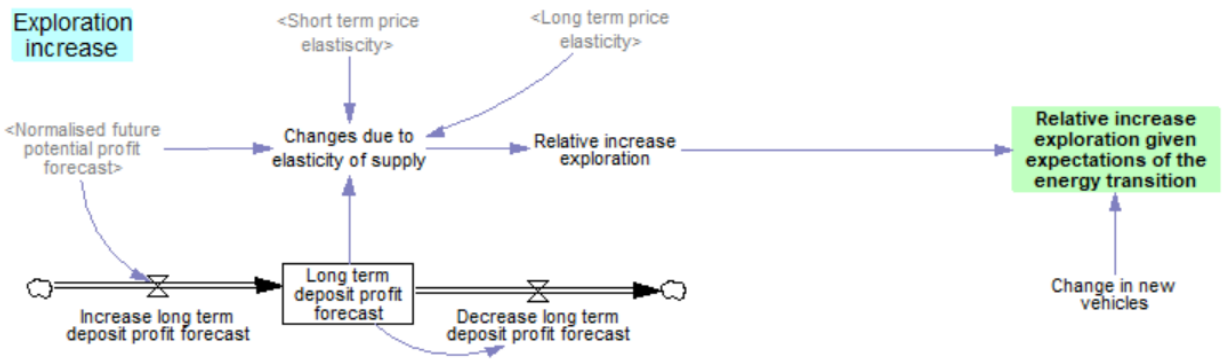


Figure 2.28: structure for exploration increase. Blue = constant, green = output.

Profit over investment ranking is not the only factor that plays a role in determining which projects are invested in first to create new brownfield or greenfield capacity. Investment attractiveness due to non-profit based factors is also important. Investment attractiveness is based on many different economic, social and environmental factors. An investment attractiveness index was published by the Fraser Institute (2020). However, many countries in the database by Mudd (2020) were not included in this publication.

Therefore, corruption index (Transparency International, 2020), which has a decent correlation with investment attractiveness (see appendix I4) was used as a proxy for investment attractiveness. This was combined with profit over investment to come to a final investment attractiveness ranking of projects. The structure for investment attractiveness is shown in figure 2.29.

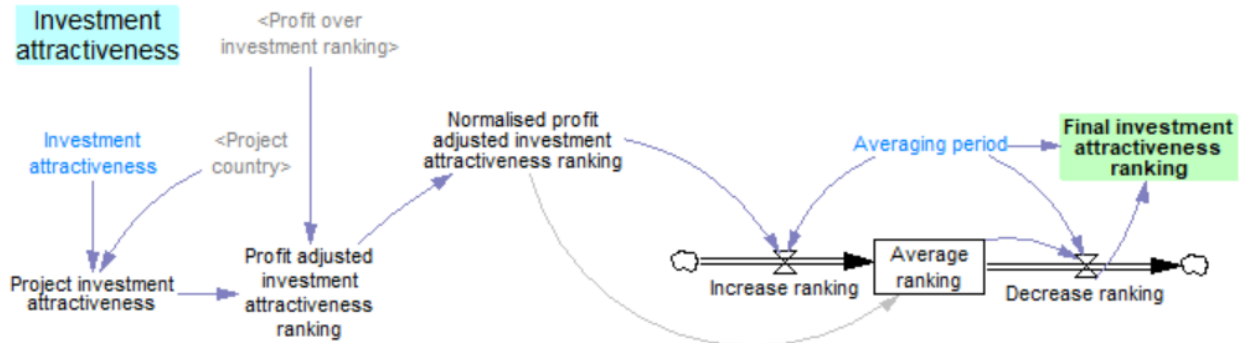


Figure 2.29: structure for investment attractiveness. Blue = constant, green = output.

2.3.4 Impacts sub-model

Mining has many sustainability impacts, including economic impacts, social impacts and different types of environmental impacts. However, due to time and data constraints, the only impact that was considered in this thesis was Global Warming Potential (GWP), which represents life cycle GHG emissions in tonne CO₂eq.

GWP was made dynamic by including an assumed constant component excluding electricity, based on various Life Cycle Assessments (LCAs) on nickel, and a component exclusively including electricity, which is based on the regional electricity mix as projected by the SSPs. More details on determining the dynamic GWP are described in appendix K. The structure for determining GWP is shown in figure 2.30.

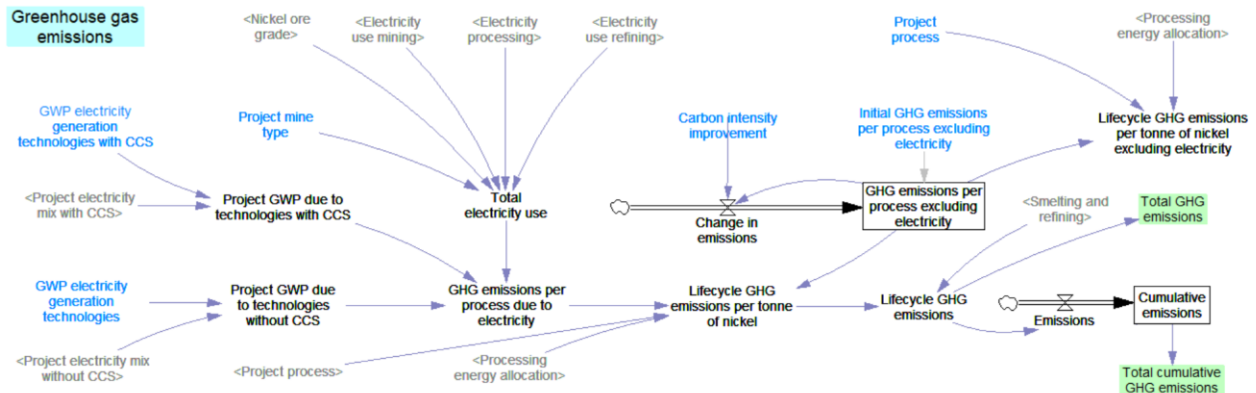


Figure 2.30: structure for determining GHG emissions. Blue = constant, green = output.

2.4 Model verification and validation

Model verification and validation are forms of model testing where errors are uncovered and models are improved to increase the confidence in their usefulness. Verification consists of testing whether the model is coded or simulated correctly. Validation consists of testing whether the model is fit for purpose. This is often done in collaboration with the model clients or audience (Pruyt, 2013). Various tests were done iteratively throughout the construction of the model. These tests are described below.

For verification, various forms of debugging were applied, both based on errors indicated by the modelling software and based on checking the model for additional errors. This includes changing the signs in certain equations when the model behaviour did not correspond with what logically should happen, adding stocks to prevent simultaneous equations in feedback loops, preventing floating point overflows by adding ZIDZ (zero if divided by zero), XIDZ (x if divided by zero), MAX (maximum) and MIN (minimum) structures, adjusting formulas in certain flows to prevent stocks from becoming negative, checking to see whether fractions add up to 1 and checking the unit consistency of the variables.

Some parts of the model include rather discrete implementations, which strictly speaking should be replaced by more continuous alternatives (Pruyt, 2013). However, when working at mine level, the implementation of certain discrete elements could not be avoided. Some discrete elements that could potentially have been avoided with extra effort, such as the calculation of new generation capacity, were also left unchanged because of the relatively minor impact they had on the overall results. However, in future adaptations of the model it is beneficial to take another look at all the discrete elements and see where these could be improved.

For validation, multiple tests are possible. One form of validation is structural validation, where tests are done to see if the model structure and boundaries are appropriate (Pruyt, 2013). The structure is mainly based on literature, but some discussion was also done with experts in the mining field, which led i.a. to the inclusion of the mothballing dynamics shown in appendix G2.1.

Most of the feedback loops in figure 2.3 were endogenously included in the model, with the exception of the impact of material scarcity, GHG emissions and a carbon tax on the ET. The impact nickel scarcity may have on the ET is an outcome of the model and GHG emissions, a carbon tax and the ET are major global developments that exceed the boundaries of the nickel system in reality too.

Sensitivity analysis and uncertainty analysis were included as part of the EMA methodology. First, parameters, functions, structures and boundaries with large impacts on the results were identified by changing certain variables and combinations of variables in initial runs of the model. The highly sensitive variables were then selected for further analysis and were included as switches and uncertainty ranges in the experimental set-up. Extreme conditions tests were also done on the model in the form of disruption scenarios. More information on the experimental set-up is given in section 2.5.

Another form of validation is replicative validation, where investigation is done to see if the results of the model correspond with historic data or the results of other models. One way of doing this is checking whether a certain model can reproduce past real data. However, for the purpose of EMA, models that produce a good fit with past data are not necessarily more useful (Pruyt, 2013).

In the case of the present model, the years between 2015 and 2020 could be compared with past developments. However, most of the initial values that were used in the model do not correspond exactly with the base year 2015 because such accurate past data was not available, especially not at the level of detail that was used in the model. Therefore, other forms of validation were deemed more useful here.

The behaviour produced by the model was compared with past behaviour to see if the overall dynamics were similar. However, it is important to keep in mind that past data does not guarantee a good fit with developments in the future (Pruyt, 2013), especially when transitions, such as the ET occur. The model outcomes were also compared with other models in literature. The results of the validation tests are discussed in sections 3.4 (structural validation) and 3.5 (replicative validation).

2.5 Experimental set-up

The software used to create the model is Vensim, specifically built for SD modelling (Ventana System, 2010). The temporal scope of the research is 2015 - 2060. 2015 is used as the base year because it is near the centre of the range of years used in the database by Mudd (2020) and most data was available for that year. 2060 was used as the final year because beyond that results were deemed too uncertain to lead to useful insights. The model is therefore simulated for 45 years. The selected numerical integration method is Euler, because of the discrete elements in the model (Pruyt, 2013) and a time step of 0.0625 was selected because it was the smallest time step that did not lead to computational difficulties. All economic data included in the model is in US\$2005 unless otherwise specified.

The software used to run the model is Python, using the EMA Workbench package (Kwakkel, 2017). This allowed multiple runs with different input values to be done and plotted. Based on the computational limitations, 1000 runs were deemed good enough to give a decent picture of the different behaviour that can be generated by the model. First 1000 runs were done using the OCP and the electrification transport scenario. Most of the results in this thesis are based on these runs. Then an additional 1000 runs were done to obtain data for the FSP and another 1000 runs to obtain data for the hydrogen transport scenario. Finally, another 1000 runs were done with lower values for global maximum capacity increase.

Different types of uncertainties were included in the model. These uncertainties can be categorized as either structural or parametric. Structural uncertainties apply to system boundaries, the conceptual model or the computer model structure (Van der Linden, 2020). This includes the underlying paradigm, methods for allocation, methods for calculating price, the choice to include by-products and the choice to mine resources for a certain period before potentially being mothballed. Parametric uncertainties apply to scenarios or parameters in the model. Figure 2.31 shows the different types of uncertainties and the methodological choices included in the simulations.

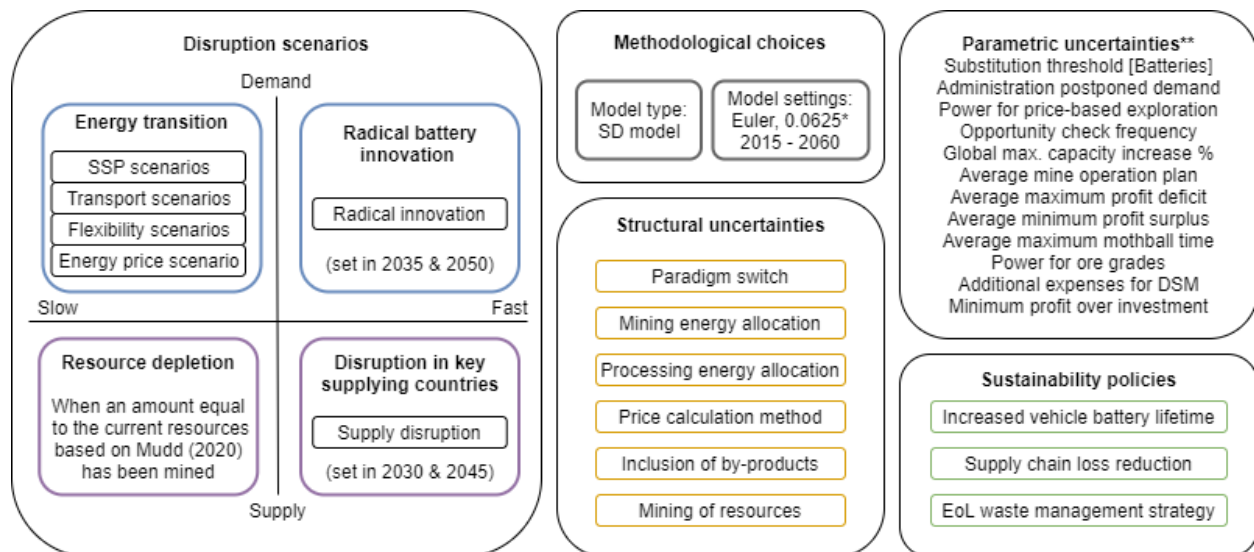


Figure 2.31: uncertainties included in the model. Switches are shown in boxes. *Euler is the numerical integration method. 0.0625 is the chosen time step. **These are the parametric uncertainties that are not included as switches in the model, but as an uncertainty range.

The scenarios in the model were designed to fit into the resilience framework by Sprecher et al. (2015). One type of disruption was selected for each of the four quadrants in figure 2.1. These disruptions are elaborated on in table 2.1. To be able to assess the impacts of certain disruptions, they were compared to a BAU situation which is considered to consist of the OCP, SSP2-baseline, a BAU electrification transport scenario and the supply disruption and radical innovation switches turned off.

Table 2.1: Disruption scenarios included in the model.

| Type | Disruption | Elaboration |
|---------------|---------------------------------------|---|
| <i>Demand</i> | | |
| Slow | Energy transition | The ET is a demand disruption that gradually takes place over time. To represent this transition, four different sets of scenarios were included: the SSP scenarios, transport scenarios, flexibility scenarios and energy price scenarios. |
| Fast | Radical battery innovation | A radical battery innovation is a demand disruption that can occur relatively quickly when a new battery is discovered. In this disruption, a new battery enters the market that doesn't require nickel. This disruption was set to occur twice, once in 2035 and once in 2050, both times halving the substitution threshold. |
| <i>Supply</i> | | |
| Slow | Resource depletion | Resource depletion is a gradual process where resources run out. This can be seen in physical terms or in terms of economic extractability. Resource depletion occurs in the FSP once current known resources according to Mudd (2020) run out. This is compared to what happens in the OCP once an amount equal to current known resources has been mined. |
| Fast | Disruption in key supplying countries | As fast disruption on the supply side, a disruption in key supplying countries was included. This disruption was set to occur in 2030 and 2045, impacting the country with the largest share of supply at those times, which would then be compromised and stop mining activities for a year. |

Structural uncertainties and scenarios were included in the model as switches. In the EMA workbench, these are referred to as categorical parameters because they consist of a limited number of options. A list of the switches included in the model is shown in table M1 in appendix M. Parameters included in the EMA workbench are referred to as real parameters as they consist of a range of possible real numbers between a minimum and a maximum value. Due to computational limitations, not all parameters in the model were given such uncertainty ranges. A selection was made based on the impact of changing a variable in initial test runs. This selection is shown in figure 2.30 and in table M2 in appendix M.

In addition to the disruption scenarios, three sustainability policies were included as switches. This includes an increase in vehicle battery lifetime, where the lifetime of batteries in EVs is doubled, a supply chain loss reduction, where losses along the forward supply chain are halved, and four EoL waste management strategies focusing on battery recycling.

In the first three strategies, EoL RR of nickel in batteries is either worse, equal to or better than the recycling of other class I products. In the fourth strategy, EoL RR is further improved by annual improvements in the EoL CR of batteries. The runs were evaluated based on various performance metrics. These are described in table M3 in appendix M.

3 Results

In this chapter, the results are described by assessing the effects of different model runs on performance metrics. This is done in the order of the research sub questions. First, demand projections are described. Second, the impacts of demand and supply disruption scenarios are covered, starting with the ET and followed by radical battery innovation, resource depletion and disruption in key supplying countries. Third, the impacts of sustainability policies are described.

The fourth and fifth sub questions are covered in sections on structural validation and on replicative validation respectively. In the structural validation, key structural and parametric uncertainties were assessed. In the replicative validation, the results were compared to historic developments and other model results in literature. New insights are also highlighted in this section. A final section is included at the end of this chapter, where the overall impacts on resilience are discussed.

All figures in this chapter only include runs for the electrification transport scenario because of the highly uncertain data for the nickel intensity of hydrogen tanks. Figure N1 in appendix N shows some results for the hydrogen transport scenario. All figures also only include OCP runs, unless indicated otherwise.

3.1 Demand projections

The demand projections for all model runs are shown in figure 3.1, divided over the different SSPs assessed in this thesis. This figure shows that an ET to limit global temperature increase to 1.5 °C generally leads to much higher nickel requirements than a BAU situation (SSP2-baseline). The density plot (right side of the figure) shows the density and range of the runs per scenario in 2060.

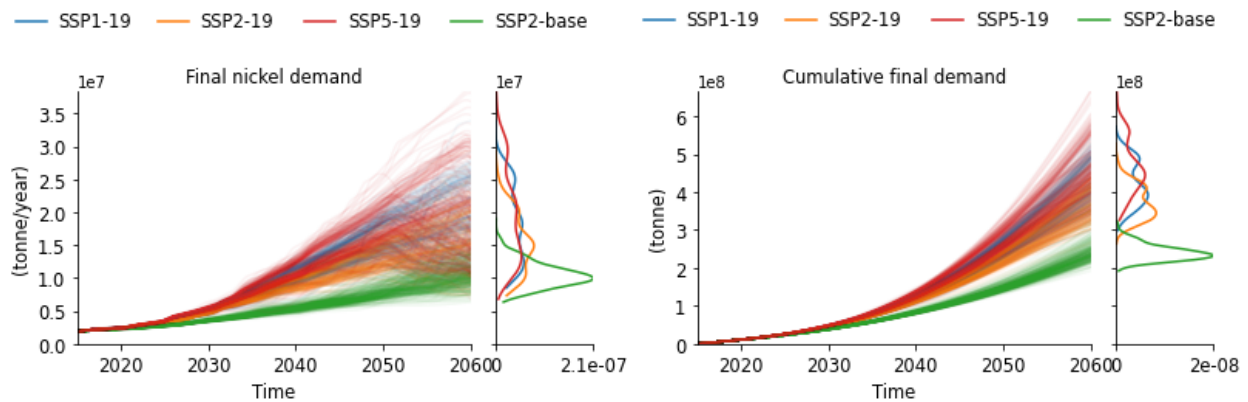


Figure 3.1: final nickel demand and cumulative final demand per assessed SSP. SSP2-baseline = BAU, the others are ET scenarios.

The final demand shown in figure 3.1 includes price effects and excludes postponed demand. Figure 3.2 shows total functional nickel demand and total substitution, which mostly consists of battery substitution. Battery substitution is shown together with demand change due to price elasticity in figure N2 in appendix N. The impacts of substitution and price elasticity on demand can be seen by comparing final demand with total functional demand, which excludes these price effects. The effect of postponed demand is shown in figure N3 in appendix N.

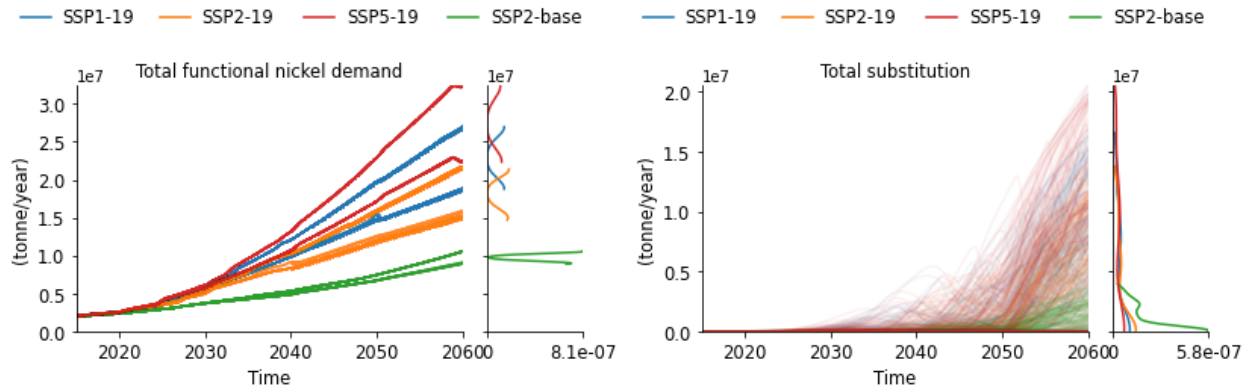


Figure 3.2: total functional nickel demand and total substitution per assessed SSP.

Figure 3.2 shows that substitution increases the higher the total functional demand becomes. The same goes for changes due to price elasticity. Substitution starts occurring around 2030 for the ET scenarios and around 2040 for the BAU scenario, which also has less substitution. Most substitution is due to the substitution of batteries because it was assumed that batteries have the lowest substitution threshold compared to other uses of nickel and in some runs radical battery innovation occurs. The forks in the total functional nickel demand are caused by battery lifetime assumptions (see section 3.3.3).

There are multiple reasons for the higher nickel demand in the ET scenarios. First, on average renewable energy generation technologies and power plants using CCS have a higher nickel intensity than fossil fuel-based power plants without CCS (see appendix C1.1). In addition, more installed capacity is required for the same electricity output because of the on average lower capacity factors (CF) of renewable energy technologies (EIA, 2019a, b). Second, SSP1 and SSP5 both project a higher GDP and a higher GDP per capita than SSP2. This means more nickel is projected for the RoE and a larger number of vehicles is projected. Finally, the EV share is lower in the BAU scenario.

Figure 3.3 shows the relative impact of the two most important contributors to nickel demand, EV battery storage and the RoE. Batteries take over as the largest demand category around 2035 - 2040 for the ET scenarios. Nickel demand for electricity generation reaches about 1 million tonnes/year by 2060 for the ET scenarios and about 200 thousand tonnes/year for BAU. Nickel demand for SBS is minimal for most combinations of SSP, flexibility scenario and EV battery lifetime, and the choice of flexibility scenario has a negligible impact on final nickel demand (see figures N4 and N5 in appendix N).

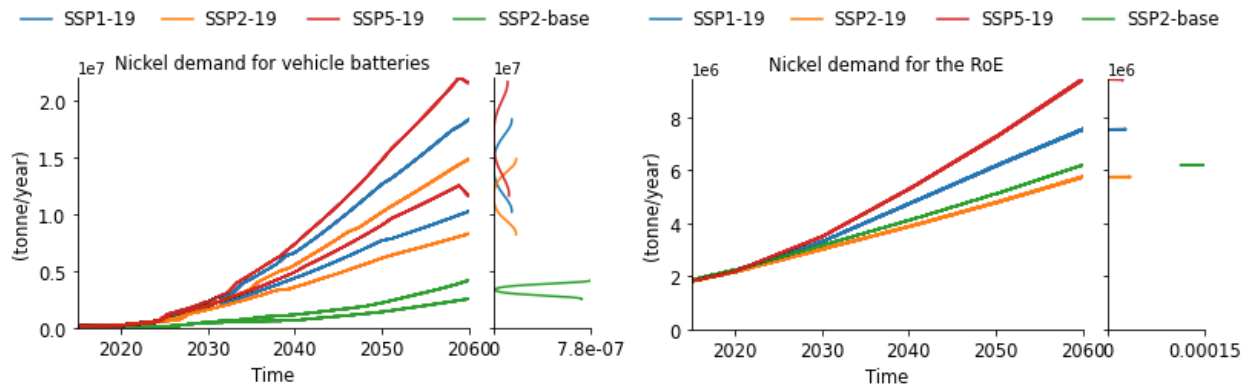


Figure 3.3: Nickel demand for vehicle batteries and the RoE.

3.2 Disruption scenarios

In this section, the impacts of the different disruption scenarios on the nickel dynamics are described. However, before doing so, the BAU situation without disruptions is covered. This is followed by disruptions due to the ET, radical battery innovation, resource depletion and supply disruptions in dominant supplying countries.

3.2.1 Business as usual

The BAU situation consists of the OCP, SSP2-baseline, an EV share based on the IEA RTS and the supply disruption and radical innovation switches turned off. The demand in the BAU situation has already been shown in section 3.1 and other performance metrics for BAU are shown in the following sections when it is compared with the disruption scenarios. In this section, single run results are shown to give a clearer picture of certain dynamics occurring without disruption.

Figure 3.4 shows the results of a single BAU run for price change vs production change. The dynamics represent hog cycles. These are cycles where supply surplus and deficit follow each other, leading to periods with higher prices and periods with lower prices (Futrell et al., 2019). Such periods can also be observed in the historic nickel price (see appendix I3.1).

Figure 3.4 shows a single run and the pattern is different for every run, so no conclusions regarding the timing or the severity of high and low prices can be made from this figure, it simply represents the behaviour. This shows there already is a certain degree of variability in prices without any disruptions.

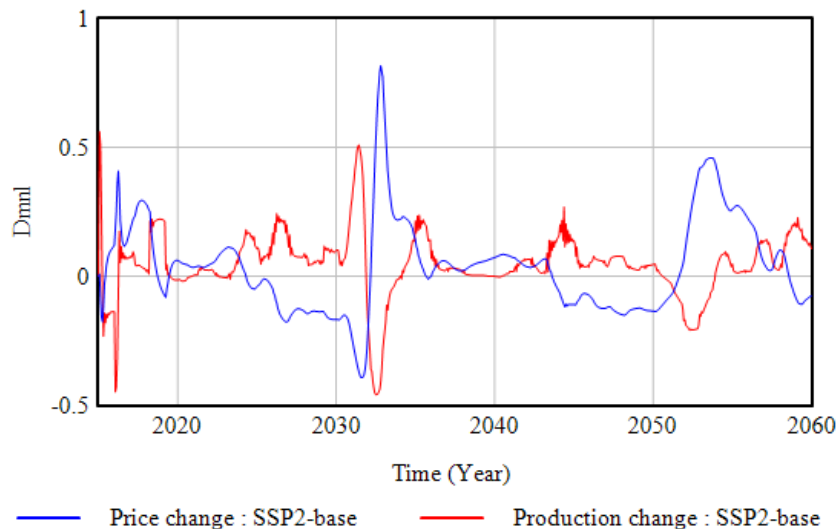


Figure 3.4: price change vs production change for a single BAU run with base settings.

Other single run results, for the share of processing per technology, the share of operating capacity per country, the number of mines producing a certain by-product, and the average periodic nickel price as an indicator for resilience for all four assessed SSPs, are shown in appendix N2. These figures are just for illustrative purposes to show the type of behaviour the model can produce.

3.2.2 Energy transition

The results in section 3.1 showed that nickel demand increases significantly due to the ET. In this section, the impact of the ET on some other key performance metrics is assessed. As the ET is the main disruption scenario of interest in this thesis, more performance metrics are assessed here than for the other disruption scenarios. This includes the analysis of supply, price, the constituents of price (average marginal costs and scarcity), the constituents of marginal costs, and sustainability indicators and externalities, such as average ore grade, average final energy use, cumulative GHG emissions and cobalt and palladium production.

Higher demand due to the ET also means higher supply is required and this can be seen in figure 3.5, which shows nickel mining and cumulative mined nickel. For nickel mining, the hog cycles are visible, although it is more difficult to see than in a single run. In some runs, it is rather extreme due to the discrete implementation of the model, but when looking at the cumulative mined nickel, it smoothes out.

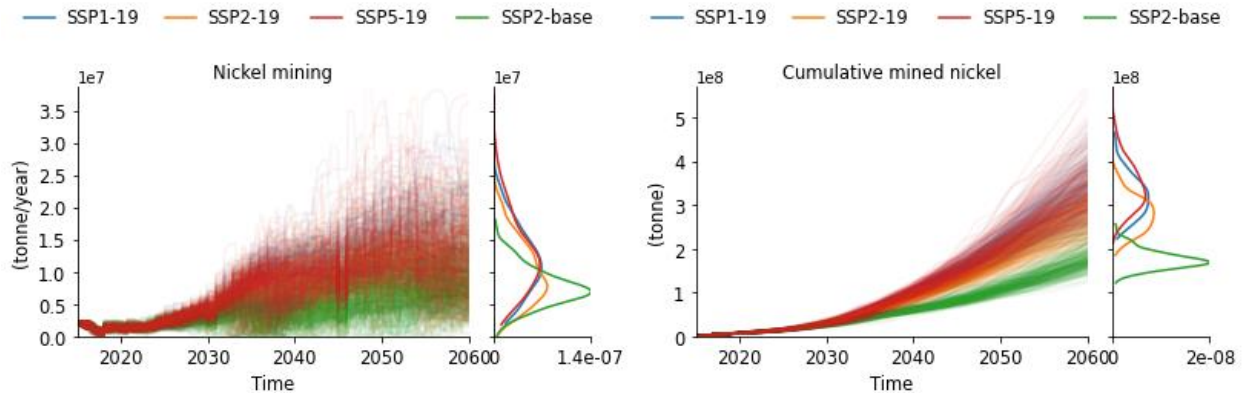


Figure 3.5: nickel mining and cumulative mined nickel per SSP.

Figure 3.6 shows the cumulative mined cobalt and palladium. Overall, the by-products were modelled in a highly uncertain way because no supply (other than from nickel deposits) and demand dynamics were included to determine their scarcity. Therefore, not much can be said about specific by-products. Possible exceptions are cobalt and palladium because 50% of these metals currently depend on nickel mining (Nassar et al., 2015), so these metals are more connected to nickel scarcity.

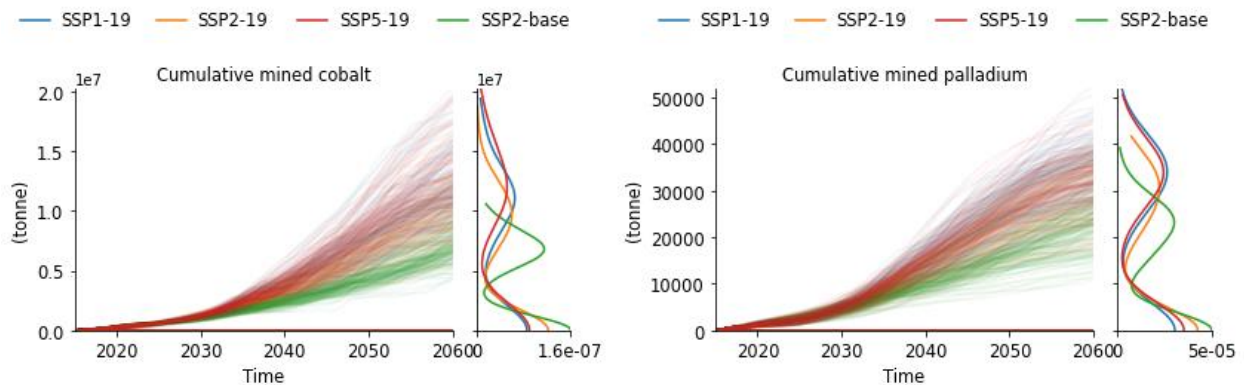


Figure 3.6: cumulative cobalt and palladium production from nickel mines per SSP.

Primary nickel processing, which shows similar behaviour to nickel mining, with slightly lower values due to losses, determines final nickel availability, together with recycling and nickel in stock. Consumption forecast, the forecasted (delayed) demand request (final nickel demand + postponed demand), over final nickel availability, determines nickel scarcity in the model. Together with average marginal costs, this determines nickel price when using the price method based on availability and consumption (see appendix I3.2). Nickel price and its two constituents are shown in figure 3.7.

The average price is higher in the ET scenarios and is initially highest for SSP1-19 and eventually for SSP5-19. Over the years, and for the different runs, the price ranges between 500 - 90000, 1500 - 175000, 500 - 140000 and 1500 - 300000 2005\$/tonne for SSP2-baseline, SSP1-19, SSP2-19 and SSP5-19 respectively. For most runs, the prices cycle around 30000 2005\$/tonne for the ET scenarios and around 15000 2005\$/tonne for the BAU scenario.

Figure 3.7 shows that not only the average scarcity is higher in the ET scenarios, which is an indication that supply cannot always keep up with demand, but the average marginal costs are also higher. The reason for this becomes more apparent by looking at important constituents of marginal cost: energy costs (figure 3.8) and carbon costs (figure 3.11). Royalties, reagents and others and by-product credits are shown in appendix N3 in figures N10 and N11.

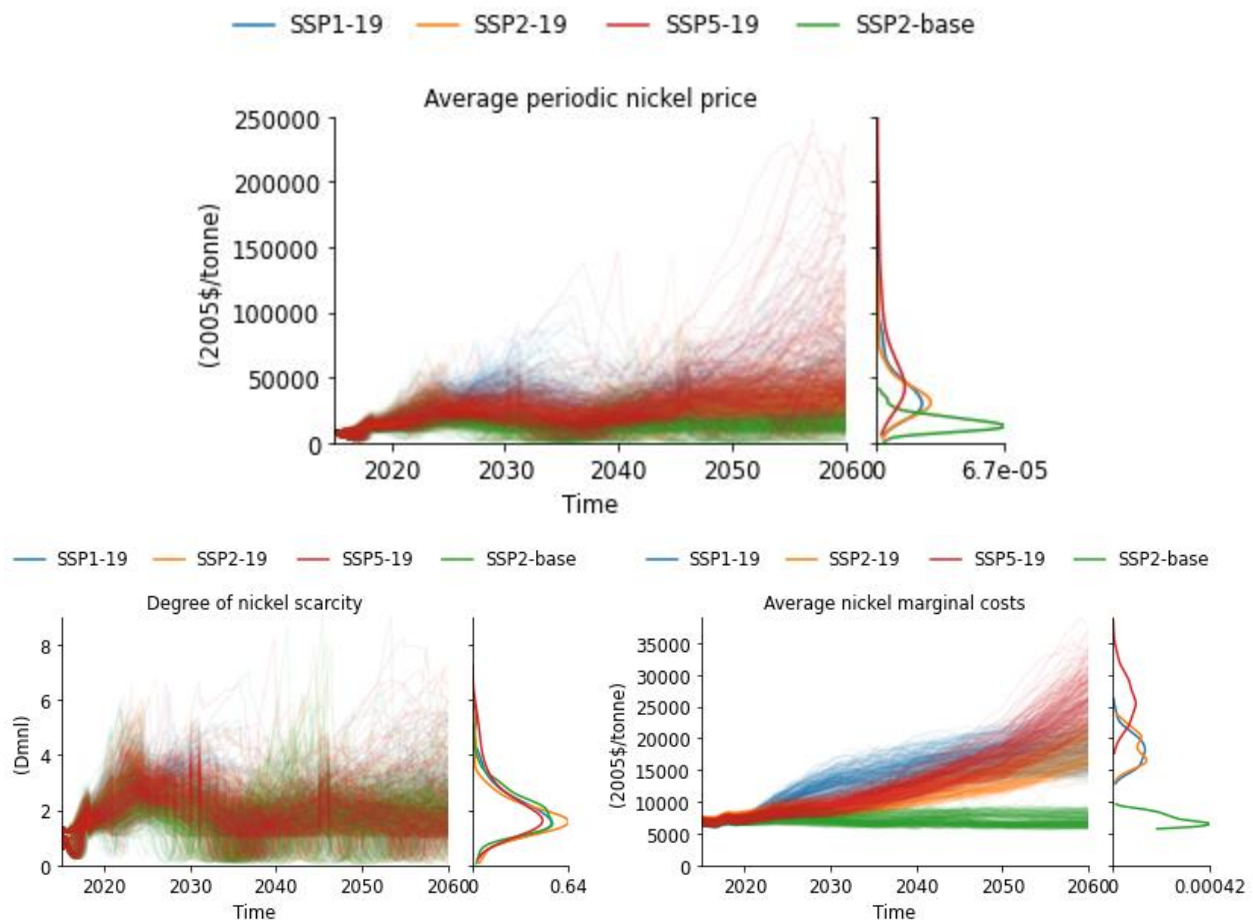


Figure 3.7: average periodic nickel price, degree of nickel scarcity and average marginal costs. Price goes up to 300000 2005\$/tonne for one run, but the graph is cut off at 250000 2005\$/tonne for better clarity.

Figure 3.8 shows the average final energy use and the average energy costs for mining, processing and refining combined. For separate depictions of mining and processing, see figures N12 and N13 in appendix N3. Energy costs increase first in the ET scenarios, after which they gradually decrease in most runs, but increase rapidly in some runs. In the BAU scenario, final energy use and thereby energy costs are mostly decreasing. There are multiple distinct pathways depending on the fuel price scenario (see appendix I1.4) and the processing energy allocation method (see section 3.4.1).

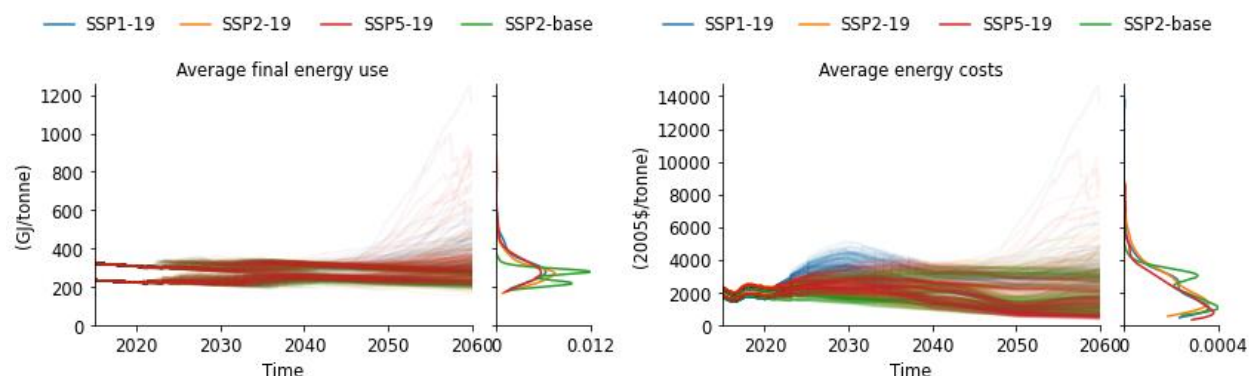


Figure 3.8: average final energy use and average energy costs.

As can be seen in figure 3.8, the average final energy use for mining and processing ranges between about 200 and 350 GJ/tonne for most runs, with a minimum of 180 GJ/tonne and a maximum of 1200 GJ/tonne by 2060. Annual total final energy use of all mines combined is shown in figure N14 in appendix N3. Most values for total final energy use in 2060 range between 0.5 and 5 EJ/year. To put this into perspective, global Total Primary Energy Supply (TPES) in 2018 was 598 EJ, Total Final Consumption (TFC) was 416 EJ and TFC for industry was 119 EJ (IEA, 2020a). Table 3.1 shows the energy-nickel nexus in numbers.

Table 3.1: The energy-nickel nexus in numbers. Ranges are shown, with an estimated average in brackets. ET includes all SSPs with a Representative Concentration Pathway (RCP) of 1.9. BAU includes SSP2-baseline.

| Scenario | Energy for nickel in 2060 (EJ/year)* | Percentage of total final consumption in 2018 (%) | Nickel for energy in 2060 (tonne/year)** | Percentage of total nickel demand in 2060 (%) |
|----------|--------------------------------------|---|--|---|
| BAU | 0.5 - 3.5 (1.6) | 0.1 - 0.8 (0.4) | 0 - 1.2E7 (4E6) | 0 - 67 (40) |
| ET | 1 - 5 (2.5) | 0.2 - 1.2 (0.6) | 0 - 3.1E7 (1E7) | 0 - 82 (59) |

*Energy refers to final energy use. Data on energy products for non-energy use is not included. Due to the large annual variability, the range with the highest density is shown. For the full range, see figure N14 (appendix N3)

**This is the total final nickel demand minus the demand for the RoE. The ranges start at 0, because in some runs, substitution has replaced the need for primary nickel demand. This is likely because nickel prices became too high in these runs.

The average energy costs are the product of the average final energy use and the energy price. Important factors that influence energy use are mine type, ore type, ore grade and energy efficiency improvements. Efficiency improvements gradually decrease energy requirements. For most runs, the laterite share increases over time. Because most laterite mines are OC, this leads to lower energy requirements for mining. However, because laterites are more energy intensive to process, this leads to higher energy requirements for processing. The fraction of OC mines and the fraction of laterite mines over time are shown in figure N15 in appendix N3.

Figure 3.9 shows that average ore grade decreases over time and this occurs faster in the ET scenarios because more is mined. One aspect is that the average ore grade for specific mines decreases faster. Another aspect is that, with a higher price, more mines with a lower initial ore grade become profitable, thereby decreasing average ore grade. The opposite is true for a lower price. Existing mines with an ore grade that has become sufficiently low become unprofitable and may even be decommissioned, thereby leading to a higher overall average ore grade that may even exceed the initial average ore grade. A lower ore grade leads to increased energy demand for mining, which can be seen in some runs in figure 3.8.

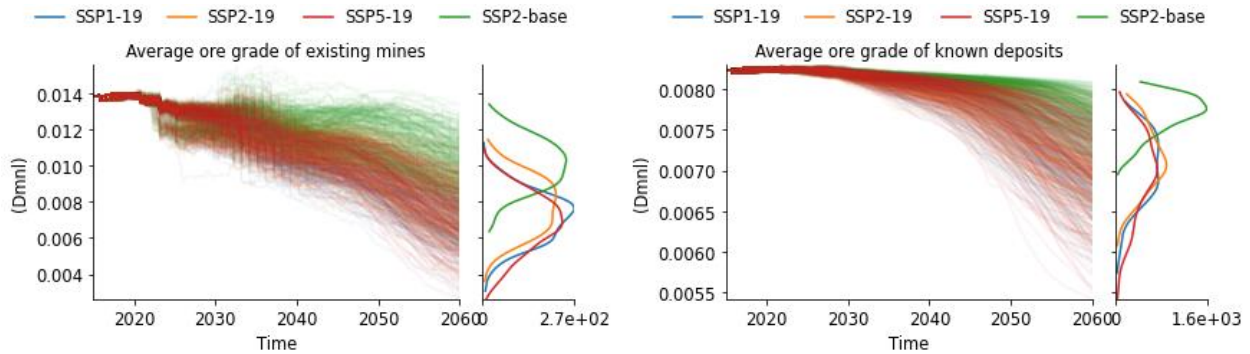


Figure 3.9: overall average nickel ore grade of existing mines and of all deposits in the database by Mudd (2020).

As stated in section 2.3.3, energy price was split into electricity price and fuel price and three scenarios were created for fuel price (see appendix I1.3). Electricity price depends on fuel price, regional renewable energy share and the carbon costs for electricity generation if a carbon price is included, which is the case in the ET scenarios.

Figure 3.10 shows electricity price for the three fuel price scenarios and per SSP. As a carbon price is introduced in the three ET scenarios, with the highest carbon price in 2030 for SSP1-19, the electricity price increases. Then, as the percentage of renewable energy in electricity generation increases, it decreases again, partially because emissions are reduced and partially because, for the same fuel price, the electricity price is assumed to be lower when there is a higher share of renewables, because more fuels are starting to be made with electricity instead of the other way around. For an increasing fuel price, electricity price ends up close to its initial price in 2060 and for a decreasing and fluctuating fuel price, electricity price ends up lower than its initial price.

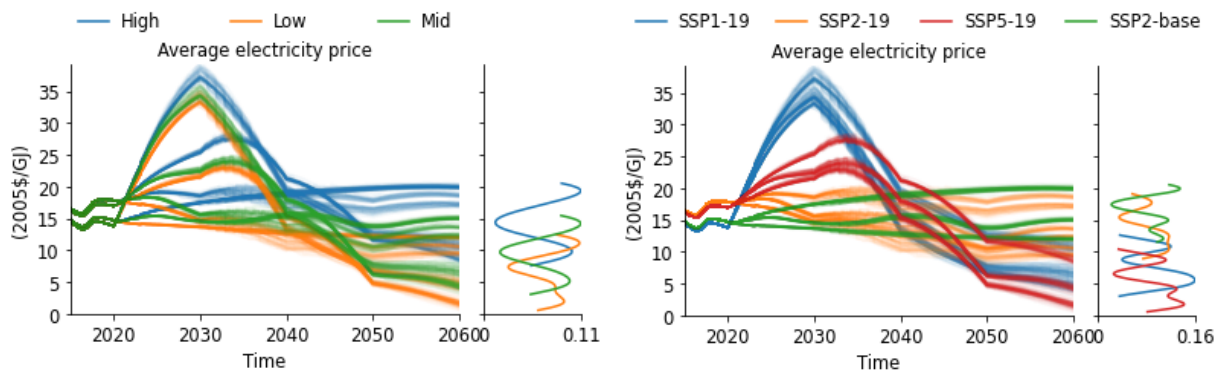


Figure 3.10: average electricity price per fuel price scenario and per SSP.

Figure 3.11 shows the cumulative GHG emissions from nickel mining and the average carbon costs due to the implementation of a carbon price. A carbon price is included for all of the ET scenarios, but excluded for the BAU scenario. It can be seen that the inclusion of a carbon price has a large impact on the marginal costs of a project. It influences marginal costs for nickel directly by taxing on-site GHG emissions, and as shown in figure 3.10, it also influences marginal costs indirectly by increasing the electricity price in the model.

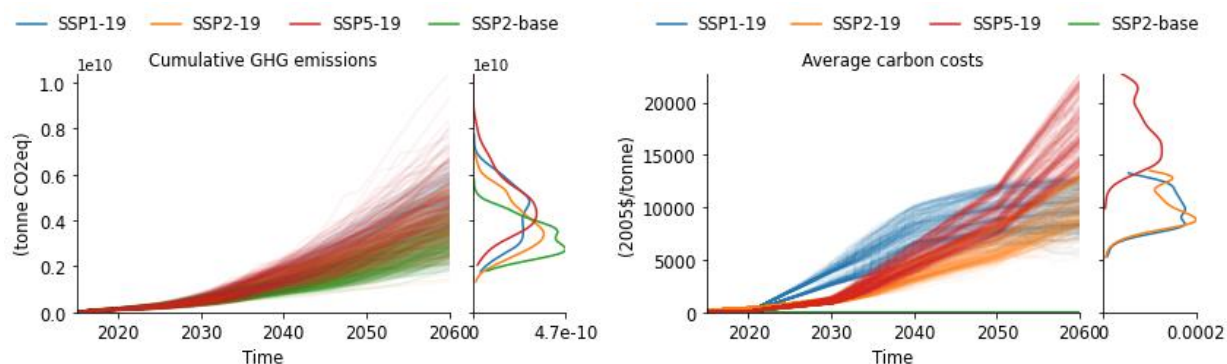


Figure 3.11: cumulative GHG emissions over time and average carbon costs per tonne of nickel.

Cumulative GHG emissions from nickel mining may be higher due to the ET, but they also may be lower in some cases for SSP1-19 and SSP2-19. The reason for this is that more nickel is required and ore grade decreases faster leading to higher energy requirements. However, at the same time, the electricity mix, which is also used for mining, is becoming increasingly less GHG intensive due to increasing shares of renewable energy. This effect may be even more pronounced if fuel use for mining also becomes more renewable, something that was not considered in the current analysis.

As can be seen in figure 3.11, cumulative GHG emissions due to nickel production range between about 1.3E9 and 1E10 tonne CO₂eq. Annual total GHG emissions due to nickel production are shown in figure N14 in appendix N3. In 2060, most values range between 2E7 and 3E8 tonne CO₂eq/year. To put this into perspective, the global total GHG emissions in 2015 were about 50E9 tonne CO₂eq/year (Ritchie & Roser, 2016). Table 3.2 shows the GHG emissions due to nickel production for BAU and the ET. Where the emissions in the ET initially start larger than those in BAU, average emissions are slightly lower in the ET by 2060 due to the increased share of renewable energy.

Table 3.2: GHG emissions due to nickel production. Ranges are shown, with an estimated average in brackets. ET includes all SSPs with an RCP of 1.9. BAU includes SSP2-baseline.

| Scenario | Nickel GHG emissions in 2060 (tonne CO ₂ eq/year) | Percentage of total GHG emissions in 2015 (%) |
|----------|--|---|
| BAU | 2E7 - 3E8 (1.3E8) | 0.04 - 0.6 (0.3) |
| ET | 2E7 - 3E8 (1.2E8) | 0.04 - 0.6 (0.2) |

The figures above show that there are many factors that influence marginal nickel costs and thereby price. Some factors, including energy efficiency improvements, more OC mining and an increasing share of renewables in the electricity mix, reduce costs, whereas other factors, such as a decreasing ore grade and more energy intensive processing methods due to the increased share of laterites, increase costs.

3.2.3 Radical innovation

The effects of the radical innovation of battery technology are shown in figure 3.12, where the results for some key performance metrics are categorized based on whether this disruption occurred or not. This figure shows that more substitution of batteries occurs in scenarios with the disruption (the lines for the years where the disruption started, 2035 and 2050 are also slightly thicker), and that final nickel demand is on average lower than the final demand in scenarios without the disruption. This also leads to lower supply, lower average prices, a higher average ore grade and lower cumulative GHG emissions.

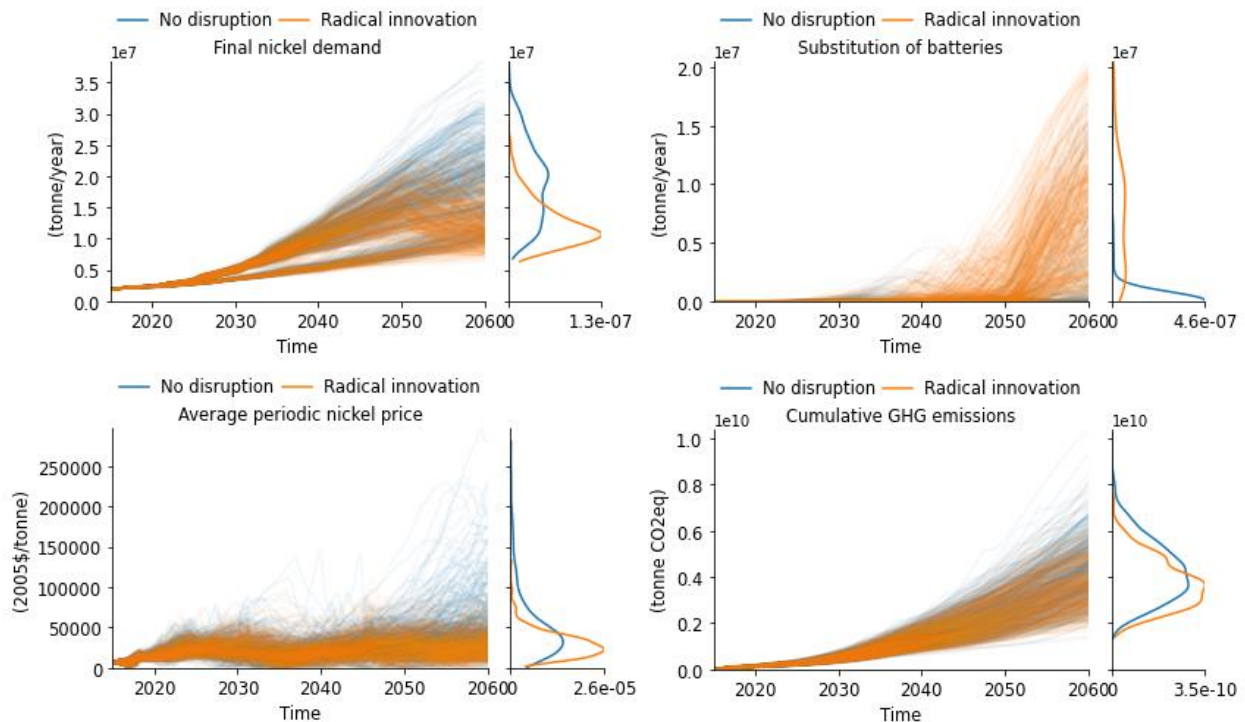


Figure 3.12: results for the impact of radical innovation that halves battery substitution threshold in 2035 and in 2050. See figure N16 in appendix N4 for more results.

It is important to keep in mind that although the GHG emissions due to nickel are less, these will occur due to the substitute material instead and without further details about the characteristics of the substitute material, it is unknown whether that will lead to more or less GHG emissions compared to nickel mining.

3.2.4 Resource depletion

For this disruption scenario, resource depletion was assumed when all the initial resources in the database by Mudd (2020) ran out. Essentially, this is what is assumed in the FSP. Therefore, first, some FSP results are shown in figure 3.13 (additional FSP results are shown in figure N17 in appendix N4). Then, resource depletion is shown for both the OCP and the FSP in figure 3.14.

In the FSP, the degree of nickel scarcity (demand/supply) and thereby nickel price become very high as of about 2045 for the ET scenarios. The reason for this sharp increase is because supply is not able to meet demand due to resource depletion from this point onward. This is further exacerbated by a positive feedback loop between price and royalties, where a higher price leads to higher royalties and vice versa. For BAU, the average periodic nickel price also becomes higher than in the OCP. The FSP runs seem like unrealistic futures, but they do illustrate what can happen when a resource becomes scarcer.

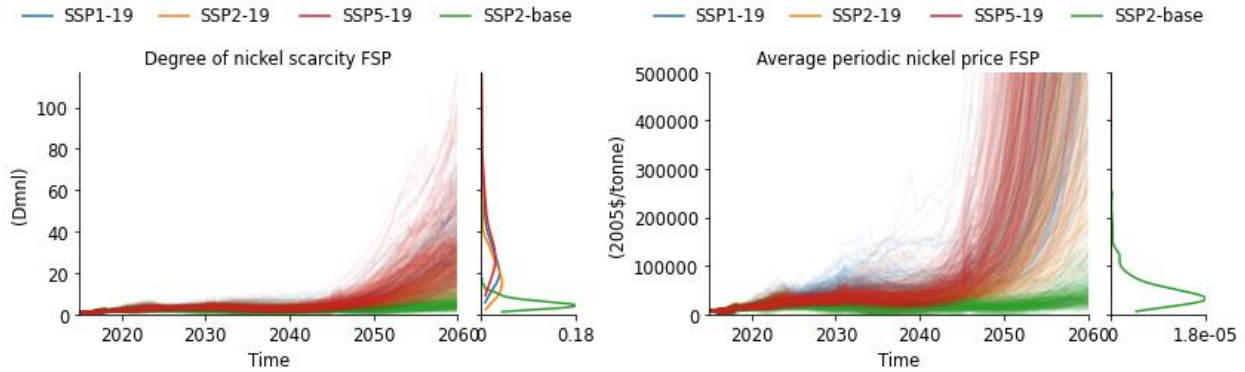


Figure 3.13: scarcity and nickel price in the FSP. Values for price go up to unrealistically high levels but they were cut off at 500000 2005\$/tonne for clarity.

Figure 3.14 shows the depletion of original resources based on Mudd (2020) in both paradigms. In the OCP, an amount of resources, equal to the original resources, are depleted between 2050 and 2060 for most ET runs. No depletion occurs for BAU. In the FSP, original resources are not depleted completely, because some deposits in the database have resources lower than the minimum capacity times the mining operation plan, so they are never activated in the model. This is discussed further in section 4.4.2.

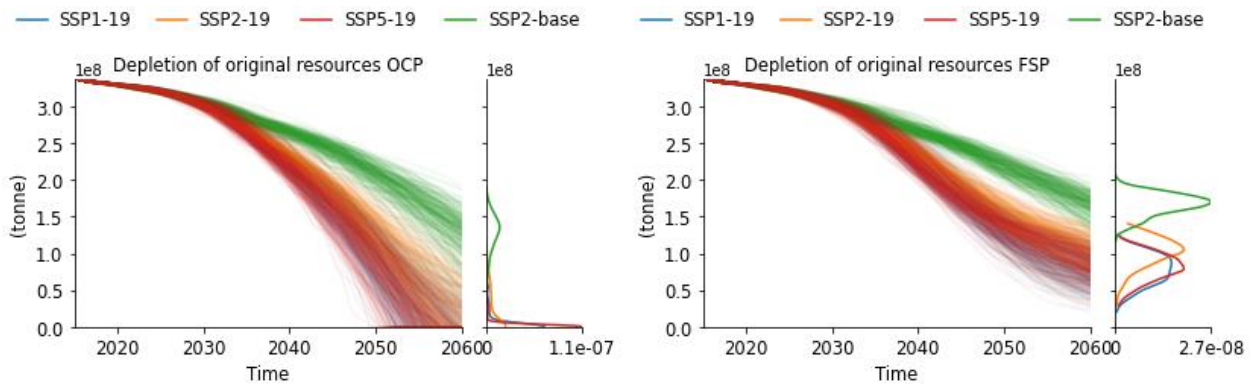


Figure 3.14: depletion of original resources for the FSP and the OCP. Note: the depletion of original resources includes losses, whereas cumulative mined nickel does not. The curve in the FSP becomes an asymptote and, based on the way it was modelled, it will never reach 0.

3.2.5 Supply disruption

Figure 3.15 shows the impact of a 1-year supply disruption in 2030 and 2045, where mining stopped in the country with the largest share of supply at those times, on some key performance metrics. A dip can be spotted in nickel processing in 2030 and in 2045, where on average the runs including the supply disruption produce less nickel. These dips are also visible in the degree of nickel scarcity in figure 3.7 and in the average periodic nickel price, but then as peaks.

This disruption can also be seen as an extreme conditions test. The behaviour that can be seen is expected. Supply disruption should lead to an increased price as scarcity increases, but the price should stabilize again once new production capacity has been added or once the disruption is over (Van der Linden, 2020). Additional results for the supply disruption are shown in figure N18 in appendix N4.

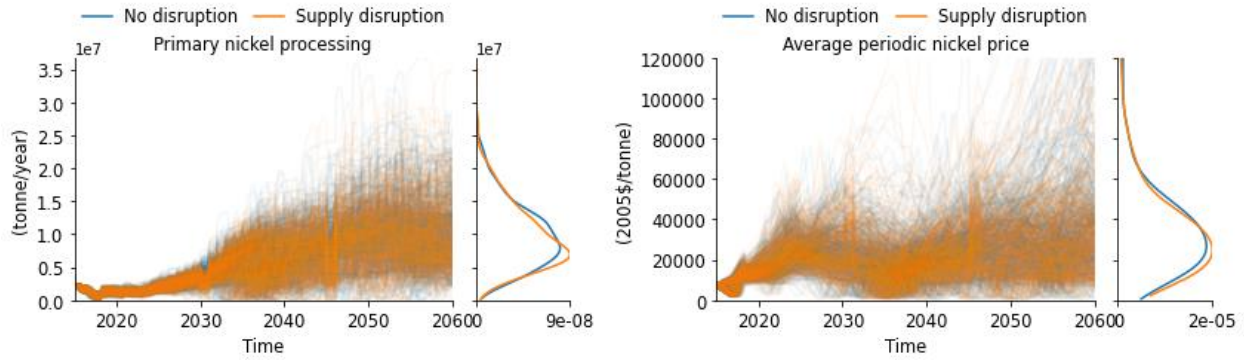


Figure 3.15: results for the influence of a 1-year supply disruption in 2030 and 2045, where mining stopped in the country with the largest share of supply at those times.

3.3 Sustainability policies

In this section, the effects of increased sustainability are assessed. First, the effects of EoL waste management of batteries are covered, followed by the effects of supply chain loss reduction and the effects of increased battery lifetime. These are all quite broad sustainability categories that are not the responsibility of a single actor but can come about through the efforts of multiple actors in different fields.

A policy that is included in the model, but is not covered in this section in much detail, is the carbon price. A carbon price was included in all ET scenarios as part of the SSPs. The carbon price is required to achieve the target of 1.5 °C temperature increase in these SSPs. Figures 3.10 and 3.11 show that the carbon price has quite a large impact on average marginal costs and thereby on average periodic nickel price. This is discussed further in section 4.4.4.

3.3.2 EoL waste management

Figure 3.16 shows the EoL RR for battery waste management for the four waste management strategies described in section 2.5, and EoL RR per SSP. In all scenarios, EoL RR first decreases due to the higher share of batteries in final demand and the lower share of stainless steel. EoL RR is impacted by the EoL waste management strategy and by the overall average nickel ore grade. As ore grade decreases, the attractiveness of recycling increases.

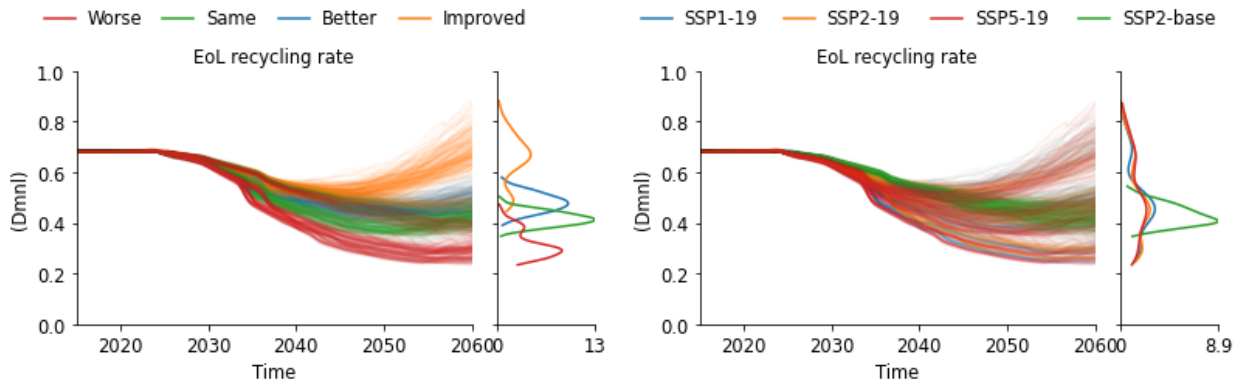


Figure 3.16: EoL RR for the four waste management strategies and per SSP. Note: no changes to stainless steel recycling were included. The main focus is on batteries, because this is projected to be the largest demand category.

This effect is especially visible when looking at the different SSPs. The BAU scenario ends up with lower EoL RRs than the ET scenarios when the waste management strategy for batteries is the same or better than for other class I applications and when waste management is improved even further, because it has higher overall average ore grades. When the waste management strategy for batteries is worse than for other class I applications, the ET scenarios lead to a lower EoL RR, because of the higher share of batteries. Only for the strategy where waste management is improved even further by improving the EoL CR, does the final EoL RR in 2060 eventually end up being higher than the initial EoL RR.

Figure 3.17 shows the impact of waste management strategy choice on cumulative mined nickel and average periodic nickel price. This shows that in the runs with improved waste management, cumulative mined nickel is lower, because more demand is covered by recycling. The average periodic nickel price is also slightly lower. However, it is important to note here that energy use and GHG emissions were not taken into account for recycling, thereby leading to a larger difference in costs compared to primary nickel processing than would occur in reality. This is discussed further in section 4.4.4. Additional results for EoL waste management are shown in figures N19 and N20 in appendix N5.

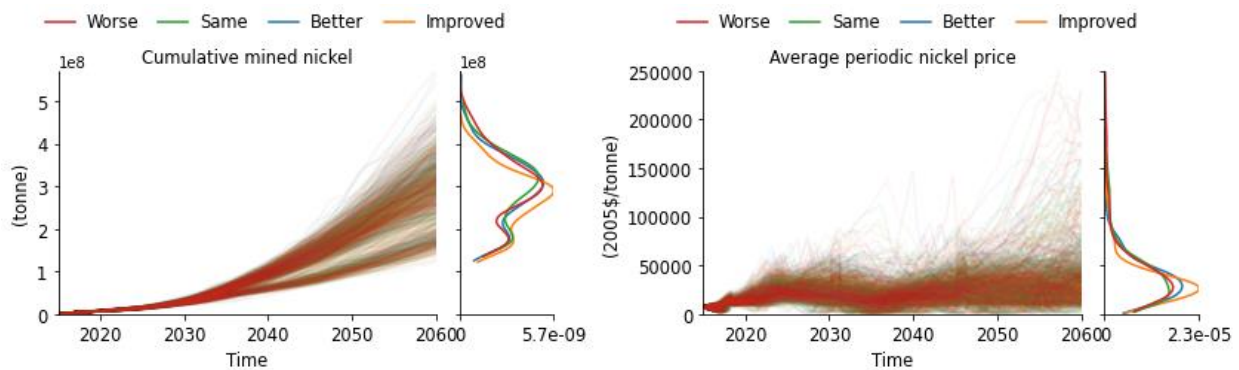


Figure 3.17: cumulative mined nickel and average periodic nickel price based on EoL waste management strategy.

3.3.2 Supply chain loss reduction

The impacts of halving forward supply chain losses are shown in figure 3.18. When the loss reduction policy is included, slightly less nickel is mined and there are less GHG emissions. It is important to note here that a lower percentage of mining losses leads to more mined nickel, while at the same time a lower percentage of processing losses means less mined nickel is required. This is probably why the values in figure 3.18 do not differ much. There is also no large impact on price or other performance metrics.

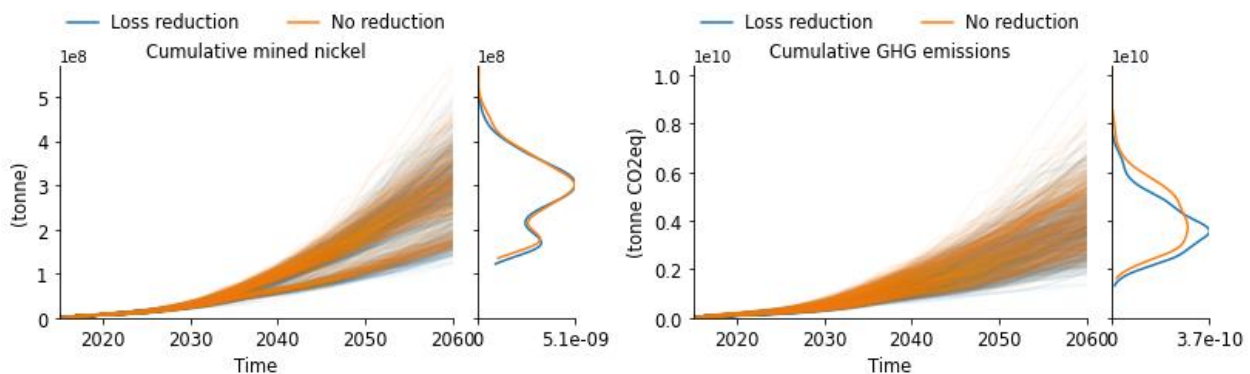


Figure 3.18: cumulative mined nickel and cumulative GHG emissions based on the inclusion of loss reduction.

3.3.3 EV battery lifetime increase

The impacts of doubling the EV battery lifetime from 8 years to 16 years (the assumed lifetime of the vehicles) on some key performance metrics are shown in figure 3.19. This measure significantly reduces nickel demand and thereby cumulative mined nickel and GHG emissions.

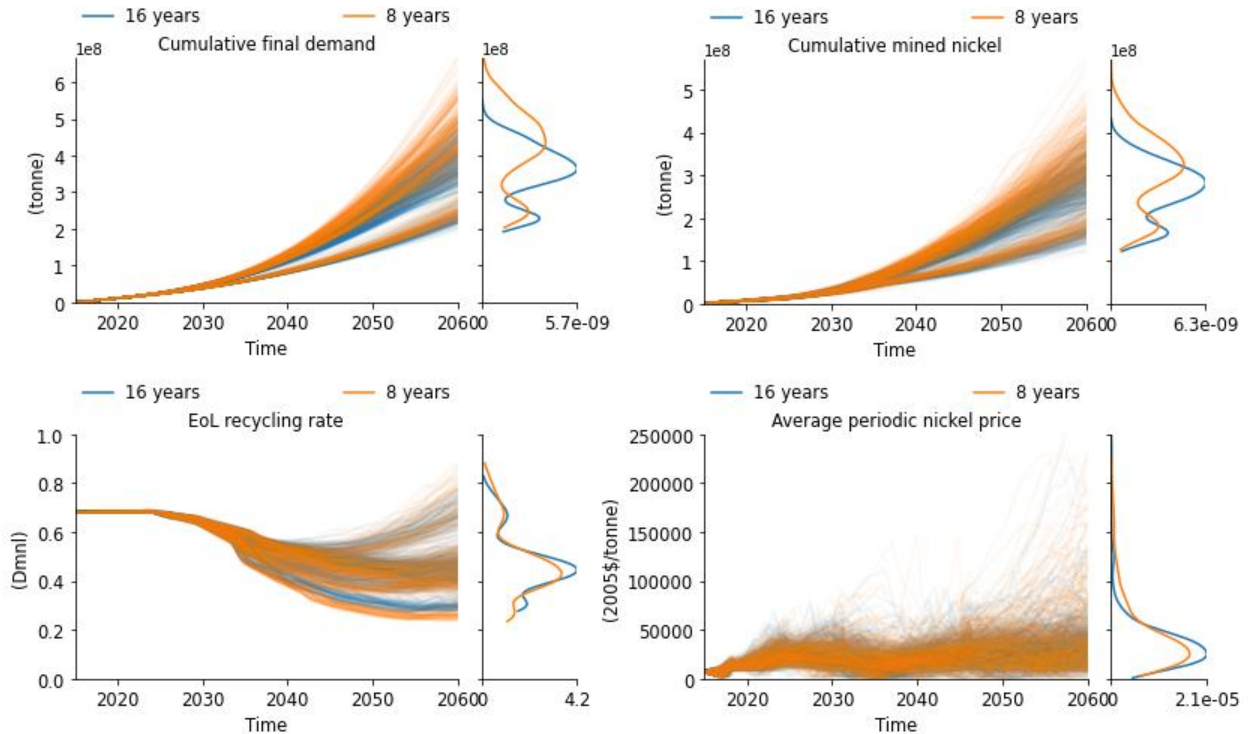


Figure 3.19: the impact of EV battery lifetime increase on various key performance metrics.

Less cumulative mined nickel also leads to a higher average ore grade, and because the percentage of batteries in scrap is highest for a lower EV battery lifetime, some runs for these scenarios also have the lowest EoL RR. The average price is slightly lower for the EV battery lifetime of 16 years. Additional results for EV battery lifetime increase are shown in figure N21 in appendix N.

3.4 Structural validation

As explained in section 2.4, the results of the uncertainty analysis are described in this section as part of the structural validation. First, structural uncertainties are explored and then parametric uncertainties. Only the most relevant results are included in the section. Others can be found in appendices N6 - N8.

3.4.1 Structural uncertainties

As shown in figure 2.31, six switches were included in the experimental set-up to explore structural uncertainties. Only the uncertainties with a large impact on the results are shown here. These are the processing energy allocation method and the inclusion of by-products. Switches with an intermediate impact (the option to mine resources) and switches with a minor impact (the mining energy allocation method and the price calculation method) on the results are shown in appendix N6. The impact of the paradigm switch was already shown in section 3.2.4.

Processing energy allocation method

Figure 3.20 shows the impact of the choice of processing energy allocation to different nickel product inputs, based on either mass or full allocation to nickel, on some of the performance metrics. This shows that if more processing energy costs and GHG emissions are allocated to nickel, average marginal costs and nickel price are higher. This allocation has a much larger impact than the mining energy allocation.

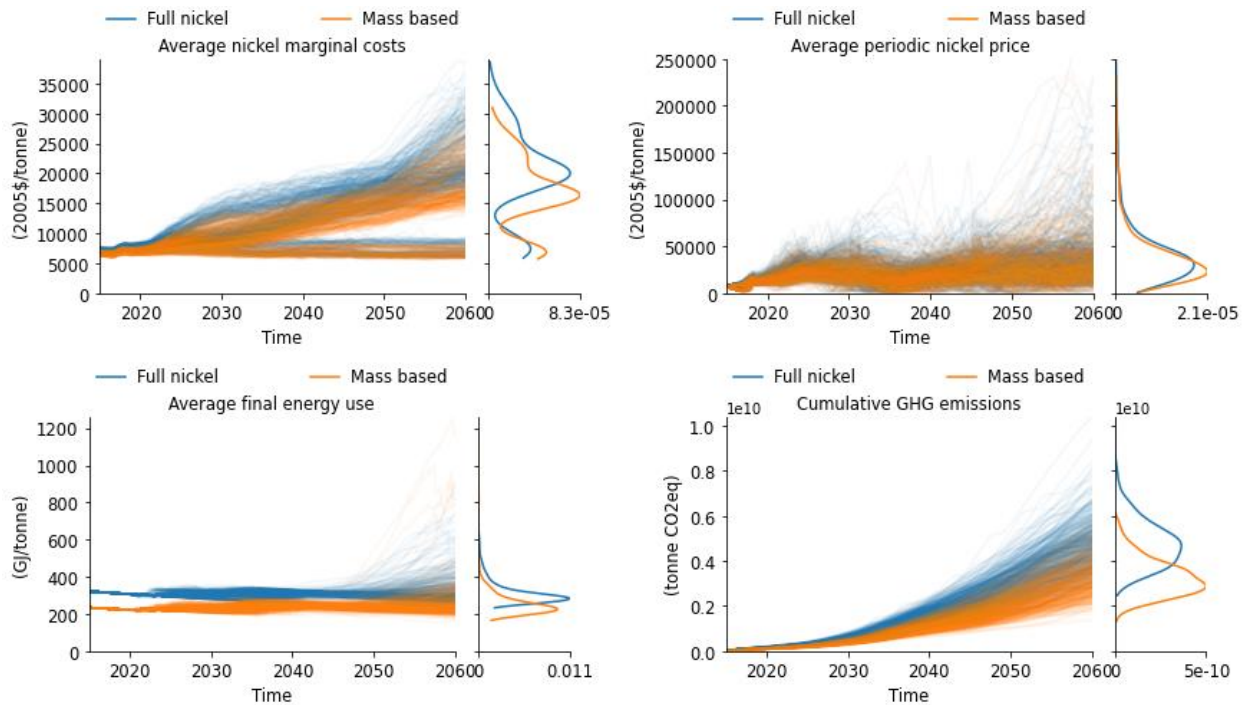


Figure 3.20: some key performance metrics categorized based on processing energy allocation method. Additional results are shown in figure N22 in appendix N6.

Inclusion or exclusion of by-products

Figure 3.21 shows the impact on some performance metrics of including or excluding by-products. In the model, by-products are only recovered if this leads to additional profit. Recovery then leads to lower costs attributed to nickel because some of the mining costs are allocated to the by-products. Therefore, it makes sense that the costs, and thereby the price, can become higher by excluding by-products.

Inclusion of by-products also makes a difference for which specific deposits become most profitable first. By including by-products, deposits with many recoverable by-products are favoured over deposits with less recoverable by-products that may be more profitable if by-products are not considered.

Figure 3.21 shows that a larger fraction of laterite mines exists when by-products are excluded. This also means the fraction of OC mines is higher and therefore average mining energy costs are lower. However, average processing energy costs and cumulative GHG emissions attributed to nickel are higher due to the more energy and carbon intensive laterite processing methods. This also means carbon costs are higher when a carbon price is included, further increasing average marginal costs and price.

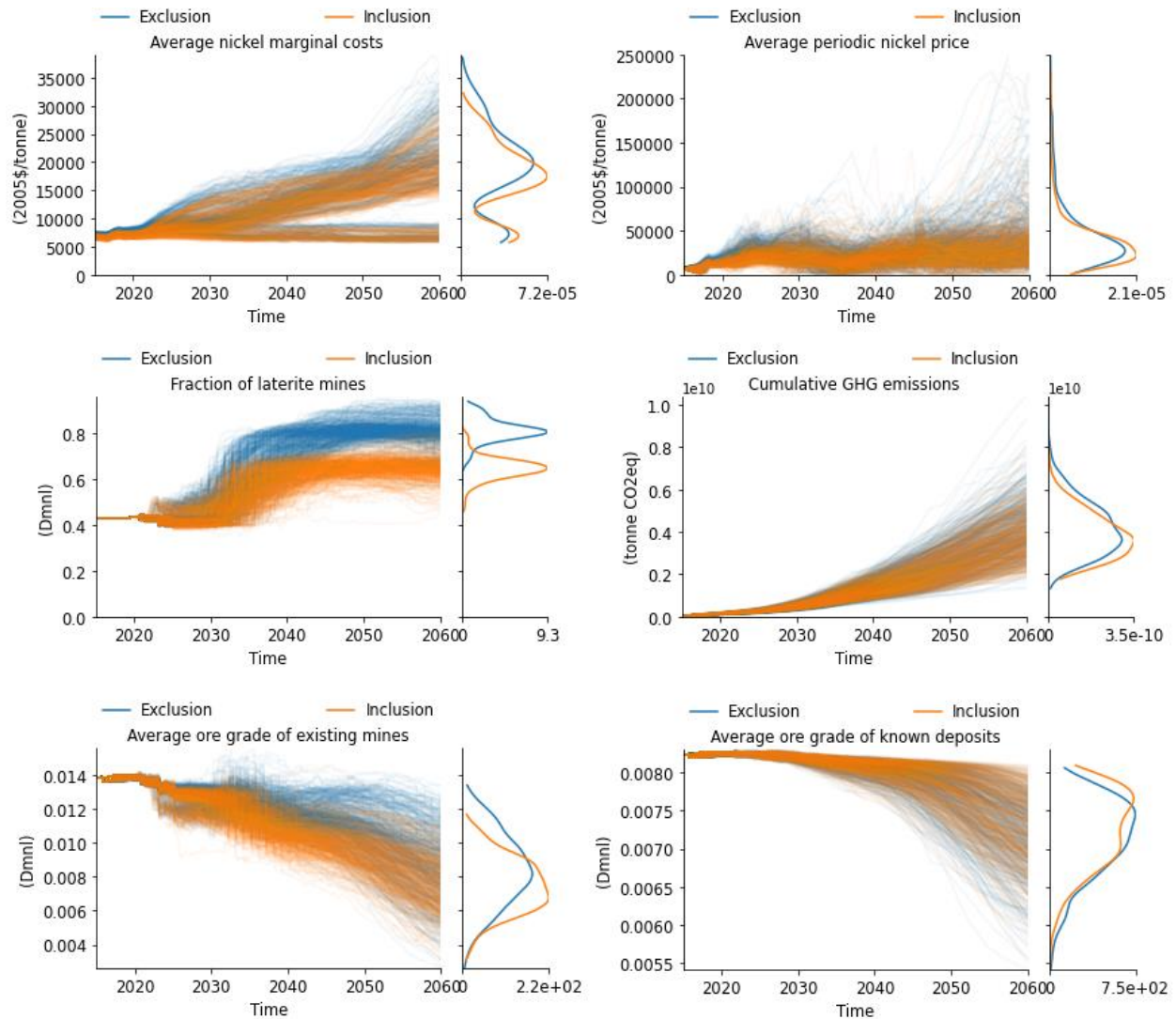


Figure 3.21: some performance metrics categorized based on the inclusion of by-products. Additional results are shown in figure N23 in appendix N6.

Average ore grade of existing mines is higher when by-products are excluded, yet average ore grade of known deposits ends up being lower. This is probably because nickel ore grade is more important for the relative profitability of mines when by-products are not considered and mines with higher ore grades are favoured over those with lower ore grades. Then as the ore grade in existing mines decreases, new deposits with higher initial ore grades become more profitable and the existing mines with the lower ore grades are decommissioned in favour of these new deposits.

3.4.2 Parametric uncertainties

Parametric uncertainties were explored by including uncertainty ranges for certain sensitive parameters. First, the parameters and switches with the largest impact on certain performance metrics at different points in time were identified (this is visualised in appendix N7). Then, influential parameters were assessed in further detail. Many results could be obtained from this. However, in this section, only the results that were deemed most relevant are included. This includes the parameters with a large impact on average final energy use and the parameters with a large impact on average periodic nickel price.

Average final energy use

Regarding average final energy use, the parameter with the largest impact is the power for ore grades (see figure N28 in appendix N7). Results for this parameter are shown in figure 3.22. Other parameters with a large impact are average maximum mothball time, power for price-based exploration and average mine operation plan. Results for these parameters are shown in figure N35 in appendix N8.

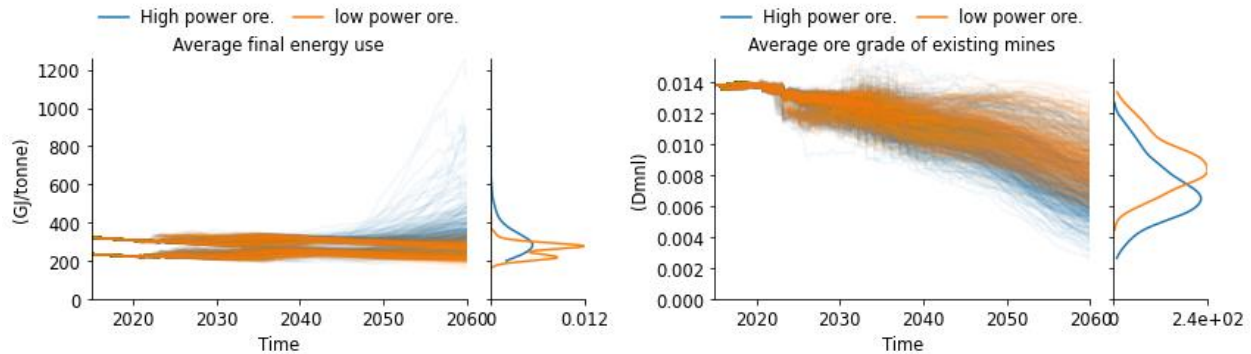


Figure 3.22: average final energy use and average ore grade of existing mines for lower values for power for ore grade (≤ 0.3) and higher values (> 0.3).

A higher power for ore grade leads to a faster decline in ore grade once the original resources in the database by Mudd (2020) are depleted, thereby leading to higher average final energy use. As is shown in figure N35 in appendix N8, the runs where final energy use shoots up in later years also have some other things in common. Most of these runs include by-products, a short average mine operation plan and a low power for price-based exploration.

Inclusion of by-products can lead to larger profitability of a deposit even if the nickel ore grade is lower than the ore grade of other deposits, which is why mines can continue to be profitable even if their energy use goes up. A shorter average mine operation plan means a larger capacity and faster depletion of the resources in a certain deposit, thereby reducing ore grade at a faster rate. A lower power for price-based exploration means more exploration and therefore more reserves for profitable mines, for which the ore grade continues to decrease, even to a point where energy use and the associated costs become much higher. If there is less exploration, these mines don't have enough resources left at a certain point and other mines that have higher ore grades, but may be less profitable in other areas, take over.

Average periodic nickel price

Regarding average periodic nickel price, parameters with a large impact include administration of postponed demand and power for price-based exploration (see figure N27 in appendix N7). Results for these parameters are shown below. Other parameters with a large impact are average maximum profit deficit as percentage of investment, average maximum mothball time, average mine operation time and minimum profit over investment. Results for these parameters are shown in figure N36 in appendix N8.

Figure 3.23 shows the impact of the administration of postponed demand. Higher values mean it takes longer for postponed demand to be registered. This leads to less variability in postponed demand and thereby also less variability in the demand request, final nickel availability and nickel price. However, it also means perceived scarcity is lower than actual scarcity. This means less nickel is mined and the difference between cumulative demand and consumption becomes larger, indicating lower resilience (see figure N37 in appendix N8). In this case, price may not be the best indicator for resilience, as price is based on perceived scarcity (which doesn't consider all postponed demand) and not on actual scarcity.

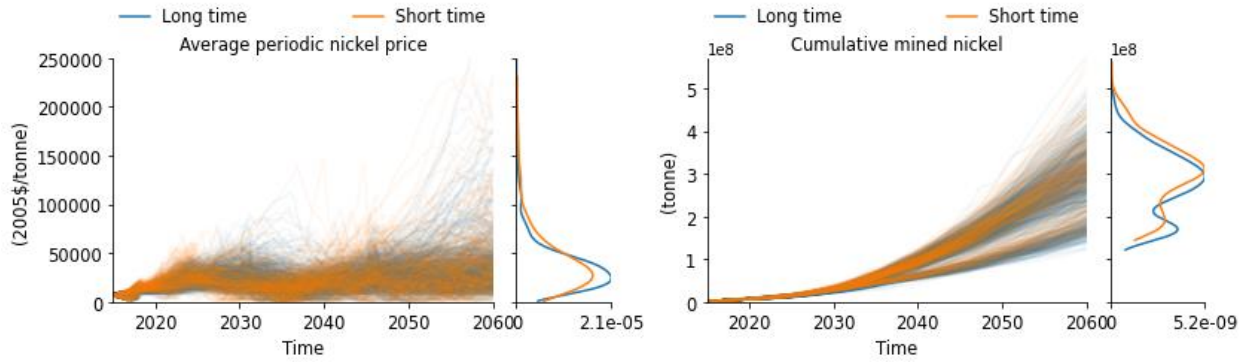


Figure 3.23: average periodic nickel price and cumulative mined nickel for lower values for administration of postponed demand (≤ 1 year) and higher values (> 1 year).

In single runs, increasing the administration of postponed demand leads to less extreme hog cycles, but at a certain point it doesn't lead to any cycles as final nickel availability consistently stays below demand. However, values where this occurs are generally higher than those included in the uncertainty range.

Administration of postponed demand is not the only variable that influences the extremity of the hog cycles. This is also impacted by exploration. Figure 3.24 shows the impact of the power for price-based exploration. Because the power is a fraction, a higher power leads to less price-based exploration, which leads to less variability in final nickel availability, but also to less cumulative mined nickel, increased nickel scarcity, higher average periodic nickel prices and reduced resilience.

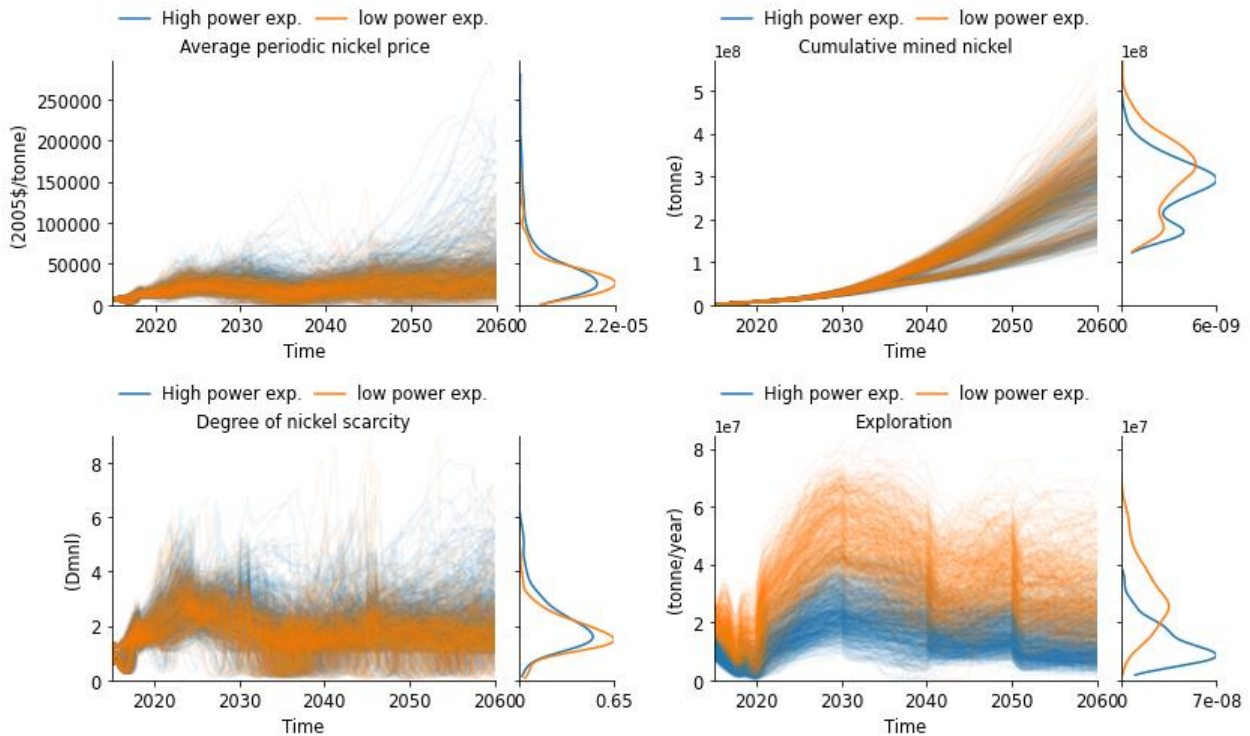


Figure 3.24: average periodic nickel price, cumulative mined nickel, degree of nickel scarcity and exploration for lower values for power for price-based exploration (≤ 0.7) and higher values (> 0.7). Additional results for exploration are shown in figure N38 in appendix N8.

Additional attention was also paid to the global maximum capacity increase percentage. In the experimental set-up, values between 10% and 50% annual increase were included. Varying between these values did not have a large impact on the overall results, indicating that a 10% global maximum annual capacity increase is generally high enough for sufficient nickel to be produced. However, an additional set of runs was done where the values were varied between 1% and 30% annual increase and, for these runs, a different global maximum capacity increase percentage did have a large impact (see figure N39 in appendix N9). The average periodic nickel price can become much higher much earlier for low global maximum capacity increase percentages, as can be seen in figure 3.25. Some other results for the additional runs are shown in figure N40 in appendix N9.

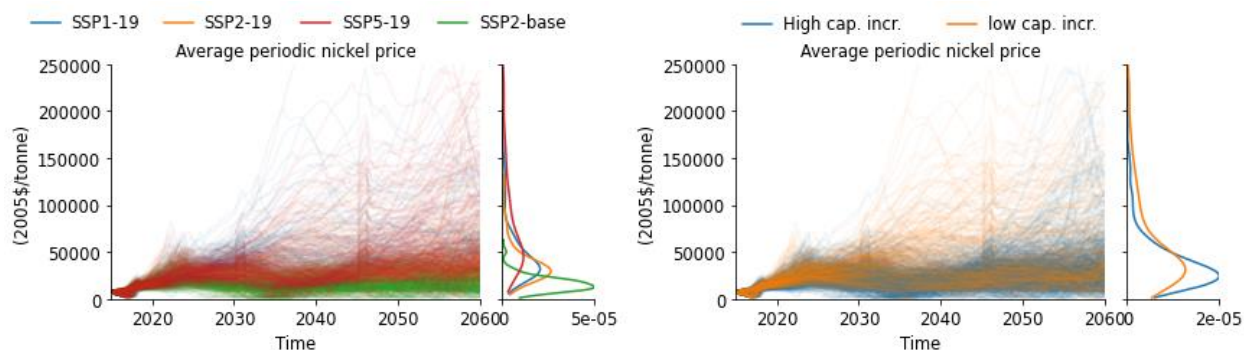


Figure 3.25: average periodic nickel price for a global maximum capacity increase percentage between 1% and 30% per SSP and for high (>0.10) and low (<= 0.10) values for global maximum capacity increase percentage. Price goes up to 350000 2005\$/tonne, but the graphs were cut off at 250000 2005\$/tonne for better clarity.

3.5 Replicative validation

In this section, the replicative validation is covered, starting with a comparison with historic developments and then a comparison with literature. A section on new insights is also included, where the results that differ from previous research due to the more detailed modelling are highlighted.

3.5.1 Comparison with historic developments

The results were compared with two historic developments: the historic annual nickel price and the historic annual change in production. The historic nickel price for the past 25 years is shown in appendix I3.1. When adjusted for inflation, the price ranges between about 5000 and 47000 2005\$/tonne. Figure 3.26 shows the inflation adjusted historic price combined with the model results for a single SSP2-baseline run and a single SSP5-19 run.

As stated in section 3.2.2, the model results show a price range between 500 and 300000 2005\$/tonne for the ET scenarios and between 500 and 90000 2005\$/tonne for the BAU scenario. For most runs, the prices cycle around 30000 2005\$/tonne for the ET scenarios and around 15000 2005\$/tonne for the BAU scenario.

These average prices are plausible considering historic developments and so is the cyclical behaviour. However, the extremes are much larger or smaller than what has historically occurred. The price goes down lower than in history, because there are more extreme heights in final nickel availability in the model. This then leads to the mothballing of many mines, after which the price shoots up again, leading to much higher variability.

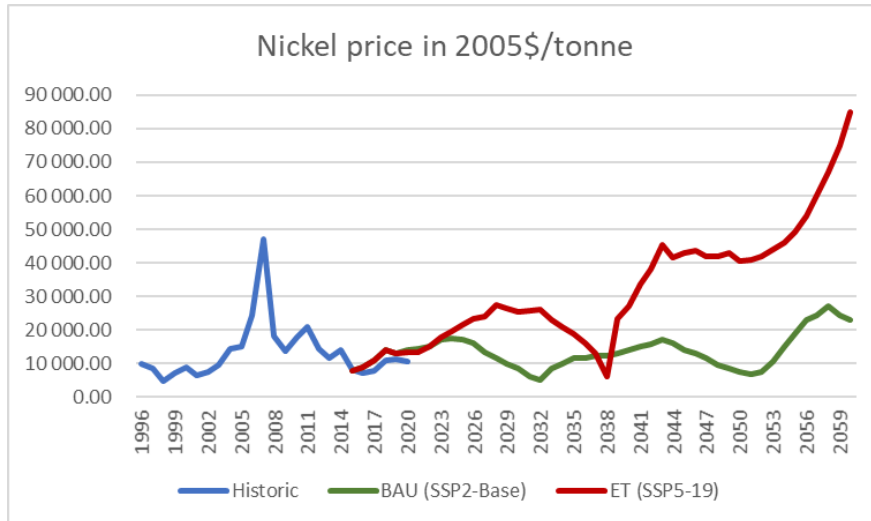


Figure 3.26: historic nickel price adjusted for inflation based on Trading Economics (2020) and model results for nickel price for runs for SSP2-baseline (BAU) and SSP5-19 (the most extreme ET scenario) with base settings. Because the raw data could not be obtained, crude annual values were copied to create this figure. Keep in mind that the results shown here are single run results and that different behaviour occurs in each run.

The average price for the BAU scenarios fits quite well with the historic prices, whereas the price peaks in the SSP5-19 scenario increase over time. This can mostly be explained by the introduction of a carbon price in this scenario (see figure 3.11). As stated in section 2.4, the model price between 2015 and 2020 does not match exactly with the historic price for this period because of the uncertainty regarding the exact timing of the initial values in the model.

Figure 3.27 shows the historic annual change in mining vs the annual change in the runs for SSP2-baseline and SSP5-19 with base settings. This figure shows that mining fluctuates more in the model, with larger extremes than what has historically been observed. This shows that the results of the model are likely to be more extreme than what can occur in reality. In fact, in other runs, even larger extremes occur. This is discussed further in section 4.4.2.

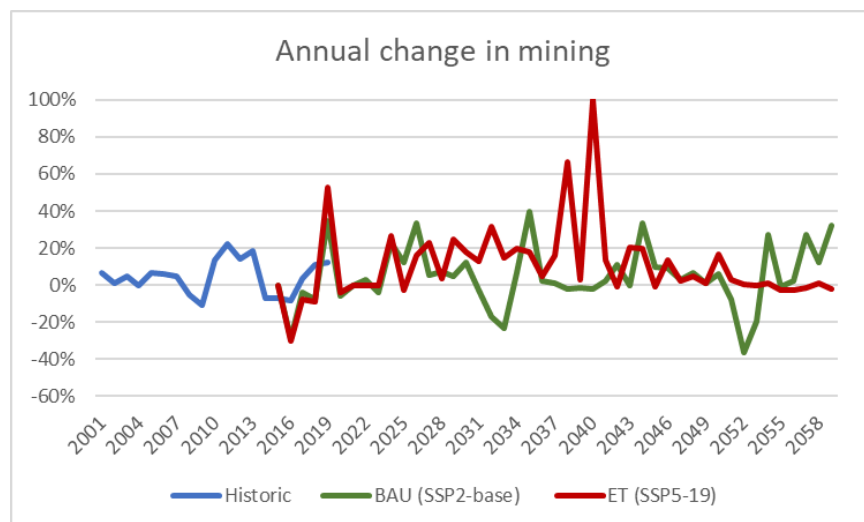


Figure 3.27: historic annual change in mining vs values for SSP2-baseline and SSP5-19 with base settings. Keep in mind that the results shown here are single run results and that different behaviour occurs in each run.

3.5.2 Comparison with literature

In this section, the results are compared with literature. The focus is on demand projections because most literature has mainly assessed this. As stated in the introduction, literature that assessed the impacts of the ET on nickel demand includes Elshkaki et al. (2017), Van der Linden (2020) and many of the papers in table A1, some of which provide data in tonnes/year. Wood Mackenzie (n.d.) also created a demand projection. The different projections are compared in figure 3.28.

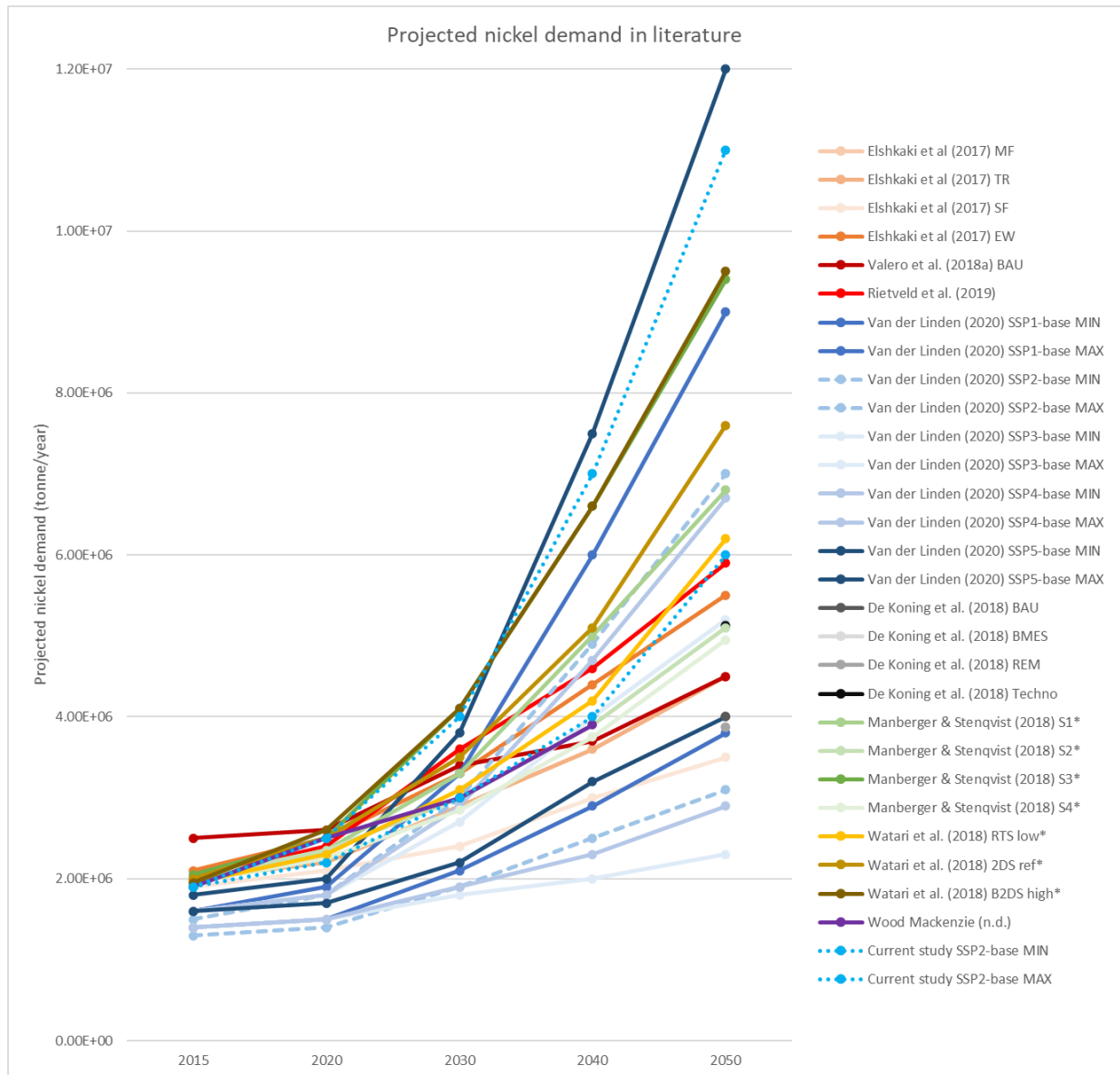


Figure 3.28: nickel demand projections in literature. Most projections go from 2015 (or earlier) to 2050. De Koning et al. (2018) only provided values for 2050. The ET scenarios in the current study have higher values, going up to 2.7E7 tonne/year in 2050 for SSP5-19, and are not included in the figure. For the abbreviations used in previous research, see that respective research. The references with a * only provided annual data for the energy system and not for the RoE, so the RoE projections by Rietveld et al. (2019) were added for better comparison. However, it is important to keep in mind that this therefore does not completely represent these studies and figure 3.29 shows that the RoE projections by Watari et al. (2018) are likely to be higher than what is implied here.

Figure 3.28 shows that the nickel demand projections for the BAU scenario in the current study range between the middle and the high end compared to projections in previous studies. Even though the same data was used for SSP2-baseline in the current study and by Van der Linden (2020), projected uncertainty ranges differ significantly (see the dotted lines in figure 3.28). For the ET scenarios, the demand projections are also much higher than what has been projected before. This is due to differing assumptions. Especially the assumptions regarding EV batteries are important, because these form the largest share of total demand.

To determine the nickel demand for EV batteries, important factors include the projected number of vehicles, the projected share of EVs in the production of new vehicles, the type of battery used, the battery capacity and lifetime assumptions. For each of these factors, the values used in the current study and in other studies are compared in appendix O. Important differences are summarized below.

First, three of the studies in figure 3.28 did not consider (or barely considered) nickel demand for EV batteries (Elshkaki et al., 2017; De Koning et al., 2018; Rietveld et al., 2019). Second, the current study projects between 2.1 billion and 2.8 billion motor vehicles (passenger vehicles, trucks and buses) by 2050. This matches reasonably well with projections by WEC (2011), IEA (2017a), IEA (2017b) and EIA (2019a). However, Valero et al. (2018a) and Van der Linden (2020) projected considerably less vehicles. Third, the current study projects a larger share of NCA+ batteries (which have the highest nickel intensity) compared to other studies, including Manberger & Stenqvist (2018) and Van der Linden (2020). Finally, the current study considers the lifetime of the battery in the vehicles, whereas the other studies only consider the lifetime of the vehicles themselves. As shown in section 3.3.3, this makes a large difference.

The above illustrates the high sensitivity of projected nickel demand to assumptions on the number of EVs, their nickel intensity and the lifetime of the batteries. By including the assumption that vehicle batteries have to be replaced once during the lifetime of an EV, combined with a large share of EVs, the current study projects a much higher nickel demand than previously anticipated. This also highlights the importance of technological developments to improve the lifetime of vehicle batteries.

Figure 3.28 showed annual demand. A comparison of cumulative demand for the current study and previous research is shown in figure O1 in appendix O and this will be covered further in section 3.5.3. A cumulative demand of $3.1E8$ - $4.3E8$ between 2016 and 2060 projected by Watari et al. (2018) comes closest to the demand projections of the current research.

3.5.3 Summary of new insights

Some results of the current work differ from previous research due to the higher level of detail included in the current model. The insights gained from this are summarised in this section. Four specific details that led to new insights are the following:

- Separate inclusion of vehicles and vehicles batteries
- Separate inclusion of individual mines and their characteristics
- Separate inclusion of a fuel and electricity price
- Separate inclusion of class I and class II nickel in scrap

The impacts of these details compared to the aggregated approach used in previous research on certain performance metrics are shown in table 3.3 and covered in further detail below. Most of the differences focus on the research by Van der Linden (2020) because a similar modelling approach was used, and her model and code could be accessed to make a clear comparison for different performance metrics.

Table 3.3: summary of the differences in input and behaviour between previous research and this thesis. Combined, the differences in average final energy use and average energy costs, as well as some additional differences influencing marginal costs, such as royalties that differ per country and a further impact due to a different by-product composition per mine, also leads to different behaviour regarding average periodic nickel price, such as increased variability in the shapes and sizes of the hog cycles.

| Performance metric | Previous research | This research |
|-------------------------------------|--|--|
| <i>Batteries</i> | <i>Aggregated with the vehicle</i> | <i>Separate from the vehicle</i> |
| Cumulative nickel demand | Battery lifetime was equal to the lifetime of EVs. | Battery lifetime was half the lifetime of the vehicle in the base scenario, leading to higher final nickel demand projections |
| <i>Mines</i> | <i>Aggregated mines</i> | <i>Separate mines</i> |
| Average ore grade of existing mines | Average ore grade always decreases over time. | Average ore grade of existing mines varies over time and can increase at certain points in time as mines with low ore grade are decommissioned when they are unprofitable for too long. |
| Average final energy use | Final energy use increases over time as ore grade decreases. Innovation can reduce the rate of increase and potentially reverse it, although the latter does not occur in the model by Van der Linden (2020) | Final energy use is impacted by multiple factors, including a varying average ore grade, a varying composition of ore type, mine type and processing methods and a varying composition of by-products that all impact the relative profitability of a mine. Then, as unprofitable mines are decommissioned, the above factors, combined with innovation, influence the average final energy use, making it decrease over time, increase over time, or even drastically increase over time. |
| <i>Energy price</i> | <i>Aggregated price</i> | <i>Separate fuel and electricity prices</i> |
| Average energy costs | In the model by van der Linden (2020) three energy price scenarios were included, similar to the ones in figure I4 in appendix I1.4. | Electricity price differs from fuel price based on electricity mix. This mix impacts potential carbon costs and the difference between fuel and electricity price. This allows inclusion of the feedback of the ET on the energy price, thereby leading to different behaviour for the nickel costs. |
| <i>Nickel scrap</i> | <i>Aggregated scrap</i> | <i>Separate class 1 and class 2 scrap</i> |
| EoL RR | EoL RR always increases over time as ore grade decreases. In fact, in the model by Van der Linden (2020), it increases further due to the increasing share of batteries because of the focus on cobalt. | Total EoL RR decreases as the percentage of class I nickel (mostly batteries) increases and the percentage of class II nickel (stainless steel) decreases, due to the much higher EoL RR of stainless steel. It can then increase again if ore grade decreases and/or if the EoL CR of batteries increases due to improved EoL management of batteries. |

Separate inclusion of vehicles and vehicle batteries

As stated in section 3.5.2, the current research projects a nickel demand for ET scenarios that is higher than what has previously been projected. An important reason for this is the separate inclusion of vehicle batteries instead of assuming the same lifetime as the vehicle. For better comparison with previous research, and as a sustainability policy (also see section 3.3.3), batteries with the same lifetime as the vehicle were also included in the current research.

The difference in cumulative final nickel demand between a short and long lifetime of EV batteries is shown in figure 3.29, as well the cumulative nickel demand reported in previous research (Watari et al., 2018; Van der Linden, 2020). The cumulative demand projected by Watari et al. (2018) comes closest to the cumulative demand projected in the current research. They even project a higher cumulative demand for their BAU scenario. However, other work projects a lower cumulative nickel demand (also see figure O1 in appendix O), and taking into account a shorter battery lifetime adds to the demand considerably.

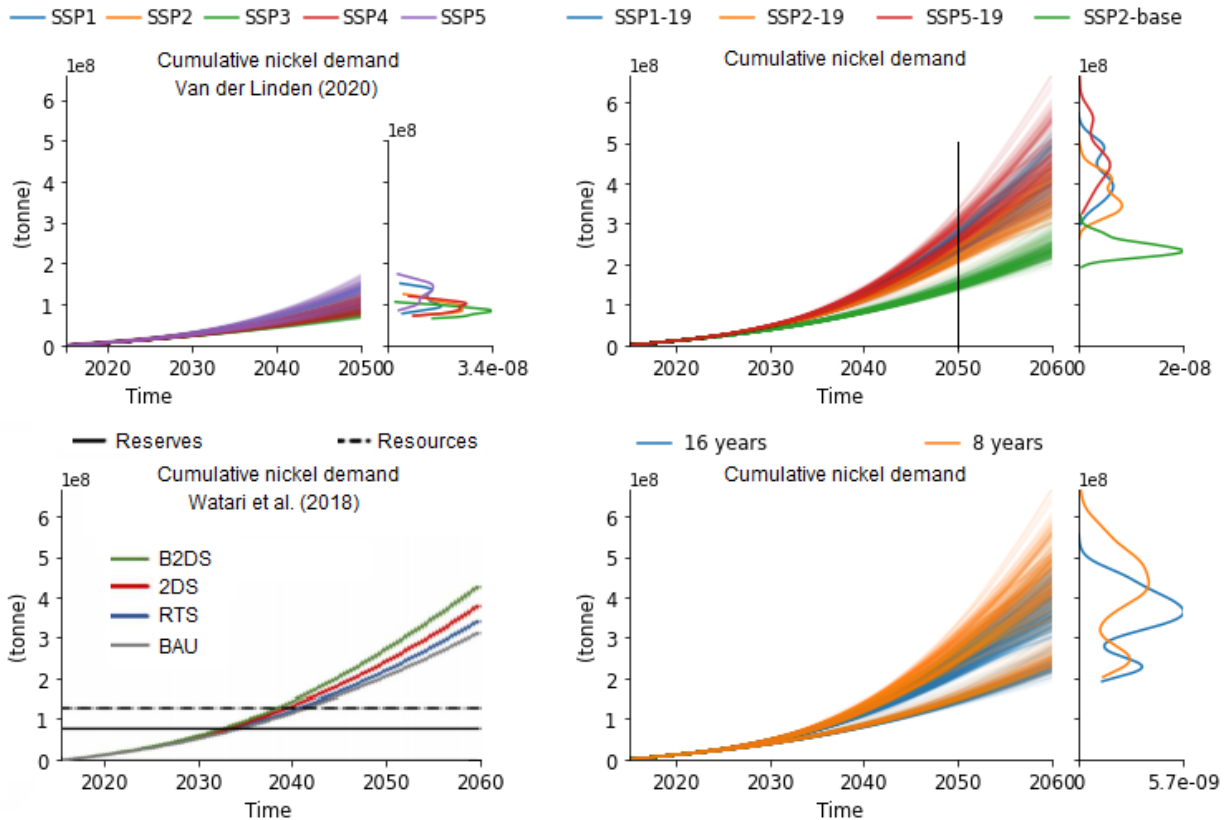


Figure 3.29: cumulative nickel demand between 2015 and 2050 projected by Van der Linden (2020; top left) and cumulative nickel demand between 2016 and 2060 projected by Watari et al. (2018; bottom left) compared to cumulative nickel demand between 2015 and 2060 for the current research with a distinction between the SSPs (top right) and a distinction between vehicle batteries that last half the lifetime of the vehicle (8 years) and vehicle batteries that last as long as the vehicle (16 years; bottom right). Van der Linden (2020) looked at all five SSPs and used a baseline RCP for each. Watari et al. (2018) used scenarios from the IEA (2017a), in line with certain temperature targets. B2DS = Beyond 2 °C Scenario; 2DS = 2 °C Scenario. The data for the nickel projections by Van der Linden (2020) was not obtained from her report directly, as she mainly reported on cobalt. Instead, it was obtained by adding a variable for cumulative demand to her model, subtracting the years before 2015 and running her model using the code she provided. The data for the nickel projections by Watari et al. (2018) was adapted from one of their figures.

Separate inclusion of individual mines and their characteristics

Because of the inclusion of individual mines, the behaviour for certain performance metrics differs compared to previous research, such as the work by Van der Linden (2020), where mines were aggregated. Specific attention is paid to nickel ore grade and final energy use.

Figure 3.30 shows the difference between the average nickel ore grade in the model by Van der Linden (2020) and the average ore grade in the current model. In the former, average ore grade always decreases over time as known resources are depleted. In the latter, the average ore grade varies more over time and can also increase at certain points as mines with low ore grades become too unprofitable and are decommissioned after a certain period of time.

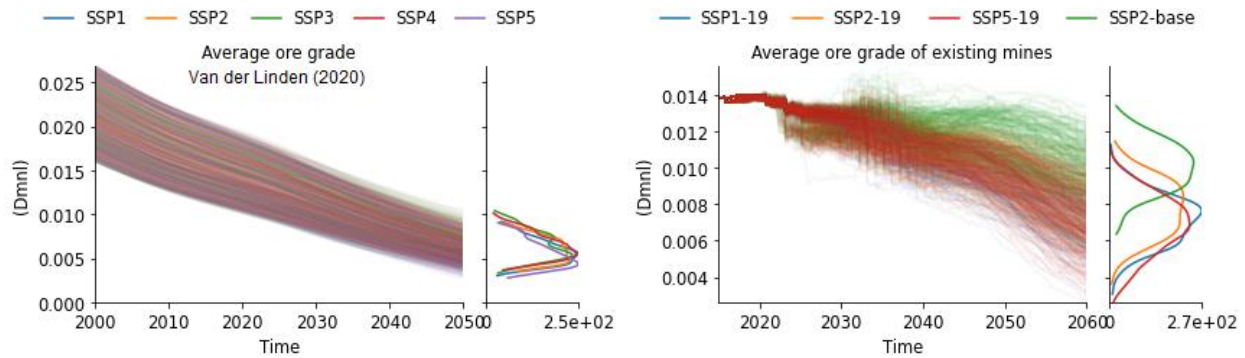


Figure 3.30: Average nickel ore grade in the model by Van der Linden (2020) compared to the average nickel ore grade of existing mines in the current model. The data for the nickel projections by Van der Linden (2020) was not obtained from her report directly. Instead, it was obtained by running her model using the code she provided.

It is important to consider that this refers to the average ore grade of existing mines. The average ore grade of known deposits generally does decrease in the current model, as can be seen in figure 3.9 (an exception is when the resources of certain deposits have a higher ore grade than the reserves, because other factors play a more important role for profitability, but this has a minor impact). However, this too would have the potential to increase if new deposits with higher ore grades are discovered. This was not included in the model.

The general trend is a decrease in all models. However, in the model by Van der Linden (2020), the decrease is relatively linear, whereas in the current model, there is an acceleration in the decrease in the ET scenarios. This is both due to the larger amount of mining and due to the switch in the way ore grade is determined once the original resources in the database by Mudd (2020) have run out.

For each individual mine, the ore grade first decreases or increases in discrete chunks based on current knowledge of the average ore grade for the different types of reserves and resources. Then, when the original resources have run out, the ore grade decays exponentially. This happens at different times for each mine and, in addition to the different times at which mines become operational, are mothballed and are decommissioned, this leads to the behaviour shown in the right-hand graph of figure 3.30. Extra attention is paid to ore grade in appendix N10, where the behaviour in both the OCP and the FSP is analysed in more detail.

Figure 3.31 shows the difference between average final energy use in the model by Van der Linden (2020) and average final energy use in the current model. In the former, energy use always increases over time as known ore grade decreases. In the latter, energy use decreases in many runs due to energy efficiency improvements, while also increasing slightly in some cases due to a decreasing ore grade. A varying composition of ore types, mine types and processing methods further complicates the behaviour.

By-products also play an important role, especially in the runs where energy use shoots up quite rapidly. In these runs, ore grades for certain prominent mines have decreased to a point where energy use significantly increases. However, because these deposits contain valuable by-products, they still remain profitable despite the high energy use. In reality, these mines would perhaps drop nickel as host metal and focus on the other metals instead. However, a change in host metal was not considered in the model.

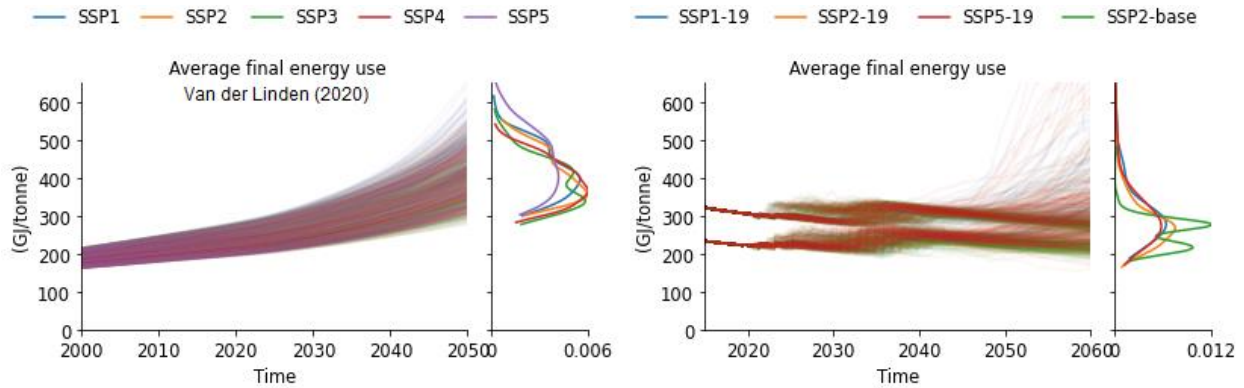


Figure 3.31: Average final energy use in the model by Van der Linden (2020) compared to average final energy use in the current model. The data for the nickel projections by Van der Linden (2020) was not obtained from her report directly. Instead, it was obtained by adding together energy use for mining and energy use for smelting and refining and running her model using the code she provided. In the right-hand figure, values go up to 1200 GJ/tonne.

Separate inclusion of electricity and fuel price

By including electricity and fuel price separately, instead of a single energy price, more complex feedbacks between the ET and the energy price (see figure 2.3) could be included based on modelled changes in electricity mix. In the model, electricity mix influences the electricity price directly, as well as indirectly through a potential carbon price. It also influences the relationship between the electricity and fuel price.

Figure 3.32 shows the difference between average energy costs in the model by Van der Linden (2020) and average energy costs in the current model. First, it is noticeable that the costs are much higher in the model by Van der Linden (2020). This has to do with different assumptions regarding initial fuel price. The details of these differences are described in figure O2 in appendix O. Total marginal costs differ less between the two models because, even though Van der Linden (2020) included transport costs separately and not as part of the energy costs, she also did not include any costs for reagents.

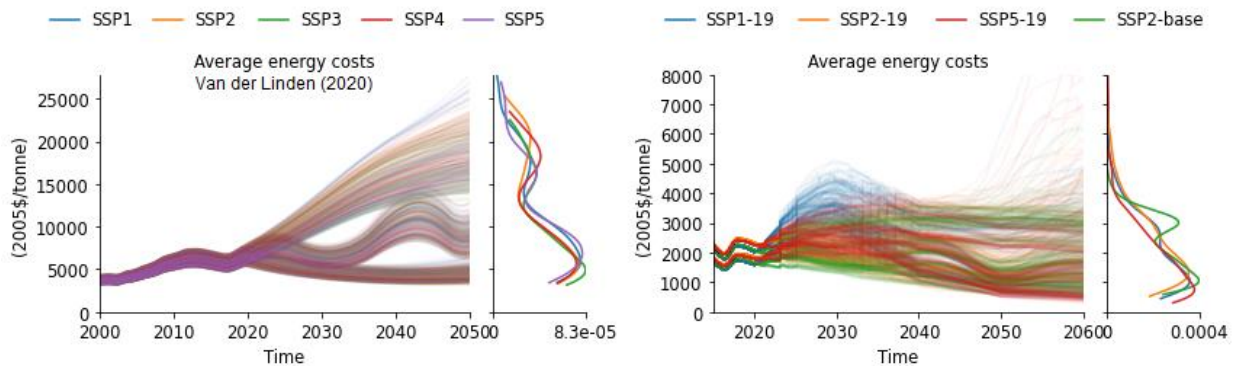


Figure 3.32: Average energy costs in the model by Van der Linden (2020) compared to average energy costs in the current model. The data for the nickel projections by Van der Linden (2020) was not obtained from her report directly. Instead, it was obtained by converting her cost data from 2000\$ to 2005\$ for better comparison and running her model using the code she provided. In the right-hand figure, values go up to 14000 2005\$/tonne.

Other differences include the impact of the different values for average final energy use and the impact of including a separate electricity price, which is mostly visible in the increased costs for SSP1-19 around 2030 due to an initial electricity mix with carbon intensive technologies combined with a high carbon price. As the electricity mix becomes more renewable, the average energy costs decrease in most runs even when fuel price increases. This is because of the large decrease in electricity price due to decreasing carbon costs, and because electricity price becomes cheaper than fuel price once more fuels start being produced with electricity than the other way around.

Separate inclusion of class I and class II nickel in scrap

Figure 3.33 shows the difference between EoL RR in the model by Van der Linden (2020) and the EoL RR in the current model. First, it is noticeable that the EoL RR starts much higher in the current model. The initial EoL RR of 68% in the current model is based on Nickel Institute (2016). The initial EoL RR for Van der Linden (2020) was calculated by multiplying her EoL PR (based on the nickel content in scrap and the average ore grade) with her EoL CR (a general range of 40 - 80% for copper, cobalt and nickel).

Another noticeable difference is the behaviour of the EoL RR. In the model by Van der Linden (2020), this increases over time as ore grade decreases and increases even further as the percentage of batteries in scrap increases. The assumption for this behaviour was that, as the percentage of batteries in cobalt scrap increases, the EoL RR for cobalt improves because cobalt is easier to extract from batteries than from other cobalt products for which the collection is not as well organised. However, this was also generalised to nickel without considering that the EoL RR for nickel is already quite high due to the well organised recycling of stainless steel.

Therefore, a distinction was made between class I (a mixture of products; over time mostly batteries) and class II (stainless steel) nickel in scrap in the current research. The EoL RR for class II was assumed to remain relatively constant at 90% (EuRIC, 2020) and the EoL RR for class I nickel was assumed to vary based on an increasing share of batteries. This initially leads to a decreasing EoL RR, as the share of batteries and thereby the share of class I nickel increases. The lower lifetime of batteries than stainless steel structures also plays a role here. Later, the EoL RR stabilizes and in many cases increases again as the ore grade decreases, with the rate of increase depending on the EoL waste management strategy.

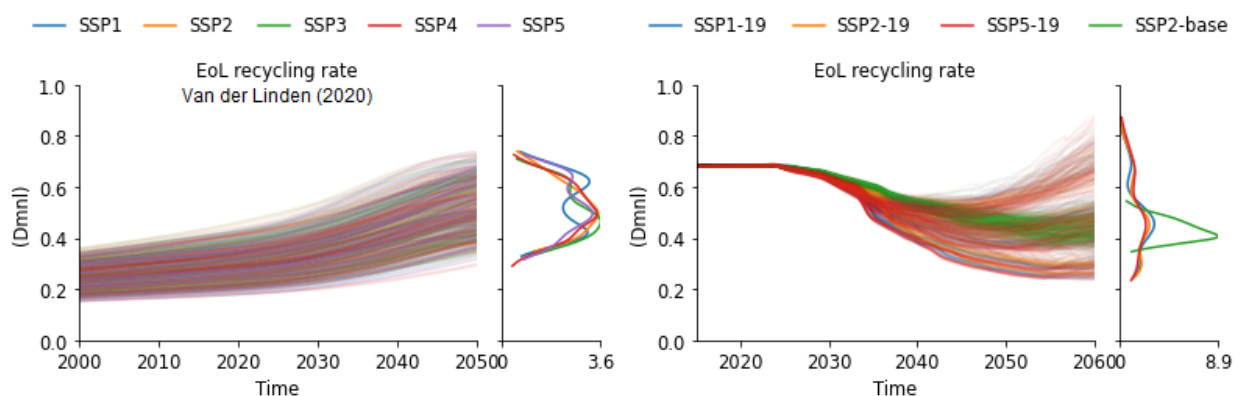


Figure 3.33: EoL RR for nickel in the model by Van der Linden (2020) compared to EoL RR for nickel in the current model. For an explanation for the differences between SSPs and EoL waste management strategies, see section 3.3.2. The data for the nickel projections by Van der Linden (2020) was not obtained from her report directly. Instead, it was obtained by multiplying her EoL CR (referred to as collection rate metal products) with her EoL PR (referred to as recycling efficiency score) to obtain EoL RR, and running her model using the code she provided.

3.6 The resilience of the nickel supply chain

In the previous sections, results were provided per sub research question. In this section, a summary is given of what these results mean for resilience. As described in section 2.1, a resilient system is one with a high resistance and/or rapidity and/or flexibility to ensure that supply can continue to meet demand.

The main indicator for resilience is considered to be the average periodic nickel price. It is normal for price to fluctuate slightly and for hog cycles to occur due to demand and supply dynamics (see section 3.2.1). However, if price fluctuates too much, it can be an indication of low resilience. When price shoots up suddenly, this is often an indication of insufficient supply to satisfy demand. If this peak in price is short lived, there is high rapidity, indicating resilience. If there is no (extreme) peak, there is high resistance, also indicating resilience. Flexibility can help by reducing demand and bringing it closer to supply.

In section 3.2, the impacts on the nickel system of the ET, radical battery innovation, resource depletion and disruption in key supplying countries, were shown. These disruptions all impact average periodic nickel price to a certain extent, but some have a larger effect than others. In addition to the disruption scenarios, other factors, such as the sustainability policies and important systemic and parametric uncertainties also impact the average periodic nickel price. Especially the combination of certain values sometimes leads to unresilient behaviour.

Energy transition

The ET has a large impact on the nickel system. Demand increases at a much higher rate than in the BAU scenario. However, in most runs, supply is able to keep up, as is indicated by the degree of nickel scarcity in figure 3.7, which does increase at points (especially at the start), but also comes back down again. However, average scarcity is higher than 1, which would be expected for a perfect match between demand and supply. This is discussed in section 4.4.3.

Figure 3.7 shows that the price for most BAU runs fluctuates around 15000 2005\$/tonne and the price for most ET runs fluctuates around 30000 2005\$/tonne. The higher price for the ET is mainly due to the carbon price in these scenarios (see figure 3.11). This does not indicate a lack of resilience, but more a shift in state, where all carbon intensive activities are more expensive due to a carbon price, including the production of potential substitutes. This also means that the higher price does not necessarily indicate higher profits for mining companies, as the costs also increase.

In most runs, the nickel system is resilient, however, when certain factors are combined, a lack of resilience can be observed. This manifests itself in a sharp increase in price that lasts for many years. The runs where price shoots up and stays up for a relatively long period have several things in common:

- Most include an ET scenario (although price in some runs with the BAU scenario also shoots up, especially between 2040 and 2050, however the peaks are lower due to lower marginal costs)
- Most do not include the radical battery innovation disruption
- In later years, many have worse EoL waste management strategies
- Many include an EV battery lifetime of 8 years
- Many have their processing energy allocated fully to nickel
- Most do not consider by-products
- Most include a high power for exploration (= low exploration)
- In runs where global maximum capacity increase percentage varies between 1 and 30%, most runs have a low global maximum capacity increase percentage.

Based on this, the nickel system can be considered conditionally resilient to the ET. Supply is able to keep up with demand if there is sufficient exploration and sufficient capacity increase. Further research is required to determine how much exploration and capacity increase is realistic and whether this is enough to prevent scarcity from becoming too high. If scarcity becomes too high, choices have to be made which part of nickel demand will be reduced and this can impact the pace of the ET.

Radical battery innovation

As shown in figure 2.1, factors that contribute to the resilience of the system include feedback loops through the price mechanism, such as price elasticity of demand (see figure N2), changing product properties, such as increasing the EV battery lifetime, and substitution which adds to the flexibility of the system.

Substitution increases the resilience of the system, but it can also be a disruption if it is too extreme. However, the radical innovation of battery technologies included in this thesis is not extreme enough to truly disrupt the nickel system, or in other words, the nickel system is resilient enough to be able to deal with this disruption, at least in the way it was modelled.

For the ET scenarios this is because it is happening at the same time as the ET, so in a way the two disruptions cancel each other out, or the radical innovation disruption at least dampens the effects of the ET by slightly reducing the average periodic nickel price again. In this sense, the radical innovation can be seen as a mechanism that improves flexibility, and thereby resilience, instead of a disruption.

For the BAU scenario, the radical battery innovation has a smaller impact because it is a disruption in battery technologies and in the BAU scenario a lower share of the demand is due to batteries. In addition, the average periodic nickel price is lower in the BAU scenario, so even though the substitution threshold has been reduced, the price of the potential substitute may still be higher than, equal to, or only slightly lower than the nickel price, which leads to less substitution.

Resource depletion

Resource depletion based on the FSP has a large impact on the nickel system. Because there is no exploration, the resources start becoming scarce as the easy to mine deposits are depleted and the price shoots up. This indicates lack of resilience. However, history has shown that it is unlikely that this will occur, because exploration has consistently led to more resources (see appendix G1.2). In addition, if substitution and other price effects were included in the FSP, these would kick in as soon as the price got too high. This is something that could be explored by adding a hybrid paradigm to the model.

In the OCP, initial resources based on the database by Mudd (2020) are depleted between 2050 and 2060 for the ET scenarios. However, because of exploration and price effects, the nickel system was resilient and able to continue functioning past this point.

Supply disruption

Regarding the disruption in key supplying countries, the overall impact is minimal. When the country with the largest share of production is compromised in 2030 and 2045, the average periodic nickel price increases. This is clearly visible in figure 3.15, but the increase is not necessarily more than the variability that occurs due to the hog cycle dynamics. This is because of the relatively high diversity of supply in the nickel system, with multiple supplying countries and a high EoL RR. Substitution also occurs as the price increases, which leads to additional balancing of the disruption.

Table 3.4 summarizes the resilience of the nickel system to the different disruptions based on the framework by Sprecher et al. (2015). In this table, the system is considered to be either resilient (green), not resilient (red) or conditionally resilient (yellow) based on the identified key uncertainties.

Table 3.4: resilience of the nickel system in the model to the disruptions assessed in this thesis. Green = resilient, red = not resilient, yellow = conditionally resilient based on key uncertainties.

| Aspects of resilience | Energy transition | Radical innovation | | Resource depletion | | Supply disruption |
|-----------------------|---|--|--|---|--|--|
| | | ET | BAU | FSP | OCP | |
| Resistance | If there is enough innovation (e.g. an increase in battery lifetime), the effects of the ET can be dampened. Carbon costs do lead to a new state. | The system is not disturbed because the ET cancels out the effects of innovation. | The system remains functional at this degree of innovation. | Without exploration to replenish supply, price becomes unrealistically high. | With sufficient exploration, supply can be replenished before the difference between demand and supply becomes too high. | There is enough diversity of supply for the price increase to not be too large. |
| Rapidity | The speed with which the nickel system can respond to the ET depends on the rate of new capacity creation. | The system is not disturbed because the ET cancels out the effects of innovation. | The system remains functional at this degree of innovation. | As resources become too scarce, the system does not return to its previous state. | If exploration is too little, the system has trouble getting back to a lower scarcity, because supply cannot keep up with increasing demand. | As soon as the disruption is over, the system returns to its previous behaviour. |
| Flexibility | As price goes up, substitution and price elasticity help prevent it from increasing even more. Discovering more substitutes would further increase flexibility. | Radical innovation leads to more substitution; increasing flexibility and dampening the impacts of the ET. | Sensitivity to substitution increases. However, substitution only occurs if the price is too high. | Substitution and price elasticity are not included in the FSP. | Substitution and price elasticity help reduce demand, thereby requiring less resources. Discovering more substitutes would further increase flexibility. | Substitution and demand reduction due to price elasticity increase as the price goes up. |

As stated in section 3.5.1, there is higher variability in average periodic nickel price in the model than what has been historically observed. However, it is important to take into account that the way the system was modelled plays a large role in this variability. This makes it difficult to determine which part of the variability is due to the actual nickel system and which part is due to the shortcomings of the modelling approach (these are discussed in section 4.4).

The model is too uncertain to clearly state anything about the actual nickel system, but it does give an indication of the factors that can have an important impact on the resilience of the nickel supply chain. Overall, the nickel system based on the OCP can be quite resilient to disturbances. However, this is under the conditions that there is sufficient exploration and capacity increase.

4 Conclusion and discussion

In this chapter, the research questions are answered in the conclusion, the societal and academic relevance is discussed, a critical reflection is given on the methods and assumptions, and recommendations for further research are provided.

4.1 General conclusion

In this thesis, the development of the global nickel supply chain, and some of its externalities, was modelled and explored between 2015 and 2060 under different disruption scenarios, sustainability policies and uncertainties. A nickel demand of 6 - 38 million tonnes per year is projected by 2060 (6 - 27 million by 2050). This is more than what has previously been projected. The highest demand occurs for SSP5-19, which has a target to limit global temperature increase to 1.5 °C alongside rapid economic growth. The main contributors to this large demand are EV batteries.

Based on the model and assumptions, the nickel system is resilient (meaning there is sufficient supply to meet demand) to partial substitution and to a one-year supply disruption compromising the top supplying country. The nickel system is conditionally resilient to ore depletion and the ET, given sufficient exploration and annual capacity increase.

To increase the resilience of the nickel system, policies that support innovation in battery material composition and lifetime, and good EoL waste management of batteries can play an important role. EoL RR first decreases in all scenarios due to a larger share of batteries and a lower share of stainless steel in scrap. However, with good EoL waste management, the EoL RR eventually surpasses the initial EoL RR again. Policies that reduce forward supply chain losses have less impact on resilience, but do reduce the cumulative GHG emissions due to the nickel industry.

Key structural uncertainties influencing the development and resilience of the nickel system include the processing energy allocation method, with full allocation to nickel leading to higher energy use, emissions, costs and nickel price; and the inclusion of by-products, where the consideration of by-products leads to prioritization of different mines and thereby different behaviour.

Key parametric uncertainties include the administration of postponed demand, which determines how quickly postponed demand is registered, and the power for price-based exploration, which determines the degree of exploration in the model. A global maximum capacity increase percentage only starts making a large difference at values lower than 10% per year. For ore grade and energy use, the power for ore grade also has a large impact.

The findings of this thesis are based on a first attempt at SD modelling of global material flows at mine level. With the used data and assumptions, the model generally leads to plausible behaviour. However, in many runs, the changes in price and production and the resulting hog cycles become quite extreme. Compared to previous research, in which mines were aggregated, some different and interesting behaviour was identified, which was made possible due to the detailed modelling and the inclusion of individual nickel mines.

This includes the potential for average ore grade to increase over time, as mines with lower ore grades are decommissioned; average final energy requirements that can decrease, increase, or increase rapidly, depending on a varying average ore grade, a varying composition of processing methods and a varying composition of by-products; and average energy costs that differ depending on the projected electricity mix in the countries containing deposits. For a more detailed description of new insights, see table 3.3.

4.2 Societal relevance

This research was not done for a single problem owner. Instead, the results can be useful for a multitude of stakeholders, including governments, companies interested in accelerating the ET and actors in the nickel industry and the mining industry in general. All these actors benefit from a nickel system that is as resilient as possible and can also help contribute to this resilience. Of further societal relevance are the externalities of nickel production. In the following sections, the implications for the ET are discussed, followed by the usefulness of the results for the mining industry, and the externalities.

4.2.1 Implications for the energy transition

On one side of the energy-nickel nexus, nickel is required to produce energy. The results indicate that there can be enough nickel for the ET, given sufficient exploration and rate of capacity increase. However, until more research has been done on how much exploration and capacity increase is realistic, no concrete conclusions can be drawn about the impact of nickel on the pace of the ET.

For stakeholders on the demand side, such as governments interested in accelerating the ET, renewable energy companies and EV companies, as well as other nickel consumers, it is useful to consider the large nickel demand that can occur due to the ET, which may lead to some problems with supply, thereby hampering the ET. In general, the faster the demand increases and the higher it becomes, the lower the resilience of the system, and the higher the chance that the demand cannot be fulfilled, as can be seen in the ET scenarios. Therefore, limiting nickel demand through innovation, is an important area these actors can focus on.

The results show that increased substitution through radical battery innovation can increase resilience. Continuing to research new battery technologies is important to realise this. The results also show that battery lifetime makes a large difference, so innovations that increase battery lifetime are also important. Of further importance is the recyclability of batteries, as an increase in EoL RR reduces primary nickel demand. This recyclability can be facilitated throughout the battery supply chain, from the design to the collection strategy, as both an improved EoL PR and EoL CR contribute to increasing the EoL RR in the future.

An important aspect of the SSPs with a target of 1.5 °C temperature increase is that they all include a carbon price. This tax is an important mechanism that governments can implement to reach the temperature increase target, and it is intended to discourage the use of fossil fuels and encourage the use of renewables. However, the model shows that it inadvertently also impacts the ET, by impacting the price of materials required for renewable energy and other low carbon intensive technologies such as EVs. The net effect of a carbon price may still be beneficial for the ET, but this feedback (also illustrated in figure 2.3) is something that should be taken into account.

4.2.2 Usefulness for the mining industry

For stakeholders on the supply side, such as investors and mining companies, the large nickel demand in the ET scenarios can be seen as an incentive to invest in nickel, to explore more and to build more mines. The resilience of the system is also relevant because a less resilient system contains more risks for individual mining companies. However, in the model, the cycles in many runs are more extreme than what would occur in reality. This is likely because, although the model is very detailed, many factors that can influence the variability in reality were not considered.

The model presented in this thesis can be seen as a basis for future research on the development of the nickel supply chain. It contains some fundamentally demonstrable and important connections between system aspects. However, the model is based mostly on literature and theory, and in some cases highly uncertain assumptions. To take this into account, uncertainty was included in the model. However, uncertainty ranges could not be included for all variables due to computational limitations. In addition, the uncertainty ranges did not prevent the large extremes in the model.

To increase the usefulness for stakeholders, the model structure and data inputs could therefore benefit from a larger degree of collaboration and expert and stakeholder input. The model is adaptable and in future adaptations, the assumptions and data inputs could be refined and improved by those who have a higher level of expertise and/or access to data. This could then lead to more valid and robust results that can be used to aid decision making.

The results shown in section 3 are all global results. However, due to the level of detail included in the model, it is also able to produce data on a regional or country level. Examples are shown in figure N43 in appendix N11. This could be of further interest for stakeholders in the mining industry, as well as for the governments of the countries in question. Once regional results become more robust, they could be useful for national policy making. For example, by tweaking the investment climate in certain countries, it becomes more likely for more mines in those countries to be favoured.

Obtaining results at mine level is also possible, but the model is not detailed enough for this to be useful. All mines are based on existing deposits, but due to the many crude assumptions that were made, the deposits were named based on the country they are located in, followed by a number, and the model should currently not be used to obtain data for specific projects.

4.2.3 Externalities of nickel production

In this thesis, final energy use and GHG emissions were modelled as sustainability impacts of nickel mining. Cobalt and palladium mining were also projected. Strictly speaking, these are not externalities, but they are included here as the by-products most dependent on nickel mining. Final energy use, GHG emissions and cobalt and palladium production are discussed below. Other externalities were not included, but could be added to the model in future research. This is discussed further in section 4.4.4.

As one side of the energy-nickel nexus, nickel required for energy infrastructure was discussed in section 4.2.1. On the other side of the energy-nickel nexus, energy is required to produce nickel. Table 3.1 in section 3.2.2 shows numbers for both sides. It shows that the final energy required for nickel production in 2060 is, on average, about 0.4% of the TFC in 2018 for BAU and about 0.6% of TFC in the ET scenarios.

It is important to note that the values for final energy required for nickel do not include data on energy products for non-energy use, which means the percentages of TFC may be slightly higher. Primary Energy Demand (PED) was also not calculated in this research. This could be done in future adaptations of the model by including data for non-energy use, as well as (dynamic) conversion efficiencies for the different electricity generation technologies. This is discussed further in section 4.4.4.

Nickel production also leads to GHG emissions, both directly on-site through fuel use and process emissions and indirectly through electricity use. Table 3.2 in section 3.2.2 shows numbers for the GHG emissions projected in the model. The values in 2060 are, on average, about 0.3% of the total GHG emissions in 2015 for BAU and about 0.2% for the ET scenarios. This is because of the higher share of renewables in the ET scenarios in 2060. However, cumulatively, the ET leads to more GHG emissions from nickel production, as can be seen in figure 3.11

Regarding cobalt, Manberger & Stenqvist (2018) project a cumulative cobalt demand between 2015 and 2060 of about $2E6 - 7.5E7$ tonnes. The projections of other literature also fall between this range, albeit for slightly different time frames (Valero et al., 2018a; Watari et al., 2018; Giurco et al., 2019; Moreau et al., 2019; Van der Linden, 2020; also see figure O3 in appendix O). In the current model, the cumulative mined cobalt is between $4E6$ and $2E7$ tonnes (see figure 3.6). Not considering losses, and matching the lower and upper bounds with each other, this is about 27 - 200% of the demand.

This is quite a decent share of the demand, considering only 50% of cobalt currently comes from nickel mining (Nassar et al., 2015). This may change in the future, but this means more cobalt can also be obtained elsewhere. In addition, the cobalt scarcity in the model is based on nickel scarcity, but if actual cobalt dynamics were included, cobalt recovery could potentially be higher. More cobalt is mined for the ET scenarios, which matches well with a higher cobalt demand for batteries in the ET.

Regarding palladium, Moreau et al. (2019) project a cumulative palladium demand between 2010 and 2050 of about 6 - 41 tonnes, and Valero et al. (2018a) project a cumulative palladium demand between 2016 and 2050 of about 7800 tonnes. In the current model, the cumulative mined palladium between 2015 and 2050 is about 8000 - 39000 tonnes (see figure 3.6). Currently, 50% of palladium comes from nickel mining (Nassar et al., 2015), so, even when considering losses, this should be more than enough to cover the demand up to 2050. However, due to the large difference between the values found in the literature, it could be beneficial to reassess palladium demand in future research.

4.3 Academic relevance

This thesis was written for the Master's programme Industrial Ecology (IE). IE is an interdisciplinary field where technical, social and environmental aspects are integrated to study complex sustainability issues. This thesis fits well within the field of IE because it focuses on two important societal developments with a clear connection to sustainability: the ET and material depletion. To model these developments, different parts of the socio-technical system of the nickel supply chain and the natural environment were integrated, and circularity was covered in both energy (renewables) and material (recycling) sense.

In addition to contributing to IE, this research has led to some new insights relevant for multiple academic fields. These fields include the energy-material nexus, supply chain resilience and SD modelling, and they are each addressed in turn below.

4.3.1 Energy-material nexus

This thesis contributes to research on the energy-material nexus by, on one side, providing insights into the energy requirements and energy costs for the nickel industry for different deposit characteristics, processing methods and regional energy mixes, and on the other side, providing insights into the nickel requirements for the ET.

Table A1 in appendix A summarizes previous research in this area. The current research adds new insights by suggesting that nickel demand for the ET may be larger than previously anticipated if a large fleet of EVs is to be produced. This large demand can compromise the resilience of the nickel supply chain under certain circumstances, which does not only have consequences for the nickel system itself, but also for the pace of the ET.

4.3.2 Supply chain resilience

This thesis also contributes to research on supply chain resilience. An existing framework for supply chain resilience (Sprecher et al., 2015) was applied to the model and the resilience of the nickel supply chain to four different disruption scenarios and other uncertainties was assessed. The results show the type of behaviour that is caused by different disruptions and the circumstances under which there is a higher and a lower resilience.

Under some circumstances, an ET, with a target to limit temperature increase to 1.5 °C, leads to lower resilience of the nickel supply chain, for example when there is no battery innovation, there is bad EoL waste management of batteries, there is limited exploration and there is a slow rate of capacity increase. Under other circumstances, the ET poses less problems for the nickel supply chain. In future research it could be useful to further investigate these circumstances, to gain more useful insights for stakeholders.

4.3.3 System dynamics research

A third area of contribution of this thesis is to the field of SD modelling. In this thesis, traditional aggregated, continuous SD modelling was adapted to include disaggregated, more discrete ABM elements, specifically the inclusion of individual mines instead of considering only one 'global mine'. As far as the author is aware, this approach is a new way of modelling material supply chains.

In reality, mines are highly heterogeneous and the disaggregated system can behave differently and more dynamically than the aggregated system. This behaviour is captured in the current model, leading to various new insights, such as the potential for average ore grade of existing mines to increase under certain circumstances. These insights were summarized in table 3.3.

This research can be considered as an experiment. It shows that it is possible to add ABM elements in Vensim and that this leads to different behaviour than the behaviour of traditional SD models. A model at mine level is a lot more complex and detailed and also adds discrete elements to a traditionally continuous form of modelling. The discrete elements make the model less elegant and perhaps also contribute to the large fluctuations in the model.

However, a working model was created, with which the research questions of this thesis could be answered. As stated in section 4.2.2, further adaptation of the model is needed to increase its usefulness for stakeholders and to be able to give any concrete policy recommendations.

Whether the hybrid form of modelling attempted in this thesis is useful for further applications, or whether a pure form of ABM may perhaps be more suitable, remains to be seen. Further research can be done to determine the applicability of the hybrid method for other materials. It is also relevant to look more at the regional data in further research, as this can lead to more concrete policy recommendations.

4.4 Limitations and recommendations for future research

The global energy and mining systems are very complex and difficult to model, especially at the detailed level that was attempted in this thesis. The created model is a good start for exploring the global nickel system and its nexus with the energy system at mine level, but there are many aspects that can be improved, regarding both the structure of the model and the data inputs.

In this section, the limitations of the model and the research are discussed and recommendations are given for future research. Some recommendations were already given in previous sections, so these are not repeated here. Many specific limitations were discussed in the detailed description of the model in the appendix, so these are also omitted here in favour of a more general discussion of the limitations. This is done per sub-model below, but first some general points are discussed.

A lot of information can be gathered from the model, but not all of it was included in the experimental set-up and/or results of this thesis. A few additional structural uncertainties are included in the model in the form of switches, including an option for stockpiling, different energy calculation methods and a different method for calculating vehicle demand. These structural uncertainties can be explored in future research.

In addition, different variables could be given an uncertainty range in future runs of the model, to see what impact this has on the results, and different performance metrics, including country and process specific performance metrics, could be chosen to assess. In future research it could also be interesting to combine certain values for variables that lead to extreme behaviour in scenarios to further understand which values lead to the lowest resilience of the system.

4.4.1 Demand system

For the demand dynamics, the focus was on the energy system, specifically electricity generation, electricity storage and road transport. These were the sectors that were expected to grow the most, but in future research it could also be interesting to take into account other parts of the energy system.

On the other hand, section 3.1 showed that the most important contributor to nickel demand is EV batteries. In future research it could therefore be interesting to simplify the rest of the energy system and focus mainly on EVs and the uncertainties involved with EVs, such as nickel intensity, lifetime, share of vehicle stock and vehicle stock projections.

SBS requirements were calculated in a relatively complex way and multiple uncertain values were used to determine what essentially is a balancing factor. Due to the uncertainties involved this led to rather erratic behaviour in figures N4 and N5 in appendix N1.

Because the numbers for SBS are relatively small compared to the other demand categories, this does not matter much for the overall results. However, a simpler method could have been used to obtain smoother results with the same amount of uncertainty. Something that can be concluded from the calculations for SBS is that if enough EVs participate in V2G, hardly any SBS is required.

Repurposing of EV batteries was included in the current analysis, but this was done in a rather crude way. Even though SBS demand is not much, an interesting avenue for further research could be to look more into vehicle battery repurposing, which could also be linked to EoL battery management and innovation in increasing battery lifetime, which are all factors that can help reduce demand for primary nickel.

Regarding hydrogen, only the hydrogen requirements of the fuel cells in the vehicles and of hydrogen tanks (assumed to be for storage outside of the vehicles) based on uncertain values from Tokimatsu et al. (2018) were taken into account. However, these results were deemed too uncertain to present in the main text. To gain more confidence regarding hydrogen requirements, additional research should be consulted.

In addition, certain hydrogen infrastructure was not taken into account in the current analysis. For example, Meylan et al. (2016) estimate that 6.12 mg nickel is required per kg of hydrogen for electrolyzers, and Kleijn & van der Voet (2010) calculated that about 2200 kg nickel is required per km of stainless-steel pipe for transporting hydrogen. However, this requires additional calculation of the amount of hydrogen required, which was not done in this analysis.

There is data on hydrogen in the SSP database (IIASA, 2018), including data on electricity produced from hydrogen. However, due to time constraints this was not added to the model. This is something that could be added in the future to create a more detailed picture of the nickel requirements for hydrogen, also outside of the road transport sector. Overall, hydrogen was not looked at that extensively or meticulously in this analysis, so this is something that would be interesting to do in future research.

In the current analysis, ambitious ET scenarios were chosen with the goal to limit global temperature increase to 1.5 °C. These scenarios will probably lead to the highest nickel requirements, but it could also be interesting to assess some other SSPs. The SSPs allow for regional distinction regarding energy mix, which impacts nickel supply, but it could also be interesting to include a regional distinction for nickel demand. This could be something as simple as a distinction between developed and developing countries, and could add some additional dynamics to the model.

Regarding the price effects included in the model, more in-depth research can be done on potential intensity changes and more in-depth research can be done regarding potential nickel substitutes and the likelihood that these could take over a certain portion of nickel demand. A large amount of substitution occurs in the current model, especially after 2050 (see figure 3.2). In future research, it could be interesting to see what happens if the possibility for such substitution is reduced.

On the other hand, the possibility for more, and different types of substitution, could also be explored. This can include material substitution, but also forms of technological substitution (see appendix E3), such as increased public transport, or vehicle sharing, or even reduced transport requirements due to increased working from home.

In the model, desubstitution can occur when the nickel price becomes more attractive than the substitute's price again. This happens immediately, as soon as the price is lower. However, once an alternative has been found, it may have established a firm foothold in the market and a threshold may need to be crossed before the demand switches back to nickel again. This is something that could be added to the model in future adaptations.

4.4.2 Supply system

The supply sub-model was adapted from Van der Linden (2020) to include individual mines and new structures were created to be able to convert resources to reserves and increase capacity for each individual mine. The structure for converting resources to reserves is rather crude, but it is the best that could be conceived at present. In future research it would be beneficial to explore alternative methods for converting resources to reserves.

For increasing capacity, a maximum global capacity increase percentage was included to prevent too many new mines from being created simultaneously. However, because of the different developing times of the mines, sometimes the percentage of new mines that started operations becomes larger than the maximum global capacity increase percentage. In future research it may be relevant to take into account the total developing capacity at a certain time, because in reality, actors in the mining industry can be aware that certain capacity is already being built elsewhere and this could impact the investing strategy.

The structure for increasing capacity was also implemented too discretely. In reality, new capacity isn't built exactly at the start of each year. This could also cause problems in the model, and it is beneficial to find a way to implement such a structure in a more continuous way in future adaptations of the model. Furthermore, the replicative validation of capacity increase could be increased by obtaining data on historic capacity changes.

Surprisingly, global maximum capacity increase percentage did not impact key performance metrics much. Anything between 10% and 50% did not lead to significant differences. However, when the values were varied between 1% and 30%, global maximum capacity increase percentage did have a large impact. In future research more attention can be paid to the exact point where global maximum capacity increase percentage starts to become a problem for the resilience of the nickel supply chain.

A relevant factor that may play a role in the small differences between 10% and 50% capacity increase, is that after a while there is already so much existing capacity, both operating and mothballed, that capacity coming back from C&M is enough to cover an increase in demand, and in the model, mines enter and exit C&M at a much faster rate than the development of new mines.

The structure for mothballing could be improved. Despite adding a maximum profit deficit and a minimum profit surplus to prevent mines from going in and out of C&M too quickly, this is still happening rather frequently, leading to large variability in final nickel availability. The model leads to much larger extremes than have been observed in history. An important avenue for future research is therefore to uncover the reason for these large extremes, which could be explained by the frequent mothballing, so the model can be adjusted accordingly and the extremes can be smoothed out more.

Because of the large extremes that occur in certain runs of the model, it can also occur that operating capacity, and thereby mining, is 0 at a certain point in time. Because of this, all the averages in the model were based on existing mines (operating + mothballed) instead of only on operating mines. In future adaptations of the model, the possibility of basing the averages on operating capacity could be explored.

As can be seen in the FSP runs, some of the deposits in the database by Mudd (2020) were never activated in the model, because their initial resources were too low. This includes deposits with the initial status of tailings. Because these deposits are never activated, there is also no exploration in their area, because exploration depends on profitability in the model.

However, in reality, exploration does not only occur in the same area that a certain mining company is located in, and mining companies can be in charge of multiple deposits. Therefore, it could be interesting in future research to adapt the model in such a way that exploration does occur in the deposits that are never activated in the current model. Avenues for including additional potential deposits in the model could also be explored. This could increase resilience through increased diversity of supply.

No data was found on historic exploration efforts for further validation of the model. However, more research should be done on how realistic the amount of exploration in the different runs is (see figure 3.24). Exploration is an important factor determining the resilience of the nickel supply chain and if it turns out that the amount of exploration is excessively high, the actual resilience could be less than what has been indicated by this research. There are also costs involved in exploration, costs that were not directly included in the model. This is also something that could be improved in future adaptations of the model.

Currently, the model only contains mining capacity and not refining capacity. This could potentially be added in future adaptations to better incorporate global transportation and geopolitical aspects. In this sense, a dynamic version could be created of the Sankey diagram in figure G3 in appendix G2. As indicated by Sprecher et al. (2015), geopolitical factors can be an important source of disruption, impacting resilience.

The nickel system appears to be quite resilient to the supply disruptions included in the current study. However, these disruptions only lasted one year. In future research, longer supply disruptions could be tested. Other types of disruptions described in section 2.1 could also be tested.

The inclusion of stockpiling also has not been tested properly, although a switch for stockpiling was included in the model. This is still quite a crude switch though, and further research should be done to improve it. Preliminary results show that turning on the stockpiling switch slightly dampens the extreme cycles in the results.

In the model, the nickel price applies to both class I and class II nickel, so even though over time there is more demand for class I nickel, this is not reflected in the supply and in many runs a shortage of class I occurs alongside oversupply of class II. This class II nickel would then have to undergo further processing to be suitable for use in batteries, which would lead to additional costs that were not considered in the model (see appendix N12 for the amount of nickel this applies to in the model).

According to Gordon (2020), the division of class I and class II should not matter for investors, who should instead look at the market holistically. Based on this, it may not matter much that the model is structured the way it is. However, it could still be interesting in future research to see if there is a way to get supply and demand to match better with each other for each individual class.

Because supply and demand of class I and class II don't always match with each other, the percentage of a certain class in scrap can be misrepresented in the model. For primary nickel scrap, these percentages were based on supply. However, for secondary nickel scrap they were based on delayed demand.

If further processing occurs (which would also lead to more primary scrap than currently included), the fractions in scrap may fit better with supply, but in all runs with a lack of resilience, the percentages in scrap may remain misrepresented. This is therefore worth looking into in future research. In addition, more research on recycling of the different demand categories of nickel, especially battery recycling, could help further improve the way recycling was modelled in this thesis.

4.4.3 Price system

The cost calculations in the model are quite simplified and many more factors than those included play a role. The same goes for the determination of investment attractiveness. An important limitation is that no distinction was made between the capital costs, the reagent costs, the development times and the by-product recovery rates of the different processing technologies. These are all factors that differ per processing method in reality. This could be included in future adaptations of the model.

As stated earlier in this section, an energy calculation method switch was included in the model, but it was not used in the experimental set-up. This switch allows the use of two alternative methods for determining final energy use, based on formulas by Valero et al. (2013) and Elshkaki et al. (2017).

Important differences between the method used in the experimental set-up on one hand and the two alternative methods on the other hand, are that for the former there is no impact of ore grade on processing, and for the latter there is less distinction between the different processing methods. Test runs indicate that changing between these methods does not have a large impact on the average periodic nickel price and on the cumulative mined nickel, but it could be interesting to assess this further in future research.

Averages in the model, such as average final energy use, were calculated based on the number of existing mines. However, relative volumes were not considered in these calculations. This is an important shortcoming that should be rectified in future adaptations of the model.

Ore grade was modelled in two steps. First, the average ore grade for the reserves and resources mentioned in the database by Mudd (2020) was used and once these original resources ran out, ore grade declined based on cumulative mined nickel and a power for ore grades (see appendix I1.1 for a more detailed explanation). In future research, it could be interesting to adapt this in such a way that the change in ore grade based on the database becomes more continuous, instead of jumping discretely from average to average.

Not much attention was paid to the DSM of manganese nodules in this thesis, even though it is 8% of current resources (see appendix G1). Further research could look into this more, especially the costs, because now a highly uncertain assumption is used of twice the energy costs of land-based mining and 2 - 20 times the capital costs. Currently, DSM is not activated in the model, probably because it is deemed too expensive. In future research it is interesting to determine a more accurate relation between DSM and land-based mining.

There are multiple limitations to the way by-products were included in the model. The main limitation is the determination of by-product scarcity. This was based on nickel scarcity and for by-products with a larger share coming from other deposit types, the scarcity was made to be more out of sync with the nickel scarcity. In future research other options for including by-product scarcity could be explored.

Nickel dynamics drive the model because, in most cases, nickel is the host metal of a certain deposit. However, nickel dynamics also drive platinum mining in the model, even though in some deposits platinum is the host metal. In these deposits, the platinum is always recovered, so in a way platinum does have a larger impact on the profitability of the deposit than the by-products. However, in future adaptations of the model, platinum could be given a more important role.

Nickel remains the host metal of all deposits throughout the model. However (especially in the runs where final energy use shoots up; see figure 3.8), it could be beneficial to include the possibility of a change in host metal to the model. This would mean that a certain by-product would take over as a host metal and nickel would become a by-product, with the potential to not be recovered, if that is economically more attractive when mining the new host metal.

The by-products were modelled in a cruder way than nickel, which makes sense because they are not the main interest of this research. However, palladium and cobalt were highlighted more in this research and it is important to note that in the case of palladium a very uncertain formula was used (see table I9 in appendix I2.1). In future research, it would be beneficial to find more accurate data for palladium.

The collection of most of the data used in the model was done with utmost care. However, due to time constraints, the search for some data, specifically the royalties, was done in a more superficial way. In future research, better data could be collected for the royalties. In addition, the potential for making the royalties more dynamic could be explored.

In the model, many economic processes that exist in reality were not included, which may have contributed to the large extremes. For example, the price in the model does not react to knowledge of the development of new mines and capacity. It only reacts once mining actually starts for a new project. In reality, price may already react when there is knowledge of increased supply in the future. This could be added in future adaptations of the model. Long-term contracts were also not included in the model. By adding such contracts in future adaptations, the variability could perhaps be dampened further.

There is a discrepancy between what is profitable in the model in initial years and what is profitable in reality based on where certain operating capacity is located. This indicates, that although many factors were considered, there are likely many more factors that play a role in the profitability and the relative attractiveness of certain projects. Research can be done to determine more of these factors that could then be included in the model.

Price was used as an indicator for resilience in this thesis. However, as stated in section 3.4.2, price is based on perceived scarcity and not on actual scarcity, because of the delay in the administration of postponed demand. This slightly reduces the usefulness of price as an indicator for resilience in some cases.

On the other hand, the inclusion of postponed demand in the model, may be the reason that scarcity fluctuates around 2 instead of around 1 in figure 3.7. Postponed demand is a difficult to model variable with a large impact on the model. In future research, more attention could be paid to the best way in which postponed demand can be included in the model.

4.4.4 Sustainability impacts

The number of assessed sustainability impacts was limited in this analysis. The focus was on final energy use and GHG emissions. In future research, it would be interesting to also assess other environmental impact categories. Once more detailed nickel LCA's become available for different processing methods, these can be incorporated in the model. In addition, more aspects than only the electricity mix could be made dynamic. Furthermore, more attention could be given to the social and economic aspects of sustainability.

The choice was made to look at final energy demand, excluding energy products for non-energy use, in this research instead of PED because this was easier to include for a dynamic energy mix. However, in future research it could also be interesting to determine PED, as this is an indicator that is more frequently used and that gives a better indication of lifecycle energy requirements. To do this, (dynamic) conversion efficiencies would have to be added to the model for the different electricity generation technologies. Data for non-energy should then also be included.

Impacts (and costs) were only included up to refining, not for other steps of the supply chain. Energy use and GHG emissions were also not included for recycling. This favours recycling more than would be realistic, which is why no comparison could be made for energy requirements and GHG emissions as a result of the different EoL waste management strategies. This could be included in future adaptations of the model.

Regarding the sustainability policies included in the model, carbon price was automatically included in the 1.5 °C ET scenarios. However, because carbon price turned out to have quite a large impact on the marginal costs and thereby the price, in future research it could be interesting to assess the impact of these scenarios without the carbon price. This may, however, mean that they would then no longer be in line with the 1.5 °C target.

Especially in SSP5-19, the carbon costs become quite high. This is mainly because renewable energy technologies were only included in the model for electricity generation, not for direct fuel use. It was assumed that, in the mining industry, fossil fuels would continue to be used for transport and heating purposes. However, especially in the ET scenarios, the share of EVs increases rapidly, so such vehicles could also potentially be used in the mining industry. Biofuels, hydrogen and other synthetic fuels could also be used in the future. In fact, the way the electricity price was calculated actually counts on such changes. This could be considered in future adaptations of the model and it would lead to lower GHG emissions and thereby lower carbon costs in the ET scenarios.

The carbon tax was the only type of environmental cost included in the model. Other costs for environmental impacts could potentially be included in future adaptations in combination with other impact categories.

In future research, it could also be interesting to look at additional sustainability policies, including energy efficiency improvements, material efficiency improvements and carbon intensity improvements in addition to the autonomous developments. This is something that was done by Manberger & Stenqvist (2018), who included scenarios with 2 - 5% material intensity improvement.

Overall, the current research has led to the generation of a large amount of data, with numerous opportunities for future research. The most important contribution of this thesis is not in the data and assumptions, but in the model itself, which can be adapted and refined in further research, where more stakeholder input is included, to make the outcomes more robust and useful for decision making.

References

- Amit, R. K., Venugopal, S. (2018). Is this time different for electric vehicle (EV) battery materials? *FISITA World Automotive Congress 2018*, 1(1), 1617-1628.
- Auping, W. L. (2011). *The Uncertain Future of Copper: An Exploratory System Dynamics Model and Analysis of the Global Copper System in the Next 40 Years* (Delft University of Technology). Retrieved from <https://repository.tudelft.nl/islandora/object/uuid%3A4998f817-848d-4879-9d5f-2c0bd9ee4c81>
- Auping, W., Pruyt, E., & Kwakkel, J. H. (2012). Analysing the uncertain future of copper with three exploratory system dynamics models. In *Proceedings of the 30th International Conference of the System Dynamics Society, St. Gallen, Switzerland, 22-26 July 2012*. System Dynamics Society. <http://resolver.tudelft.nl/uuid:afda83f7-66fd-452c-baf2-b021007704a0>
- Auping, W. L. (2018). Modelling Uncertainty: Developing and Using Simulation Models for Exploring the Consequences of Deep Uncertainty in Complex Problems. Ede, NL: GVO Drukkers & Vormgevers. <https://doi.org/10.4233/uuid:0e0da51a-e2c9-4aa0-80cc-d930b685fc53>
- Bankes, S. C. (1993). Exploratory Modeling for Policy Analysis. *Operations Research*, 41(3), 435-449.
- Bleiwas, D.I. (1984). Nickel Availability – Market Economy countries: A mineral Availability Program Appraisal. Information Circular, Bureau of Mines, United States.
- Blok, K., & Nieuwlaar, E. (2021). *Introduction to energy analysis* (3rd edition), London and New York: Routledge, Taylor & Francis Group.
- BNEF (2019). *2H 2019 Battery Metals Outlook: Demand Realities*. Bloomberg finance L.P.
- Borshchev, A., & Filippov, A. (2004). *From System Dynamics and Discrete Event to Practical Agent Based Modeling: Reasons, Techniques, Tools*. In Proceedings of the 22nd International Conference of the System Dynamics Society, July 25-29, 2004, Oxford, England.
- Brown, T., Schlachtberger, D., Kies, A., Schramm, S., & Greiner, M. (2018). Synergies of sector coupling and transmission reinforcement in a cost-optimised, highly renewable European energy system. *Energy*, 160, 720-739.
- Bustamante, M. L., & Gaustad, G. (2016). Materials Research to Enable Clean Energy: Leverage Points for Risk Reduction in Critical By-product Material Supply Chains. In *REWAS 2016* (pp. 193-201). Springer, Cham.
- Choi, C. H., Cao, J., & Zhao, F. (2016). System dynamics modeling of indium material flows under wide deployment of clean energy technologies. *Resources, Conservation and Recycling*, 114, 59-71.
- Committee for mineral reserves international reporting standards (CRIRSCO, 2019). *International reporting template for the public reporting of exploration targets, exploration results, mineral resources and mineral reserves*. Retrieved from: [http://www.criusco.com/templates/CRIRSCO International Reporting Template November 2019.pdf](http://www.criusco.com/templates/CRIRSCO%20International%20Reporting%20Template%20November%202019.pdf)
- Crundwell, F., Moats, M., Ramachandran, V. & Robinson, T., & Davenport, W. (2011). *Nickel Production, Price and Extractions Costs*. Extractive Metallurgy of Nickel, Cobalt and Platinum Group Metals. 21-37. doi: 10.1016/B978-0-08-096809-4.10002-4

- De Koning, A., Kleijn, R., Huppel, G., Sprecher, B., van Engelen, G., & Tukker, A. (2018). Metal supply constraints for a low-carbon economy? *Resources, Conservation and Recycling*, 129, 202-208.
- Dry, M. (2013). Early evaluation of metal extraction projects. *Alta Nickel-Cobalt-Copper Conference*. Perth, Australia. Retrieved from: <https://www.researchgate.net/publication/290390996> EARLY EVALUATION OF METAL EXTRACTION PROJECTS
- Eckelman, M. J. (2010). Facility-level energy and greenhouse gas life-cycle assessment of the global nickel industry. *Resources, conservation and recycling*, 54(4), 256-266.
- Energy Information Administration (EIA, 2019a). *International Energy Outlook 2019: With projections to 2050*. Retrieved from <https://www.eia.gov/outlooks/ieo/pdf/ieo2019.pdf>
- Elshkaki, A. (2013). An analysis of future platinum resources, emissions and waste streams using a system dynamic model of its intentional and non-intentional flows and stocks. *Resources Policy*, 38(3), 241-251.
- Elshkaki, A., Reck, B. K., & Graedel, T. E. (2017). Anthropogenic nickel supply, demand, and associated energy and water use. *Resources, Conservation and Recycling*, 125, 300-307.
- EuRIC (2020). Metal Recycling Fact Sheet [brochure]. Retrieved from <https://www.euric-aisbl.eu/position-papers/item/335-euric-unveils-metal-recycling-brochure>
- Forrester, J. (1958). Industrial dynamics. A major breakthrough for decision makers. *Harvard Business Review*, 36 (4), 37-66. doi: 10.1225/58404
- Forrester, J. (1961). *Industrial Dynamics*. Cambridge, MA: MIT Press.
- Forrester, J. (1995). The beginning of system dynamics. *The McKinsey Quarterly* (4), 4–16.
- Fraser Institute (2020). *Survey of Mining Companies 2019*. Retrieved from <https://www.fraserinstitute.org/studies/annual-survey-of-mining-companies-2019>
- Futrell, G.A., Mueller, A.G., & Grimes, G. (2019). *Understanding Hog Production and Prices Cycles*. Retrieved from: <https://swine.extension.org/understanding-hog-production-and-price-cycles/>
- Giurco, D., Dominish, E., Florin, N., Watari, T., & McLellan, B. (2019). Requirements for minerals and metals for 100% renewable scenarios. In *Achieving the Paris Climate Agreement Goals* (pp. 437-457). Springer, Cham.
- Gloeser-Chahoud, S., Kuehn, A., & Tercero Espinoza, L. A. (2016). Global use structures of the magnetic materials neodymium and dysprosium. A scenario-based analysis of the effect of the diffusion of electromobility on the demand for rare earths. *Working Paper Sustainability and Innovation*. 48(17). 1-54.
- Golroudbary, S. R., Calisaya-Azpilcueta, D., & Kraslawski, A. (2019). The Life Cycle of Energy Consumption and Greenhouse Gas Emissions from Critical Minerals Recycling: Case of Lithium-ion Batteries. *Procedia CIRP*, 80, 316-321. <https://doi.org/10.1016/j.procir.2019.01.003>
- Gordon, M. (2020). *Nickel Class 1 & 2: Why does it matter for investors*. Crux investor. Retrieved from: <https://articles.cruxinvestor.com/class-1-class-2-why-does-it-matter-for-investors>

- Grosjean, C., Miranda, P. H., Perrin, M., & Poggi, P. (2012). Assessment of world lithium resources and consequences of their geographic distribution on the expected development of the electric vehicle industry. *Renewable and Sustainable Energy Reviews*, 16(3), 1735-1744.
- Harmsen, J. H. M., Roes, A. L., & Patel, M. K. (2013). The impact of copper scarcity on the efficiency of 2050 global renewable energy scenarios. *Energy*, 50, 62-73.
- Hoenderdaal, S., Espinoza, L. T., Marscheider-Weidemann, F., & Graus, W. (2013). Can a dysprosium shortage threaten green energy technologies? *Energy*, 49, 344-355.
- Houari, Y., Speirs, J., Candelise, C., & Gross, R. (2014). A system dynamics model of tellurium availability for CdTe PV. *Progress in Photovoltaics: Research and Applications*, 22(1), 129-146.
- Hydrogen Council (HC, 2017). Hydrogen Scaling up. Retrieved from: <https://hydrogencouncil.com/wp-content/uploads/2017/11/Hydrogen-scaling-up-Hydrogen-Council.pdf>
- International Energy Agency (IEA, 2017a). *Energy Technology Perspectives 2017: Catalysing Energy Technology Transformations*. Retrieved from https://webstore.iea.org/download/direct/1058?fileName=Energy_Technology_Perspectives_2017-PDF.pdf
- International Energy Agency (IEA, 2017b). *The Future of Trucks: implications for energy and the environment*. Retrieved from <https://webstore.iea.org/download/direct/288>
- International Energy Agency (IEA, 2020a). *Key World Energy Statistics 2020*. Retrieved from: https://webstore.iea.org/download/direct/4093?fileName=Key_World_Energy_Statistics_2020.pdf
- International Institute for Applied Systems Analysis (IIASA, 2018). *SSP Database: Shared Socioeconomic Pathways – version 2.0, December 2018*. Retrieved from: <https://tntcat.iiasa.ac.at/SspDb/dsd?Action=htmlpage&page=about>
- International Renewable Energy Agency (IRENA (2017). *Electricity Storage and Renewables: Costs and markets to 2030*. Retrieved from: https://www.irena.org/DocumentDownloads/Publications/IRENA_Electricity_Storage_Costs_2017.pdf
- International Renewable Energy Agency (IRENA, 2018). *Hydrogen from Renewable Power: Technology outlook for the energy transition*. Retrieved from: <https://www.irena.org/publications/2018/Sep/Hydrogen-from-renewable-power>
- Kleijn, R., & Van der Voet, E. (2010). Resource constraints in a hydrogen economy based on renewable energy sources: An exploration. *Renewable and sustainable energy reviews*, 14(9), 2784-2795.
- Kushnir, D., & Sandén, B. A. (2012). The time dimension and lithium resource constraints for electric vehicles. *Resources Policy*, 37(1), 93-103.
- Kwakkel, J. H. (2017). The Exploratory Modeling Workbench: An open-source toolkit for exploratory modeling, scenario discovery, and (multi-objective) robust decision making. *Environmental Modelling and Software*, 96, 239–250. doi: 10.1016/j.envsoft.2017.06.054
- Kyle, J. (2010) Nickel laterite processing technologies – where to next? *In ALTA 2010 Nickel/Cobalt/Copper Conference, 24 - 27 May, Perth, Western Australia*. <https://researchrepository.murdoch.edu.au/id/eprint/4340/>
- Lempert, R. J., Popper, S., & Bankes, S. (2003). *Shaping the next One Hundred Years: New methods for quantitative, long term policy analysis*. Santa Monica, CA: RAND.

- Månberger, A., & Stenqvist, B. (2018). Global metal flows in the renewable energy transition: Exploring the effects of substitutes, technological mix and development. *Energy policy*, 119, 226-241.
- Meylan, F. D., Moreau, V., & Erkman, S. (2016). Material constraints related to storage of future European renewable electricity surpluses with CO₂ methanation. *Energy Policy*, 94, 366-376.
- Moreau, V., Dos Reis, P. C., & Vuille, F. (2019). Enough Metals? Resource Constraints to Supply a Fully Renewable Energy System. *Resources*, 8(1), 29.
- Mudd, G. M. (2010). Global trends and environmental issues in nickel mining: Sulfides versus laterites. *Ore Geology Reviews*, 38(1-2), 9-26.
- Mudd, G. (2020). *Nickel Resources Database* [personal communication, 10 November, 2020]
- Nassar, N. T., Graedel, T. E., & Harper, E. M. (2015). By-product metals are technologically essential but have problematic supply. *Science advances*, 1(3)
- Nickel institute (n.d.). *About Nickel*. Retrieved from: <https://nickelinstitute.org/about-nickel/>
- Nickel Institute (2016). *Nickel Recycling*. Retrieved from: https://www.nickelinstitute.org/media/2273/nickel_recycling_2709_final_nobleed.pdf
- Nickel Institute (2020). *Life Cycle Assessment of Nickel Products: Reference year 2017*. Final Report.
- Pehl, M., Arvesen, A., Humpenöder, F., Popp, A., Hertwich, E. G., & Luderer, G. (2017). Understanding future emissions from low-carbon power systems by integration of life-cycle assessment and integrated energy modelling. *Nature Energy*, 2(12), 939-945.
- Pruyt, E. (2013). *Small system dynamics models for big issues: Triple jump towards real-world complexity*. Delft: TU Delft Library. 324p.
- Riahi, K., Van Vuuren, D. P., Kriegler, E., Edmonds, J., O'Neill, B. C., Fujimori, S., ... & Lutz, W. (2017). The shared socioeconomic pathways and their energy, land use, and greenhouse gas emissions implications: an overview. *Global Environmental Change*, 42, 153-168.
- Rietveld, E., Boonman, H., van Harmelen, T., Hauck, M., Bastein, T. (2019). *Global Energy Transition and Metal Demand - An Introduction and Circular Economy Perspectives*. TNO. Doi: 10.13140/RG.2.2.25790.54086
- Ritchie, H., & Roser, M. (2016). *Greenhouse Gas Emissions*. Our World in Data. Retrieved from: <https://ourworldindata.org/greenhouse-gas-emissions#:~:text=Greenhouse%20gases%20are%20measured%20in,were%20around%2035%20billion%20tonnes>
- Rogelj, J., Luderer, G., Pietzcker, R. C., Kriegler, E., Schaeffer, M., Krey, V., & Riahi, K. (2015). Energy system transformations for limiting end-of-century warming to below 1.5 C. *Nature Climate Change*, 5(6), 519.
- Schmidt, T., Buchert, M., & Schebek, L. (2016). Investigation of the primary production routes of nickel and cobalt products used for Li-ion batteries. *Resources, Conservation and Recycling*, 112, 107-122.
- Sprecher, B., Daigo, I., Murakami, S., Kleijn, R., Vos, M., & Kramer, G. J. (2015). Framework for resilience in material supply chains, with a case study from the 2010 rare earth crisis. *Environmental science & technology*, 49(11), 6740-6750.

- Sprecher, B., Reemeyer, L., Alonso, E., Kuipers, K., & Graedel, T. E. (2017). How “black swan” disruptions impact minor metals. *Resources Policy*, 54, 88-96.
- Stamp, A., Wäger, P. A., & Hellweg, S. (2014). Linking energy scenarios with metal demand modeling—The case of indium in CIGS solar cells. *Resources, Conservation and Recycling*, 93, 156-167.
- Strategic Dialogue on Sustainable Raw Materials for Europe (STRADE, 2016). *European Policy Brief: The Cost Competitiveness of Mining Operations in the European Union*. No.08/2016. Retrieved from: <https://st6.ning.com/topology/rest/1.0/file/get/3410397167?profile=original>
- Sumitomo Metal Mining Col, Ltd (SMM, n.d.). *Producing High-Quality Products form Low-Grade Nickel Oxide Ore*. Retrieved from: https://www.smm.co.jp/E/csr/activity_highlights/persistence/highlights1.html
- Tokimatsu, K., Höök, M., McLellan, B., Wachtmeister, H., Murakami, S., Yasuoka, R., & Nishio, M. (2018). Energy modeling approach to the global energy-mineral nexus: Exploring metal requirements and the well-below 2° C target with 100 percent renewable energy. *Applied energy*, 225, 1158-1175.
- Transparency International (2020). *Corruption Perception Index 2019*. Retrieved from <https://www.transparency.org/en/cpi/2019/index/nzl>
- United States Geological Survey (USGS, 2020a). *National Minerals Information Centre: Nickel Statistics and Information*. Retrieved from: <https://www.usgs.gov/centers/nmic/nickel-statistics-and-information>
- Valero, A., Valero, A., & Domínguez, A. (2013). Exergy replacement cost of mineral resources. *Journal of environmental accounting and management*, 1(1), 147-148.
- Valero, A., Valero, A., Calvo, G., & Ortego, A. (2018a). Material bottlenecks in the future development of green technologies. *Renewable and Sustainable Energy Reviews*, 93, 178-200.
- Van der Linden (2020). Exploration of the Cobalt System: Scenarios for a critical material for the energy system. *Delft University of Technology*. <https://repository.tudelft.nl/islandora/object/uuid%3Ae51dbb87-09f7-4c33-a956-226874a1e7b7?collection=education>
- Ventana System. (2010). *Vensim reference manual*. Harvard, MA: Ventana Systems, Inc.
- Vesborg, P. C., & Jaramillo, T. F. (2012). Addressing the terawatt challenge: scalability in the supply of chemical elements for renewable energy. *Rsc Advances*, 2(21), 7933-7947.
- Watari, T., McLellan, B., Ogata, S., & Tezuka, T. (2018). Analysis of potential for critical metal resource constraints in the international energy agency’s long-term low-carbon energy scenarios. *Minerals*, 8(4), 156.
- Watari, T., McLellan, B. C., Giurco, D., Dominish, E., Yamasue, E., & Nansai, K. (2019). Total material requirement for the global energy transition to 2050: A focus on transport and electricity. *Resources, Conservation and Recycling*, 148, 91-103.
- WBMS (2018) *Nickel Workbook June 2018* [personal communication, 12 May, 2020]
- World Energy Council (WEC, 2011). *Global Transport Scenarios 2050*. Retrieved from: https://www.worldenergy.org/assets/downloads/wec_transport_scenarios_2050.pdf
- Wood Mackenzie (n.d.): Figure in Els, F. (2018). *Electric vehicle demand will double nickel price – as soon as 2022*. Retrieved from: <http://www.mining.com/electric-vehicle-demand-will-double-nickel-price-soon-2022>

Zerrahn, A., Schill, W. P., & Kemfert, C. (2018). On the economics of electrical storage for variable renewable energy sources. *European Economic Review*, 108, 259-279.

Appendices

The Future of Nickel in a Transitioning World

Exploratory System Dynamics Modelling and Analysis of the Global Nickel Supply Chain and its Nexus with the Energy System



Universiteit
Leiden

Jessie Bradley
2156164; 4908244
Supervisor 1: Benjamin Sprecher
Supervisor 2: Willem Auping
MSc. Industrial Ecology
Leiden University & TU Delft
18/3/2021

Table of Contents Appendices

| | |
|--|----|
| List of figures and tables appendices | 4 |
| List of abbreviations appendices | 9 |
| Appendix A: Literature on materials for the energy transition | 13 |
| Appendix B: Detailed model structure | 16 |
| Appendix C: Background, assumptions & data: energy system | 21 |
| Appendix C1: Electricity generation | 21 |
| Appendix C1.1: Nickel intensities of electricity generation technologies | 22 |
| Appendix C1.2: Lifetimes of electricity generation technologies | 23 |
| Appendix C2: Storage technologies | 24 |
| Appendix C2.1: Nickel intensities of storage technologies | 24 |
| Appendix C2.2: Lifetimes of storage technologies | 25 |
| Appendix C3: Transport technologies | 26 |
| Appendix C3.1: Battery capacities of vehicle technologies | 26 |
| Appendix C3.2: Lifetimes of vehicle technologies | 27 |
| Appendix C4: Relationships between the sectors | 28 |
| Appendix D: Background, assumptions & data: energy scenarios | 30 |
| Appendix D1: Electricity generation scenarios | 30 |
| Appendix D1.1: SSP data | 31 |
| Appendix D2: Storage scenarios | 33 |
| Appendix D2.1: Flexibility scenarios | 34 |
| Appendix D2.2: PHS, CSP TES and V2G shares | 36 |
| Appendix D2.3: Battery repurposing | 37 |
| Appendix D2.4: Behind the meter storage | 37 |
| Appendix D2.5: Battery market shares | 38 |
| Appendix D3: Transport scenarios | 39 |
| Appendix D3.1: Electrification scenarios | 40 |
| Appendix D3.2: Hydrogen scenarios | 41 |
| Appendix D4: VRE share | 43 |
| Appendix E: Background, assumptions & data: price effects | 44 |
| Appendix E1: Resource depletion paradigms | 44 |
| Appendix E2: Price elasticity | 45 |

| | |
|--|-----------|
| Appendix E3: Substitution | 45 |
| Appendix E4: Intensity improvement | 47 |
| Appendix F: Demand sub model input and data sources | 50 |
| Appendix G: Background, assumptions & data: supply dynamics | 54 |
| Appendix G1: Nickel resources | 54 |
| Appendix G1.1: Exploration | 54 |
| Appendix G1.2: Resources to reserves | 55 |
| Appendix G2: Production capacity | 57 |
| G2.1 Operating and mothballed capacity | 58 |
| G2.2 Creating new capacity | 60 |
| Appendix G3: Supply chain | 60 |
| G3.1 Nickel processing | 61 |
| G3.2 Losses and recycling | 62 |
| Appendix H: Supply sub model input and data sources | 65 |
| Appendix I: Background, assumptions & data: price dynamics | 68 |
| Appendix I1 Cost structure | 68 |
| Appendix I1.1: Energy for mining processing and transport | 68 |
| Appendix I1.2: Alternative energy calculation methods | 72 |
| Appendix I1.3: Processing energy cost allocation | 72 |
| Appendix I1.3: Energy price | 74 |
| Appendix I1.5: Royalties and taxes | 76 |
| Appendix I1.6: Reagents and other costs | 77 |
| Appendix I1.7: Carbon price | 77 |
| Appendix I2: By-products | 78 |
| Appendix I2.1: By-products in the model | 78 |
| Appendix I2.2: Mining energy cost allocation | 81 |
| Appendix I3: Nickel price and profit | 81 |
| Appendix I3.1: Historic nickel price | 82 |
| Appendix I3.2: Price calculation | 82 |
| Appendix I3.3: Profit calculation | 83 |
| Appendix I4: Investment attractiveness | 83 |
| Appendix J: Price sub model input and data sources | 85 |

| | |
|--|------------|
| Appendix K: Background, assumptions & data: impacts | 89 |
| Appendix K1: Greenhouse gas emissions | 89 |
| Appendix K2: SSP regional data | 93 |
| Appendix L: Impacts sub model input and data sources | 100 |
| Appendix M: Switches, base values and performance metrics | 101 |
| Appendix N: Additional results | 105 |
| Appendix N1: Additional demand projections | 105 |
| Appendix N2: Additional BAU single run results | 107 |
| Appendix N3: Additional energy transition results | 109 |
| Appendix N4: Additional results for other disruptions | 112 |
| Appendix N5: Additional sustainability policy results | 113 |
| Appendix N6: Additional structural uncertainty results | 115 |
| Appendix N7: Identification of influential parameters | 118 |
| Appendix N8: Additional parametric uncertainty results | 121 |
| Appendix N9: Results for a reduced global capacity increase | 123 |
| Appendix N10: Focus on ore grade | 125 |
| Appendix N11: Results for top supplying countries | 128 |
| Appendix N12: Class I vs class II nickel | 129 |
| Appendix O: Comparison with previous research | 130 |
| References appendices | 134 |

List of figures and tables appendices

Figures

| | | |
|-----------|--|----|
| Figure B1 | <i>More detailed version of the XLRM framework applied to the nickel model in this thesis</i> | 16 |
| Figure B2 | <i>Complete demand sub-model</i> | 17 |
| Figure B3 | <i>Complete supply sub-model</i> | 18 |
| Figure B4 | <i>Complete price sub-model</i> | 19 |
| Figure B5 | <i>Complete impacts sub-model</i> | 20 |
| Figure C1 | <i>Physical components of the energy system</i> | 21 |
| Figure C2 | <i>Nickel containing components considered in this thesis and their relationships</i> | 28 |
| Figure D1 | <i>SSPs and RCPs</i> | 30 |
| Figure D2 | <i>Profiles of the storage capacity scenarios discussed by Zerrahn et al. (2018) and those used in the model</i> | 35 |
| Figure D3 | <i>Types of grid electricity storage considered in this thesis and types of SBS</i> | 37 |
| Figure D4 | <i>The four transport scenarios included in this thesis</i> | 40 |
| Figure D5 | <i>Vehicle market shares for the ET and BAU electrification scenarios</i> | 41 |
| Figure D6 | <i>Vehicle market shares for the ET and BAU hydrogen scenarios</i> | 42 |
| Figure E1 | <i>Various options at different levels to fulfil the functions of moving 1 km and delivering 1 kWh of electricity</i> | 46 |
| Figure E2 | <i>Variables that influence nickel intensity in batteries, vehicles and electricity generation technologies</i> | 48 |
| Figure G1 | <i>Global distribution and ore type of nickel resources and reserves per country</i> | 54 |
| Figure G2 | <i>Nickel reserves, production and R/P ratio from 2000 to 2019</i> | 56 |
| Figure G3 | <i>Static nickel material flow diagram for the year 2015</i> | 57 |
| Figure G4 | <i>Mechanism for mothballing and restarting</i> | 60 |
| Figure I1 | <i>Final energy intensity range for nickel production</i> | 69 |
| Figure I2 | <i>Final energy demand for various processing methods broken down by energy type and processing stage. Full allocation to nickel was applied</i> | 73 |
| Figure I3 | <i>Final energy demand for various processing methods broken down by energy type and processing stage. Mass based allocation was applied</i> | 74 |
| Figure I4 | <i>Fuel price scenarios used in the model</i> | 74 |
| Figure I5 | <i>Calculated costs for reagents and other per processing energy allocation method</i> | 77 |
| Figure I6 | <i>Nickel price for the past 25 years in US\$/tonne</i> | 82 |

| | | |
|------------|--|-----|
| Figure I7 | <i>Correlation between investment attractiveness and corruption</i> | 83 |
| Figure N1 | <i>Impact of the transport scenario on final demand and substitution</i> | 105 |
| Figure N2 | <i>Demand changes due to price elasticity and battery substitution per assessed SSP</i> | 105 |
| Figure N3 | <i>Demand request and postponed demand for the OCP and the FSP</i> | 106 |
| Figure N4 | <i>Nickel demand for electricity generation capacity and SBS per SSP</i> | 106 |
| Figure N5 | <i>Nickel demand for SBS per flexibility scenario and for EV battery lifetime</i> | 107 |
| Figure N6 | <i>Share of processing per technology for a single run with base settings</i> | 107 |
| Figure N7 | <i>Share of operating capacity per country for a single run with base settings</i> | 108 |
| Figure N8 | <i>Number of mines from which certain by-products are recovered for a single run with base settings</i> | 108 |
| Figure N9 | <i>Resilience for the four assessed SSPs for single runs with base settings</i> | 109 |
| Figure N10 | <i>Average marginal costs for royalties and reagents and other costs</i> | 109 |
| Figure N11 | <i>By-product credits and average marginal costs for deposits</i> | 109 |
| Figure N12 | <i>Average final energy use for mining and processing</i> | 110 |
| Figure N13 | <i>Average energy costs for mining per SSP and average energy costs for processing & refining per SSP, per fuel price scenario and per processing energy allocation method</i> | 110 |
| Figure N14 | <i>Total annual final energy use and total annual GHG emissions of all mines combined</i> | 111 |
| Figure N15 | <i>Fraction of existing mines per mine type and per ore type</i> | 111 |
| Figure N16 | <i>Additional results for the radical battery innovation disruption</i> | 112 |
| Figure N17 | <i>Additional results for the FSP</i> | 112 |
| Figure N18 | <i>Additional results for the influence of a 1-year supply disruption in 2030 and 2045 where mining stopped in the country with the largest share of supply at those times</i> | 113 |
| Figure N19 | <i>Additional results for EoL waste management</i> | 113 |
| Figure N20 | <i>Total recycling per EoL waste management strategy and per SSP</i> | 114 |
| Figure N21 | <i>Additional results for EV battery lifetime increase</i> | 114 |
| Figure N22 | <i>Additional results for processing energy allocation method</i> | 115 |
| Figure N23 | <i>Additional results for by-product inclusion</i> | 115 |
| Figure N24 | <i>Results for the option to mine resources just before a mine is potentially mothballed</i> | 116 |
| Figure N25 | <i>Results for the mining energy allocation method</i> | 117 |
| Figure N26 | <i>Results for the price method</i> | 117 |
| Figure N27 | <i>Variables with the highest impact on average periodic nickel price at different points in time</i> | 118 |
| Figure N28 | <i>Variables with the highest impact on average final energy use at different points in time</i> | 118 |
| Figure N29 | <i>Variables with the highest impact on final nickel demand at different points in time</i> | 119 |

| | | |
|------------|--|-----|
| Figure N30 | <i>Variables with the highest impact on nickel mining at different points in time</i> | 119 |
| Figure N31 | <i>Variables with the highest impact on average ore grade of existing mines at different points in time</i> | 119 |
| Figure N32 | <i>Variables with the highest impact on average ore grade of all deposits at different points in time</i> | 120 |
| Figure N33 | <i>Variables with the highest impact on cumulative GHG emissions at different points in time</i> | 120 |
| Figure N34 | <i>Variables with the highest impact on EoL RR at different points in time</i> | 120 |
| Figure N35 | <i>Average final energy use and average ore grade of existing mines for various parameters</i> | 121 |
| Figure N36 | <i>Degree of nickel scarcity and the average periodic nickel price for various parameters</i> | 122 |
| Figure N37 | <i>Difference between cumulative demand and consumption per SSP and for lower values for administration of postponed demand (≤ 1 year) and higher values (> 1 year)</i> | 123 |
| Figure N38 | <i>Additional results for exploration</i> | 123 |
| Figure N39 | <i>Variables with the highest impact on average periodic nickel price at different points in time for a global maximum capacity increase percentage between 1% and 30%</i> | 124 |
| Figure N40 | <i>Results for performance metrics for global maximum capacity increase ($\leq 0.10 = \text{low}$, $> 0.10 = \text{high}$)</i> | 124 |
| Figure N41 | <i>The impact of SSP, by-product inclusion, power for ore grade (high > 0.3; low ≤ 0.3) and power for price-based exploration (high > 0.7; low ≤ 0.7) on average ore grade of existing mines and average ore grade of known deposits for the OCP</i> | 126 |
| Figure N42 | <i>The impact of mining resources, loss reduction, average maximum mothball time (long > 20 years; short ≤ 20 years) and global maximum capacity increase (high > 0.25; low ≤ 0.25) on average ore grade of existing mines and average ore grade of known deposits for the FSP</i> | 127 |
| Figure N43 | <i>Share of operating capacity for top supplying countries per SSP</i> | 128 |
| Figure N44 | <i>Additional processing required when less class I nickel is produced than required and more class II is produced than required</i> | 129 |
| Figure O1 | <i>Cumulative nickel demand reported in previous research and in the current study for both the BAU scenario and the ET scenarios</i> | 132 |
| Figure O2 | <i>Difference in fuel price in the model by Van der Linden (2020) and the current model</i> | 132 |
| Figure O3 | <i>Cumulative cobalt demand reported in previous research and cumulative <u>mined</u> cobalt in the current study</i> | 133 |

Tables

| | | |
|----------|--|----|
| Table A1 | <i>Research done on the material requirements of the ET</i> | 13 |
| Table C1 | <i>Nickel intensities of electricity generation technologies</i> | 22 |
| Table C2 | <i>Lifetimes of electricity generation technologies</i> | 23 |
| Table C3 | <i>Lithium-ion battery chemistries, energy densities, nickel intensities, market share and applications for 2018</i> | 25 |

| | | |
|-----------|--|----|
| Table C4 | <i>Lifetimes of battery technologies</i> | 26 |
| Table C5 | <i>Battery capacity of vehicles</i> | 27 |
| Table C6 | <i>Lifetimes of vehicle technologies</i> | 27 |
| Table D1 | <i>The four selected scenarios consisting of marker scenarios compatible with RCP 1.9 and a BAU scenario</i> | 31 |
| Table D2 | <i>Data for the SSP1-19 scenario</i> | 31 |
| Table D3 | <i>Data for the SSP2-19 scenario</i> | 32 |
| Table D4 | <i>Data for the SSP5-19 scenario</i> | 32 |
| Table D5 | <i>Data for the SSP2-baseline scenario</i> | 32 |
| Table D6 | <i>The three flexibility scenarios used in the nickel model</i> | 35 |
| Table D7 | <i>Values for storage as fraction of electricity demand used in the flexibility scenarios and additional values in profiles by Zerrahn (2018) and Sinn (2017).</i> | 35 |
| Table D8 | <i>Data for the battery market shares</i> | 38 |
| Table D9 | <i>Vehicle market shares for the ET electrification scenario</i> | 40 |
| Table D10 | <i>Vehicle market shares for the BAU electrification scenario</i> | 41 |
| Table D11 | <i>Vehicle market shares for the ET hydrogen scenario</i> | 42 |
| Table D12 | <i>Vehicle market shares for the BAU hydrogen scenario</i> | 42 |
| Table D13 | <i>Assumptions for basing variable changes on VRE share</i> | 43 |
| Table E1 | <i>How different types of potential are determined in the two paradigms</i> | 45 |
| Table E2 | <i>Potential nickel substitution in stainless steel and batteries</i> | 45 |
| Table F1 | <i>Values and data sources used for the constants and lookups in the demand sub model.</i> | 50 |
| Table G1 | <i>Different types of mining capacity included in the model and the status they have at the start of the model</i> | 58 |
| Table G2 | <i>Nickel mine production (tonne/year), number of operating mines and estimated average operating capacity (tonne/year)</i> | 59 |
| Table G3 | <i>Principal nickel processing methods and the number (and percentage) of deposits with this method in the database by Mudd (2020)</i> | 61 |
| Table G4 | <i>Losses at different stages of the supply chain</i> | 64 |
| Table H1 | <i>Values and data sources used for the constants and lookups in the supply sub model</i> | 65 |
| Table I1 | <i>Final energy requirements for processes</i> | 69 |
| Table I2 | <i>Average nickel content of the different final and intermediate products</i> | 72 |
| Table I3 | <i>Nickel containing countries per region as classified by IASA (2018)</i> | 75 |
| Table I4 | <i>Renewable energy shares for SSP1-19 per region</i> | 75 |
| Table I5 | <i>Renewable energy shares for SSP2-19 per region</i> | 75 |

| | | |
|-----------|--|-----|
| Table I6 | <i>Renewable energy shares for SSP5-19 per region</i> | 75 |
| Table I7 | <i>Renewable energy shares for SSP2-baseline per region</i> | 76 |
| Table I8 | <i>Royalties per country as fraction of sales</i> | 76 |
| Table I9 | <i>By-product data</i> | 79 |
| Table I10 | <i>Fraser investment attractiveness score, corruption perception score and normalised corruption perception score per country in the model</i> | 84 |
| Table J1 | <i>Values and data sources used for the constants and lookups in the price sub model</i> | 85 |
| Table K1 | <i>GWP of nickel processing technologies for the current electricity mix</i> | 90 |
| Table K2 | <i>Contribution of electricity to the GWP of nickel processing technologies and final values used for GWP (in kg CO2 eq./kg Ni) excluding electricity in the model</i> | 91 |
| Table K3 | <i>GWP for electricity generation technologies</i> | 92 |
| Table K4 | <i>Electricity mix per region for SSP1-19</i> | 93 |
| Table K5 | <i>Electricity mix per region for SSP2-19</i> | 94 |
| Table K6 | <i>Electricity mix per region for SSP5-19</i> | 96 |
| Table K7 | <i>Electricity mix per region for SSP2-baseline</i> | 97 |
| Table L1 | <i>Values and data sources used for the constants and lookups in the impacts sub model.</i> | 100 |
| Table M1 | <i>Switches included in the model, the number of options per switch and the base value</i> | 101 |
| Table M2 | <i>Key uncertainties in the model, their range and their base values</i> | 102 |
| Table M3 | <i>Performance metrics assessed in the results</i> | 103 |
| Table O1 | <i>Differences in the assumptions used for factors determining the amount of nickel in EV batteries and in the RoE for Van der Linden (2020) and the current study</i> | 130 |

List of abbreviations appendices

| | |
|------|---|
| A&C | Availability and Consumption |
| ACEA | European Automobile Manufacturers Association |
| ATES | Aquifer Thermal Energy Storage |
| ATL | Atmospheric Leaching |
| B2DS | Beyond 2 °C Scenario |
| BAU | Business As Usual |
| BEV | Battery Electric Vehicle |
| BF | Blast Furnace |
| BP | British Petroleum |
| BNEF | Bloomberg New Energy Finance |
| CCS | Carbon Capture and Storage |
| CE | Consumer Electronics |
| CF | Capacity factor |
| CAC | Cumulative Availability Curve |
| CAES | Compressed Air Energy Storage |
| CHP | Combined Heat and Power |
| CPI | Corruption Perception Index |
| C-Si | Crystalline silicon |
| CSP | Concentrated Solar Power |
| C&M | Care and Maintenance |
| DNI | Direct Nickel |
| DSM | Deep Sea Mining |
| DSO | Direct Shipping Ore |
| EAF | Electric Arc Furnace |
| EB | Electric Bus (E-Bus) |
| EC | European Commission |
| EIA | Energy Information Administration |
| EITI | Extractive Industries Transparency Initiative |
| EoL | End of Life |

| | |
|-----------|---|
| EoL CR | End of Life Collection Rate |
| EoL PR | End of Life Processing Rate |
| EoL RR | End of Life Recycling Rate |
| E/P | Energy/Power |
| ERC | Exergy Replacement Costs |
| EROI | Energy Return on energy Investment |
| ET | Energy Transition |
| ETr | Electric Truck (E-Truck) |
| EuRIC | European Recycling Industries' Confederation |
| EV | Electric Vehicle |
| FC-Bus | Fuel Cell Bus |
| FCH | Fuel Cells and Hydrogen |
| FC-Truck | Fuel Cell Truck |
| FC(E)V | Fuel Cell (Electric) Vehicle |
| FSP | Fixed Stock Paradigm |
| GDP | Gross Domestic Product |
| GHG | Greenhouse Gas |
| GWP | Global Warming Potential |
| GVR | Grand View Research |
| HC | Hydrogen Council |
| HEV | Hybrid Electric Vehicle |
| HL | Heap Leaching |
| HM | Hydrometallurgical |
| HPAL | High Pressure Acid Leaching |
| HVAC | Heating, Ventilation and Air Conditioning |
| IAM | Integrated Assessment Model |
| ICA | International Copper Association |
| ICE | Internal Combustion Engine |
| IDE-JETRO | Institute of Developing Economies - Japan External Trade Organisation |
| IE | Industrial Ecology |
| IEA | International Energy Agency |

| | |
|-------|--|
| IIASA | International Institute for Applied Systems Analysis |
| IGCC | Integrated Gasification Combined Cycle |
| IHA | International Hydropower Association |
| IO | Input-Output |
| IPCC | Intergovernmental Panel on Climate Change |
| IRENA | International Renewable Energy Agency |
| IRR | Internal Rate of Return |
| ISSF | International Stainless-Steel Forum |
| IW | International Waters |
| LCA | Life Cycle Assessment |
| LCO | Lithium Cobalt Oxide |
| LFP | Lithium Iron Phosphate |
| LMO | Lithium Manganese Oxide |
| MFA | Material Flow Analysis |
| NCA | Nickel Cobalt Aluminium |
| NI | Nickel Institute |
| NMC | Nickel Manganese Cobalt |
| NMH | Nickel Metal Hydride |
| NPV | Net Present Value |
| OC | Open Cut |
| OCP | Opportunity Cost Paradigm |
| OECD | Organisation of Economic Cooperation and Development |
| PED | Primary Energy Demand |
| PHEV | Plug-in Hybrid Electric Vehicle |
| PHS | Pumped Hydro Storage |
| PM | Pyrometallurgical |
| PNG | Papua New Guinea |
| PPP | Purchasing Power Parity |
| PV | Photovoltaics |
| PWC | PricewaterhouseCoopers |
| RCP | Representative Concentration Pathway |

| | |
|--------|--|
| RE | Renewable Energy |
| REN21 | Renewable Energy Network 21 |
| RKEF | Rotary Kiln Electric arc Furnace |
| RoE | Rest of the Economy |
| R/P | Reserves over production ratio |
| RTS | Reference Technology Scenario |
| SBS | Stationary Battery Storage |
| SD | System Dynamics |
| SEC | Specific Energy Consumption |
| SMM | Sumitomo Metal Mining |
| SSP | Shared Socioeconomic Pathway |
| STRADE | Strategic Dialogue on Sustainable Raw Materials for Europe |
| TES | Thermal Energy Storage |
| TMR | Total Material Requirements |
| T&DI | Transmission and distribution infrastructure |
| UG | Underground |
| UN | United Nations |
| UNEP | United Nations Environment Programme |
| USA | United States of America |
| USDOE | United States Department of Energy |
| USGS | United States Geological Survey |
| USSEC | United States Securities and Exchange Commissions |
| V2G | Vehicle to Grid |
| VRE | Variable Renewable Energy |
| WEC | World Energy Council |
| WWF | World Wildlife Fund |
| XLRM | Exogenous uncertainties, levers, relationships and metrics |

Appendix A: Literature on materials for the energy transition

Table A1: research done on the material requirements of the ET. Nickel is highlighted in bold. Bottleneck materials can create constraints for the production of e.g. renewable energy infrastructure based on certain deployment targets. There is a risk of supply shortages for these materials (Valero et al., 2018a). The literature review to obtain these articles was done at the end of 2019. Articles published later on are not included. Abbreviations are described below.

| Topic | Scope | Components | Materials | Scenarios | Bottleneck | Source |
|--|---------------------|--|--|--|--|------------------------------|
| 'Requirements for Minerals and Metals for 100% Renewable Scenarios' | Global, 2015 - 2050 | Solar PV, wind, EVs, batteries | Li, Co, Ag | 1.5 °C, 100% renewable, 5 supply scenarios | Cumulative total demand for Li and Co exceeds reserves. | Giurco et al. (2019) |
| 'Dynamic Energy Return on Energy Investment (EROI) and material requirements' for the global energy transition | Global, 1995 - 2060 | Solar PV, CSP, wind, EV batteries, T&DI | Mg, V, Al, Cr, Zn, Ni , Mo, Cd, In, Cu, Pb, Te, Mn, Ga, Ag, Sn | Green growth scenario. Bottom-up assessment | Risk for Te, In, Ga, Ag, Sn based on reserves. Risk for Te, In based on resources | Capellan-Perez et al. (2019) |
| 'Enough Metals? Resource Constraints to Supply a Fully Renewable Energy System' | Global 2010 - 2050 | Solar PV, CSP, wind, hydro, ocean and various battery technologies | Al, Br, Cd, Cr, Co, Cu, Ga, Au, In, Zr, Fe, La, Pb, Li, Zn, Mg, Mn, Mo, Nd, Ni , Pd, Pt, Re, Ti, Sn, Rh, Ag, Ta, Te | IPCC, IEA, WWF/Ecofys, and IRENA scenarios | Risk for Cd, Co, Au, Pb, Ni , Ag, Sn, Zn based on current reserves. | Moreau et al. (2019) |
| 'Environmental Implications of Future Demand Scenarios for Metals' | Global, 2010 - 2050 | Focus on the electricity system, with different mixes. | Fe, Al, Cu, Zn, Pb, Ni , Mn | Adapted versions of the UN's GEO-4 scenarios | Not mentioned; focus is on environmental implications | Van der Voet et al. (2019) |
| Global Energy Transition and Metal Demand - An Introduction and Circular Economy Perspectives | Global, 2011 - 2050 | Focus on the electricity system | Ag, Al, Au, B, Cd, Ce, La, Co, Cr, Cu, Dy, Fe, Ga, Gd, Sm, Tb, In, Li, Mg, Mn, Mo, Nd, Ni , Pb, Pr, Pt, Pd, Se, Si, Sn, Ta, Te, Ti, V, Zn | Include an IO model. Use the B2D scenario by the IEA | Production needs speeding up for: Au, B, Cd, Ce, La, Cu, Dy, Ga, Gd, Sm, Tb, Li, Nd, Pb, Pr, Pt, Pd, Sn, Te, Ti, V | Rietveld et al. (2019) |
| 'Total material requirement for the global energy transition to 2050: A focus on transport and electricity' | Global, 2015 - 2050 | Fossil, ICE, EV, CSP, PV, hydro, wind, nuclear, ocean, bio, CCS, geothermal | Te, Ag, Ni , Mo, Cu, Al, Fe, Pt, Co, Li | Scenarios in ETP 2017 by the IEA. Stock-flow dynamics and TMR | Not mentioned | Watari et al. (2019) |
| 'Critical Metal Resource Constraints in the International Energy Agency's Long-Term Low-Carbon Energy Scenarios' | Global, 2015 - 2060 | Solar power, wind power, EVs | In, Ga, Se, Te, Cd, Ag, Dy, Nd, Li, Co, Ni , Pt, Fe, Al, Cu | Scenarios in ETP 2017 by the IEA. Use a top-down, bottom-up and integrated model | Risk for solar and EVs. Risk for In, Te, Ag, Li, Ni , Pt, Se. Recycling leads to 20-70% less demand. | Watari et al. (2018) |
| 'Scenarios for Demand Growth of Metals in Electricity Generation Technologies, Cars, and Electronic Appliances' | Global, 2000 - 2050 | PV, CSP, wind, hydro, biomass, other RE, nuclear, coal, oil, gas, CCS, CHP, ICE, EVs | Cu, Co, Nd, Ta, Li | SSPs as implemented by the IMAGE IAM. | Demand for Co and Li expected to increase by a factor 10 - 20+ due to future EV demand | Deetman et al. (2018) |

| | | | | | | |
|--|---------------------|---|---|--|---|------------------------------|
| 'Material bottlenecks in the future development of green technologies' | Global 2016 - 2050 | Wind, solar PV, CSP, EVs | Ag, Al, Cd, Ce, Co, Cr, Cu, Dy, Fe, Ga, Gd, Ge, In, La, Li, Mg, V, Mn, Mo, Nb, Nd, Ni , Pd, Pr, Pt, Si, Sn, Ta, Te, Ti, Zn | Use a BAU scenario. Use both a bottom-up and a top-down approach | Risk for solar PV, wind, CSP, EVs. Risk for Ag, Cd, Co, Cr, Cu, Ga, In, Li, Mn, Ni , Sn, Te, Zn. | Valero et al. (2018a) |
| 'Global material requirements for the energy transition. An exergy flow analysis of decarbonisation pathways' | Global, 2025 - 2050 | Wind, solar PV, solar thermal, CSP, geothermal, gas, nuclear, hydro, ICE, EVs | Ag, Al, As, V, Cd, Ce, Co, Cr, Cu, Dy, Fe, Ga, Gd, Ge, In, K, La, Li, Mg, Mn, Mo, Nb, Nd, Ni , P, Pb, Pd, Pr, Pt, Si, Sn, Ta, Te, Ti, Zn | IEA and Greenpeace scenarios | Demand for Co, Li, Mg, Ti and Zn will increase by at least six-fold in terms of ERC. | Valero et al. (2018b) |
| 'Modelling the material and energy costs of the transition to low-carbon energy' | Global, 2000 - 2050 | Wind solar PV, CSP, hydro, coal, gas, oil, nuclear | Cu, Al, Fe | Garcia-Olivares et al. (2012), Ecofys/ WWF and IEA | Not mentioned | Vidal et al. (2018) |
| 'Metal supply constraints for a low-carbon economy?' | Global, 2000 - 2050 | PV, wind, hydro, Nuclear, gas, coal, CCS, CHP, ICE, EVs | Fe, Al, Cu, Ni , Cr, In, Nd, Dy, Li, Pb, Zn | Own scenarios. Include an IO model and LCA data. | Risk for Solar PV and EVs. Risk for Dy, In, Li, Nd | De Koning et al. (2018) |
| Global metal flows in the energy transition: Exploring effects of substitutes, technology mix and development | Global, 2015 - 2060 | Solar PV, CSP, wind, EVs, batteries, fuel cells | Co, Cu, Dy, Ga, In, Li, Nd, Ni , Pt, Se, Ag, Te | Scenarios in ETP 2017 by the IEA. | Risk for EVs. Risk for Co, Li | Manberger & Stenqvist (2018) |
| 'Exploring metal requirements and the well-below 2 °C target with 100 percent renewable energy' | Global, 2010 - 2100 | PV, wind, EVs, nuclear, coal, oil, gas, CCS, hydro, H2, biomass, T&DI, geothermal | Si, Ag, In, Ga, Cd, Se, Te, Cu, Fe, W, Nd, Dy, Li, Co, Ni , Mn, Hf, Mo, V, Y, Nb, Zr, Pd, Pt, Al, Ti, La, Mg, Cr, | Own; 100% renewable; gas & renewables; coal & nuclear | Risk for solar PV, wind, FCV. Risk for In, Se, Te, Dy, Zr, Ni , Pt, Y, V, Li, La | Tokimatsu et al. (2018) |
| Energy modeling approach to the global energy-mineral nexus: a first look at metal requirements and the 2°C target | Global, 2010 - 2100 | PV, wind, EVs, nuclear, coal, oil, gas, CCS, hydro, H2, biomass, T&DI, geothermal | Si, Ag, In, Ga, Cd, Se, Te, Cu, Fe, Nd, Dy, Li, Co, Ni , Mn, Hf, Mo, V, Nb | Coal & nuclear, BAU and net ZERO; gas & renewables, BAU and net ZERO | Risk for solar PV, nuclear, EVs. Risk for In, Se, Te, Li, Co, Ni , Mn | Tokimatsu et al. (2017) |
| Material constraints for 100 % global renewable energy | Global, to 2050 | Solar, wind and potentially others | 28 metals (could not access past the abstract) | IPCC, WWF and IEA scenarios | Could not access | Emdadi et al. (2017) |
| 'Critical minerals and energy-Impacts and limitations of the energy transition | Global, 2010 - 2050 | Solar PV, Wind, fuel cells | Co, Cu, Ga, In, Li, Mg, Ni , Pt, Pd, Ir, Se, Te, Zn, Nd, Dy, Y, Ru, Rh, Os | Scenarios based on the IEA | Risk for solar PV and wind. Risk for In, Se, Te, Dy, Nd | McLellan et al. (2016) |
| 'Role of critical metals in the future markets of clean energy technologies' | Global, 2010 - 2050 | Solar, wind, EV, batteries, fuel cells, hydrogen storage, LED, electrolysis | Ru, Pt, Ag, Nd, Pr, Dy, Tb, Ga, Pd, Au, Ge, In, Ce, La, Co, Y, Eu, Te | Based on IPCC scenarios, TIMES model | Risk for solar, wind, EVs, fuel cells. Risk for Ag, Co, Dy, In, La, Pt, Ru, Te | Grandell et al. (2016) |

| | | | | | | |
|--|--------------------------------|--|--|---|--|-------------------------------|
| 'Metal Demand to Meet SDG Energy-related Goals' | Global, 2010 - 2100 | Solar PV, T&DI | Cu, In | WEC Jazz scenario as BAU scenario | Risk for both Cu and In | Murakami et al. (2015) |
| 'Raw Materials for Renewable Energy Technologies' | Global, 2012 - 2030 | Solar PV, wind, EVs | Fe, Al, Cu, Nd, Dy, Li, Co, Mn, Ni, Ag | Based on a Greenpeace scenario | Risk for Dy, Co, Li, Nd, Ag | Mocker et al. (2015) |
| Integrated life-cycle assessment of electricity-supply scenarios' | Global, 2010 - 2050 | Solar PV, CSP, wind, hydro, coal, natural gas | Fe, Al, Cu | Apply LCA. Use IEA BLUE Map and Baseline scenarios | Supply may be a concern for Cu | Hertwich et al. (2015) |
| 'Global Flows of Critical Metals Necessary for Low-Carbon Technologies: The Case of Neodymium, Cobalt, and Platinum' | Global, 2005 | Motor magnets, battery electrodes, fuel cell electrolytes | Nd, Co, Pt | Global MFA, including 231 countries and regions, using trade data | Not mentioned | Nansai et al. (2014) |
| 'Exploring rare earths supply constraints for the emerging clean energy technologies and the role of recycling' | Global, 2000 - 2050 (and 2100) | Wind turbines, EVs | Nd, Dy | Own supply and demand scenarios | China is likely to play a dominant role regarding dy. | Habib & Wenzel (2014) |
| 'Dynamic analysis of the global metals flows and stocks in electricity generation technologies' | Global, 2010 - 2050 | Oil, coal, gas, nuclear, CSP, PV, biomass, wind, hydro, geothermal | Ag, Al, Cd, Cr, Cu, Fe, Ga, Ge, In, Mo, Ni, Pb, Se, Te, Zn, Nd, Dy, Mg, Mn | GEO-3 scenarios. Dynamic MFA | Risk for Solar PV. Risk for Ag, Ge, In, Te | Elskaki & Graedel (2013) |
| 'A global renewable mix with proven technologies and common materials' | Global | Generation, power system and transport | Cu, Al, Nd, Li, Ni, Zn, Pt | Propose an alternative energy mix to fossil fuels | Risk for vehicles. Risk for Li, Ni, Pt | Garcia-Olivares et al. (2012) |
| 'Evaluating Rare Earth Element Availability: A Case with Revolutionary Demand from Clean Technologies' | Global, 2010 - 2035 | Wind, EVs | Ce, Dy, Eu, Gd, La, Nd, Pr, Sm, Tb, Y | Own scenarios | Risk for wind, EVs. Risk for Nd, Dy | Alonso et al. (2012) |
| 'Metal requirements of low-carbon power generation' | Global, 2007, mixes up to 2050 | Coal, natural gas, oil, CCS, nuclear, wind, hydro, solar, biomass, CHP | U, Ag, Mo, Sn, Zn, Cu, Al, Ni, Fe | Own scenarios and the IEA Blue Map scenario | Significant upscaling of mining is required. | Kleijn et al. (2011) |
| 'Resource constraints in a hydrogen economy based on renewable energy sources: An exploration' | Global, 2050 | Solar PV, wind, T&DI, hydrogen system, fuel cells, motors | Cd, Te, Se, Ga, In, Ge, Ru, Fe, Ag, Cu, Pb, Nd, Ni, Cr, Pt | Market first scenario. Assumed hydrogen economy | Bulk materials are also at risk due to the sheer size of the ET. | Kleijn & van der Voet (2010) |

Abbreviations: CSP = Concentrated Solar Power; T&DI = Transmission and distribution infrastructure; IPCC = Intergovernmental Panel on Climate Change; WWF = World Wildlife Fund; WEC = World Energy Council; IEA = International Energy Agency; IRENA = International Renewable Energy Agency; UN = United Nations; LCA = Life Cycle Assessment; IO = Input-Output; MFA = Material Flow Analysis; TMR = Total Material Requirements; RE = renewable energy; PV = Photovoltaics; CHP = Combined Heat and Power; BAU = Business as Usual; ICE = Internal Combustion Engine; EV = Electric Vehicle; FCV = Fuel Cell Vehicle; CCS = Carbon Capture & Storage; ERC = Exergy Replacement Costs; SSP = Shared Socioeconomic Pathway; IAM = Integrated Assessment Model. For the abbreviations of specific scenarios used in certain publications, see those publications.

Appendix B: Detailed model structure

This appendix contains a more elaborate version of the XLRM (Exogenous uncertainties, levers, relationships and metrics) framework (figure B1) applied to nickel and the complete structures of the four sub models (figures B2 - B5).

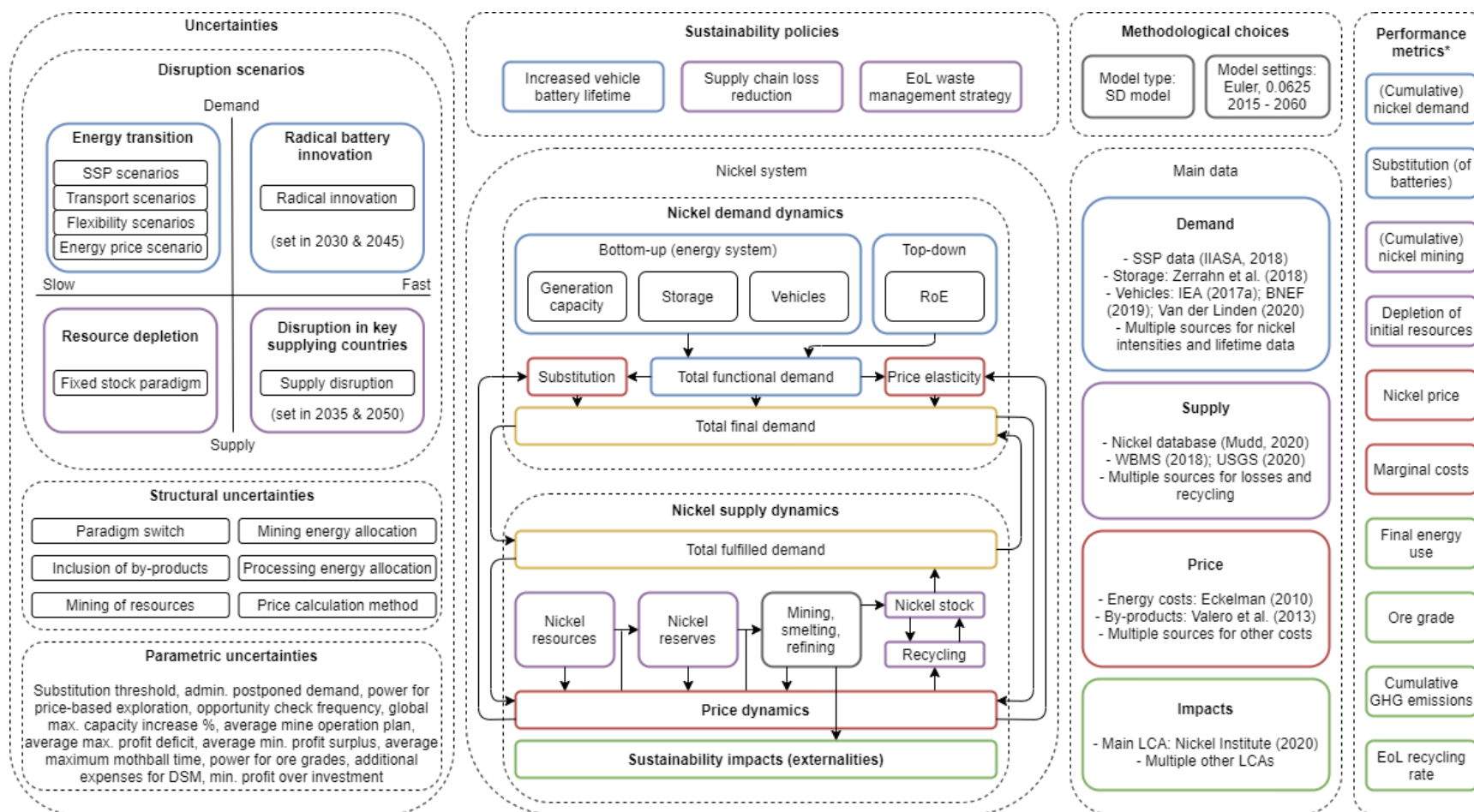


Figure B1: more detailed version of the XLRM framework applied to the nickel model. *Only the main performance metrics are included.

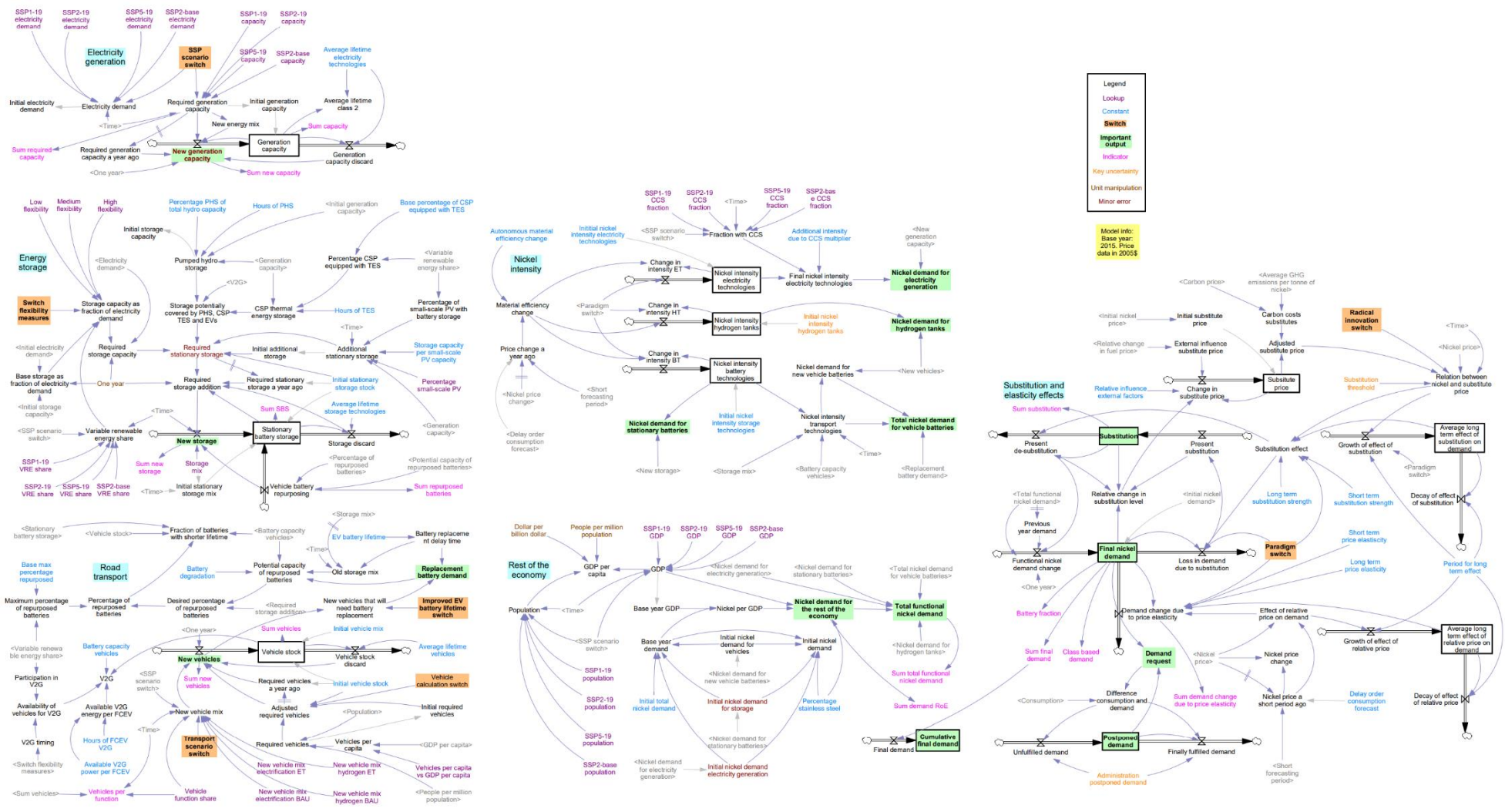


Figure B2: complete demand sub-model. The legend is included in the figure.

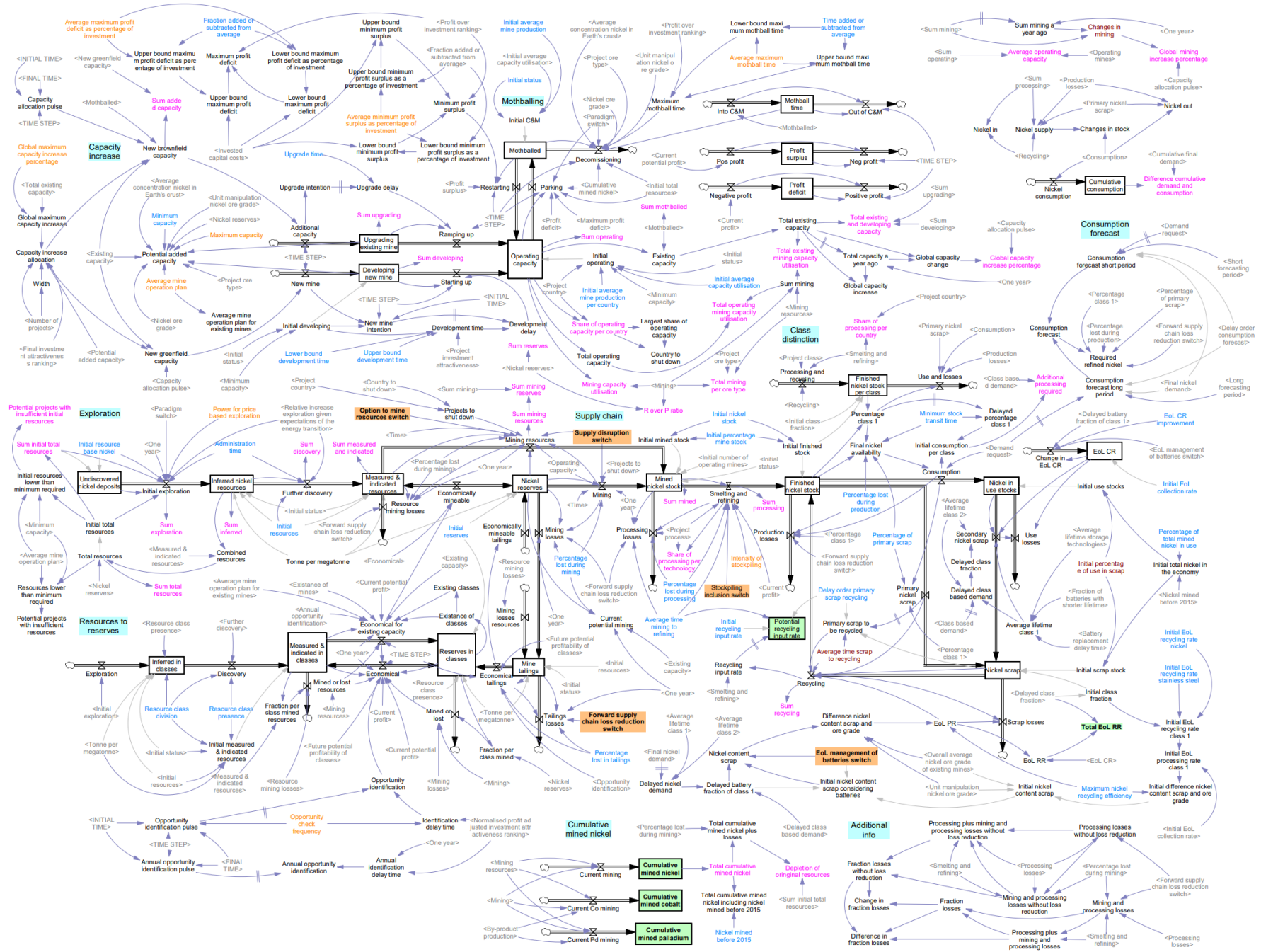


Figure B3: complete supply sub-model. For the legend, see figure B2.

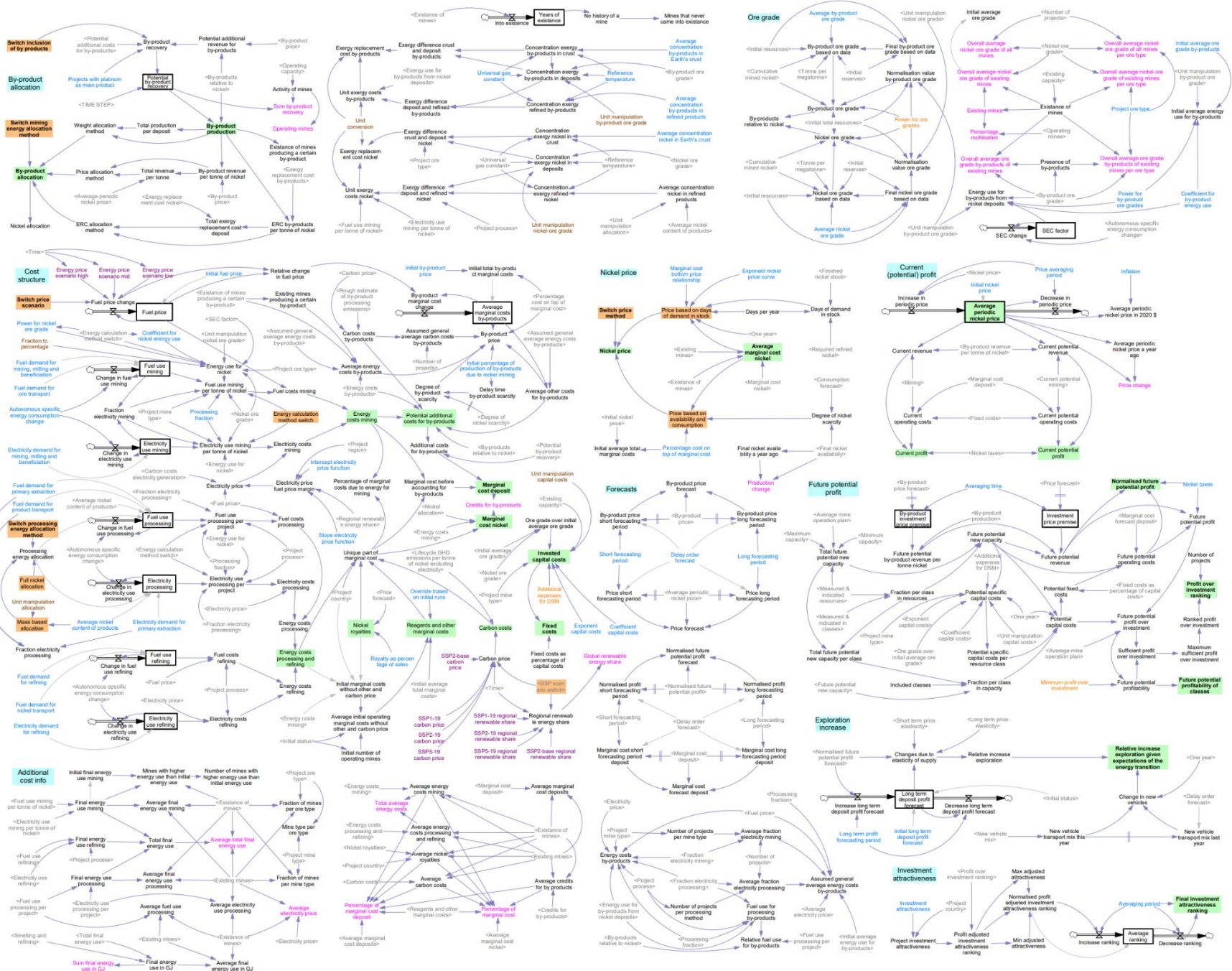


Figure B4: complete price sub-model. For the legend, see figure B2.

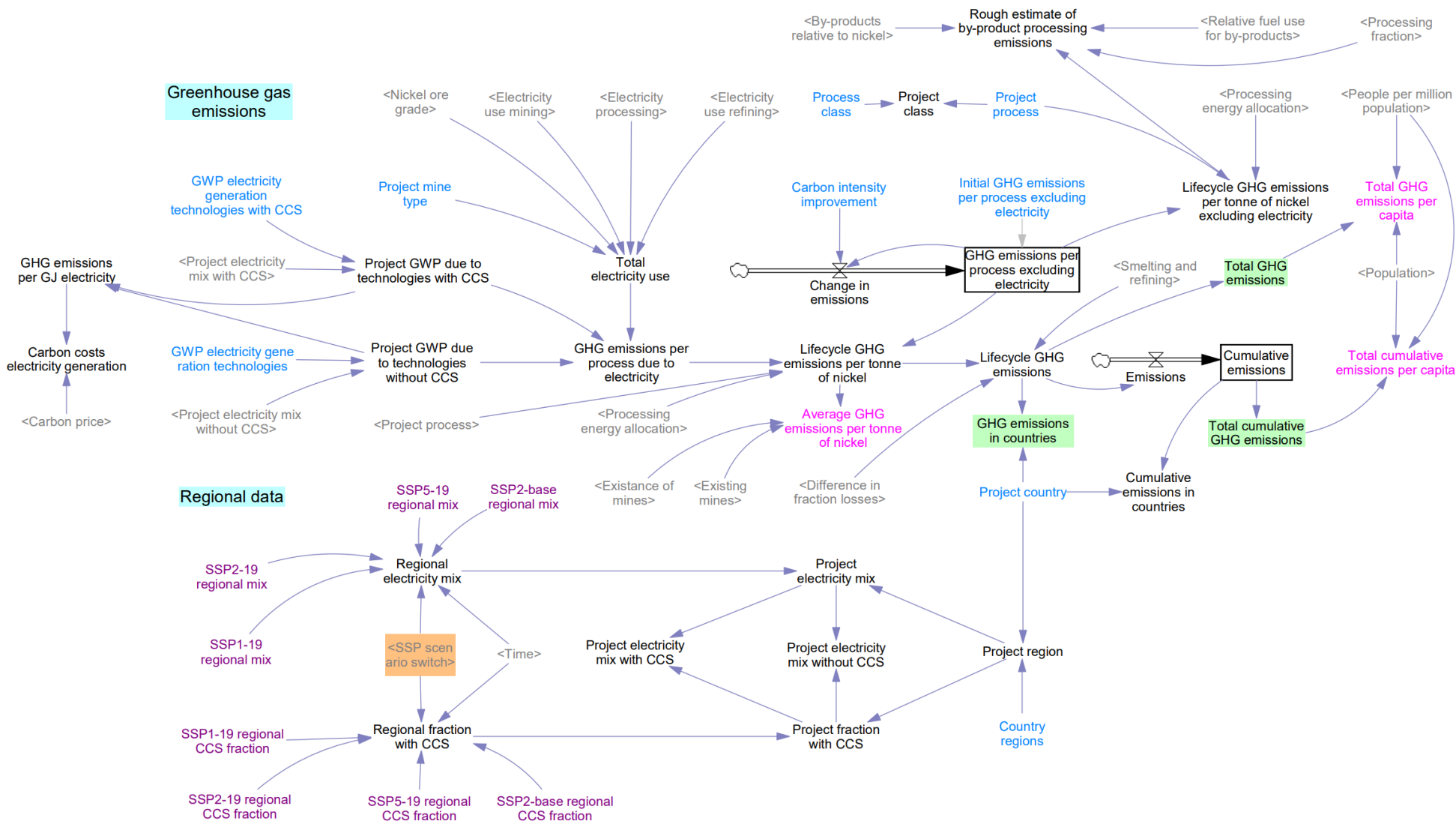


Figure B5: complete impacts sub-model. For the legend, see figure B2.

Appendix C: Background, assumptions & data: energy system

This appendix contains background information that can be consulted to provide some more context for the concepts related to the energy system discussed in the main text. Assumptions are also explained and values used in the model for nickel intensity and component lifetime are shown.

Physical components of the energy system are shown in figure C1. These components can be divided into energy carriers (fuels, heat and electricity) and supply chain categories (supply, T&DI, storage and use). Many of these components contain nickel, but most data is available on the power sector, storage and the road transport sector. These are also the sectors which are expected to change most in the Energy Transition (ET) through increased electrification of the energy system (Blok & Nieuwlaar, 2021) and are thus the focus of this thesis. In future research, the other components could also be assessed.

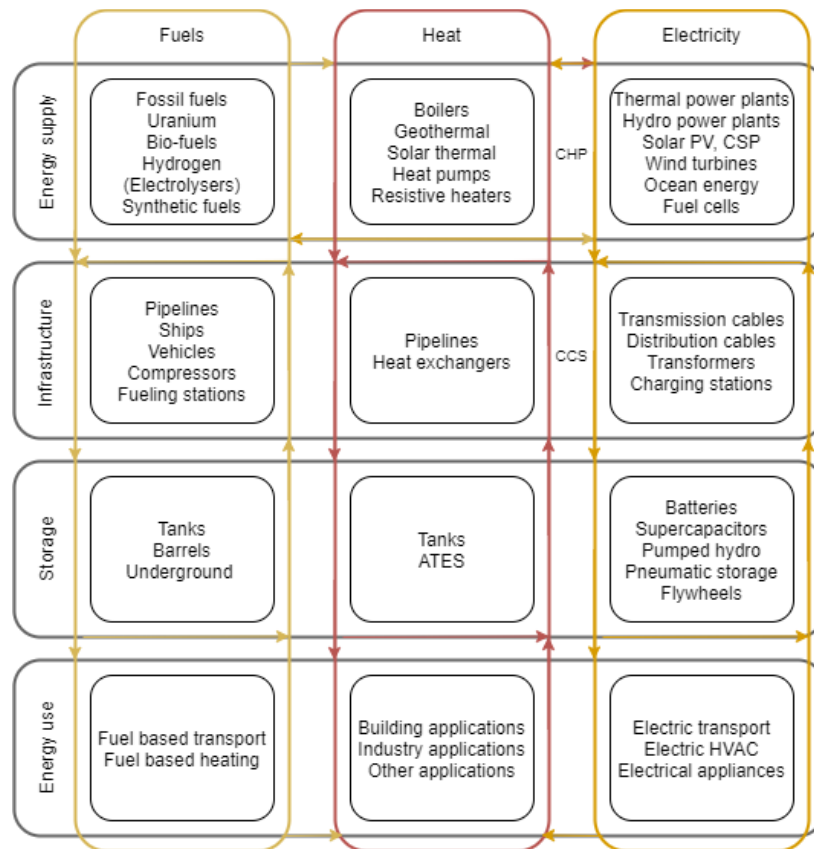


Figure C1: physical components of the energy system. ATES = Aquifer Thermal Energy Storage, HVAC = Heating, Ventilation and Air Conditioning. Created with information from Hadjipaschalis et al. (2009); Blok & Nieuwlaar (2021); and Brown et al. (2018).

Appendix C1: Electricity generation

Nickel is used in virtually all electricity generation technologies, including fossil fuel-based generation, nuclear, bio-energy, wind, solar (PV and CSP), geothermal, hydropower and ocean energy. It is also used for CCS and in hydrogen infrastructure and fuel cells. Nickel used in electricity generation technologies is mainly in the form of stainless steel (Nickel Institute, n.d.).

Appendix C1.1: Nickel intensities of electricity generation technologies

Table C1: nickel intensities of electricity generation technologies (tonne/GW). n = number of sources on which the values were based. More details regarding this table are discussed below. CCS was included in the model by multiplying intensities for bio, oil, coal and natural gas by 1.1, 2.3, 2.1 and 1.8 respectively, based on the difference between the values with and without CCS. C-Si = Crystalline silicon.

| Component | Min. intensity | Avg. intensity | Max. intensity | n | Sources |
|----------------------|----------------|----------------|----------------|---|---|
| Solar PV (C-Si) | 1 | 30 | 88 | 3 | Kleijn et al. (2011); Elshkaki & Graedel (2013); Fizaine & Court (2015) |
| Solar PV (thin film) | 16 | 16 | 16 | 1 | |
| Average solar PV | 1 | 30 | 86 | - | Based on 97% market share c-Si (IEA PVPS, 2019) |
| CSP (parabolic) | 940 | 940 | 940 | 1 | Pihl et al. (2012) |
| CSP (tower) | 1800 | 1800 | 1800 | 1 | |
| Average CSP | 1069 | 1069 | 1069 | - | Based on 85% market share parabolic (GVR, 2019) |
| Wind | 111 | 523 | 920 | 6 | Kleijn et al. (2011); Elshkaki & Graedel (2013); Moss et al. (2013b); Fizaine & Court (2015); World Bank (2017); Rietveld et al. (2019) |
| Geothermal | 240 | 60198 | 120155 | 2 | Moss et al. (2013a); Valero et al. (2018b) |
| Hydro power | 31 | 57 | 79 | 2 | Kleijn et al. (2011); Moss et al. (2013a) |
| Ocean Energy | 0.2 | 0.2 | 0.2 | 1 | Moss et al. (2013a) |
| Nuclear | 256 | 398 | 638 | 3 | Kleijn et al. (2011); Moss et al. (2011); Fizaine & Court (2015) |
| Bio-energy | 20 | 753 | 1486 | 2 | Kleijn et al. (2011); Ashby (2013) |
| Bio-energy + CCS | 69 | 802 | 1535 | - | The difference between oil + CCS and oil was added to the bio-energy values |
| Oil | 37 | 37 | 37 | 1 | Kleijn et al. (2011) |
| Oil + CCS | 86 | 86 | 86 | 1 | |
| Coal | 176 | 179 | 182 | 2 | Kleijn et al. (2011); De Koning et al. (2018) |
| Coal + CCS | 352 | 370 | 387 | 2 | |
| Natural gas | 77 | 89 | 100 | 2 | |
| Natural gas + CCS | 154 | 160 | 166 | 2 | |

In the model, current market shares of PV technologies are used. This may change in the future, but as the intensity of thin film is within the range of intensities of C-si, and the numbers are already very uncertain, it is assumed to remain constant. CSP shares are also assumed to remain constant.

Kleijn et al. (2011) reported two types of biofuel (rapeseed and wood CHP). An average of these two types was taken when considering their data. The value for rapeseed was relatively high, because of the substantial inputs required per unit biomass along the life cycle (Kleijn et al., 2011). The rapeseed oil was used in an oil-fired power plant, so for bio-energy + CCS, the difference between oil + CCS and oil was added to the bio-energy values.

Data for electricity generation was reported in t/GWh by Kleijn et al. (2011) and De Koning et al. (2018). Capacity Factors (CFs) reported by the EIA (2019b,c) for the year 2010 (the closest year available to the base year of 2000 used by De Koning et al. (2018)) were used to convert the values in t/GWh to t/GW. It is not ideal to be using CFs because they differ per year and per country by a few percentage points. However, given the large uncertainty already surrounding the numbers, the values for the USA for 2010 were assumed to be representative enough.

The nickel intensities reported by Moss et al. (2013a) were used by Rietveld et al. (2019) and Watari et al. (2019) and they were also used for some of the technologies in this thesis. However, there are some concerns about the magnitude of the intensities. Especially the nickel intensity for geothermal is very large, at 120155 t/GW. This is about 500 times more than the value reported by Valero et al. (2018b).

It is unclear how Valero et al. (2018b) obtained their value, but Moss et al. (2013a) based their value on an LCA by Sullivan et al. (2010), who report steel requirements for geothermal that are about 16 times as much as the steel requirements they report for coal. This is mainly due to the large steel requirement of the well, but the steel requirements for the plant are still 4 times as much as the steel requirements for the coal plant. The capital costs for a geothermal plant and well are comparable to the capital costs for various fossil fuel powered plants (EIA, 2020a), so it seems strange that a geothermal plant can have so much more steel. This should be looked into in further research.

The high temperatures in large parts of the geothermal plant and well mean that there is probably a higher percentage of nickel in the steel than in plants that deal with lower temperatures. However, the value provided by Moss et al. (2013a) still seems disproportionately high. On the other hand, Moss et al. (2013a) report a very low value for ocean energy of 0.22 t/GW. This is about half a million times less than the value reported for geothermal energy and it is also a lot less than values reported for other technologies. However, this was the only value that could be found for ocean energy and because ocean energy does not play a large role in the SSP scenarios, it will not have a large impact on the final results.

Appendix C1.2: Lifetimes of electricity generation technologies

Table C2: lifetimes of electricity generation technologies (years). n = number of sources on which the values were based. None of the literature distinguished between power plants with or without CCS, so the same value was assumed. Sources: Tidball et al. (2010); Turconi et al. (2013); Raugai & Leccisi (2016); Valero et al. (2018a); Manberger & Stenqvist (2018); Tokimatsu et al (2018); Kis et al. (2018) Watari et al. (2019)

| Component | Min. lifetime | Avg. lifetime | Max. lifetime | n |
|--------------------|---------------|---------------|---------------|---|
| Solar PV | 15 | 27 | 40 | 8 |
| CSP | 20 | 28 | 30 | 5 |
| Wind | 15 | 24 | 30 | 8 |
| Geothermal | 20 | 37 | 60 | 4 |
| Hydro power | 30 | 57 | 100 | 4 |
| Ocean Energy | 30 | 30 | 30 | 1 |
| Nuclear | 40 | 49 | 60 | 6 |
| Bio-energy (+CCS) | 15 | 34 | 45 | 5 |
| Oil (+CCS) | 20 | 32 | 40 | 4 |
| Coal (+CCS) | 30 | 41 | 60 | 5 |
| Natural gas (+CCS) | 20 | 33 | 45 | 5 |

Appendix C2: Storage technologies

Nickel is also used in most storage technologies. Moss et al. (2013a) provided an indication of the nickel or stainless steel required for various technologies, including flywheels, Compressed Air Energy Storage (CAES; pneumatic storage), Thermal Energy Storage (TES) and Pumped Hydro Storage (PHS), but they did not provide concrete nickel intensities for each technology.

Storage can be divided into short-term storage (often measured in hours), such as PHS and battery storage and long-term storage (often measured in weeks or months), such as long-term TES and hydrogen storage (Blok & Nieuwlaar, 2021). In this thesis only short-term storage was considered explicitly. It is assumed that most short-term storage technologies, except PHS (97% of storage capacity in 2017), TES at CSP sites (which can have a significant contribution in the future) and batteries (whose share is growing rapidly), make up a sufficiently small share of the total storage capacity to be neglected in this analysis (IRENA, 2017).

Regarding batteries, different types are used for various mobile and stationary storage applications. These types include lead acid batteries, nickel-based batteries, such as Nickel-Iron (NiFe), Nickel-Cadmium (NiCd) and Nickel-Metal Hydride (NMH), and lithium-ion batteries. Many lithium-ion batteries, which have high energy densities and are therefore most suitable for EVs and stationary storage, also contain a large nickel fraction. This type of batteries includes Nickel Cobalt Aluminium (NCA) batteries and various Nickel Manganese Cobalt (NMC) batteries. The advantage of using nickel in batteries is increased storage capacity and energy density at a lower cost (Nickel Institute, 2018).

Appendix C2.1: Nickel intensities of storage technologies

The main focus of this thesis is on battery storage. Nickel required for PHS and CSP TES was assumed to already be accounted for in the infrastructure required for hydropower and CSP respectively. Moss et al. (2013a) provide a value of 60 tonne/GW for PHS, which is included in the range for hydropower (table C1). Nickel required for hydrogen storage is considered only in relation to FCVs.

According to Tokimatsu et al. (2018), the nickel intensity in the stainless steel of hydrogen storage tanks is between 93 and 132 kg/vehicle, with an average of 112 kg/vehicle. When referring to hydrogen storage tanks, Tokimatsu et al. (2018) presumably refer to the infrastructure and not to the tank in the vehicle. However, the value still seems rather high and it is not clear how they obtained it. The value should be treated with care, but if it is a decent approximation, it would mean that FCVs have a higher total intensity (including infrastructure) than Battery Electric Vehicles (BEVs).

Different types of lithium-ion battery chemistries and their energy density, nickel intensity, market share and applications are shown in table C3. In 2018, the market share of nickel containing lithium-ion batteries was 53%, but this share is expected to grow to 85% by 2030 (BNEF, 2019). The nickel ratio of NMC batteries has also increased over the years, leading to higher energy densities. However, the decreased cobalt content makes the batteries more prone to explosions (van der Linden, 2020).

Energy densities were obtained from Wentker et al. (2019). Nickel Institute (2018) also provided values for energy density, but these are slightly more outdated and lower. However, because Wentker et al. (2019) did not include values for Lithium Manganese Oxide (LMO) and Lithium Cobalt Oxide (LCO) batteries, these values were taken from Nickel Institute (2018) and increased based on the average difference between the other values of the two sources.

Table C3: lithium-ion battery chemistries (BNEF, 2019), energy densities (Wentker et al., 2019; Nickel Institute, 2018), nickel intensities (calculated), market share and applications for 2018 (BNEF, 2019). EV = passenger electric vehicles, ETr = E-trucks, EB = E-buses, CE = consumer electronics, SBS = stationary battery storage. The energy density applies to the mass of the whole battery, the nickel intensity applies to the mass of the nickel. It was assumed that the cathode is 30% of the total weight of the battery (Dunn et al., 2012). More details are discussed below.

| Battery | Components (and cathode composition (%)) | Energy density (kWh/kg) | Nickel intensity (kg/kWh) | Market share | Current applications |
|------------------------------|--|-------------------------|---------------------------|--------------|----------------------|
| <i>Not containing nickel</i> | | | | 47% | |
| LFP | Lithium (7%), iron (60%), phosphate (33%) | 0.21 | 0 | 19% | CE, EV, ETr, EB, SBS |
| LMO | Lithium (6%) manganese (94%), oxide | 0.22 | 0 | 2% | CE, EV |
| LCO | Lithium (11%), cobalt (89%), oxide | 0.26 | 0 | 26% | CE |
| <i>Containing nickel</i> | | | | 53% | |
| NMC 111 | Lithium (11%), nickel (30%), manganese (29%), cobalt (30%) | 0.25 | 0.36 | 14% | CE, EV, ETr, EB, SBS |
| NMC 442 | Lithium (11%), nickel (37%), manganese (34%), cobalt (18%) | 0.26 | 0.43 | 14% | SBS |
| NMC 532 | Lithium (11%), nickel (45%), manganese (26%), cobalt (18%) | 0.26 | 0.52 | | EV |
| NMC 622 | Lithium (11%), nickel (54%), manganese (17%), cobalt (18%) | 0.27 | 0.60 | 15% | CE, EV, ETr |
| NMC 811 | Lithium (11%), nickel (72%), manganese (8%), cobalt (9%) | 0.28 | 0.77 | 3% | CE |
| NCA | Lithium (11%), nickel (73%), cobalt (14%), aluminium (2%) | 0.28 | 0.78 | 7% | EV, ETr |
| NCA+ | Lithium (11%), nickel (82%), cobalt (5%), aluminium (2%) | 0.29 | 0.85 | | EV |

Since 2010, energy density has changed quite a lot and it will continue to increase in the future (BNEF, 2019). Ilika (2019) expects energy density to reach 0.5 kWh/kg by 2030. This is not explicitly included in the model, but is (at least partially) reflected in the model through intensity changes, storage mix changes and substitution. This is discussed in more detail in appendix E4.

Van der Linden (2020) obtained nickel intensity data for different battery chemistries from Olivetti et al. (2017). However, Olivetti et al. (2017) do not include data for NMC 422, NMC 532 and NCA+. In this thesis, nickel intensity was determined by combining energy density, the nickel fraction per cathode and the cathode fraction per battery, as described by BNEF (2019), who also calculated intensities but did not report them. BNEF (2019) also included production losses in their calculations, but that is not done in this thesis, because the production losses are already included in the model. According to Dunn et al. (2012), the cathode fraction of the total battery weight is about 30% for LMO batteries. Assuming this also applies to NCA and NMC batteries, leads to values that are very similar to the values by Olivetti et al. (2017).

Appendix C2.2: Lifetimes of storage technologies

The lifetimes for PHS and CSP TES were assumed to be equal to the lifetimes of hydro power and CSP respectively. The lifetimes of battery technologies are shown in table C4. As indicated by IRENA (2017), lifetime can increase over time. This is not taken into account in the nickel model. Instead, both the lifetime ranges IRENA (2017) provides for 2016 and 2031 were used to determine an average lifetime. Potential future lifetime prolongation may be (partially) taken into account in the intensity reduction.

Table C4: Lifetimes of battery technologies (years). *n* = number of sources on which the values were based. The other category consists mostly of LFP, so data for LFP was used. Source: IRENA (2017). The average lifetime here is 16 years, but 18 years is used in the model to match the data on repurposing of EV batteries (see appendix C3.2).

| Component | Min. lifetime | Avg. lifetime | Max. lifetime | n |
|-------------|---------------|---------------|---------------|---|
| NCA+ | 5 | 16 | 31 | 1 |
| NCA | 5 | 16 | 31 | 1 |
| NMC811 | 5 | 16 | 31 | 1 |
| NMC622 | 5 | 16 | 31 | 1 |
| NMC532 | 5 | 16 | 31 | 1 |
| NMC422 | 5 | 16 | 31 | 1 |
| NMC111 | 5 | 16 | 31 | 1 |
| Other (LFP) | 5 | 16 | 31 | 1 |

Appendix C3: Transport technologies

In the transport sector, nickel is used in trains, aircrafts, and various land-based vehicles, for example in the form of coatings. Nickel is especially required in EV batteries, which can be used in passenger vehicles, trucks and buses (Nickel Institute, n.d.; BNEF, 2019). Battery demand is expected to grow most and is thus assessed in most detail. Coatings and other applications are included as part of the Rest of the Economy (RoE).

Passenger vehicles can be divided into different types based on the type of powertrain. The most common types include the ICEs, Hybrid Electric Vehicles (HEVs), Plug-in Hybrid Electric Vehicles (PHEVs), BEVs and FCVs. ICE vehicles run solely on a certain fuel (not considering the small start-up and auxiliary electrical systems battery), whereas the other four contain a larger, often lithium-ion, battery.

In addition to a battery, FCVs, which run on hydrogen, also have a nickel containing fuel cell. Moreover, hydrogen infrastructure has to be built to supply the FCVs, including nickel-containing storage tanks. As stated in appendix C2.1, Tokimatsu et al. (2018) provide values on the nickel intensity of fuel cells and storage infrastructure in kg per vehicle. The storage tanks are also relevant for hydrogen storage for other purposes, including long- term storage of grid electricity. However, in this thesis hydrogen is only considered in relation to FCVs.

Appendix C3.1: Battery capacities of vehicle technologies

Table C5 shows the battery capacity of different vehicle types. According to Speirs et al. (2014), the capacities of PHEV and BEV batteries are about 10 - 20 times larger than the capacities of HEV and FCV batteries. Values provided by FCH (2010), though outdated, corroborate this. Based on this, and the values provided by Van der Linden (2020) and InsideEVs (2020) for PHEV and BEV capacities, the battery capacities of HEV and FCV were determined. In a similar manner, Fuel Cell Bus and Truck (FC-Bus and FC-Truck) values were derived from electric bus and truck (E-Bus and E-Truck) values.

Based on the market share of the battery types in 2018 (BNEF, 2019), a static average nickel intensity of 0.56 kg/kWh was calculated. Multiplying this by the battery capacity of the different vehicles led to a static nickel intensity per vehicle type. These calculated intensities were quite similar to values that could be found in the literature (USDOE, 2011; Tokimatsu et al., 2018; Valero et al., 2018a; Watari et al., 2019).

Table C5: Battery capacity of vehicles (GWh/vehicle). *n* = number of sources on which the values are based. Also see Manberger & Stenqvist (2018) for similar values and a more detailed division of vehicle types.

| Component | Min. capacity | Avg. capacity | Max. capacity | n | Sources |
|-----------|---------------|---------------|---------------|---|---|
| ICE | 0 | 0 | 0 | - | |
| HEV | 1E-06 | 4E-06 | 6E-06 | - | Calculated based on Speirs et al. (2014) and FCH (2010) |
| PHEV | 9E-06 | 1.8E-05 | 4.2E-05 | 2 | Van der Linden (2020); InsideEVs (2020) |
| BEV | 2E-05 | 7.1E-05 | 1.2E-04 | 2 | |
| FCV | 1E-06 | 4E-06 | 6E-06 | - | Calculated based on Speirs et al. (2014) and FCH (2010) |
| E-Bus | 1.5E-04 | 1.85E-04 | 2.20E-04 | 1 | Van der Linden (2020) |
| E-Truck | 7E-05 | 1.1E-04 | 1.5E-04 | 1 | |
| FC-Bus | 8E-06 | 9E-06 | 1.1E-05 | - | Calculated based on Speirs et al. (2014) |
| FC-Truck | 4E-06 | 6E-06 | 8E-06 | - | |

For FCVs, an average calculated intensity of 2 kg/vehicle is similar to the values reported by Tokimatsu et al. (2019), who only considered the fuel cell and not the battery. On the other hand, Watari et al. (2019) reported 1 kg/vehicle for the whole vehicle. Based on this, and the fact that all these factors are already uncertain, it is assumed that the calculated value based on the battery capacity is enough to encompass both battery and fuel cell, so no additional variables were added to the model to account for the fuel cell.

In the model, the battery capacities are used instead of the static average intensities. This is because the market share of the different batteries changes significantly over time for the different storage functions (stationary, passenger vehicles, buses and trucks) and these changes are reflected in the model using battery scenarios provided by BNEF (2019). This is discussed in more detail in appendix D2.5.

The values for BEV and PHEV differ significantly per vehicle model (InsideEVs, 2020) and battery capacities also change over time. To increase range, it is assumed that over time, as energy density increases, battery capacity will also increase, unless size is reduced to reduce weight. Batteries that have already been made, degrade over time and their capacity reduces. This is mostly not considered in the model, however, a capacity reduction of 75% is considered for the repurposing of batteries (Walker et al., 2015; Assuncao et al., 2016; De Rousseau et al., 2017 White et al., 2020).

Appendix C3.2: Lifetimes of vehicle technologies

Table C6: Lifetimes of vehicle technologies (years). *n* = number of sources on which the values were based. Sources: Ercan et al. (2016); Zhou et al. (2017); Deetman et al. (2018); Manberger & Stenqvist (2018); Watari et al. (2019); Nordelof et al. (2019); ACEA (2020); Statista (2020). The average lifetime here is 13 years, but 16 years is used in the model (see below).

| Component | Min. lifetime | Avg. lifetime | Max. lifetime | n |
|-------------------|---------------|---------------|---------------|---|
| Passenger vehicle | 10 | 13 | 15 | 4 |
| Bus | 12 | 13 | 16 | 3 |
| Truck | 9 | 13 | 17 | 3 |

According to ACEA (2020) and Statista (2020), the lifetimes of different vehicles have been increasing over time. To take this into account, a lifetime of 16 years was selected for all vehicle functions. This also makes it exactly twice the lifetime of an EV battery inside a vehicle, reported as 8 years (Walker et al., 2015; Assuncao et al., 2016; De Rousseau et al., 2017 White et al., 2020). With a second-life of 10 years for repurposed batteries (at 70 - 80% of initial capacity), the total lifetime would be 18 years. This value is also used for the storage technologies instead of 16, so it matches (see table C4).

Van der Linden (2020) used values for passenger vehicles, buses and trucks of 20, 30 and 18 years respectively. However, the 18 years refers to the infrastructure for trucks, not the trucks themselves and no sources could be found for the 20 and 30 years, so these values were not considered. They would, however bring the range closer to an average lifetime of 16 years, further supporting this choice.

Appendix C4: Relationships between the sectors

The nickel containing components included explicitly in this thesis are shown in figure C2. The three sectors discussed above are interconnected in multiple ways. To smooth the increased variability when integrating renewables in electricity systems, various flexibility measures are required. Storage options are one form, but there are also other measures, including grid expansion, flexible dispatch, active demand response and various other forms of sector coupling, which is the increased interaction between supply sectors and end users. An example is using excess electricity to create other energy carriers, like hydrogen and synthetic fuels. Curtailment, which is simply the reduction or restriction of the output of a generator, is also an option (Brown et al., 2018; Zerrahn et al., 2018).

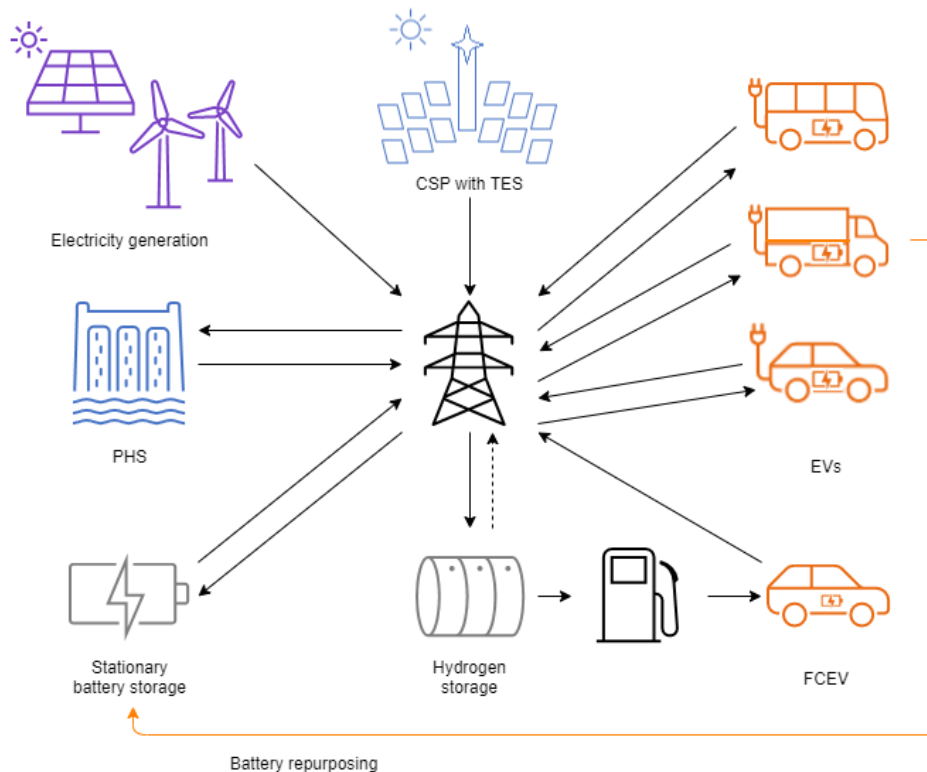


Figure C2: Nickel containing components considered in this thesis and their relationships. The solid lines indicate relationships included in the nickel model. The dotted lines indicate relationships that are not explicitly included in the model. The black lines are energy flows, the orange line is a material flow. The black components are just for illustrative purposes. Any nickel used in these components is not considered.

Increased flexibility means less SBS is required. A form of flexibility applied explicitly in the model is the use of EVs for storage. This is a form of demand response, also known as Vehicle to Grid (V2G) storage, where EVs can be charged when supply is high and discharged to the grid when supply is low and the vehicles are not in use. This can significantly reduce the need for SBS (IRENA, 2017; Brown et al., 2018).

FCVs can also be used for V2G. In this case, the fuel cell in the vehicle is used as a 'power plant', with hydrogen as fuel. The available energy from FCVs doesn't depend on the battery capacity as for BEVs and PHEVs, but on the hydrogen storage capacity and the fuel cell capacity. It is assumed that each FCV has a capacity of 10 KW that can be used for 6 hours per day, based on Oldenbroek et al. (2017).

SBS can consist of new batteries, with a lifetime of about 18 years, but also of repurposed EV batteries. Vehicles have a lifetime of about 16 years, but EV batteries can be used in vehicles for only about 8 years before they have degraded too much to be suitable for vehicles and need to be replaced. However, at this point they still have 70 - 80% of their initial capacity and can still be used for 10 more years as stationary storage (Walker et al., 2015; Assuncao et al., 2016; De Rousseau et al., 2017 White et al., 2020).

Appendix D: Background, assumptions & data: energy scenarios

This appendix contains background information that can be consulted to provide some more context for the scenarios used as input in the model. Assumptions are also explained and values used in the model for the different scenarios are shown.

Large changes are expected in the energy system in the coming decades, but there are many ways in which these developments can occur. Multiple organisations, including the IPCC, IEA, IRENA, WEC, Shell, British Petroleum (BP), the European Commission (EC) and Greenpeace, have created scenarios (Dagnachew et al., 2019). In this thesis some of the more ambitious ones were selected to explore the nickel requirements. These are pathways that conform to the 1.5 °C temperature increase target. Below, first electricity generation scenarios are described, followed by storage scenarios and transport scenarios.

Appendix D1: Electricity generation scenarios

The selected scenarios for electricity generation are the results of IAMs that combine SSPs with Representative Concentration Pathway (RCP) 1.9. SSPs are five narratives that vary based on socio-economic developments, such as Gross Domestic Product (GDP) and population (figure D1a). The SSPs have been used by multiple IAMs, so there are multiple scenarios per SSP. However, for each SSP a certain IAM is known as the marker model that produces a set of marker scenarios per RCP. The marker scenarios can be considered as the representatives of a certain SSP, while the results of other IAMs can be used to indicate uncertainty (IIASA, 2018).

RCPs are pathways that vary based on the level of radiative forcing. Radiative forcing is the difference between radiation arriving at and leaving Earth and its atmosphere. When the incoming radiation is larger than the outgoing radiation, caused by the increase of Greenhouse Gases (GHGs), the temperature will rise. RCP 1.9 indicates a radiative forcing of 1.9 W/m². This is the level of radiative forcing likely to limit temperature increase to 1.5°C (Hausfather, 2018). The different levels of radiative forcing, and the associated temperature increase, used in the RCPs are shown in figure D1b.

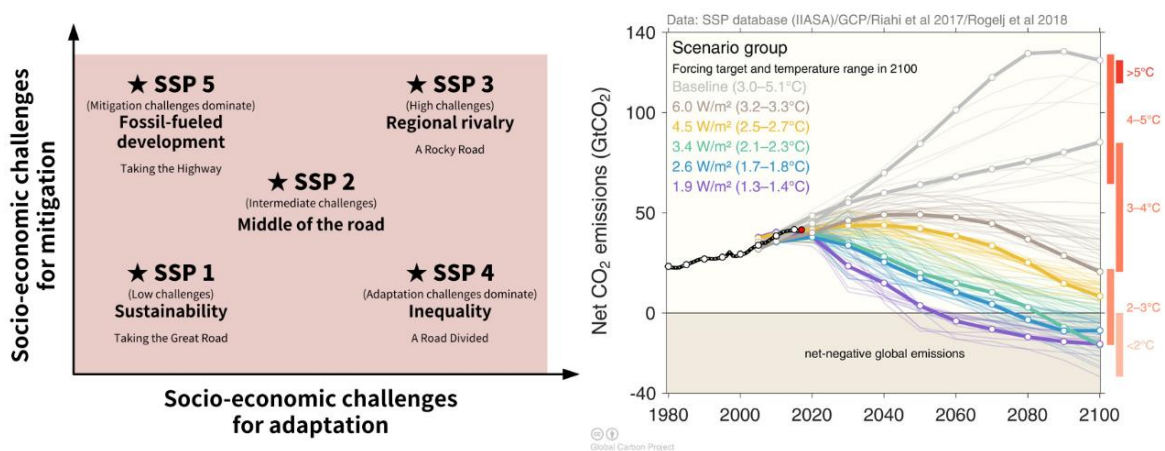


Figure D1: a. SSPs (O'Neill et al., 2017) b. RCPs (Hausfather, 2018)

Of the marker scenarios, only three of the five SSPs are compatible with RCP 1.9; SSP1-19, SSP2-19 and SSP5-19. These are used in the nickel model, together with the baseline scenario for SSP2, which is used as a BAU scenario. However, the model is made in such a way that other scenarios can also be added. The four selected scenarios are explained in more detail in table D1.

Table D1: the four selected scenarios consisting of marker scenarios compatible with RCP 1.9 and a BAU scenario. The values for these scenarios are shown in appendix D1.1 (Riahi et al., 2017; IIASA, 2018).

| Scenario | Model | Elaboration |
|--------------------------------------|-----------------|---|
| 1 Sustainability, SSP1-19 | IMAGE | Gradual shift to a more sustainable world with increased equality and respect for environmental boundaries. Emphasis on economic growth shifts to emphasis on well-being. Lower resource and energy intensity. Developments are compatible with limiting global temperature increase to 1.5 °C |
| 2 Middle of the road, SSP2-19 | MESSAGE-GIOBIOM | Continuation of historical trends with slow progress toward achieving sustainability goals. Inequality only improves slowly. Environmental degradation with some improvements, including lower resource and energy intensity. Developments are compatible with limiting global temperature increase to 1.5 °C |
| 3 Fossil-fueled development, SSP5-19 | REMIND-MAGPIE | Focus on competitive markets and technological, social and economic development to achieve sustainability. Rapid economic growth through exploitation of fossil fuels and resource and energy intensive lifestyles. Developments are compatible with limiting global temperature increase to 1.5 °C |
| 4 BAU, SSP2-Baseline | MESSAGE-GLOBIOM | Same as SSP-19. The main difference is that the developments are BAU and not compatible with limiting global temperature increase to 1.5 °C, instead leading to an increase of about 3.8 °C. |

Appendix D1.1: SSP data

The tables below show SSP scenario estimates for various variables used in the model between 2005 and 2100. Exact data for all variables in the base year 2015 could not be found, so it is assumed to be between the 2010 and 2020 values estimated in the SSP scenarios. Because these values are estimates and the values for 2015 are a further extrapolation, they may deviate from reality. However, they were deemed good enough for a starting value estimate.

Table D2: data for the SSP1-19 scenario (IIASA, 2018). Some values based on additional assumptions (see below).

| SSP1 RCP 1.9 | 2005 | 2010 | 2020 | 2030 | 2040 | 2050 | 2060 | 2070 | 2080 | 2090 | 2100 |
|--|----------|----------|----------|----------|----------|----------|----------|----------|----------|----------|----------|
| Population (million) | 6531 | 6922 | 7576 | 8062 | 8389 | 8531 | 8492 | 8299 | 7967 | 7510 | 6958 |
| GDP (PPP) (billion US\$2005/yr) | 57408 | 68462 | 101815 | 155855 | 223196 | 291301 | 356291 | 419291 | 475419 | 524876 | 565390 |
| Carbon price (US\$2005/t CO ₂) | 0 | 0 | 0 | 304 | 546 | 651 | 708 | 652 | 520 | 335 | 239 |
| Secondary energy (electricity) (GWh/yr) | 1.82E+07 | 2.13E+07 | 2.41E+07 | 2.26E+07 | 2.75E+07 | 3.53E+07 | 4.25E+07 | 4.87E+07 | 5.23E+07 | 5.26E+07 | 5.03E+07 |
| Variable renewable energy share | 0.01 | 0.02 | 0.07 | 0.11 | 0.45 | 0.67 | 0.69 | 0.64 | 0.66 | 0.72 | 0.72 |
| PV capacity (GW) | 4 | 39 | 279 | 386 | 2357 | 3018 | 2479 | 1121 | 1247 | 1519 | 1674 |
| CSP capacity (GW) | 0 | 1 | 8 | 19 | 577 | 1979 | 3691 | 5179 | 5960 | 6357 | 6204 |
| Wind capacity (GW) | 59 | 196 | 490 | 527 | 1490 | 2887 | 2990 | 2299 | 2386 | 2821 | 2567 |
| Assumed geothermal capacity (GW) | 10 | 11 | 17 | 27 | 88 | 136 | 181 | 226 | 271 | 317 | 360 |
| Total biomass capacity (GW) | 67 | 81 | 185 | 224 | 315 | 430 | 577 | 665 | 711 | 742 | 824 |
| Hydro capacity (GW) | 871 | 1028 | 1314 | 1431 | 1730 | 1820 | 1877 | 1936 | 1991 | 2050 | 2078 |
| Nuclear capacity (GW) | 403 | 423 | 452 | 452 | 373 | 214 | 184 | 185 | 236 | 305 | 306 |
| Total oil capacity (GW) | 405 | 435 | 325 | 249 | 31 | 9 | 8 | 8 | 7 | 6 | 5 |
| Total coal capacity (GW) | 967 | 1139 | 1089 | 872 | 254 | 210 | 268 | 346 | 336 | 283 | 193 |
| Total gas capacity (GW) | 1011 | 1171 | 1616 | 1469 | 1072 | 1552 | 2139 | 2639 | 2657 | 2253 | 1886 |
| Assumed ocean capacity (GW) | 0 | 0 | 0 | 0 | 0 | 0 | 0 | 0 | 0 | 0 | 0 |
| Fraction of bio + CCS | 0.00 | 0.00 | 0.00 | 0.30 | 0.96 | 0.98 | 1.00 | 1.00 | 1.00 | 1.00 | 1.00 |
| Fraction of coal + CCS | 0.00 | 0.00 | 0.00 | 0.01 | 0.55 | 0.91 | 1.00 | 1.00 | 1.00 | 1.00 | 1.00 |
| Fraction of gas + CCS | 0.00 | 0.00 | 0.01 | 0.07 | 0.56 | 0.92 | 0.99 | 0.98 | 0.96 | 0.95 | 0.87 |
| Fraction of oil + CCS | 0.00 | 0.00 | 0.01 | 0.13 | 0.69 | 0.94 | 0.99 | 0.99 | 0.99 | 0.98 | 0.96 |

Table D3: data for the SSP2-19 scenario (IIASA, 2018). Some values based on additional assumptions (see below).

| SSP2 RCP 1.9 | 2005 | 2010 | 2020 | 2030 | 2040 | 2050 | 2060 | 2070 | 2080 | 2090 | 2100 |
|--|----------|----------|----------|----------|----------|----------|----------|----------|----------|----------|----------|
| Population (million) | 6503 | 6867 | 7611 | 8262 | 8787 | 9169 | 9385 | 9457 | 9407 | 9254 | 9032 |
| GDP (PPP) (billion US\$2005/yr) | 56533 | 67506 | 100897 | 141177 | 180978 | 223260 | 268958 | 321282 | 378016 | 438379 | 504585 |
| Carbon price (US\$2005/t CO ₂) | 0 | 0 | 32 | 95 | 268 | 436 | 710 | 1156 | 1884 | 3068 | 4998 |
| Secondary energy (electricity) (GWh/yr) | 1.81E+07 | 2.10E+07 | 2.63E+07 | 3.16E+07 | 4.46E+07 | 6.24E+07 | 8.30E+07 | 1.01E+08 | 1.14E+08 | 1.25E+08 | 1.38E+08 |
| Variable renewable energy share | 0.01 | 0.03 | 0.09 | 0.28 | 0.42 | 0.46 | 0.47 | 0.52 | 0.58 | 0.65 | 0.75 |
| PV capacity (GW) | 3 | 38 | 257 | 1227 | 2489 | 4654 | 6952 | 9976 | 11665 | 14006 | 17851 |
| CSP capacity (GW) | 0 | 2 | 2 | 12 | 56 | 154 | 341 | 659 | 1120 | 1760 | 2706 |
| Wind capacity (GW) | 55 | 255 | 654 | 2183 | 4718 | 6720 | 8592 | 11241 | 14350 | 17454 | 21263 |
| Geothermal capacity (GW) | 10 | 16 | 15 | 36 | 112 | 168 | 219 | 270 | 278 | 287 | 296 |
| Total biomass capacity (GW) | 28 | 40 | 64 | 57 | 34 | 29 | 60 | 136 | 208 | 210 | 176 |
| Hydro capacity (GW) | 855 | 1128 | 1225 | 1634 | 2124 | 2342 | 2555 | 2681 | 2749 | 2795 | 2826 |
| Nuclear capacity (GW) | 406 | 415 | 511 | 763 | 1248 | 2244 | 3659 | 4459 | 4605 | 4151 | 3286 |
| Total oil capacity (GW) | 408 | 233 | 88 | 45 | 19 | 11 | 10 | 1 | 0 | 0 | 0 |
| Total coal capacity (GW) | 1208 | 1554 | 1613 | 1175 | 478 | 103 | 39 | 16 | 5 | 1 | 0 |
| Total gas capacity (GW) | 891 | 1065 | 1774 | 2134 | 2605 | 2539 | 2271 | 1574 | 1480 | 1503 | 1793 |
| Assumed ocean capacity (GW) | 0 | 0 | 0 | 341 | 1523 | 2633 | 3667 | 5283 | 7093 | 8899 | 11415 |
| Fraction of bio + CCS | 0.00 | 0.00 | 0.00 | 0.09 | 0.59 | 0.85 | 0.85 | 0.91 | 0.97 | 0.97 | 0.97 |
| Fraction of coal + CCS | 0.00 | 0.00 | 0.00 | 0.32 | 1.00 | 0.99 | 1.00 | 1.00 | 1.00 | 1.00 | 1.00 |
| Fraction of gas + CCS | 0.00 | 0.00 | 0.00 | 0.16 | 0.71 | 0.90 | 0.87 | 0.87 | 0.87 | 1.00 | 1.00 |
| Fraction of oil + CCS | 0.00 | 0.00 | 0.00 | 0.19 | 0.77 | 0.91 | 0.91 | 0.92 | 0.94 | 0.99 | 0.99 |

Table D4: data for the SSP5-19 scenario (IIASA, 2018). Some values based on additional assumptions (see below).

| SSP5 RCP 1.9 | 2005 | 2010 | 2020 | 2030 | 2040 | 2050 | 2060 | 2070 | 2080 | 2090 | 2100 |
|--|----------|----------|----------|----------|----------|----------|----------|----------|----------|----------|----------|
| Population (million) | 6505 | 6894 | 7552 | 8054 | 8403 | 8579 | 8589 | 8457 | 8200 | 7831 | 7375 |
| GDP (PPP) (billion US\$2005/yr) | 56690 | 67570 | 101900 | 162800 | 246600 | 338400 | 440600 | 560000 | 686500 | 819000 | 960100 |
| Carbon price (US\$2005/t CO ₂) | 0 | 0 | 7 | 96 | 349 | 629 | 1204 | 1724 | 2904 | 4681 | 7464 |
| Secondary energy (electricity) (GWh/yr) | 1.84E+07 | 2.15E+07 | 2.92E+07 | 3.33E+07 | 4.46E+07 | 6.99E+07 | 9.70E+07 | 1.21E+08 | 1.42E+08 | 1.62E+08 | 1.78E+08 |
| Variable renewable energy share | 0.01 | 0.03 | 0.06 | 0.12 | 0.28 | 0.45 | 0.57 | 0.65 | 0.70 | 0.74 | 0.77 |
| PV capacity (GW) | 1 | 39 | 265 | 360 | 1108 | 3444 | 8102 | 14540 | 22640 | 30590 | 36790 |
| CSP capacity (GW) | 0 | 1 | 4 | 66 | 685 | 3009 | 6551 | 9700 | 12420 | 15000 | 17940 |
| Wind capacity (GW) | 40 | 180 | 515 | 1262 | 3688 | 7680 | 11770 | 15430 | 19070 | 22960 | 24560 |
| Geothermal capacity (GW) | 8 | 12 | 14 | 33 | 43 | 43 | 42 | 40 | 39 | 39 | 39 |
| Total biomass capacity (GW) | 24 | 35 | 46 | 78 | 310 | 458 | 536 | 626 | 721 | 760 | 756 |
| Hydro capacity (GW) | 702 | 743 | 702 | 891 | 2105 | 3539 | 4102 | 4326 | 4515 | 4683 | 4798 |
| Nuclear capacity (GW) | 401 | 404 | 482 | 831 | 1627 | 2295 | 2659 | 2854 | 2809 | 2662 | 2485 |
| Assumed total oil capacity (GW) | 322 | 317 | 229 | 110 | 0 | 0 | 0 | 0 | 0 | 0 | 0 |
| Total coal capacity (GW) | 1134 | 1299 | 1297 | 650 | 134 | 1 | 0 | 0 | 0 | 0 | 0 |
| Total gas capacity (GW) | 925 | 1147 | 2241 | 2761 | 1752 | 1165 | 731 | 384 | 150 | 85 | 45 |
| Assumed ocean capacity (GW) | 0 | 0 | 0 | 0 | 0 | 0 | 0 | 0 | 0 | 0 | 0 |
| Fraction of bio + CCS | 0.00 | 0.00 | 0.00 | 0.66 | 0.96 | 0.99 | 1.00 | 1.00 | 1.00 | 1.00 | 1.00 |
| Fraction of coal + CCS | 0.00 | 0.00 | 0.00 | 0.00 | 0.00 | 0.08 | 0.19 | 0.53 | 0.53 | 0.53 | 0.53 |
| Fraction of gas + CCS | 0.00 | 0.00 | 0.00 | 0.02 | 0.20 | 0.46 | 0.76 | 0.84 | 0.81 | 0.70 | 0.26 |
| Fraction of oil + CCS | 0.00 | 0.00 | 0.00 | 0.23 | 0.39 | 0.51 | 0.65 | 0.79 | 0.78 | 0.75 | 0.60 |

Table D5: data for the SSP2-baseline scenario (IIASA, 2018). Some values based on assumptions (see below).

| SSP2 Baseline | 2005 | 2010 | 2020 | 2030 | 2040 | 2050 | 2060 | 2070 | 2080 | 2090 | 2100 |
|--|----------|----------|----------|----------|----------|----------|----------|----------|----------|----------|----------|
| Population (million) | 6503 | 6867 | 7611 | 8262 | 8787 | 9169 | 9385 | 9457 | 9407 | 9254 | 9032 |
| GDP (PPP) (billion US\$2005/yr) | 56533 | 67529 | 101245 | 143070 | 185955 | 231300 | 280515 | 336849 | 398498 | 465847 | 539332 |
| Carbon price (US\$2005/t CO ₂) | 0 | 0 | 0 | 0 | 0 | 0 | 0 | 0 | 0 | 0 | 0 |
| Secondary energy (electricity) (GWh/yr) | 1.81E+07 | 2.10E+07 | 2.63E+07 | 3.27E+07 | 3.90E+07 | 4.73E+07 | 5.89E+07 | 7.18E+07 | 8.24E+07 | 9.32E+07 | 1.05E+08 |
| Variable renewable energy share | 0.01 | 0.03 | 0.07 | 0.10 | 0.13 | 0.15 | 0.18 | 0.21 | 0.22 | 0.24 | 0.28 |
| PV capacity (GW) | 3 | 38 | 257 | 256 | 238 | 160 | 382 | 899 | 1336 | 2097 | 3375 |
| CSP capacity (GW) | 0 | 2 | 2 | 2 | 0 | 0 | 0 | 0 | 0 | 0 | 0 |
| Wind capacity (GW) | 56 | 255 | 541 | 932 | 1419 | 2122 | 3134 | 4362 | 5091 | 6253 | 7950 |
| Geothermal capacity (GW) | 10 | 16 | 15 | 7 | 0 | 0 | 0 | 0 | 0 | 0 | 0 |
| Total biomass capacity (GW) | 28 | 41 | 65 | 51 | 32 | 61 | 59 | 69 | 124 | 168 | 220 |
| Hydro capacity (GW) | 855 | 1127 | 1219 | 1300 | 1449 | 1496 | 1560 | 1661 | 1771 | 1831 | 1848 |
| Nuclear capacity (GW) | 406 | 415 | 511 | 437 | 281 | 165 | 217 | 379 | 670 | 1172 | 1765 |
| Total oil capacity (GW) | 408 | 233 | 88 | 45 | 19 | 11 | 10 | 1 | 0 | 0 | 0 |
| Total coal capacity (GW) | 1209 | 1551 | 1634 | 1400 | 1246 | 1402 | 1794 | 2189 | 2619 | 2696 | 2397 |
| Total gas capacity (GW) | 887 | 1065 | 1777 | 2939 | 4651 | 6273 | 8174 | 10346 | 11574 | 12596 | 14292 |
| Assumed ocean capacity (GW) | 0 | 0 | 0 | 0 | 8 | 33 | 50 | 81 | 188 | 547 | 865 |
| Fraction of bio + CCS | 0 | 0 | 0 | 0 | 0 | 0 | 0 | 0 | 0 | 0 | 0 |
| Fraction of coal + CCS | 0 | 0 | 0 | 0 | 0 | 0 | 0 | 0 | 0 | 0 | 0 |
| Fraction of gas + CCS | 0 | 0 | 0 | 0 | 0 | 0 | 0 | 0 | 0 | 0 | 0 |
| Fraction of oil + CCS | 0 | 0 | 0 | 0 | 0 | 0 | 0 | 0 | 0 | 0 | 0 |

There was some missing data in the SSP database. None of the scenarios reported any data for ocean energy. For SSP1-19, data for geothermal was also missing, and for SSP5-19 there was no data for oil. In addition, there was a discrepancy between the sum of the reported values for technologies and the reported total. This may be partially due to rounding errors, however, for some scenarios the difference is quite large. Instead of ignoring this difference it was attributed to the technologies for which data was missing.

For SSP2-19 and SSP2-baseline, the difference was attributed to ocean energy. For SSP2-19 this becomes quite a large number by 2100 and for SSP2-baseline it is also relatively large compared to other minor renewables. However, because the nickel intensity used for ocean energy is very small, it is not assumed to affect the model results much.

For SSP1-19, the difference was attributed to geothermal energy instead of ocean energy because it was assumed that it is more likely for ocean energy to have a lower capacity than geothermal, because geothermal is a more mature technology. However, this does not explain why ocean energy becomes more in SSP2-19 and SSP2-baseline. This is an important point of uncertainty that should be considered. For SSP5-19, the difference was attributed to oil, because, especially in the earlier years, this fits better with the other scenarios and it fits with the fossil-fueled development narrative of SSP5. After 2040, the difference becomes slightly negative for most years and it is assumed oil becomes 0 for all these years.

In the SSP database, the values for installed capacity did not distinguish between power plants with or without CCS, but the values for electricity generation did. However, the electricity generation shares for plants with and without CCS cannot simply be converted to capacity shares. It was assumed that the CF remains similar when adding CCS, however there is an energy penalty that needs to be taken into account. This means that for the same net energy output, a larger capacity is required for power plants with CCS, because some of the produced energy is used for the CCS (Blok & Nieuwlaar, 2021).

The energy penalty for implementing CCS depends on many factors, including power plant type and CCS type. In the literature ranges have been reported of between 15 and 28% for pulverised coal, 5 - 20% for Integrated Gasification Combined Cycle (IGCC) and 15 - 16% for natural gas combined cycle (Budinis et al., 2018). In this thesis a value of 15% is used for all technologies.

In the SSP database, no distinction is made between oil-fired power plants with or without CCS. It is assumed that the share with CCS is similar to the shares for bio, coal and natural gas and therefore an average of those shares was used. The share of oil in total electricity generation is relatively small, so regardless of what is assumed, it will not make much difference.

Appendix D2: Storage scenarios

Modelling storage is very complex and includes many considerations and assumptions. The required storage is determined by the amount of electricity generated by Variable Renewable Energy (VRE) sources (wind and solar), as well as by the application of other flexibility measures. Zerrahn et al. (2018) reviewed the literature on storage requirements for various VRE shares and they concluded that the amount of storage required as a percentage of total annual electricity demand decreases significantly when other flexibility measures and curtailment are taken into account.

Appendix D2.1: Flexibility scenarios

Zerrahn et al. (2018) created three profiles of required storage capacity as a percentage of electricity demand per VRE share, that can be seen as scenarios. Their analysis was for Germany, but they also assessed other research from different countries with similar results. In the first scenario, all renewable surplus energy is integrated. Zerrahn et al. (2018) argue that this is a highly unlikely scenario, because it does not make economic sense to have that much storage capacity. In the second scenario, curtailment is allowed, greatly reducing the required storage capacity, and in the third scenario, additional flexibility is added, reducing the required storage capacity even further, while also decreasing curtailment.

Several adjustments were made to the profiles described by Zerrahn et al. (2018) to obtain three flexibility scenarios used in the model: a high, medium and low flexibility scenario. First, as argued by Zerrahn et al. (2018), the scenario in which all renewable surplus energy is integrated (adapted from Sinn, 2017), was discarded based on its high unlikelihood. Second, the scenario with additional flexibility was also discarded. Zerrahn et al. (2018) based this on V2G storage, which is already explicitly included in the model. The scenario could also be achieved through flexible electric heaters or the production of hydrogen, which is not considered explicitly in the model. However, it was assumed that such flexibility could also be used instead of curtailment in the second scenario derived from Zerrahn et al. (2018).

Furthermore, the research assessed by Zerrahn et al. (2018) only applied to developed countries with well-established electricity grids. This allows for a lot more flexibility than what is possible in smaller off-grid systems or less reliable grids in developing countries (IRENA, 2017). Therefore, the second scenario by Zerrahn (2018) was used in this thesis as the high flexibility scenario in a global setting. To account more for the, on average lower flexibility in a global setting, medium and low flexibility scenarios were created that shifted the data by Zerrahn (2018) a respective 10% and 20% to the left on the VRE share scale.

In their profiles, Zerrahn et al. (2018) do not include base storage as a fraction of electricity demand that is required regardless of VRE share. This storage was assumed to be equivalent to the storage capacity in the base year (2015) as VRE share was still relatively low then. The storage capacity in the base year was determined as follows: first the PHS capacity in 2017 of 4530 GWh was determined by multiplying the reported total storage capacity of 4670 GWh by the reported share of PHS of 97% (IRENA, 2017). This capacity was then divided by the capacity in GW reported by IHA (2018) to obtain an E/P (Energy/Power) ratio of 30 hours of storage. Based on IRENA (2017), it was further calculated that EV batteries were 2.7% of the total storage capacity.

It was assumed that the E/P ratio, the 97% and the 2.7% remained relatively stable between 2015 and 2017. Based on this and the PHS of 144 GW in 2015 (IHA, 2016), the total storage capacity in 2015 in GWh was calculated. The EV battery share was then removed from the total storage capacity, because not all EV batteries are actually used for V2G, with the exception of a share equivalent to the VRE share in 2015 (IRENA, 2017). VRE share is also used to determine the percentage of EVs being used for V2G in the model.

The remaining storage capacity of 4280 GWh was then divided by the total electricity demand in 2015 (IRENA, 2017) to obtain a fraction of 0.00017. The same procedure was followed to determine storage as a fraction of electricity demand for the IRENA (2017) REmap scenario. The three scenarios used in this thesis are summarised in table D6 and the data used is shown in table D7 and figure D2.

Table D6: the three flexibility scenarios used in the nickel model.

| Scenario | Elaboration |
|---------------|--|
| 1 Low flex | Base storage as a fraction of electricity demand plus the second profile proposed by Zerrahn et al. (2018) shifted 20% to the left on the VRE share scale. In addition, it is assumed $\frac{1}{3}$ of the vehicles participating in V2G are available at the right time. |
| 2 Medium flex | Base storage as a fraction of electricity demand plus the second profile proposed by Zerrahn et al. (2018) shifted 10% to the left on the VRE share scale. In addition, it is assumed $\frac{1}{2}$ of the vehicles participating in V2G are available at the right time. |
| 3 High flex | Base storage as a fraction of electricity demand plus the second profile proposed by Zerrahn et al. (2018) including the option for curtailment. It is argued in this thesis that the curtailment could also be replaced by other flexibility measures. In addition, it is assumed $\frac{2}{3}$ of the vehicles participating in V2G are available at the right time. |

Table D7: values for storage as fraction of electricity demand used in the flexibility scenarios (orange) and additional values in profiles by Zerrahn (2018) and Sinn (2017). Values closer to 90% for the shifted scenarios are assumptions made to fit the curve ending at 0.00215 at 90% based on Zerrahn (2018).

| VRE share | 15% | 20% | 25% | 30% | 35% | 40% | 45% | 50% | 55% | 60% | 65% | 70% | 75% | 80% | 85% | 90% |
|-------------------------------------|---------|----------|----------|----------|----------|----------|----------|----------|----------|----------|----------|----------|----------|----------|----------|----------|
| Zerrahn (2018) | | | | | | | | | | | | | | | | |
| increased flex | 0 | 0 | 0 | 0 | 0 | 0 | 0 | 0.000006 | 0.000024 | 0.00004 | 0.000056 | 0.000084 | 0.000206 | 0.00048 | 0.000998 | 0.002154 |
| Zerrahn (2018) | 0 | 0 | 0 | 0 | 0 | 0.000016 | 0.000036 | 0.00007 | 0.000108 | 0.000216 | 0.000352 | 0.00046 | 0.000628 | 0.000924 | 0.001386 | 0.002154 |
| Zerrahn (2018) shifted 10% | 0 | 0 | 0 | 0.000016 | 0.000036 | 0.00007 | 0.000108 | 0.000162 | 0.000216 | 0.000318 | 0.000406 | 0.000502 | 0.000628 | 0.000924 | 0.001386 | 0.002154 |
| Zerrahn (2018) shifted 20% | 0 | 0.000016 | 0.000036 | 0.00007 | 0.000108 | 0.000162 | 0.000216 | 0.000284 | 0.000352 | 0.000406 | 0.00046 | 0.000544 | 0.000628 | 0.000924 | 0.001386 | 0.002154 |
| Zerrahn (2018); Sinn (2017) no flex | 0 | 0.00002 | 0.00004 | 0.0001 | 0.0003 | 0.0008 | 0.0024 | 0.00426 | 0.0062 | 0.0083 | 0.0102 | 0.0124 | 0.015 | 0.0184 | 0.0254 | 0.033 |
| Increased flex | 0.00017 | 0.00017 | 0.00017 | 0.00017 | 0.00017 | 0.00017 | 0.00017 | 0.000176 | 0.000194 | 0.00021 | 0.000226 | 0.000254 | 0.000376 | 0.00065 | 0.001168 | 0.002324 |
| High flex | 0.00017 | 0.00017 | 0.00017 | 0.00017 | 0.00017 | 0.000186 | 0.000206 | 0.00024 | 0.000278 | 0.000386 | 0.000522 | 0.00063 | 0.000798 | 0.001094 | 0.001556 | 0.002324 |
| Mid flex | 0.00017 | 0.00017 | 0.00017 | 0.000186 | 0.000206 | 0.00024 | 0.000278 | 0.000332 | 0.000386 | 0.000488 | 0.000576 | 0.000672 | 0.000798 | 0.001094 | 0.001556 | 0.002324 |
| Low flex | 0.00017 | 0.000186 | 0.000206 | 0.00024 | 0.000278 | 0.000332 | 0.000386 | 0.000454 | 0.000522 | 0.000576 | 0.00063 | 0.000714 | 0.000798 | 0.001094 | 0.001556 | 0.002324 |
| No flex | 0.00017 | 0.00019 | 0.00021 | 0.00027 | 0.00047 | 0.00097 | 0.00257 | 0.00443 | 0.00637 | 0.00847 | 0.01037 | 0.01257 | 0.01517 | 0.01857 | 0.02557 | 0.03317 |

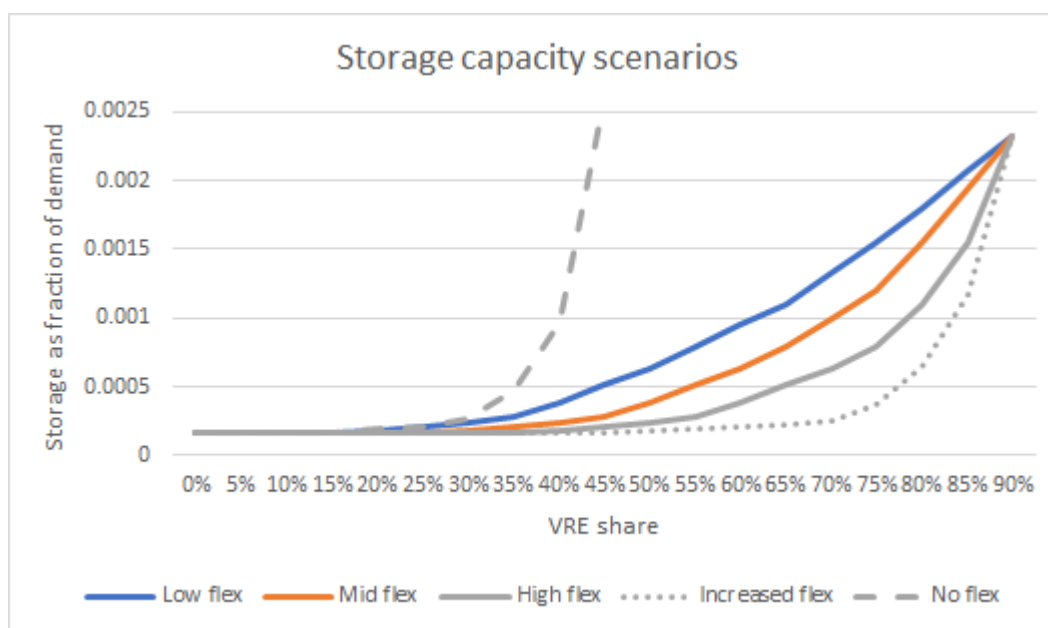


Figure D2: profiles of the storage capacity scenarios discussed by Zerrahn et al. (2018; grey) and those used in the model (solid lines). Data for this figure is shown in table D7. The 'no flex' scenario goes up to a fraction of 0.033 at 90% (Sinn, 2017). The other scenarios converge at 90% based on Zerrahn et al. (2018). A base storage fraction of 0.00017 was added to the scenarios based on IHA (2016), IHA (2018) and IRENA (2017).

The shift of 10% and 20% may seem arbitrary, however, the 20% shifted profile actually fits better with the more market-based forecast made by IRENA (2017). IRENA (2017) modelled the potential storage capacity growth from 2017 to 2030. Here they included potential storage additions for PHS, CSP TES, EV storage (split into passenger vehicles, commercial vehicles, buses and 2 & 3 wheelers), SBS (split into rooftop PV, retrofit rooftop PV and utility scale) and a small 'other' category including CAES, flywheels and other TES.

At a 34% VRE share in 2030 in IRENAs (2017) REmap scenario, the calculated storage as a fraction of total electricity demand is between 0.00028 and 0.00037. This corresponds with the 0.00028 at 35% in the low flexibility scenario and is a lot more than what is expected based on Zerrahn et al. (2018).

It is important to note that the calculated values for the REmap scenario only include a fraction (based on VRE share) of EV storage, as the primary function of EVs is providing a transportation service. Therefore, the number of batteries goes up regardless of grid storage requirements. This also applies to stationary storage, due to behind-the-meter storage opportunities for small scale PV systems to increase self-sufficiency (IRENA, 2017). This is discussed further in appendix D2.4.

It is very uncertain how flexibility will develop in the future and this is also a dynamic factor that will probably increase over time with increased sector coupling and innovation. The research done by Zerrahn (2018) described a static situation with different possible VRE shares and this is also used in this thesis. However, it is important to keep in mind that in reality it is more likely that the values are closer to the low flex scenario in earlier years and closer to the high flex scenario in later years.

In theory, curtailment is always possible, but this would require more electricity generation capacity, and thus more nickel. It is unclear how curtailment is taken into account in the SSP scenarios. Some other flexibility measures could also require more nickel, but this is not taken into account in this thesis, because the assessment of what this flexibility could be is beyond the scope of this research.

Appendix D2.2: PHS, CSP TES and V2G shares

Once other flexibility has been accounted for, the remaining storage requirements can be fulfilled by the available storage options. The four storage options included in this thesis are PHS, CSP TES, SBS and EV battery storage (V2G).

Over the past five years, the percentage of hydropower capacity that functioned as PHS was consistently 12% (IHA 2016-2020). According to Achkari & El Fadar (2020), 45% of CSP capacity is currently equipped with TES. However, because it is cost-effective, it is assumed this will increase over the years. This increase is based on the increase in VRE share to fit with the SSP narratives (see table D1).

The hours of storage or E/P ratio was assumed to be 30 hours for PHS, based on reported energy and power by IRENA (2017) and IHA (2018) for 2017. The E/P ratio for CSP TES was assumed to be between 5 and 9 hours (IRENA, 2017). These values are used in the model in combination with data on hydropower and CSP capacity respectively to determine the amount of storage that can be covered by PHS and CSP TES in different scenarios.

V2G requires willingness to participate by the vehicle owners. In this thesis, the availability of vehicles for V2G is linked to the share of VRE. It is assumed that the willingness of vehicle owners to participate depends on the incentives they receive and that these incentives depend on the amount of storage that is needed, which increases as the share of VRE increases.

Appendix D2.3: Battery repurposing

All storage not covered by EVs, PHS and CSP TES is assumed to be covered by SBS. For stationary storage, it is generally cheaper to repurpose batteries than to purchase new ones (Walker et al., 2015; BNEF, 2016). However, the quality is lower and some studies have come to more negative conclusions regarding the economics (De Rousseau et al., 2017). In addition, there may be warranty issues and not all EV companies want to be involved with repurposing (BNEF, 2016). According to BNEF (2016) about a third of the EV batteries will be given a second life as stationary storage by 2025. It is assumed that over time this will increase as VRE share increases and more storage is required.

Appendix D2.4: Behind the meter storage

According to IRENA (2017), up to 40% of annual small-scale PV installations included battery storage in Germany in recent years, with an assumed capacity of 1.2 - 2 kWh/kW small-scale PV. However, this percentage was probably lower in other countries and also lower for the existing stock. To match with an initial installed stationary battery capacity of 11 GWh, of which about 3 - 4 GWh was assumed to be small-scale (IRENA, 2017; Olson & Bakken, 2019), it is assumed that the percentage of small-scale PV installations including battery storage was equal to the modelled VRE share in 2015. It is also assumed that this percentage will increase over time as the price for battery storage decreases. Based on this, the percentage of small-scale PV installations with battery storage is assumed to increase as VRE share increases. The different types of storage considered in the model are shown in figure D3.

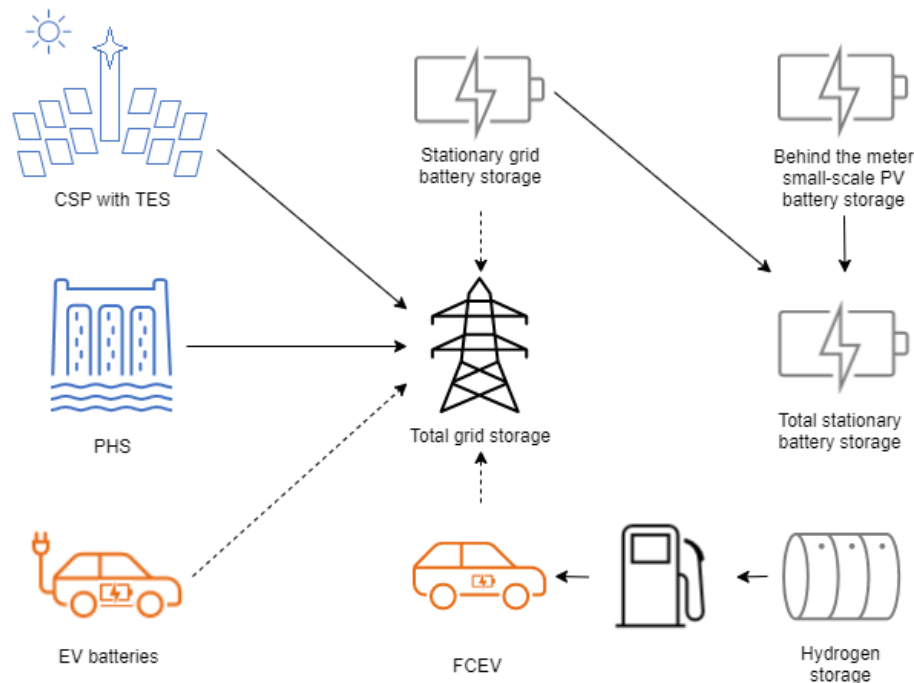


Figure D3: types of grid electricity storage considered in this thesis and types of SBS. The dotted line indicates that not all EVs are used for V2G. Strictly speaking, CSP with TES may not be grid storage, but it does reduce the requirements for grid storage and is therefore included. The same goes for V2G.

Regarding the percentage of total PV that will be small-scale over the years, there has been a general trend of increasing utility-scale share (Radoia, 2019) and this is expected to continue in the future, from about 50% in 2016 to about 67% in 2050. An additional 18% in 2016 and 15% in 2050 is commercial and industrial capacity and the remaining 32% and 18% respectively consists of off-grid, microgrid and residential applications (Olson & Bakken, 2019). It is assumed that the latter category will have its own battery storage. This is included in the model with the assumption that the 2015 values are the same as the 2016 values and the 2050 values will not change further.

Due to the many assumptions involved, the way storage is modelled in this thesis is very uncertain. However, a general conclusion that can be drawn, also found by Zerrahn et al. (2018), is that not much SBS is needed for the grid in the future if EVs can indeed cover a large part of the storage requirements.

Appendix D2.5: Battery market shares

The market share and the current applications of different battery types are included in table C3 for 2018. However, this is expected to change significantly in the future. BNEF (2019) expects the nickel-containing share to rise to 85% by 2030, especially due to an increased share of NMC 811. These changes are included in the model by creating a lookup based on the expectations of BNEF (2019) until 2030 with further extrapolation to 2100. This is shown in table D8.

Table D8: data for the battery market shares (BNEF, 2019). Some values are based on assumptions (see text).

| Battery scenario | 2015 | 2018 | 2020 | 2022 | 2024 | 2026 | 2028 | 2030 | 2040 | 2050 | 2060 | 2070 | 2080 | 2090 | 2100 |
|---------------------------|------|------|------|------|------|------|------|------|-------|------|-------|------|-------|------|------|
| Stationary | | | | | | | | | | | | | | | |
| NCA+ share | 0 | 0 | 0 | 0 | 0 | 0 | 0 | 0 | 0 | 0 | 0 | 0 | 0 | 0 | 0 |
| NCA share | 0 | 0 | 0 | 0 | 0 | 0 | 0 | 0 | 0 | 0 | 0 | 0 | 0 | 0 | 0 |
| NMC 811 share | 0 | 0 | 0 | 0.05 | 0.12 | 0.16 | 0.2 | 0.24 | 0.355 | 0.47 | 0.585 | 0.7 | 0.815 | 1 | 1 |
| NMC 622 share | 0 | 0.15 | 0.29 | 0.4 | 0.4 | 0.34 | 0.29 | 0.24 | 0.16 | 0.08 | 0 | 0 | 0 | 0 | 0 |
| NMC 532 share | 0 | 0 | 0 | 0 | 0 | 0 | 0 | 0 | 0 | 0 | 0 | 0 | 0 | 0 | 0 |
| NMC 422 share | 0.04 | 0.19 | 0.15 | 0.14 | 0.12 | 0.17 | 0.17 | 0.17 | 0.135 | 0.1 | 0.065 | 0 | 0 | 0 | 0 |
| NMC 111 share | 0.73 | 0.35 | 0.26 | 0.05 | 0 | 0 | 0 | 0 | 0 | 0 | 0 | 0 | 0 | 0 | 0 |
| Other | 0.23 | 0.31 | 0.3 | 0.36 | 0.36 | 0.33 | 0.34 | 0.35 | 0.35 | 0.35 | 0.35 | 0.3 | 0.185 | 0 | 0 |
| Passenger vehicles | | | | | | | | | | | | | | | |
| NCA+ share | 0.18 | 0.19 | 0.21 | 0.25 | 0.24 | 0.27 | 0.31 | 0.35 | 0.39 | 0.43 | 0.47 | 0.51 | 0.55 | 0.59 | 0.63 |
| NCA share | 0 | 0.02 | 0.04 | 0.04 | 0.03 | 0.03 | 0.03 | 0 | 0 | 0 | 0 | 0 | 0 | 0 | 0 |
| NMC 811 share | 0 | 0.01 | 0.08 | 0.3 | 0.47 | 0.57 | 0.61 | 0.65 | 0.61 | 0.57 | 0.53 | 0.49 | 0.45 | 0.41 | 0.37 |
| NMC 622 share | 0.28 | 0.5 | 0.5 | 0.34 | 0.23 | 0.11 | 0.03 | 0 | 0 | 0 | 0 | 0 | 0 | 0 | 0 |
| NMC 532 share | 0.36 | 0.15 | 0.08 | 0.03 | 0 | 0 | 0 | 0 | 0 | 0 | 0 | 0 | 0 | 0 | 0 |
| NMC 422 share | 0 | 0 | 0 | 0 | 0 | 0 | 0 | 0 | 0 | 0 | 0 | 0 | 0 | 0 | 0 |
| NMC 111 share | 0.07 | 0.04 | 0.01 | 0 | 0 | 0 | 0 | 0 | 0 | 0 | 0 | 0 | 0 | 0 | 0 |
| Other | 0.11 | 0.09 | 0.08 | 0.04 | 0.03 | 0.02 | 0.02 | 0 | 0 | 0 | 0 | 0 | 0 | 0 | 0 |
| Trucks | | | | | | | | | | | | | | | |
| NCA+ share | 0 | 0.02 | 0.04 | 0.05 | 0.05 | 0.03 | 0.04 | 0.05 | 0.06 | 0.07 | 0.08 | 0.09 | 0.1 | 0.11 | 0.12 |
| NCA share | 0.23 | 0.18 | 0.17 | 0.14 | 0.12 | 0.13 | 0.14 | 0.15 | 0.16 | 0.17 | 0.18 | 0.19 | 0.2 | 0.21 | 0.22 |
| NMC 811 share | 0 | 0 | 0.05 | 0.13 | 0.2 | 0.27 | 0.28 | 0.29 | 0.3 | 0.31 | 0.32 | 0.33 | 0.34 | 0.35 | 0.36 |
| NMC 622 share | 0.08 | 0.2 | 0.27 | 0.2 | 0.13 | 0.07 | 0.05 | 0.03 | 0 | 0 | 0 | 0 | 0 | 0 | 0 |
| NMC 532 share | 0 | 0 | 0 | 0 | 0 | 0 | 0 | 0 | 0 | 0 | 0 | 0 | 0 | 0 | 0 |
| NMC 422 share | 0 | 0 | 0 | 0 | 0 | 0 | 0 | 0 | 0 | 0 | 0 | 0 | 0 | 0 | 0 |
| NMC 111 share | 0.23 | 0.11 | 0 | 0 | 0 | 0 | 0 | 0 | 0 | 0 | 0 | 0 | 0 | 0 | 0 |
| Other | 0.46 | 0.49 | 0.47 | 0.48 | 0.5 | 0.5 | 0.49 | 0.48 | 0.48 | 0.45 | 0.42 | 0.39 | 0.36 | 0.33 | 0.3 |
| Buses | | | | | | | | | | | | | | | |
| NCA+ share | 0 | 0 | 0 | 0 | 0 | 0 | 0 | 0 | 0 | 0 | 0 | 0 | 0 | 0 | 0 |
| NCA share | 0 | 0 | 0 | 0 | 0 | 0 | 0 | 0 | 0 | 0 | 0 | 0 | 0 | 0 | 0 |
| NMC 811 share | 0 | 0 | 0 | 0 | 0.01 | 0.08 | 0.17 | 0.26 | 0.3 | 0.34 | 0.38 | 0.42 | 0.46 | 0.5 | 0.54 |
| NMC 622 share | 0 | 0.03 | 0.04 | 0.06 | 0.09 | 0.08 | 0.06 | 0.04 | 0 | 0 | 0 | 0 | 0 | 0 | 0 |
| NMC 532 share | 0 | 0 | 0 | 0 | 0 | 0 | 0 | 0 | 0 | 0 | 0 | 0 | 0 | 0 | 0 |
| NMC 422 share | 0 | 0 | 0 | 0 | 0 | 0 | 0 | 0 | 0 | 0 | 0 | 0 | 0 | 0 | 0 |
| NMC 111 share | 0.02 | 0 | 0 | 0 | 0 | 0 | 0 | 0 | 0 | 0 | 0 | 0 | 0 | 0 | 0 |
| Other | 0.98 | 0.97 | 0.96 | 0.94 | 0.9 | 0.84 | 0.77 | 0.7 | 0.7 | 0.66 | 0.62 | 0.58 | 0.54 | 0.5 | 0.46 |

The BNEF (2019) values were placed two years (3 years for 2015) before the forecast by BNEF (2019) to account for manufacturing time. The extrapolations from 2030 onward were partially based on Van der Linden (2020). In this thesis, it is assumed that after 2030 the changes are relatively slow over a 10-year period, but of course the uncertainty of all changes after 2030 is very high.

Van der Linden (2020) increased the share of NMC811 and decreased the share of NCA+ over time. However, in this thesis, this is switched around to reflect the relative difficulty of obtaining cobalt. In addition, it is likely that higher energy density is preferred in the future and even if NMC gets a higher energy density than NCA+, this is likely due to an increased nickel content, which is also reflected by increasing the NCA share. This is an assumption without accounting for substitution. If nickel becomes scarce, substitution will occur in the model, which includes switching to batteries containing less nickel.

In the thesis by Van der Linden (2020), the values for trucks stagnate, however, in this thesis, the NCA and NMC 811 shares keep growing and LFP is reduced to create a scenario where more nickel is required. If substitution occurs in the model, it follows that a switch is made back to increasing LFP or another technology that does not contain (as much) nickel.

Appendix D3 Transport scenarios

The transport scenarios were designed to stay close to the narratives of the different SSPs by relating the number of vehicles to GDP and population. Our World in Data (2014) created a chart in which they compared the number of motor vehicles per 1000 inhabitants to Purchasing Power Parity (PPP) adjusted GDP per capita. Their definition of motor vehicles includes passenger vehicles, trucks and buses. This chart was used to estimate the number of required vehicles based on GDP growth after first converting 2014 US\$ to 2005 US\$ to match the SSP data. This value was adjusted based on the initial number of vehicles in 2015, which was about 1.28 billion according to Statista (2018a).

Based on Van der Linden (2020), the passenger vehicle share of total motor vehicles for all SSPs was consistently around 75% in 2015, flattening off at about 80% by 2050. The truck share was roughly 24% in 2015, flattening off at about 19% by 2050. The bus share is the remainder. These figures are all rough estimates, but they do indicate the relatively large share of passenger vehicles and small share of buses.

An important category that was not included is the 2 & 3 wheelers. According to IRENA (2017), a relatively large share of batteries was used in 2 & 3 wheelers in 2017, about 105 GWh, which was 65% of non-PHS storage. However, in the future this share is expected to decrease to about 7% in 2030 in the IRENA (2017) REmap scenario. Due to lack of data, this category was excluded.

In total, four transport scenarios were constructed, based on two important uncertainties: BAU vs ET and electrification vs hydrogen. The distinction between BAU vs ET is determined by the SSPs, where the SSPs with a target of 1.5 °C temperature increase (SSP1-19, SSP2-19 and SSP5-19) are considered as ET scenarios and SSP2-baseline is considered as the BAU scenario. The four transport scenarios and their data sources are shown in figure D4 and described further in sections D3.1 and D3.2.

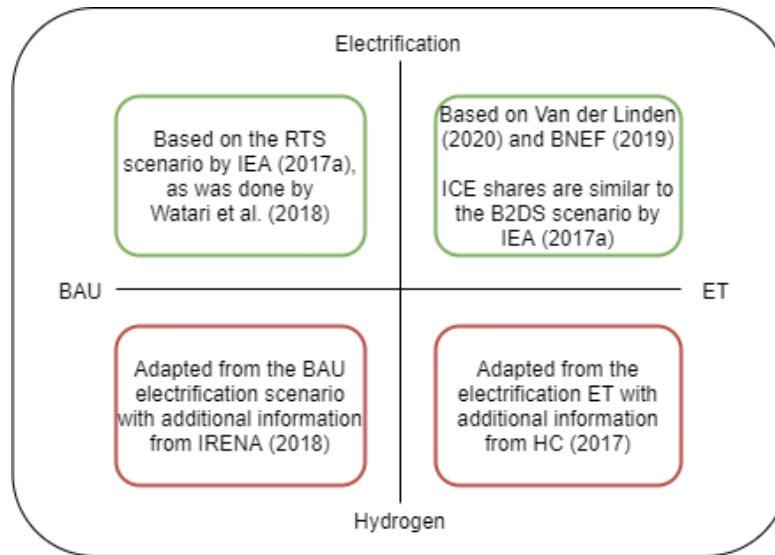


Figure D4: the four transport scenarios included in this thesis.

Appendix D3.1: Electrification scenarios

The ET electrification scenario is based on Van der Linden (2020), who considered ICEs, PHEVs and BEVs for passenger vehicles, and ICEs and a general category of EVs for buses and trucks. The values up to 2050 were based on Van der Linden (2020) and thereafter the values were linearly extrapolated. In the shares reported by Van der Linden (2020), HEV and FCV were not included. It was assumed that the HEV share is a fraction of the ICE share that increases over time. This fraction was assumed to be equal to the combined BEV and PHEV share. It was further assumed that the FCV remains zero in this scenario. The ICE shares in this scenario are similar to those in the Beyond 2 Degrees Scenario (B2DS) by the IEA (2017a).

The BAU electrification scenario was based on the Reference Technology Scenario (RTS) by the IEA (2017a), as was done by Watari et al. (2018). For buses and trucks, the ET values were shifted by 10 years. Vehicle shares for the ET and BAU electrification scenarios are shown in table D9 and D10 respectively and in figure D5. The numbers in the tables may not exactly match the figures of the sources they are based on, partially due to additional assumptions and partially due to the fact that many were estimated based on graphs in the publications.

Table D9: vehicle market shares for the ET electrification scenario. Based on BNEF (2019) & Van der Linden (2020)

| Electrification ET | 2000 | 2010 | 2020 | 2030 | 2040 | 2050 | 2060 | 2070 | 2080 | 2090 | 2100 |
|---------------------------------|------|-------|-------|-------|-------|-------|------|------|------|------|------|
| Passenger vehicle shares | | | | | | | | | | | |
| ICE | 1 | 0.990 | 0.872 | 0.487 | 0.184 | 0.01 | 0 | 0 | 0 | 0 | 0 |
| HEV | 0 | 0.005 | 0.062 | 0.211 | 0.245 | 0.09 | 0 | 0 | 0 | 0 | 0 |
| PHEV | 0 | 0.005 | 0.016 | 0.069 | 0.075 | 0.16 | 0.1 | 0 | 0 | 0 | 0 |
| BEV | 0 | 0 | 0.05 | 0.233 | 0.496 | 0.74 | 0.9 | 1 | 1 | 1 | 1 |
| FCEV | 0 | 0 | 0 | 0 | 0 | 0 | 0 | 0 | 0 | 0 | 0 |
| Bus shares | | | | | | | | | | | |
| ICE | 1 | 0.9 | 0.48 | 0.28 | 0.19 | 0.095 | 0 | 0 | 0 | 0 | 0 |
| BEV | 0 | 0.1 | 0.52 | 0.72 | 0.81 | 0.905 | 1 | 1 | 1 | 1 | 1 |
| FCEV | 0 | 0 | 0 | 0 | 0 | 0 | 0 | 0 | 0 | 0 | 0 |
| Truck shares | | | | | | | | | | | |
| ICE | 1 | 1 | 0.99 | 0.92 | 0.81 | 0.69 | 0.57 | 0.45 | 0.33 | 0.21 | 0.09 |
| BEV | 0 | 0 | 0.01 | 0.08 | 0.19 | 0.31 | 0.43 | 0.55 | 0.67 | 0.79 | 0.91 |
| FCEV | 0 | 0 | 0 | 0 | 0 | 0 | 0 | 0 | 0 | 0 | 0 |

Table D10: vehicle market shares for the BAU electrification scenario. Based on IEA (2017a)

| Electrification BAU | 2000 | 2010 | 2020 | 2030 | 2040 | 2050 | 2060 | 2070 | 2080 | 2090 | 2100 |
|---------------------------------|------|-------|-------|------|------|------|------|------|------|------|------|
| Passenger vehicle shares | | | | | | | | | | | |
| ICE | 1 | 0.990 | 0.990 | 0.78 | 0.69 | 0.49 | 0.23 | 0 | 0 | 0 | 0 |
| HEV | 0 | 0.005 | 0.005 | 0.12 | 0.19 | 0.28 | 0.40 | 0.47 | 0.31 | 0.15 | 0.00 |
| PHEV | 0 | 0.005 | 0.005 | 0.05 | 0.07 | 0.14 | 0.22 | 0.30 | 0.38 | 0.46 | 0.53 |
| BEV | 0 | 0 | 0 | 0.05 | 0.05 | 0.09 | 0.15 | 0.23 | 0.31 | 0.39 | 0.47 |
| FCEV | 0 | 0 | 0 | 0 | 0 | 0 | 0 | 0 | 0 | 0 | 0 |
| Bus shares | | | | | | | | | | | |
| ICE | 1 | 0.9 | 0.9 | 0.48 | 0.28 | 0.19 | 0.10 | 0 | 0 | 0 | 0 |
| BEV | 0 | 0.1 | 0.1 | 0.52 | 0.72 | 0.81 | 0.91 | 1 | 1 | 1 | 1 |
| FCEV | 0 | 0 | 0 | 0 | 0 | 0 | 0 | 0 | 0 | 0 | 0 |
| Truck shares | | | | | | | | | | | |
| ICE | 1 | 1 | 1 | 0.99 | 0.92 | 0.81 | 0.69 | 0.57 | 0.45 | 0.33 | 0.21 |
| BEV | 0 | 0 | 0 | 0.01 | 0.08 | 0.19 | 0.31 | 0.43 | 0.55 | 0.67 | 0.79 |
| FCEV | 0 | 0 | 0 | 0 | 0 | 0 | 0 | 0 | 0 | 0 | 0 |

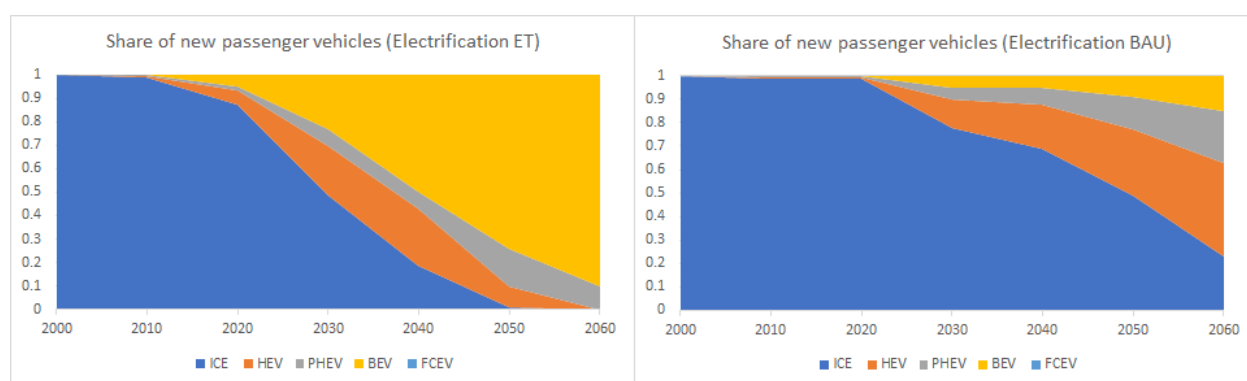


Figure D5: vehicle market shares for the ET (left) and BAU (right) electrification scenarios.

Appendix D3.2: Hydrogen scenarios

In the hydrogen scenarios, BEVs and PHEVs are complemented by FCVs, which were expected to replace some of the BEVs and PHEVs (and in the case of trucks, ICEs) in the electrification scenario. Multiple organizations have created hydrogen outlooks, including IEA and IRENA. In this thesis, the Hydrogen Council (HC) roadmap (HC, 2017) was used to include a relatively extreme ET hydrogen scenario, in which about 25% of the world's passenger vehicles, 30% of trucks and 25% of buses are running on hydrogen by 2050.

Based on HC (2017), the percentage of FCV sales was expected to be 0 in 2015 for all transport functions, 3% for passenger vehicles, 2.5% for trucks and 10% for buses in 2030 and 35% for passenger vehicles, 45% for trucks and 50% for buses in 2050 for the ET hydrogen scenario. The values for the intermediate years were based on linear extrapolation.

IRENA (2018, p.31), who estimated the economic potential of hydrogen produced from renewable electricity, state the following about the HC roadmap: 'While the Hydrogen Council roadmap is industry's consensus vision of hydrogen's potential in the economy under the right circumstances (e.g. alignment of policies, regulations, codes and standards), it is just one vision of numerous potential outcomes'. IRENA (2018) estimates a substantially lower amount of hydrogen by 2050 (about 10x less). However, the HC (2017) roadmap was selected to show the potential impact an ET with such a large amount of FCVs could have.

The BAU hydrogen scenario is more in line with the projections by IRENA (2018), as the ET hydrogen scenario values were divided by 10 for this scenario. Vehicle shares for the ET and BAU hydrogen scenarios are shown in table D11 and D12 respectively and in figure D6.

Table D11: vehicle market shares for the ET hydrogen scenario

| Hydrogen ET | 2000 | 2010 | 2020 | 2030 | 2040 | 2050 | 2060 | 2070 | 2080 | 2090 | 2100 |
|--------------------------|------|-------|-------|-------|-------|-------|-------|-------|-------|-------|-------|
| Passenger vehicle shares | | | | | | | | | | | |
| ICE | 1 | 0.990 | 0.872 | 0.487 | 0.184 | 0.01 | 0 | 0 | 0 | 0 | 0 |
| HEV | 0 | 0.005 | 0.062 | 0.211 | 0.245 | 0.09 | 0 | 0 | 0 | 0 | 0 |
| PHEV | 0 | 0.005 | 0.016 | 0.062 | 0.050 | 0.098 | 0.109 | 0.109 | 0.109 | 0.109 | 0.109 |
| BEV | 0 | 0 | 0.05 | 0.210 | 0.331 | 0.452 | 0.502 | 0.502 | 0.502 | 0.502 | 0.502 |
| FCEV | 0 | 0 | 0 | 0.03 | 0.19 | 0.35 | 0.389 | 0.389 | 0.389 | 0.389 | 0.389 |
| Bus shares | | | | | | | | | | | |
| ICE | 1 | 0.9 | 0.48 | 0.28 | 0.19 | 0.095 | 0 | 0 | 0 | 0 | 0 |
| BEV | 0 | 0.1 | 0.47 | 0.62 | 0.51 | 0.405 | 0.448 | 0.448 | 0.448 | 0.448 | 0.448 |
| FCEV | 0 | 0 | 0.05 | 0.1 | 0.3 | 0.5 | 0.552 | 0.552 | 0.552 | 0.552 | 0.552 |
| Truck shares | | | | | | | | | | | |
| ICE | 1 | 1 | 0.99 | 0.897 | 0.618 | 0.380 | 0.141 | 0 | 0 | 0 | 0 |
| BEV | 0 | 0 | 0.01 | 0.078 | 0.145 | 0.171 | 0.196 | 0.222 | 0.247 | 0.273 | 0.299 |
| FCEV | 0 | 0 | 0 | 0.025 | 0.238 | 0.45 | 0.663 | 0.778 | 0.753 | 0.727 | 0.701 |

Table D12: vehicle market shares for the BAU hydrogen scenario

| Hydrogen BAU | 2000 | 2010 | 2020 | 2030 | 2040 | 2050 | 2060 | 2070 | 2080 | 2090 | 2100 |
|--------------------------|------|-------|-------|-------|------|-------|------|------|------|------|------|
| Passenger vehicle shares | | | | | | | | | | | |
| ICE | 1 | 0.99 | 0.99 | 0.78 | 0.69 | 0.49 | 0.23 | 0 | 0 | 0 | 0 |
| HEV | 0 | 0.005 | 0.005 | 0.12 | 0.19 | 0.28 | 0.40 | 0.47 | 0.31 | 0.15 | 0 |
| PHEV | 0 | 0.005 | 0.005 | 0.05 | 0.06 | 0.12 | 0.19 | 0.27 | 0.36 | 0.44 | 0.52 |
| BEV | 0 | 0 | 0 | 0.05 | 0.05 | 0.08 | 0.12 | 0.18 | 0.23 | 0.28 | 0.33 |
| FCEV | 0 | 0 | 0 | 0.003 | 0.01 | 0.035 | 0.06 | 0.08 | 0.11 | 0.13 | 0.15 |
| Bus shares | | | | | | | | | | | |
| ICE | 1 | 0.9 | 0.9 | 0.48 | 0.28 | 0.19 | 0.10 | 0 | 0 | 0 | 0 |
| BEV | 0 | 0.1 | 0.095 | 0.51 | 0.69 | 0.76 | 0.84 | 1 | 1 | 1 | 1 |
| FCEV | 0 | 0 | 0.005 | 0.01 | 0.03 | 0.05 | 0.07 | 0.09 | 0.11 | 0.13 | 0.15 |
| Truck shares | | | | | | | | | | | |
| ICE | 1 | 1 | 1 | 0.99 | 0.92 | 0.81 | 0.69 | 0.57 | 0.45 | 0.33 | 0.21 |
| BEV | 0 | 0 | 0 | 0.01 | 0.06 | 0.15 | 0.24 | 0.34 | 0.44 | 0.54 | 0.64 |
| FCEV | 0 | 0 | 0 | 0.003 | 0.02 | 0.05 | 0.07 | 0.09 | 0.11 | 0.13 | 0.15 |

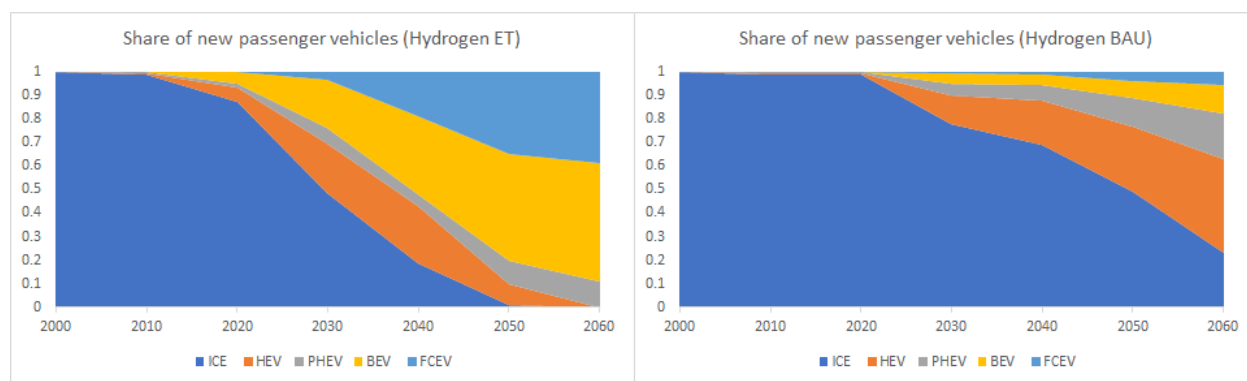


Figure D6: vehicle market shares for the ET (left) and BAU (right) hydrogen scenarios.

Appendix D4 VRE share

In the model, many variables depend on VRE share. With lack of other data to back up the reasoning, this was done to stay close to the SSP narratives. The main assumption here is that a favourable environment for VRE would also be a favourable environment for these variables. The variables depending on VRE share, including the reasoning per variable, are summarised in table D13. In future research other ways of representing these variables could be explored.

Table D13: assumptions for basing variable changes on VRE share

| Variable | Formula | Reasoning for dependence on VRE share | Additional reasoning for the formula |
|--|-----------------------------|--|---|
| Storage capacity as fraction of electricity demand | Complex, see figure D2 | The larger the VRE share, the larger the variability in the electricity network and the more storage required. | Storage demand grows exponentially as VRE share increases. |
| Percentage small scale PV with battery storage | $y = x$ | It is assumed the price for battery storage decreases over time. This is linked to the VRE share to fit with a narrative where more storage is required and thus more innovation occurs in that area. | No additional values in the formula, because the initial VRE percentage matches the initial percentage of small-scale PV with battery storage |
| Participation in V2G | $y = x$ | It is assumed incentives to participate in V2G are larger in a society with more VRE because more storage is required. | No additional values in the formula |
| Maximum percentage of repurposed batteries | $y = 0.22 + x$ (Max = 1) | It is assumed that as the requirement for storage increases, due to increasing VRE share, the amount of repurposing also increases. However, this is a maximum value. If the storage requirements are less, repurposing will also be less. | According to BNEF (2016), 33% of EV batteries can be repurposed by 2025. Based on the modelled values, it is assumed that VRE share is about 11% by 2025, so 22% is used as base value. |
| Percentage CSP equipped with TES | $y = 0.38 + x$ (Max = 1) | It is assumed the price for TES decreases over time. This is linked to the VRE share to fit with a narrative where more storage is required and thus more innovation occurs in that area. | According to Achkari & El Fadar (2020), 45% of CSP was equipped with TES in 2020. Modelled VRE share is about 7% in 2020*, so 38% is used as a base value. |

* This differs per SSP and is slightly different than the actual value in 2020, because the SSP scenarios are outdated.

Appendix E: Background, assumptions & data: price effects

This appendix contains background information that can be consulted to provide some more context for the paradigms used in the model; the Opportunity Cost Paradigm (OCP) and the Fixed Stock Paradigm (FSP), and the price effects influencing demand (price elasticity, substitution and intensity changes).

Functional demand for a certain product or service is not the only thing that influences supply. Price dynamics also have an effect, though these are only relevant in the OCP. To take into account these effects, Auping (2011) and van der Linden (2020) included demand change due to price elasticity and demand change due to substitution in their copper and cobalt models. This is also applied in the nickel model. In addition, intensity improvements through innovation were included.

Appendix E1: Resource depletion paradigms

Two paradigms in research depletion studies with different perspectives on resource scarcity are the FSP and the OCP (Castillo & Eggert, 2019; van der Linden, 2020). In the FSP, which has a physical view on scarcity, natural scientists argue that there is a limited stock of minerals on Earth and this may not be enough to meet increasing demand. This suggests absolute scarcity of minerals and is reflected in peak models, which show a certain point in time where the maximum rate of extraction is reached, which will thereafter only decline (Castillo & Eggert, 2019).

In the OCP, an economic approach, economists argue that markets will adapt as prices are driven up by depletion, discouraging consumption and encouraging technological development, exploration, recycling and substitution. This is reflected in Cumulative Availability Curves (CAC), which show the mass of materials that can be extracted based on costs per unit of mass. At higher costs, more material can be extracted (Castillo & Eggert, 2019).

Both approaches have benefits and drawbacks. Proponents of the OCP argue that fixed stock thinking is not adaptive enough and does not reflect real world market responses. In turn, proponents of the FSP argue that prices are not an adequate warning for mineral scarcity, as price trends for abundant and scarce minerals do not differ much and external mining costs are not reflected by markets (Henckens et al., 2016; Castillo & Eggert, 2019). These diverging views should be taken into account when interpreting research depletion studies.

The papers in appendix A contain predominantly fixed stock elements, such as an expected production peak (Valero et al., 2018a), and while viewing some aspects, such as energy demand and technology mix, as dynamic, many view other aspects, such as production, metal intensity and resources and reserves as static. In reality, these factors are all dynamic and potentials are always changing based on new discoveries and price fluctuations (Manberger & Stenqvist, 2018; Bucholz & Brandenburg, 2018). The most dynamic elements are included by Manberger & Stenqvist (2018), who focus specifically on the effects of substitution, technological development and technological diversity. These factors are considered to be important in the OCP.

The models assessing single materials also contain more OCP elements. Van der Linden (2020) explicitly considered both paradigms and Castillo & Eggert (2019) attempted to reconcile the paradigms and created a modified CAC, which they applied to copper. Table E1 shows how each paradigm considers different types of potential for obtaining resources. The types of potential are based on Blok & Nieuwlaar (2021). Hybrid paradigms are also possible, but these are not considered in this thesis.

Table E1: how different types of potential are determined in the two paradigms.

| Potential | Fixed stock paradigm | Opportunity cost paradigm |
|---------------------------|--|--|
| Theoretical potential | Fixed resources | Resources can increase through exploration |
| Technical potential | Fixed extractable resources | Extractability of resources can increase through innovation. Innovation can also lead to product property changes, thereby reducing demand |
| Economic/market potential | Resources can change to reserves (and back) when price changes | Resources can change to reserves (and back) when price changes. There are also feedback mechanisms, through elasticity and substitution that can influence demand and thereby price. |

Appendix E2: Price elasticity

Price elasticity of demand describes the degree of responsiveness of consumers to changes in price. In general, as demand increases, so does price. In turn, an increased price can lead to reduced demand. Price elasticity of demand is therefore a negative number. In addition to price elasticity of demand, there is also price elasticity of supply, which is a positive value (Harris & Roach, 2018).

Price elasticity can differ depending on the time frame. Short-term price elasticity reflects sudden changes in price, whereas long-term price elasticity describes long-term changes. The latter is usually higher than the former because consumers have more time to respond (Blok & Nieuwlaar, 2021). The values for short- and long-term price elasticity, as well as the method for determining the effect of relative price on demand and the average long-term effect were taken from Van der Linden (2020).

Appendix E3: Substitution

Nickel has some very good properties which make it an important material for various applications. It is highly corrosion and heat resistant, highly ductile, has catalytic properties and is fully recyclable (Nickel Institute, n.d.). Currently, nickel is mainly used in stainless steel and an important future demand category is likely to be batteries. Therefore, specific attention is paid to these two categories.

Substitution can be divided into two types: material substitution, where a different material is used in the same technology, and technological substitution, where a different technology is used to provide the same function (Sprecher et al., 2015). Examples for both types are shown in table E2. Substitution can occur at different levels of the system. This is illustrated in figure E1. At each branch in the chain, a switch can be made, leading to different nickel demand. The larger the number of switches that can be made, and the easier this can be done, the higher the flexibility of the system, one of the three aspects of resilience.

Table E2: potential nickel substitution in stainless steel and batteries (Deloitte, 2015a; Sverdrup & Olafsdottir, 2019; BNEF, 2019; IEA, 2020b; USGS, 2020a). The focus here is on substitution in the energy system, but substitution can also occur in the RoE. * The batteries in this list can contain many different materials.

| Application | Why nickel is used | Potential material substitution | Potential technological substitution |
|-----------------|--|--|---|
| Stainless steel | Erosion, corrosion and heat resistance | Molybdenum, niobium, cobalt, vanadium, chromium, titanium | Energy generation technologies that require less stainless steel. |
| Batteries | Higher energy densities | LFP, LMO, LCO, sodium-ion, liquid, magnesium-based, fluoride-ion, chloride-ion, metal-air* | Other forms of storage and flexibility options and other forms of transportation and vehicle types. |

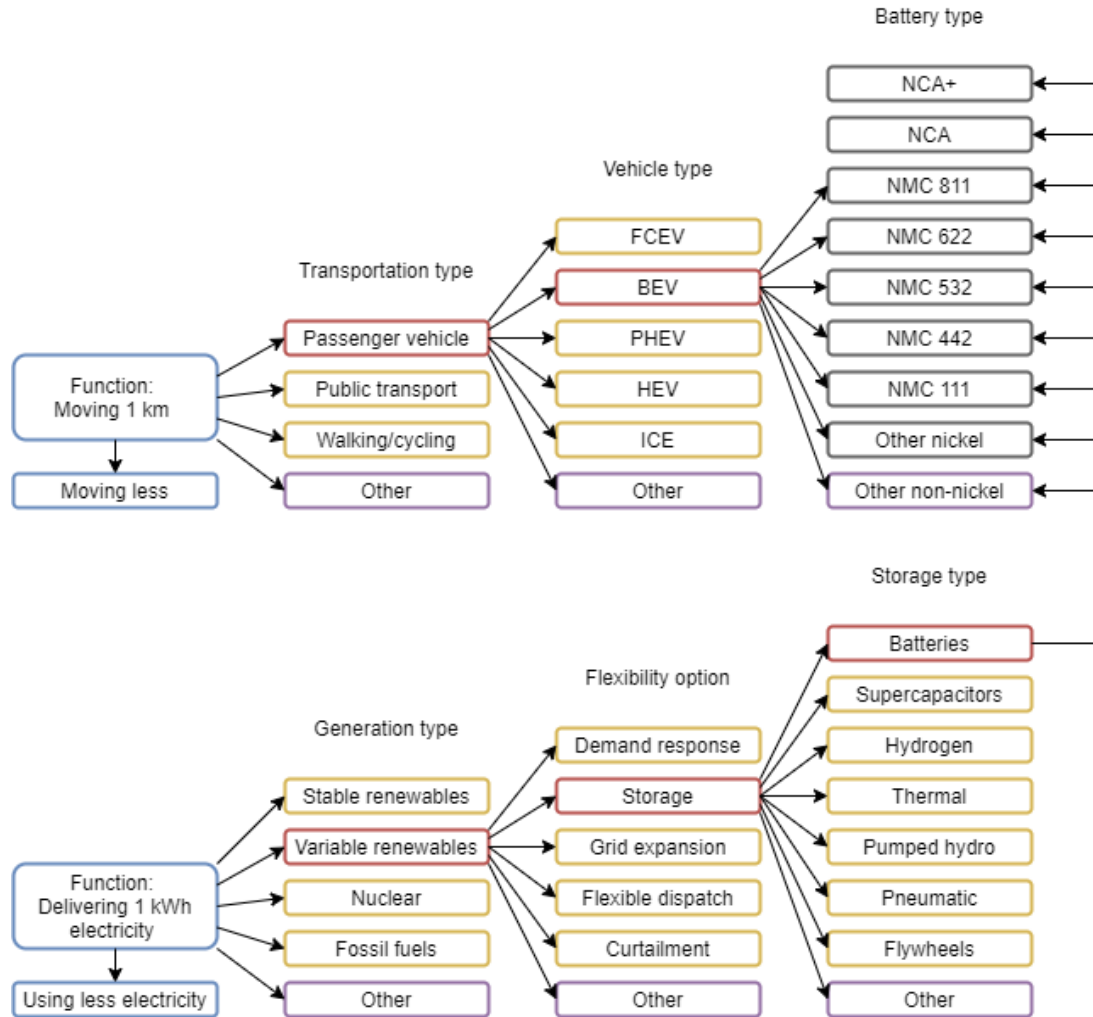


Figure E1: Various options at different levels to fulfil the functions of moving 1 km and delivering 1 kWh of electricity. Created with information from Hadjipaschalis et al. (2009), Brown et al. (2018) and BNEF (2019).

In the model, technological substitution is not considered explicitly, but the technology mix of generation technologies, storage and transportation does differ for the different ET scenarios. Material substitution (and potential resubstitution) is based on the relation between the nickel price and the substitute price and an assumed substitution threshold per demand category that indicates the difficulty of substitution.

The substitute price is based on the initial substitute price and on the relative change in energy price (Van der Linden, 2020). Carbon costs equal to those for nickel were also included, because this was deemed more accurate than not including carbon costs at all, since carbon costs were also included for nickel. Additional factors, such as scarcity of the substitute, also influence the substitute price, but other than scarcity induced in the model by increasing substitution, this was not taken into account.

Especially for batteries, a wide range of materials could become substitutes, so it is difficult to determine an initial substitute price. Because of the large uncertainty involved regardless of the chosen method, the simple method of using the initial nickel price was chosen. This makes the two prices equal at the start, which means the substitution threshold determines whether substitution occurs.

The substitution threshold is an arbitrary, highly uncertain value in this thesis that can be played around with to obtain different substitution effects. The substitution threshold will prevent substitution from occurring at the start despite equal prices and only once the nickel price becomes sufficiently high, will substitution kick in. To get some kind of basis regarding the relative substitution threshold of different demand categories, the following literature was consulted.

Svedrup & Olafsdottir (2019) assessed long-term stainless-steel supply using the integrated System Dynamics (SD) WORLD6 model. In this assessment, they looked at iron, nickel, magnesium and chromium. Their analysis shows that nickel is a key element that can limit stainless steel production due to potential supply constraints after 2045. Svedrup & Olafsdottir (2019) also discuss potential substitutes. Currently, there is no exact replacement for nickel in stainless steel while retaining quality, but molybdenum, niobium, cobalt and vanadium can be used to fulfil some of nickel's functions. However, these materials currently have higher prices and lower production volumes than nickel, which means substantial substitution with these materials is currently not viable (Svedrup & Olafsdottir, 2019). Van der Linden (2020) agrees that nickel's application in stainless steel is hard to substitute and her assumed substitution threshold values for nickel are used in the model for stainless steel.

Regarding batteries, there are various technologies currently in use that do not contain nickel, such as LFP, LMO and LCO batteries. There are also batteries that require less nickel, such as certain NMC batteries. However, the current trend is toward increasing the fraction of nickel in NMC batteries and batteries in general, due to the higher energy density and because cobalt is scarcer than nickel (BNEF, 2019). This is something that could be reversed if nickel becomes scarcer, but it is also important to keep in mind that more of a certain material is required if the energy density is lower.

In the future, the continued research and improvements in battery technology will likely lead to at least increased diversity of technologies, but also to potential disruption of the prominence of lithium-ion in battery technologies. Potential disruptive technologies, some with much greater energy densities than lithium-ion batteries, include sodium-ion batteries, liquid batteries, magnesium-based batteries, fluoride-ion batteries, chloride-ion batteries and metal-air batteries (Deloitte, 2015a; IEA, 2020b).

It is difficult to model such disruptions, but the diversity of technologies as well as the fact that batteries are a relatively new demand category for nickel means the flexibility is likely to be higher than for stainless steel. Therefore, a lower substitution threshold is used (Van der Linden, 2020). In addition, a disruption scenario was created in which the impact of a radically new storage technology was assessed (See section 2.5 in the main text). For other applications, a substitution threshold in between the thresholds for batteries and stainless steel is used.

Appendix E4: Intensity improvement

Intensity improvement is a form of incremental innovation that can be achieved by changing product properties in two ways. First, by using resources in a more efficient manner to fulfil the same function, and second, by improving the functionality without using more resources. In the model, the units for intensity are tonne/GW, tonne/GWh and tonne/vehicle for electricity generation technologies, battery storage technologies and transport technologies respectively. The units for hydrogen tanks are also tonne/vehicle.

These units show that intensity does not only change when the number of tonnes decreases, but also when the amount of GW or GWh increases. Figure E2 shows how the nickel intensity of batteries and vehicles was calculated, as well as the general components that determine intensity for the different types of demand. The green variables lead to a higher, and the red variables lead to a lower nickel intensity.

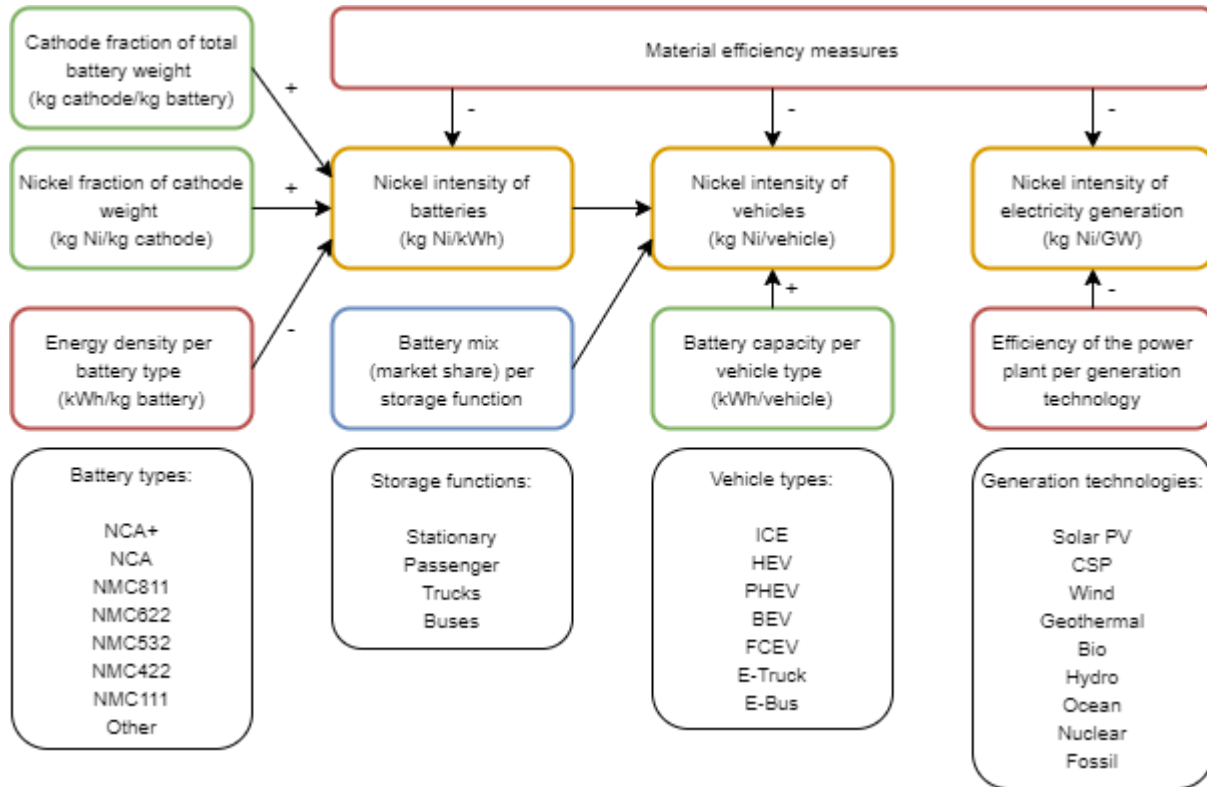


Figure E2: variables that influence nickel intensity in batteries, vehicles and electricity generation technologies. The battery types, storage functions, vehicle types and generation technologies are also included for extra clarification. Green = variable that leads to a higher nickel intensity; Red = variable that leads to a lower nickel intensity; Blue = variable that could lead to a higher or lower nickel intensity.

IEA (2019) assessed possibilities for increasing material efficiency. They estimated a reduced steel use potential of up to 32% for buildings by 2060 relative to 2017 in their material efficiency scenario, applying this to 10% of buildings. Assuming linear change, this is an overall reduction of 0.07% per year. For their RTS, they assumed no material intensity changes.

Although the values from IEA (2019) applied to steel in buildings, the intensity improvement is assumed to also apply to nickel in all energy system applications in the model. Furthermore, it is assumed that this is the autonomous intensity improvement that would occur if price remained stable. However, a price-based element was also added because it is assumed that increasing price will lead to more innovation and decreasing price to less (Blok & Nieuwlaar, 2021).

The other factors that influence nickel intensity are assumed not to be as related to nickel price as material efficiency. In addition, it is assumed that the cathode fraction of total battery weight, the nickel fraction of cathode weight and energy density remain relatively constant per battery type. They differ for the different battery types, but this is taken into account in the market share (storage mix) and substitution parts of the model.

Energy density is expected to continue increasing in the future (Deloitte, 2015a; BNEF, 2019; Ilika, 2019). However, this is mostly either because of increased nickel share, which is taken into account in the market share, or because of a completely new technology that does not contain nickel, which is considered in the radical innovation disruption scenario (See section 2.5 in the main text).

A higher battery capacity increases the range of an EV. As energy density increases, battery capacity of vehicles will also increase, unless battery size is reduced, which has benefits for the weight of the vehicle. However, density increase and capacity increase are assumed to cancel each other out with respect to their effect on nickel intensity and are therefore not considered further.

For electricity generation technologies, increased energy efficiency will reduce nickel intensity. It is assumed that additional material requirements due to energy efficiency increase are negligible. However, there is a theoretical maximum to energy efficiency and it cannot continue increasing indefinitely. In addition, for some technologies, the efficiency is already very high. Because of the uncertainty on how to treat energy efficiency changes, they are not considered in the model. Instead, the upper value in the range for material efficiency of 0.07% per year is used, with the reasoning that even if this is an overestimation, it can be considered to also partially include intensity reduction due to energy efficiency improvements.

Lifetime extension is also a product property change that reduces the requirement for new nickel. However, with the exception of vehicle battery lifetime extension, this is not considered in the model, which is another reason to use the upper value in the range for material efficiency. In the model, not all infrastructure reaches the end of its expected lifetime. Some capacity, including coal, oil, natural gas and nuclear, is retired early because of the ET. This is based on the SSPs and is shown in the model as a negative inflow.

Increased nickel requirements due to the ET can be seen as a disturbance according to the supply chain resilience framework by Sprecher et al. (2015). Price elasticity, substitution and intensity changes (changing product properties) can increase the resilience of the supply chain and minimise the impact of the ET, thereby also reducing potential limitations of nickel availability on the pace of the ET. All three price effects increase resilience but in extreme events they can function as disruptor themselves. This is considered in the radical innovation disruption scenario.

Appendix F: Demand sub model input and data sources

Table F1: values and data sources used for the constants and lookups in the demand sub model. A range is included and a row is highlighted yellow if uncertainty is assessed for a specific variable. Dmnl = dimensionless.

| Element | Unit | Type | Min | Max | Explanation/assumptions | Source |
|---|-----------------|----------|---|-----|--|-------------------------------------|
| <i>Socio-economic data (see tables D2 - D5)</i> | | | | | | |
| Population | Million people | Lookup | Selected SSP scenarios | | Population | IIASA (2018) |
| GDP | Billion \$/year | Lookup | Selected SSP scenarios | | GDP (PPP) in US\$2005 | IIASA (2018) |
| <i>Electricity generation data (see tables D2 - D5)</i> | | | | | | |
| Electricity demand | GWh/year | Lookup | Selected SSP scenarios | | Obtained from the secondary energy (electricity) section of the database | IIASA (2018) |
| VRE share | Dmnl | Lookup | Selected SSP scenarios | | Based on the share of wind and solar energy in total electricity supply | IIASA (2018) |
| Required generation capacity | GW | Lookup | Selected SSP scenarios | | Obtained from the technological indicators (capacity) section | IIASA (2018) |
| Initial generation capacity | GW | Constant | Selected SSP scenarios | | Based on modelled data because actual data could not be found. | IIASA (2018) |
| Percentage small scale PV | Dmnl | Lookup | The share of small-scale PV is assumed to be 32% in 2015 and 18% from 2050 onward | | | Olson & Bakken (2019) |
| Fraction with CCS | Dmnl | Lookup | Selected SSP scenarios | | Based on calculated fraction of CCS in electricity generation. Used a value of 15% to take into account the energy penalty of CCS. | IIASA (2018); Budinis et al. (2018) |
| <i>Storage data</i> | | | | | | |
| Initial stationary storage stock | GWh | Constant | 11 | | For 2017, but assumed to be applicable enough for 2015 | IRENA (2017) |
| Storage mix | Dmnl | Lookup | See table D8 | | See the text below table D8 | BNEF (2019); Van der Linden (2020) |
| Storage capacity as fraction of electricity demand | Dmnl | Lookup | See table D7 | | Base storage as fraction of electricity demand + values for one of the flexibility scenarios. | Zerrahn (2018) |
| Hours of PHS | Hour | Constant | 30 | | Calculated based on reported energy and power. | IRENA (2017); IHA (2018) |
| Percentage PHS of total hydro capacity | Dmnl | Constant | 0.12 | | Remained unchanged in the past 5 years and is assumed to remain so. | IHA (2016-2020) |
| Hours of TES | Hour | Constant | 7 | | IRENA (2017) assumed 5 - 9 hours | IRENA (2017) |
| Base % of CSP equipped with TES | Dmnl | Constant | 0.38 | | See table D13 | Achkari & El Fadar (2020) |
| <i>Transportation data</i> | | | | | | |
| Initial vehicle stock | Vehicle | Constant | 1.28E9 | | Passenger vehicles and commercial vehicles (trucks and buses) | Statista (2018a) |
| Initial vehicle mix | Dmnl | Constant | See table D9 | | Based on the average of 2000 and 2010 values of the new vehicle mix. | BNEF (2019); Van der Linden (2020) |

| | | | | | |
|---|----------------|----------|--|--|---|
| New vehicle mix electrification ET | Dmnl | Lookup | See table D9 | See the text above table D9 | BNEF (2019); Van der Linden (2020) |
| New vehicle mix electrification BAU | Dmnl | Lookup | See table D10 | See the text above table D10 | IEA (2017a); Watari et al. (2018) |
| New vehicle mix hydrogen ET | Dmnl | Lookup | See table D11 | See the text above table D11 | HC (2017) |
| New vehicle mix hydrogen BAU | Dmnl | Lookup | See table D12 | See the text above table D12 | IRENA (2018) |
| Vehicle function share | Dmnl | Lookup | The shares of passenger vehicles, buses and trucks are assumed to be 75%, 24% and 1% respectively in 2015 and 80%, 19% and 1% respectively from 2050 onward. | | Van der Linden (2020) |
| Vehicles/capita vs GDP/capita | Vehicle/capita | Lookup | See model | Relationship between the number of vehicles per capita and GDP/capita | Our World in Data (2014) |
| Battery capacity vehicles | GWh/vehicle | Constant | See table C5 | All battery capacities are kept constant because it is assumed that any changes in capacity are covered by intensity changes. | See table C5 |
| Battery degradation | Dmnl | Constant | 0.75 | Repurposed batteries have about 70 - 80% of the initial capacity | Walker et al. (2015); White et al. (2020) |
| EV battery lifetime | Year | Constant | 8 | Half of the assumed vehicle lifetime of 16 years. | Walker et al. (2015); White et al. (2020) |
| Base max % repurposed | Dmnl | Constant | 0.22 | See table D13 | BNEF (2016) |
| Available V2G power per FCV | GW/vehicle | Constant | 1E-5 | Based on Oldenbroek et al. (2017) | Oldenbroek et al. (2017) |
| Hours of FCV V2G | Hour | Constant | 6 | | |
| V2G timing | Dmnl | Constant | Depending on the flexibility scenario, this is 0.33 for low flexibility, 0.5 for medium flexibility and 0.67 for high. | | Assumption |
| <i>RoE data</i> | | | | | |
| Initial total nickel demand | Tonne/year | Constant | 1.896e+06 | This was the total nickel demand in the base year, 2015 | Statista (2018b) |
| Percentage stainless steel | Dmnl | Constant | 0.7 | Assumed to stay more or less the same within the ROE category | Nickel Institute (n.d.) |
| <i>Lifetime data</i> | | | | | |
| Average lifetime electricity technologies | Year | Constant | See table C2 | Based on the average of values provided by multiple sources. | See table C2 |
| Average lifetime storage technologies | Year | Constant | 18 | This value falls within the range provided by IRENA (2017) and fits with use in vehicles of 8 years and additional stationary use of 10 years. | IRENA (2017) |
| Average lifetime vehicles | Year | Constant | 16 | If a battery is used in a vehicle for 8 years each vehicle would require exactly two batteries during its lifetime | See table C6 |

| <i>Nickel intensity data</i> | | | | | | |
|---|---------------|----------|---|---|---|--|
| Initial nickel intensity electricity technologies | Tonne/GW | Constant | See table C1 | | Based on the average of values provided by multiple sources. | See table C1 |
| Initial nickel intensity storage technologies | Tonne/GWh | Constant | See table C3 | | Calculated by combining energy density, the nickel fraction per cathode and the cathode fraction per battery | See table C3 |
| Initial nickel intensity hydrogen tanks | Tonne/vehicle | Constant | 0.112 | | Presumably refers to infrastructure, not the tank on board a vehicle. Still, the value should be treated with caution because it seems quite high. | Tokimatsu et al. (2018) |
| Autonomous material efficiency change | Dmnl | Constant | -0.0007 | | Determined based on assumptions of linear change and comparability of steel in buildings and nickel in other infrastructure. Because this is the upper value of a range starting at 0, it is assumed to also partially include energy efficiency and lifetime changes | IEA (2019) |
| Additional intensity due to CCS multiplier | Dmnl | Constant | CCS was included in the model by multiplying intensities for bio, oil, coal and natural gas by 1.1, 2.3, 2.1 and 1.8 respectively, based on the difference between values with and without CCS (see table C1) | | | See table C1 |
| <i>Substitution data</i> | | | | | | |
| Substitution threshold stainless steel | Dmnl | Constant | 7.5 | | Van der Linden (2020) assumed a range of 5 - 10 for nickel | Van der Linden (2020) |
| Substitution threshold batteries | Dmnl | Constant | 2.5 | 5 | Batteries are assumed to be easiest to substitute. Half of the substitution threshold for steel is assumed | Assumption |
| Substitution threshold other applications | Dmnl | Constant | 6.25 | | Because of the variety of different applications, this is assumed to equal the full range of substitution possibilities from the min for batteries to the max for stainless steel (2.5 - 10). | Assumption |
| Short term substitution strength | 1/year | Constant | 0.04 | | Van der Linden (2020) assumed a range of 0.02 - 0.06. | Auping & Pruyt (2013); Van der Linden (2020) |
| Long term substitution strength | 1/year | Constant | 0.125 | | Van der Linden (2020) assumed a range of 0.1 - 0.15. | |
| Period for long term effect | Year | Constant | 10 | | Number of years it takes for the long-term substitution strength and the long-term price elasticity to apply. Van der Linden (2020) used a range of 5 - 15. | Auping & Pruyt (2013); Van der Linden (2020) |
| Relative influence external factors | Dmnl | Constant | 0.5 | | Relative influence of the energy price and other potential external factors on the substitute price compared to the influence of substitution itself. | Van der Linden (2020) |

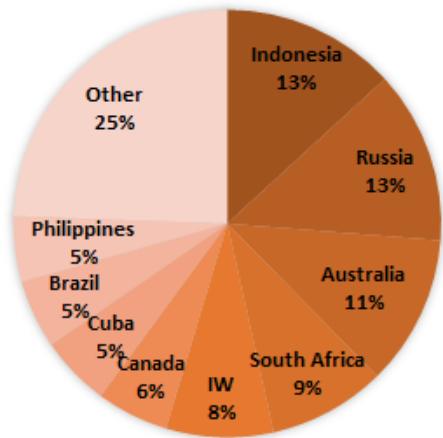
| <i>Price elasticity data</i> | | | | | | |
|---------------------------------|--------|----------|--------|---|---|--|
| Short term price elasticity | 1/year | Constant | -0.05 | | Based on Van der Linden (2020), but made negative because it applies to demand. Van der Linden (2020) used ranges of 0.02 - 0.08 and 0.1 - 0.25 for short term and long-term price elasticity respectively. | Auping & Pruyt (2013); Van der Linden (2020) |
| Long term price elasticity | 1/year | Constant | -0.175 | | | |
| <i>Postponed demand data</i> | | | | | | |
| Administration postponed demand | Year | Constant | 0.5 | 2 | The time it takes to include postponed demand in the new demand request. Van der linden (2020) used an administration time of 15 here, but this is assumed to be much too high. | Assumption |

Appendix G: Background, assumptions & data: supply dynamics

This appendix contains background information that can be consulted to provide some more context for the concepts related to the supply dynamics discussed in the main text. Assumptions are also explained.

Appendix G1: Nickel resources

NICKEL RESOURCES: 292 MT



NICKEL RESERVES: 42 MT

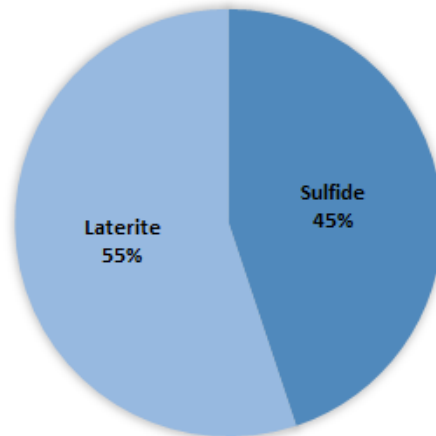
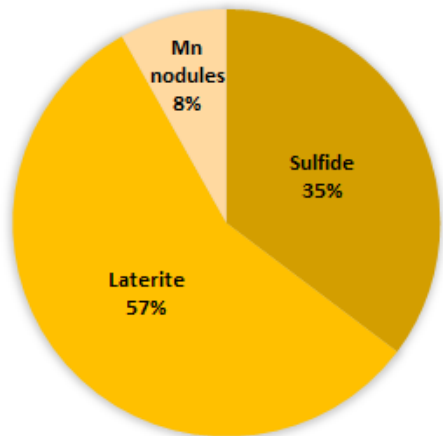
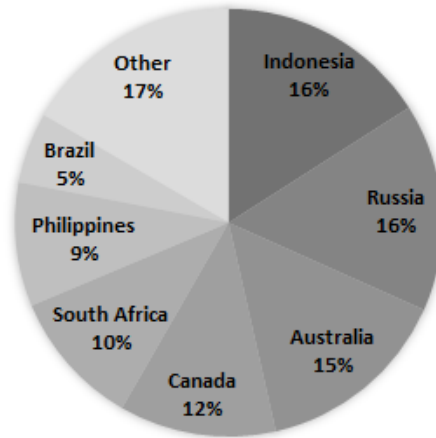


Figure G1: Global distribution (top) and ore type (bottom) of nickel resources and reserves per country. Total resources are estimated to be 334 Mt. IW = International Waters, which is where deep-sea deposits are located in the form of manganese nodules (included as sulfides in the model). Created with data from Mudd (2020).

Appendix G1.1: Exploration

In the model, exploration is included when the OCP is switched on. Exploration is split into initial exploration, which converts nickel in the resource base to inferred resources, and further discovery which converts nickel in the inferred resources to measured and indicated resources.

At first, exploration was calculated by multiplying the undiscovered nickel deposits (based on an initial resource base of 1.5E11 tonnes) with the ratio of current resources over the resource base and a price-based factor that combines profit with expectations for the ET, based on van der Linden (2020). However, this often led to behaviour where supply did not meet demand over time. Therefore, an additional power for price-based exploration was included to bring demand and supply closer together. The formula for exploration is shown in equation 1.

$$E = \frac{R_I}{B_I} * B * (P + V)^x \quad (1)$$

In which:

- E = exploration
- RI = initial resources
- BI = initial resource base
- B = resource base
- P = normalised profit
- V = expectations of the ET = change in new vehicles
- x = power for price-based exploration

Including factor x can lead to insights on potential additional exploration efforts that could be required for supply to continue meeting demand. The idea behind the addition of this factor is that in the future, price (and expectations) is a more important determinant of additional exploration efforts than historic exploration. The choice was made here for x to apply to both price and expectations instead of only to price, based on the way the variables were created. In future adaptations, it could also only be applied to price to see what impact that has.

Appendix G1.2: Resources to reserves

The next part of the supply chain is the conversion of measured and indicated resources to reserves. In the model by Van der Linden (2020) this happened in a continuous way. However, at the level of individual mines, reserves are declared in chunks. To model this, a variable was added for opportunity identification, in which each mine checks once every few years for an opportunity to declare new reserves.

A class system was constructed where the resources were divided into ten equal classes (eleven when including reserves). Each class was assumed to have different capital costs associated with creation of new capacity. This made it possible for some classes to be economical at a certain time step while other classes were not, thereby converting resources to reserves in chunks at each opportunity check.

Two routes for converting resources to reserves were created based on whether there is already existing capacity (which has already been invested in) in a certain area. If there is, an opportunity check is performed on an annual basis and new reserves are first declared for existing capacity based on current potential profitability of that capacity and additional desired operation time at that capacity. Any remaining resources can then be converted via the second route for which an opportunity check is done once every few years. Based on future potential profitability, this can lead to increasing capacity (or to creating entirely new capacity in a new area) through new investment.

Reserves can also be converted back to resources when they are no longer profitable. When the current profit (based on operating capacity) and the current potential profit (based on operating and mothballed capacity) become negative, reserves are converted back to resources during an opportunity check. The structure for converting resources to reserves is shown in figure 2.15 (main text). A duplicate structure was added to implement the class system while preventing complications in the main supply chain.

During mining, 20% was assumed to be lost (Johnson et al., 2008; Eckelman, 2010), ending up in tailings. With sufficient incentive, tailings can be mined again. Tailings were assumed to have the same difficulty of mining as class 10 resources. This is the most difficult to mine class, but it can be profitable at times. If it turns out that tailings are easier to mine, a different class can be assigned to them in future adaptations. This is a simplified estimation and any differences in ore grade are ignored. However, because this is a relatively small part of the model, with a relatively small impact on overall behaviour, it is not included in more detail. Losses from mining tailings were assumed to be 5%. See appendix G3.2 for more on losses.

Tailings will have an Open Cut (OC) or Underground (UG) mine linked to them. Because no data was collected for the energy requirements for tailings, the energy requirements for the connected OC or UG mine were used, although this may be an over- or underestimation. In future adaptations of the model, this could be adjusted.

The development of nickel reserves, production and the ratio between the two (R/P ratio) between 2000 and 2019 is shown in figure G2. The changes are more in line with the OCP, as, despite increased production, reported reserves are increasing and reported resources have remained constant (USGS, 2020a). The R/P ratio shows the number of years of a resource left if production and reserves remain constant (Blok & Nieuwlaar, 2021). However, this is not the case and the R/P ratio has remained relatively stable over the years as new resources were discovered.

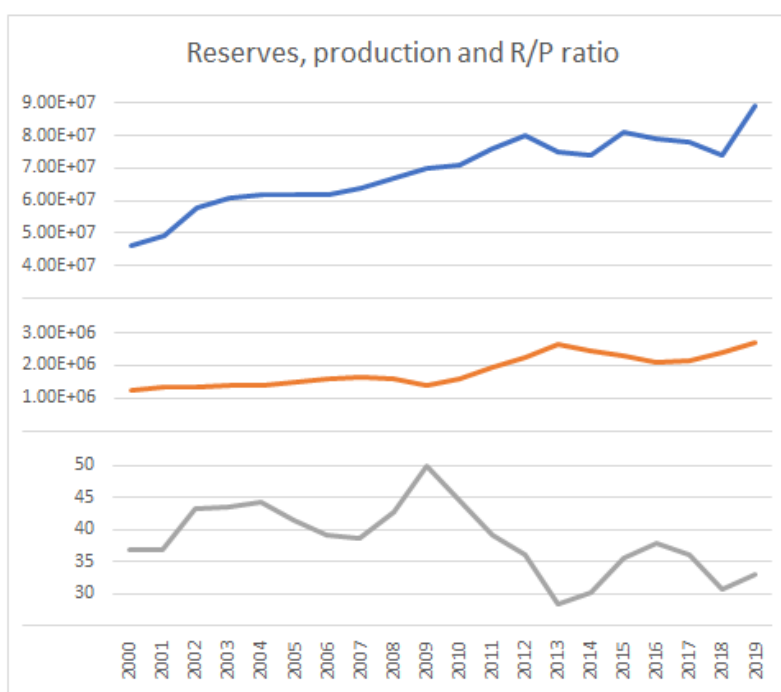


Figure G2: from top to bottom: nickel reserves (tonne), production (tonne/year) and R/P ratio (year) from 2000 to 2019. Resources were consistently reported as 130 million tonnes over these years (USGS, 2020a). Note: there is a discrepancy between the values reported by USGS (2020a) and the data from Mudd (2020) as shown in figure G1.

Appendix G2: Production capacity

Production capacity can be split into mining capacity and refining capacity. In this thesis, the focus is on mining capacity. It is acknowledged that refining capacity can differ significantly from mining capacity in terms of location and size and that there is international trade, as is illustrated in figure G3. If the refining capacity is not close to the mining capacity, there will be additional delays in the system, which reduces the stability and thereby the resilience of the system. In addition, it can create complex geopolitical dynamics that could lead to disruptions in the nickel supply chain. However, these additional complexities are beyond the scope of this research.

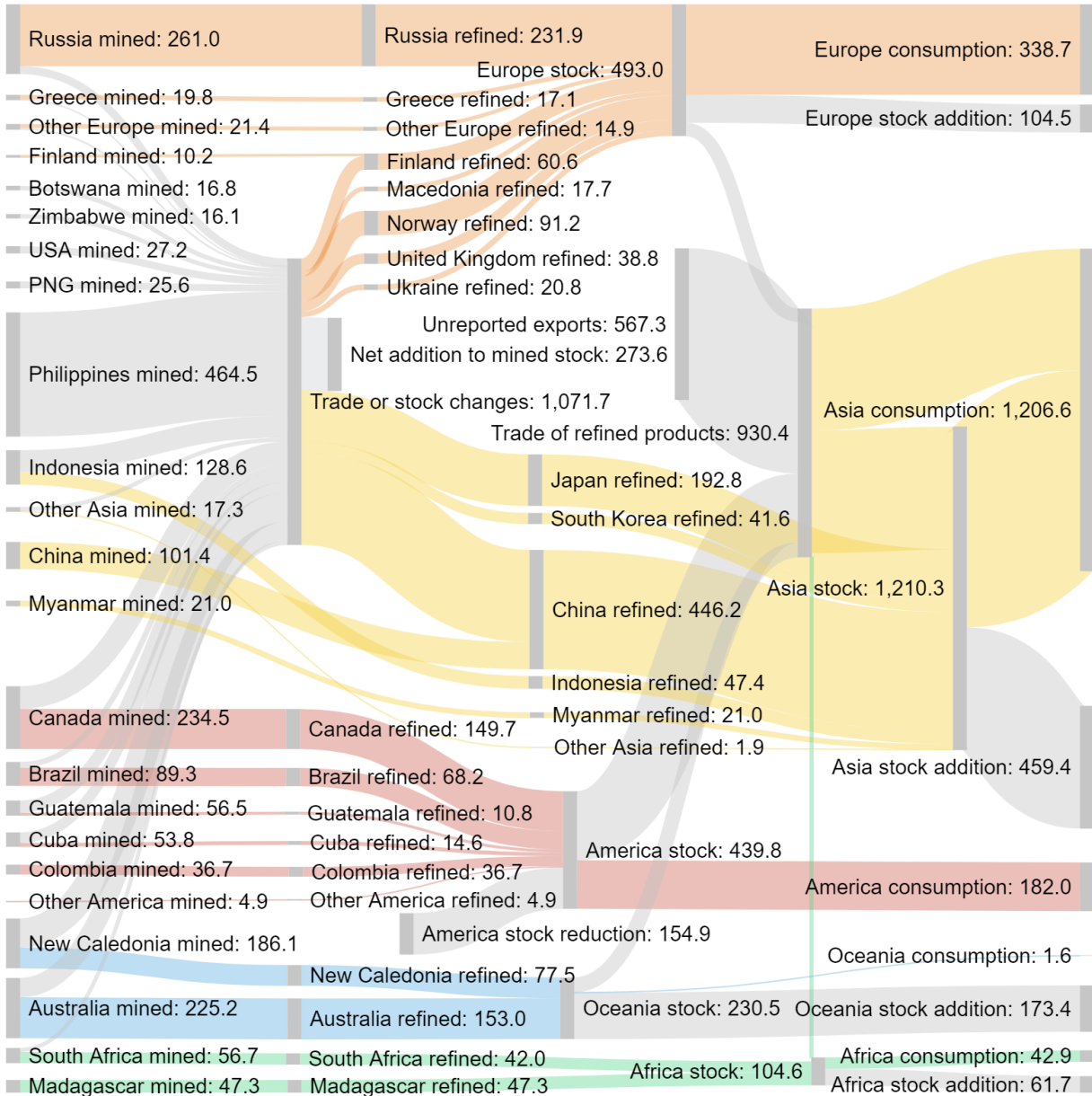


Figure G3: Static nickel material flow diagram for the year 2015 (excluding disposal and recycling). Unit: kilo tonnes. Created with data from WBMS (2018). Total mining was about 2.1 million tonnes. This is close to a total value of 2.3 million tonnes reported by USGS (2020a). The regional classification by IIASA (2018) was used.

Regarding mining capacity, a distinction is made between different types. These are elaborated on in table G1. The database by Mudd (2020) includes 652 different projects, each with a certain status. These statuses are also included in table G1 and linked to a type of mining capacity. As the nickel price goes up, it becomes attractive to mine in more areas so the availability of mining capacity increases, either through adding greenfield or brownfield capacity or by taking mothballed capacity out of Care and Maintenance (C&M). The mechanisms for doing so in the model are discussed in the following sections.

Table G1: different types of mining capacity included in the model and the status they have at the start of the model. Between brackets, the number of projects with a certain initial status in the database by Mudd (2020) is shown. Tailings are included here as greenfield, because the tailings in the database are connected to past projects that were not included as operating or mothballed in the model. New tailings created in the model can be considered part of brownfield capacity once it becomes economical to mine them.

| Type of capacity | Status | Elaboration |
|---------------------|--|--|
| Greenfield capacity | Deposit (527), tailings (5) or development (1) | Completely new mine (at least in the model), either for a deposit or for old tailings, either to be developed or under development |
| Brownfield capacity | Operating (64) | Capacity addition to an existing operating mine |
| Operating capacity | | Existing operating capacity |
| Mothballed capacity | Maintenance (55) | Existing capacity in C&M |

G2.1 Operating and mothballed capacity

Existing capacity of a certain project is either operating or mothballed. When a mine is mothballed, operations are stopped for a certain period of time and a mine is put into C&M. This can happen when the price becomes too low for operation to be beneficial. If the mine is mothballed for a certain period of time (longer than the maximum mothball time) without restarting, it is assumed to be decommissioned. Initial values for operating and mothballed capacity and the mechanism for mothballing are explained below.

Nickel mine production per country in the base year 2015 (WBMS, 2018) and the number of operating mines in each country around that time (Mudd, 2020) are shown in table G2. Based on this data, average operating capacity in the base year was estimated. In the model, initial operating capacity per project is assumed to equal average annual production in the country the project is located in plus an additional percentage based on assumed initial average capacity utilisation, with a minimum capacity of the minimum capacity set in the model.

It was assumed that the initial average mothballed capacity for projects with the status 'maintenance' is the same as the initial average production for projects with the status 'operating', which is about 34000 tonnes/year based on the data by WBMS (2018) and Mudd (2020), plus an additional percentage based on assumed initial average capacity utilisation.

Table G2: nickel mine production (tonne/year), number of operating mines and estimated average operating capacity (tonne/year). Only the countries with operating capacity and production in 2015 are included in this table. Note: WBMS (2018) reported mine production for Myanmar, Kosovo, Botswana, Spain and Norway, but these countries were not reported as operating mines by Mudd (2020). On the other hand, for Zambia, Solomon Islands and the Dominican Republic, WBMS (2018) did not report any production, but Mudd (2020) did report operating capacity. This discrepancy is probably because the data in the database by Mudd (2020) spans over multiple years and does not apply exactly to 2015, so some mines may have closed or opened slightly after 2015. Nevertheless, it was chosen to stick with the data from Mudd (2020), and production without operating capacity was ignored and operating capacity without production was given the minimum operating capacity as production. For Zimbabwe, the status for some of the mines was left blank by Mudd (2020), so based on the data by WBMS (2018) it was assumed that one of the mines with proved reserves was operating and the others were deposits.

| Country | Production in 2015 (WBMS, 2018) | Operating mines (Mudd, 2020) | Average production |
|---------------|---------------------------------|------------------------------|--------------------|
| Australia | 225300 | 7 | 32186 |
| PNG | 25600 | 1 | 25600 |
| Indonesia | 129000 | 7 | 18429 |
| Philippines | 465000 | 9 | 51667 |
| New Caledonia | 186100 | 3 | 62033 |
| Brazil | 89000 | 3 | 29667 |
| Canada | 235000 | 6 | 39167 |
| Russia | 261000 | 2 | 130500 |
| Turkey | 8600 | 1 | 10000 |
| Albania | 6700 | 1 | 10000 |
| Finland | 10300 | 3 | 10000 |
| China | 101400 | 2 | 50700 |
| Zimbabwe* | 16110 | 1 | 16110 |
| USA | 27200 | 2 | 13600 |
| Guatemala | 56510 | 2 | 28255 |
| Colombia | 36700 | 1 | 36700 |
| Greece | 19800 | 3 | 10000 |
| Madagascar | 47300 | 1 | 47300 |
| Cuba | 53800 | 3 | 17933 |
| Morocco | 200 | 1 | 10000 |
| South Africa | 56700 | 2 | 28350 |

The mechanism for mothballing is shown in figure G4. When it becomes unprofitable for mines to continue operating, they don't shut down immediately because there are also costs involved with putting a mine into C&M. Therefore, a certain profit deficit was allowed in the model and mothballing occurs only once the profit deficit exceeds the maximum profit deficit, which was assumed to be a certain percentage of initial investment. The same happens, but then the other way around when restarting a mine again. A different maximum profit deficit and minimum profit surplus was set for each mine based on their profit over investment, because it was assumed that mines with a larger profit over investment could take more risks and by waiting slightly longer before mothballing and waiting slightly shorter before starting up again.

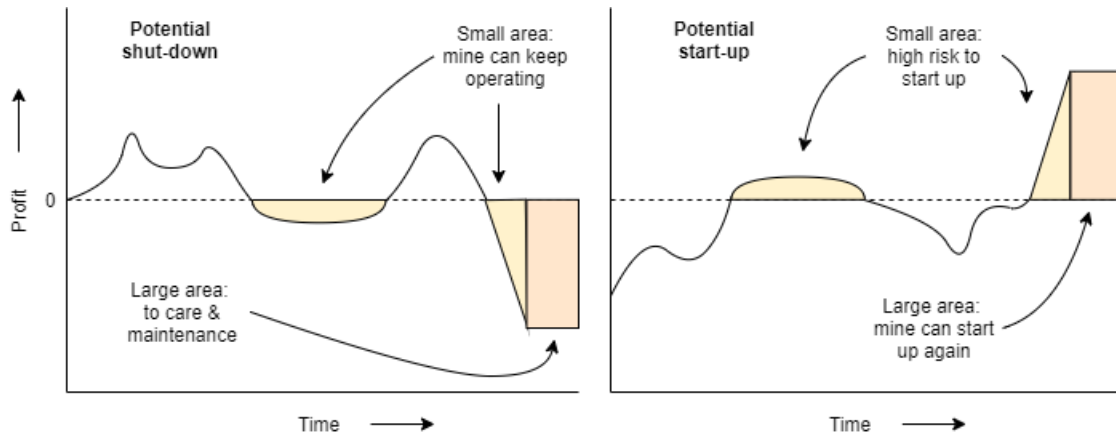


Figure G4: mechanism for mothballing (right) and restarting (left).

G2.2 Creating new capacity

For creating new capacity, the model first checks whether there are enough reserves available to create a certain minimum capacity that can run for the duration of the average mine operation plan. It then checks whether there is already existing, developing or upgrading capacity that can mine the reserves and if there are enough reserves left to create additional capacity, this intention is 'made clear to potential investors'.

However, not all mines can be invested in at once and some have a better business case than others (a higher profitability and/or other forms of investment attractiveness). It is assumed that there is a global maximum capacity increase percentage, based on historic global capacity increase. This limits the amount of new capacity that can be created in a year and the Vensim function 'allocation by priority' was used to allocate this capacity over the projects with the highest investment attractiveness. If a certain mine that is allocated new capacity already has existing capacity, the capacity is allocated as brownfield capacity. If there is no existing capacity, the capacity is allocated as greenfield capacity.

It was assumed that greenfield capacity takes longer to develop than brownfield capacity and a development time of between 5 and 10 years (Extractives Hub, n.d.) is attributed to a certain project based on investment attractiveness. It was assumed that countries with a better investment climate often have less corruption and other inefficiencies, thereby increasing the likelihood of faster development. Development time can differ quite a lot per processing method, however, this was not included in the model. This is an important aspect that could be included in future adaptations. For brownfield capacity, the upgrade time was assumed to be about 3 years.

Appendix G3: Supply chain

The nickel (closed loop) supply chain broadly includes the following steps: mining (including mining, milling and beneficiation), processing (including smelting and refining), product production, use and recycling. Mining is determined by the availability of reserves and the availability of operating capacity. The other supply chain stages are discussed below.

G3.1 Nickel processing

Sulfides and laterites require different forms of processing and are used to create different products. Nickel products can be divided over two classes (class I and class II). Sulfides are used to create class I products and laterites, which can be subdivided over limonites and saprolites, can be used to create both class I and class II products (Schmidt et al., 2016).

Class I products are refined products that consist of more than 99% nickel and Class II products are non-refined products that consist of less than 99% nickel. Class I products are suitable for most uses of nickel, including battery production. Class II products are mostly used for stainless steel production (Gigametals Corporation, 2019). A certain percentage of stainless steel is currently also supplied by class I. However, as it is expected that in the future battery demand will grow, it is assumed most stainless steel will be produced from class II, so class I demand is assumed to consist only of battery and 'other' demand.

There are various primary extraction methods for the different nickel ore types, broadly categorised as either Hydrometallurgical (HM, metal extraction through leaching with solvents) or Pyrometallurgical (PM, metal extraction through high temperature). The processing methods included in the database by Mudd (2020) are explained in table G3. New processing methods could be developed in the future, but these are not considered in the current model. This is something that could be added in future adaptations.

*Table G3: principal nickel processing methods and the number (and percentage) of deposits with this method in the database by Mudd (2020). 86 deposits (13%) were undefined. *F in the database by Mudd (2020).*

| Processing method | | Deposits | Elaboration (Kyle, 2010; Meshram et al., 2018) |
|------------------------------------|------------------------------------|-----------|--|
| <i>Nickel sulfides</i> | | | |
| PM* | Pyrometallurgical | 406 (62%) | After beneficiation, flotation produces nickel concentrate which is then smelted, usually in a flash smelting furnace to produce nickel matte. |
| HM | Hydrometallurgical | 5 (1%) | Processing of nickel sulfides via a HM route |
| <i>Nickel laterites (HM)</i> | | | |
| HPAL | High Pressure Acid Leaching | 90 (14%) | A process used for limonite ores where the ore is leached in sulphuric acid at elevated temperature (240 - 270 °C). |
| DNI | Direct Nickel | 1 (0.2%) | A relatively new process used for limonite and saprolite ores where nickel is recovered under ambient conditions with a tank-leach method. |
| HL | Heap Leaching | 9 (1%) | A process used for saprolite and limonite ores where the ore is irrigated with sulphuric acid after being stacked in heaps. |
| ATL | Atmospheric Pressure Tank Leaching | 1 (0.2%) | A process used for limonite and saprolite ores where the ore is leached in mineral acid at atmospheric pressure. |
| <i>Nickel laterites (PM)</i> | | | |
| RKEF | Rotary Kiln Electric arc Furnace | 14 (2%) | A process used for saprolite ores where the ore is mixed with coke, dried and calcinated in a rotary kiln (900 - 1000 °C) and smelted in an electric furnace (1550 °C) |
| <i>Nickel laterites (combined)</i> | | | |
| C | Caron | 1 (0.2%) | A process used for limonite (and some saprolite) ores where the ore is first roasted at about 850 °C and then leached in an ammonia solution. |
| <i>Incomplete</i> | | | |
| DSO | Direct Shipping Ore | 32 (5%) | Ore that is shipped directly to a different location. |
| B | Beneficiation | 7 (1%) | Treatment of ore to improve properties for smelting. |

Each processing method has different characteristics that impact its attractiveness. This includes energy requirements, reagent requirements, capital costs, nickel losses and environmental impacts. Due to time constraints, it was not possible to gather data for each processing method for each characteristic. Only energy requirements, nickel losses and GHG emissions were obtained for some processes and estimated for others, which influenced energy costs and costs due to carbon taxes. For reagent costs and capital costs, the same values were used for all processing methods, even though this is not the case. This is an important shortcoming that should be taken into account when analysing the results.

When distinguishing between the processing methods in table G3, certain assumptions were made. First, all sulfide processing was treated the same, and for HM sulfide processing, the values for PM sulfide processing were used. DSO and beneficiation indicate incomplete processing close to the mining facility. However, it was assumed that further processing would occur later on. Beneficiation applies to 7 projects in the database; 5 Deep Sea Mining (DSM) projects, 2 sulfide projects and 1 laterite project. The laterite project was changed to undefined and for the rest the values for PM sulfide processing were used.

DSO applies to 32 projects in the database, all laterites in Asian countries, including Indonesia, the Philippines, Myanmar and PNG (which is considered part of Asia by IIASA, 2018), many of which supply China (see figure G3). It was assumed that this ore is used to feed the nickel pig iron industry in China (Prasetyo, 2018). Pig iron is produced through PM processing of saprolites, usually by using a Blast Furnace (BF; see figure 2.19 in the main text). The values for pig iron production were applied to the deposits indicated as DSO in the database by Mudd (2020).

Some projects in the database by Mudd (2020) had an undefined processing method. For some an assumption was made based on other information in the database and the processing method was added to the database. Others received the label undefined. For these projects (all laterites), HPAL was assumed, based on the expected increase in class I nickel demand due to increasing battery demand.

A further assumption in this thesis is that all HM processing of laterites leads to class 1 nickel. Due to the small concentration of HL, ATL and DNI in the database, less attention was paid to accuracy here. In future adaptations this may need to be adjusted.

G3.2 Losses and recycling

After processing, the finished nickel is used to produce various products. During product fabrication a small fraction of the nickel is lost permanently and a larger fraction becomes primary scrap. Because this scrap is easily collected at the production facilities, it is assumed all of it can be recycled (ICA, n.d.). The rest of the nickel ends up in the products and becomes part of the use stock.

Nickel stays in use for the lifetime of products, which can differ per product. In the model, the average lifetime of stainless steel in electricity generation technologies was used as a proxy for the average lifetime of class II nickel. The average lifetime of batteries was used as a proxy for class I nickel.

After use, some of the nickel is collected and some is lost based on the End-of-Life Collection Rate (EoL CR). The collected nickel goes to the scrap stock as secondary scrap. Part of the scrap is recycled and the rest is lost based on the End-of-Life Processing Rate (EoL PR), which is determined based on the difference between the nickel content of scrap and average nickel ore grade. The idea is that if these two values come closer together, more recycling occurs (Van der Linden, 2020). The product of EoL CR and EoL PR is the End-of-Life Recycle Rate (EoL RR) (Gloser et al., 2013), which was 68% for Nickel in 2010 according to Nickel Institute (2016). This value was assumed to be the same in the base year (2015).

It is important to note here that different sources use different EoL RRs for nickel. Manberger & Stenqvist (2018) used a value of 60%, which matches with the values reported by UNEP (2011) of 57 - 63%. Van der Linden (2020) did not report EoL RR directly. She used values between 40% and 80% for EoL CR for copper, cobalt and nickel and she calculated EoL PR based on the nickel content in scrap and the nickel ore grade. However, this led to an initial EoL RR of about 20% - 40%, which is much lower than what was reported in other research.

Van der Linden (2020) also assumed that the cobalt and nickel content of scrap would increase as the portion of the demand from batteries increased, because of better organized collection. This may be true for cobalt, but most nickel recycling occurs in alloy state, for example in the form of stainless steel and the collection of stainless steel is already well organised, which is why nickel already has quite a high EoL RR (Nickel Institute, 2020; ISSF, 2021). Therefore, the increased share of batteries is likely to lead to a decrease in EoL RR instead of an increase.

To obtain a better understanding of the impact of an increasing share of batteries, a distinction was made between class I (a mixture of products) and class II (stainless steel) nickel in scrap. According to EuRIC (2020), the EoL RR for stainless steel is 90%. Based on this value and the 68% total EoL RR, the initial average EoL RR for class I nickel was determined based on the initial relative share of class I and class II nickel.

An initial EoL CR was also assumed for class I and class II nickel. For class I nickel, this was assumed to be 60%, based on Van der Linden (2020). For class II nickel, this was assumed to be 95%. Based on the initial EoL RR and the assumed initial EoL CR, the initial nickel content of scrap, which determines EoL PR in the model, was calculated.

This nickel content of scrap was assumed to remain constant for class II nickel, but to change for class I nickel based on the battery share. Three EoL waste management strategies were included that influenced this, one where batteries increase the extractable nickel content of scrap compared to other class I products, one where they have no effect and one where they reduce the extractable nickel content of scrap compared to other class I products. A fourth EoL waste management strategy was also included where batteries increase the extractable nickel content of scrap, as well as where the EoL CR of batteries increases over time (about 2% per year was assumed).

Another indicator for recycling is the recycling input rate. This is the fraction of total metal supply derived from recycling that determines how much nickel is required from primary processing to be able to fulfil the demand (van der Linden, 2020). UNEP (2011) report a nickel recycling input rate between 29% and 41%. This indicator is also included in the model.

At each stage of the supply chain, losses occur. This includes mining losses, processing losses, production losses, use losses and scrap losses. These losses are shown in table G4. According to Johnson et al. (2008), refining losses are negligible, so for processing losses only the primary extraction method was considered. Meshram et al. (2018) show that even within certain processing methods, the nickel recovery can differ based on specific locations and ore types (on a more detailed level than simply the distinction between sulfides and laterites). To keep it simple, average values were used.

Table G4: losses at different stages of the supply chain. These values are generally a lot higher than what was used by Van der Linden (2020) (between 4 and 8% per operation stage). *Assumed to apply to PM sulfide processing.

| Process | Losses (%) | Source |
|---|--------------|---|
| <i>Mining</i> | | |
| Mining | 20 | Johnson et al. (2008); Eckelman (2010) |
| <i>Primary processing</i> | | |
| RKEF (Ferronickel) | 5 | Johnson et al. (2008); Eckelman (2010); Norgate & Jahanshahi (2011) |
| BF (Nickel pig iron) | 8 | Eckelman (2010) |
| Caron (Nickel oxide) | 13 | Average of Johnson et al. (2008) and Norgate & Jahanshahi (2011) |
| Flash (Matte)* | 5 | Eckelman (2010) |
| HPAL | 8 | Norgate & Jahanshahi (2011); Khoo et al. (2017) |
| HL | 27 | Norgate & Jahanshahi (2011) |
| ATL | 20 | Norgate & Jahanshahi (2011) |
| DNI | 6 | Khoo et al. (2017) |
| <i>Further in the supply chain</i> | | |
| Production of batteries (used for all class I) | 7.5 | BNEF (2019) |
| Production of stainless steel (used for all class II) | 1 | Johnson et al. (2008); Eckelman (2010) |
| Use and scrap | EoL RR = 68% | Nickel Institute (2016). Changes over time in the model. |

Appendix H: Supply sub model input and data sources

Table H1: values and data sources used for the constants and lookups in the supply sub model. A range is included and the row is highlighted in yellow if uncertainty is assessed for a specific variable. Dmnl = dimensionless.

| Element | Unit | Type | Min | Max | Explanation/assumptions | Source |
|-----------------------------------|-----------|----------|------------------------|-----|--|--|
| <i>Resource and reserve data</i> | | | | | | |
| Initial resources | Mt nickel | Constant | Values in the database | | Initial measured, indicated and inferred resources, assumed to apply to 2015. Total resources including reserves are reported. Resources were calculated by subtracting reserves from total resources. | Mudd (2020) |
| Initial reserves | Mt nickel | Constant | Values in the database | | Initial proved and probable reserves, assumed to apply to 2015 | Mudd (2020) |
| Initial status | Dmnl | Constant | Either a 1 or a 0 | | Indicates whether a resource has a deposit, tailings, or operating, mothballed or developing capacity | Mudd (2020) |
| Administration time | Year | Constant | 15 | | Factor taken from van der Linden (2020) that plays a role in exploration when exploration otherwise becomes too high. Van der Linden (2020) used a range of 10 - 20. | Auping & Pruyt (2013) |
| Initial resource base nickel | Tonne | Constant | 1.5E11 | | Van der Linden (2020) obtained this value from USGS. | Van der Linden (2020) |
| Power for price-based exploration | Dmnl | Constant | 0.5 | 1 | Included in the model to give more weight to the price-based element of determining exploration. | Assumption |
| Opportunity check frequency | Year | Constant | 2 | 3 | Represents how often mining companies check whether new reserves can be declared. | Assumption |
| Resource class presence | Dmnl | Constant | Either a 1 or a 0 | | Used to distinguish between resources and reserves. Class 0 = reserves, the rest are resources | Assumption |
| Resource class division | Dmnl | Constant | 0.1 | | 10% because there are 10 resource classes, not including class zero, which represents the reserves. | Assumption |
| <i>Mining and refining data</i> | | | | | | |
| Initial nickel stock | Tonne | Constant | 486500 | | Total metal exchange stocks for 2015, including the London metal exchange and the Shanghai metal exchange. | WBMS (2018) |
| Initial percentage mine stock | Dmnl | Constant | 0.77 | | Calibrated to match initial nickel price | Assumption |
| Percentage lost during mining | Dmnl | Constant | 0.2 | | Losses during mining, milling and beneficiation. | Johnson et al. (2008); Eckelman (2010) |
| Percentage lost in tailings | Dmnl | Constant | 0.05 | | This is a relatively small part of the model, so less attention is paid to the details of this variable. | Assumption |
| Percentage lost during processing | Dmnl | Constant | See table G4 | | Different values apply to different processing methods | See table G4 |

| | | | | | |
|---|--------|----------|-----------------------------------|--|-------------------------|
| Average time mining to refining | Year | Constant | 0.1 | The time it takes for the ore to get from the mine to the processing plant. Assumption by van der Linden (2020), who used a range of 0.09 - 0,11. | Van der Linden (2020) |
| Nickel mined before 2015 | Tonne | Constant | 60000000 | Historically mined nickel, originally obtained from USGS. | Nickel Institute (2016) |
| <i>Production, use and recycling data</i> | | | | | |
| Minimum stock transit time | Year | Constant | 0.04 | Van der Linden (2020) used 0.05. Here 0.04 was used because it brought the two price calculation methods closest together. | Van der Linden (2020) |
| Percentage lost during production | Dmnl | Constant | See table G4 | Different values apply to different nickel containing products | See table G4 |
| Percentage of primary scrap | Dmnl | Constant | 0.325 | Van der Linden (2020) used a range between 0.25 and 0.4 to represent the percentage of primary scrap for copper, cobalt and nickel. | Van der Linden (2020) |
| Percentage of total mined nickel in use | Dmnl | Constant | 0.57 | This is an assumption by the Nickel Institute, based on the long lifetime of nickel products. | Nickel Institute (2016) |
| Initial EoL RR nickel | Dmnl | Constant | 0.68 | EoL RR for nickel in 2010; assumed to be similar in 2015 | Nickel Institute (2016) |
| Initial EoL RR stainless steel | Dmnl | Constant | 0.9 | Assumed to apply to nickel containing stainless steel. | EuRIC (2020) |
| Initial EoL CR | Dmnl | Constant | 0.6 (class I); 0.95 (class II) | Van der Linden (2020) reported a range between 0.6 and 0.8 (but used a range between 0.4 and 0.8) for copper, cobalt and nickel, based on a report by Gloser et al. (2013) on copper. 0.6 was selected for class I nickel to obtain a better matching initial nickel content of scrap (0.01 - 0.02 according to Van der Linden (2020)). For class II, consisting entirely of stainless steel, an EoL CR of 0.95 was chosen to match with an EoL RR for stainless steel of 0.9 (EuRIC, 2020). | Assumption |
| EoL CR improvement | 1/Year | Constant | 0.02 | Improvements in collection rate in EoL management strategy 4. | Assumption |
| Initial percentage of use in scrap | Dmnl | Constant | 0.001 | Calibrated to make a smoother start. | Assumption |
| Maximum nickel recycling efficiency | Dmnl | Constant | 0.95 | Value used for nickel by van der Linden (2020). This value was also used as the EoL PR for class II nickel, which together with the EoL CR leads to an EoL RR of 0.9 (EuRIC, 2020). | Van der Linden (2020) |
| Average time scrap to recycling | Year | Constant | 1 | Van der Linden (2020) assumed a range between 0.38 and 0.42. Here a value of 1 was assumed to prevent an unrealistically high peak at the start. | Assumption |

| | | | | | | |
|--|------------|----------|--------------|------|---|--------------------------|
| Initial recycling input rate | Dmnl | Constant | 0.35 | | Although it is based on relatively old data, this is assumed to be the initial fraction of finished nickel stock coming from recycled scrap. | UNEP (2011) |
| <i>Mining and refining capacity data</i> | | | | | | |
| Global maximum capacity increase percentage | Dmnl | Constant | 0.1 | 0.5 | Based on 22% production increase between 2010 and 2011 (highest since 2000, but the economic crisis may have something to do with this, which means there may have been underutilised existing capacity). | USGS (2020a) |
| Minimum capacity | Tonne/year | Constant | 10000 | | Assumption based on annual production data by USGS (2020a) | Assumption |
| Maximum capacity | Tonne/year | Constant | 1E5 | 1E6 | Maximum capacity of a single mine. | Assumption |
| Average mine operation plan | Year | Constant | 10 | 20 | This is the designed production lifetime of the mine based on reserves and expected economic conditions. | Extractives Hub (n.d.) |
| Development time | Year | Constant | 5 | 10 | This is the time it takes to develop a new mine. Both the lower bound and the upper bound are included in the model and a different value is selected per mine based on project investment attractiveness. | Extractives Hub (n.d.) |
| Upgrade time | Year | Constant | 3 | | It is assumed that it takes less time to increase the capacity of an existing mine than to create a new mine. | Assumption |
| Initial average mine production | Tonne/year | Constant | 34000 | | Based on production data in 2015 (WBMS, 2018) and the operating status reported by Mudd (2020) | WBMS (2018); Mudd (2020) |
| Initial average mine production per country | Tonne/year | Constant | See table G2 | | | |
| Initial average capacity utilisation | Dmnl | Constant | 0.8 | | Van der Linden (2020) used a range for minimum capacity utilisation between 0.7 and 0.9. | Assumption |
| Average maximum profit deficit as percentage of investment | Dmnl | Constant | 0.03 | 0.08 | A lower and an upper bound are included in the model with a respective distance of -0.2 and +0.2 from the average and a different value is selected per mine based on profit over investment ranking. | Assumption |
| Average minimum profit surplus as percentage of investment | Dmnl | Constant | 0.03 | 0.08 | | Assumption |
| Average maximum mothball time | Year | Constant | 10 | 30 | A lower and an upper bound are included in the model with a respective distance of -5 and +5 from the average and a different value is selected per mine based on profit over investment ranking. According to Ashby et al. (2016) mines can remain in C&M for several decades. | Assumption |

Appendix I: Background, assumptions & data: price dynamics

This appendix contains background information that can be consulted to provide some more context for the concepts related to the price dynamics discussed in the main text. Assumptions are also explained and values used in the model are shown.

Appendix I1 Cost structure

The cost structure consists of capital costs and operating costs. The latter can be divided into fixed and variable costs. The cost structure for nickel mining is complex. Detailed data is available, but costs a lot of money to obtain, so in this thesis many assumptions and approximations were made. More detailed data could however be plugged into the model in the future.

The cobalt model of Van der Linden (2020) was used as a basis for the costs included in this thesis. The cobalt model includes energy costs as the main determinant for mining costs and smelting and refining costs. It also includes transport costs, taxes and a carbon price. Van der Linden (2020) only included marginal (variable) costs. This is reasonable for a global model, but when individual mines are considered, capital costs and fixed operating costs become more important.

Capital costs were based on capacity. Although capital costs differ per processing technology, only data for the exponential relationship between capacity and capital costs for HPAL technology was found (Dry, 2013) and this was used to represent the capital costs for all projects. Values for the components used in this relationship are shown in appendix J. In future research it would be useful to include processing technology specific capital costs. Fixed operating costs were assumed to be about 2% of capital costs. This is an estimated 1% for labour and an estimated 1% for other costs based on Dry (2013).

The variable operating costs included in the model consist of energy costs for mining, processing and transport (based on energy use and energy price); reagents and other on-site costs; royalties and taxes; and a carbon price. These are different for each mine and depend on multiple factors, such as ore type (sulfide or laterite), ore grade, mine type (UG or OC), processing method, country, energy type, transport distance and by-products (Bleiwas, 1984; Eckelman, 2010; STRADE, 2016).

Appendix I1.1: Energy for mining processing and transport

The broad final energy intensity range of nickel production is shown in figure I1. In general, sulfides require less energy than laterites and a PM route is less energy intensive than a HM route (Eckelman, 2010).

There are various steps in the production of nickel that each require a certain amount of energy. These steps include mining, milling and beneficiation, primary extraction, refining and transport. The energy requirements also differ per processing method. Values for each step are shown per processing method in table I1 and elaborated on below.

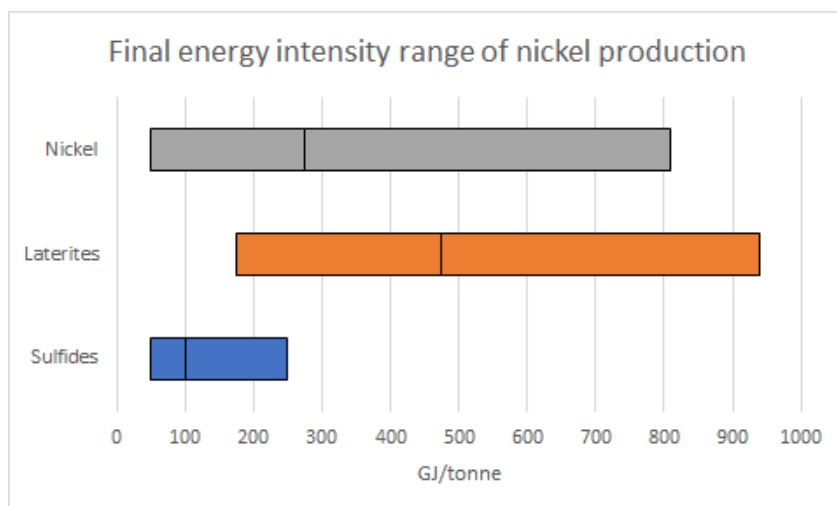


Figure 11: final energy intensity range for nickel production. Averages are indicated by vertical lines. Nickel pig iron production is not included in this figure. Adapted from Eckelman (2010).

Table I1: final energy requirements for processes. The values in plain text were obtained from Eckelman (2010). The bold values were switched around compared to what was stated by Eckelman (2010) based on his figures. The values in italics were estimated based on Norgate & Jahanshahi (2011), Northey et al. (2014) and Khoo et al. (2017). Combined OC and UG mining was assumed to be an average of OC and UG mining. DSM was assumed to be twice as much as this (highly uncertain assumption). Transport fuel takes into account average distances, but more may be used for international trade. This was not considered. Further details are described below.

| Type | Fuel | Electricity | Transport fuel |
|--|------------|-------------|----------------|
| <i>Mining, milling and beneficiation (GJ/tonne ore)</i> | | | |
| OC mine | 0.141 | 0.060 | - |
| UG mine | 0.066 | 0.149 | - |
| Combined OC and UG | <i>0.1</i> | <i>0.1</i> | - |
| DSM | <i>0.2</i> | <i>0.2</i> | - |
| Milling and beneficiation | 0 | 0.200 | - |
| Nickel ore | - | - | 0.245 |
| <i>Primary extraction/smelting (GJ/tonne product; also GJ/tonne nickel with mass-based allocation)</i> | | | |
| RKEF (Ferronickel) | 117 | 25 | 2 |
| BF (Nickel pig iron) | 27 | 2 | 0.1 |
| Caron (Nickel oxide) | 406 | 22 | 1 |
| Flash (Matte) | 21 | 16 | 1 |
| HPAL | 339 | 11 | 1 |
| HL | 263 | 9 | 1 |
| ATL | 208 | 7 | 1 |
| DNI | 321 | 10 | 1 |
| <i>Refining (GJ/tonne nickel)</i> | | | |
| Electrorefining | 0 | 15.3 | - |
| Electrowinning | 5.7 | 7.2 | - |
| Refined nickel | - | - | 2 |

When looking at energy requirements, it is important to distinguish between fuel and electricity use. This is relevant both for determining costs and for determining GHG emissions, which add to environmental impacts, but also to costs when a carbon price is implemented. Biofuels or other more sustainable fuels may be used in the mining industry in the future. However, in the model, fuels were assumed to remain fossil fuels. The same goes for transport fuels. In future research this could be linked more to the SSPs and the assumptions for electrification and hydrogen use in trucks. For electricity more diversity was assumed based on the SSPs and costs and emissions depend on the electricity mix of the country a certain mine is located in. This mix was estimated based on regional SSP data for five broad regions. (see section I1.4)

Eckelman (2010) provides data for the average final fuel and electricity requirements of UG and OC mining and the final electricity requirements for milling and beneficiation in MJ/tonne ore. Based on this, values for combined UG and OC mining (average of the two) and for DSM (2 times the average) were also determined. The value for DSM is a highly uncertain assumption.

An important determinant for the energy demand of mining is ore grade, as the higher the ore grade, the lower the energy requirements per tonne of nickel. Ore grade is included in the model by first taking average ore grades of a project for proved and probable reserves and for measured, indicated and inferred resources as reported in the database (Mudd, 2020) and using those averages until the original resources in the database run out.

Ore grade was reported by Mudd (2010) for reserves and for reserves and resources combined. The latter was assumed to apply to resources, which was assumed to work as a rough estimation but is not that accurate because it also contains the influence of the reserves. In future research this data could be manipulated in such a way that the ore grade for only resources is obtained.

Once the resources have run out, and if through exploration in the OCP more resources are discovered in a certain area, ore grade is expected to decay exponentially based on equation 2 (Van der Linden, 2020). The normalisation value in this equation was determined based on the initial total resources of a certain deposit and the final ore grade in the database.

$$OG = e^{-\left(\frac{C}{N}\right)^x} \quad (2)$$

In which:

- OG = Ore Grade
- C = Cumulative mined nickel
- N = Normalisation value ore grade
- x = Power for ore grades

Sometimes the ore grade in the database by Mudd (2020) for the resources of a certain project is larger than the ore grade for the reserves. It was assumed that this is because factors other than ore grade make the resources less economically attractive. Because of this, and because different projects with different ore grades become profitable at different times, overall average ore grade can increase and decrease over time. However, the general trend is expected to be a decrease. Based on relative ore grade, it is also possible to determine how much by-product can be produced for each tonne of nickel that is produced.

In addition to energy requirements for mining, Eckelman (2010) provides data for final fuel and electricity requirements of some representative companies using different primary extraction methods, as well as average data for various refining methods. The values in table I1 are based mainly on Eckelman (2010), because he included multiple processes and most other consulted sources reported energy demand in terms of Primary Energy Demand (PED) and not in terms of final energy demand for the production facilities. Final energy demand was used here because these values were used to determine costs for the facilities and it was assumed that all the costs for upstream energy use are already included in fuel and electricity prices.

There was a discrepancy between the values reported by Eckelman (2010) for fuel use for ferronickel and nickel pig iron (where nickel pig iron had a much higher fuel use per tonne product than ferronickel) and the figures he presented (where ferronickel had a much higher PED than pig iron per tonne product). By switching the values around, they fit much better with the figures and this also matches other literature.

No concrete data was provided by Eckelman (2010) for HM processing of laterite ores, so these values were estimated based on qualitative information and other sources. For transport, the values were assumed to equal the value for matte, since both cases concern transport of an intermediate product to a refinery. Since the main goal of using these numbers in the model is to favour a certain project over another, the exact numbers matter less than the relative order. However, there are some allocation issues that can influence this order. These issues are discussed in appendix I1.3.

Northey et al. (2014) provided electricity and fuel requirements for pyrometallurgy of sulfide ores and hydrometallurgy of laterite ores via HPAL. According to these values, HPAL requires about 23 times more fuel and 0.73 times more electricity than the PM route of obtaining class I nickel. This is quite a large difference and when applied to the data by Eckelman (2010), HPAL becomes very energy intensive, with higher values than Caron. This is not the case according to Norgate & Jahanshabi (2011). Therefore, the values calculated in this manner were used as upper range values for HPAL.

Norgate & Jahanshabi (2011) provided embodied energy values for ferronickel, Caron, HPAL, HL and ATL. Embodied energy is in terms of PED and it is important to keep in mind that other factors than electricity and fuel use also play a role when determining PED, such as the amount of sulfur used in the processing (especially for HPAL) and the amount of potential energy sources used as reductants (Nickel Institute, 2020). Despite this, it was assumed that the order of the processes (from high to low embodied energy: Caron, HPAL, ferronickel, HL, ATL) would remain more or less the same.

Norgate & Jahanshabi (2011) allocated embodied energy to all valuable co-products, including the iron in ferronickel on a mass basis. Their order from highest to lowest energy requirements matches table I1, with the exception of ferronickel. However, their value for ferronickel is relatively high compared to other sources (Eckelman, 2010 and Nickel Institute, 2020) when a similar mass-based allocation is applied. This is likely to be the reason for the difference in order.

The value given by Norgate & Jahanshabi (2011) for HPAL is 0.48 times the embodied energy for Caron and this was used in combination with the Caron values from Eckelman (2010) to determine lower range estimates for HPAL. The averages of the lower and upper estimates are shown in table I1. The values by Norgate & Jahanshabi (2011) for HL and ATL are 0.78 and 0.61 times the embodied energy of HPAL respectively. This was applied to the HPAL values to estimate the HL and ATL values. The values for DNI were based on Khoo et al. (2017), who reported a value for DNI that was 0.95 times the value for HPAL. This approach is an approximation that does not take into account differences in the fractions of energy supplied by fuel and electricity.

Appendix I1.2: Alternative energy calculation methods

In addition to the method for determining energy use in appendix I1.2, an alternative method was included in the model, based on an exponential function relating ore grade and energy use. The two methods differ in two important ways. The alternative method includes the impact of ore grade on processing energy requirements (whereas the method in appendix I1.2 only includes the impact of ore grade on mining energy requirements), but there is also less distinction between the different processing methods.

In initial runs, changing the energy calculation method did not have a very large impact on key performance metrics, so it was not considered in the main text of this thesis. However, the different methods could be explored further in future research and are therefore included in this appendix.

For the alternative method, two different functions relating ore grade and energy use were found, one based on Valero et al. (2013) and one based on Elshkaki et al. (2017). Values for the components of these functions are shown in appendix J. The function by Valero et al. (2013) was included because all the functions for calculating energy requirements for by-products were also based on their work (see table I9). However, these functions should be treated with care as various discrepancies were identified (also see section I2.1). Valero et al. (2013) reported ore grade as a percentage, but this leads to results that deviate widely from the other methods, which is why a fraction was used instead.

Appendix I1.3: Processing energy cost allocation

For the method described in appendix I1.1, different allocation methods can be used to attribute energy use to the constituents of a certain nickel product. The two methods covered in this thesis are mass-based allocation, as done by Norgate & Jahanshahi (2011) and full allocation to nickel, as done by Nickel Institute (2020). The allocation method is very important for the relative order of energy requirements for certain processing methods, so both methods are included in the model as a switch. Table I2 shows the assumptions on nickel content of different nickel products that were used in the mass-based allocation. It was assumed that all HM processing of laterites led to class I nickel.

Table I2: average nickel content of the different final and intermediate products. NI = Nickel Institute. EAF = Electric Arc Furnace.

| Product | Range | Value used in this thesis | Source |
|--------------------------|----------|---------------------------|----------------------------|
| Class 1 (refined) nickel | > 99% | 100% | Eckelman (2010) |
| Nickel oxide sinter | 75 - 78% | 77% | Eckelman (2010) |
| Ferronickel | 15 - 45% | 27% | Eckelman (2010); NI (2020) |
| Nickel pig iron (BF) | 1.5 - 8% | 5% | Eckelman (2010) |
| Nickel pig iron (EAF) | 8 - 17% | - | Eckelman (2010) |
| Cu-Ni matte | 40 - 80% | 70% | Eckelman (2010) |
| Ni-Co sulfate | 55 - 60% | 58% | SMM (n.d.) |

Figure I2 and figure I3 show the energy requirements for each processing path for the full allocation to nickel and mass-based allocation respectively. To obtain these figures, the following assumptions were made. Values for mining, milling and beneficiation in GJ/tonne ore were converted to GJ/tonne nickel based on an assumed average ore grade of 0.013. For the laterite routes, OC mining was assumed and for the sulfide route, UG mining was assumed. The value for milling and beneficiation in table I1 was assumed to apply to all processes. For mining, no allocation to by-products is included in the figures.

For primary extraction, values in GJ/tonne nickel product were assumed to be equal to GJ/tonne nickel through mass-based allocation for figure I3. For figure I2, these values were divided by average nickel content (table I2). For refining, values in GJ/tonne nickel were used. Electrorefining was applied to the sulfide route and electrowinning was applied to the laterite routes. In the model, values for certain processes may differ based on different combinations of mine type and extraction method and an ore grade that changes over time, leading to a wide variety of costs.

According to Eckelman (2010), pyrometallurgy of sulfide ores requires the least primary energy on a contained nickel basis, followed by pyrometallurgy of laterite ores. Then comes hydrometallurgy of laterite ores and Caron and finally pig iron production. This matches with the representation in figure I2, with the exception of ferronickel, which has a higher value than the HM processes. This may be because figure I2 is in terms of final energy and does not include the energy contained in the sulfur used in HM processes which contributes to a significant fraction of the PED (Nickel Institute, 2020).

In the model, energy use is determined by the factors discussed above, the ore grade development and the autonomous specific energy consumption (SEC) change which is assumed to be 1% per year due to technological developments that lead to efficiency improvements (Blok & Nieuwlaar, 2021).

All HM laterite processing was treated the same as HPAL regarding nickel recovery. It was assumed that all lead to the production of class I nickel. However, if this is not the case, figures I2 and I3 may need to be adapted slightly. Because there are relatively few deposits included in the database by Mudd (2020) with HL, ATL or DNI as processing method, this was not assessed further.

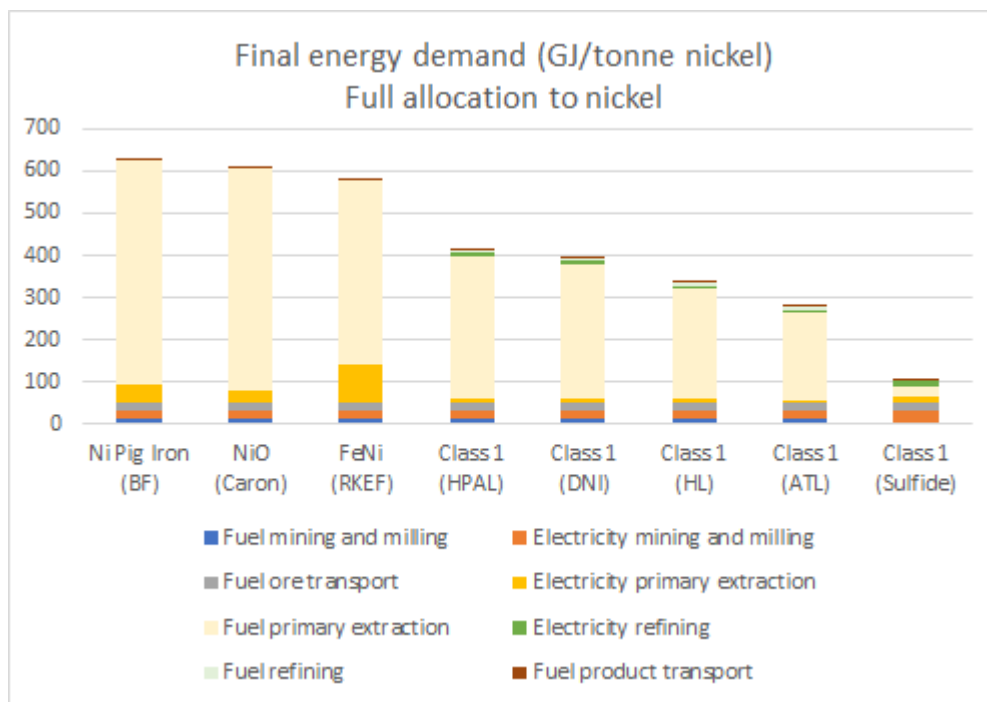


Figure I2: final energy demand for various processing methods broken down by energy type and processing stage. Full allocation to nickel was applied. An ore grade of 0.013 was assumed to determine the energy demand for mining. Product transport includes the transport of both intermediate products and refined products. Based on data from Eckelman (2010), Norgate & Jahanshahi (2011), Northey et al. (2014), Khoo et al. (2017) and Nickel Institute (2020).

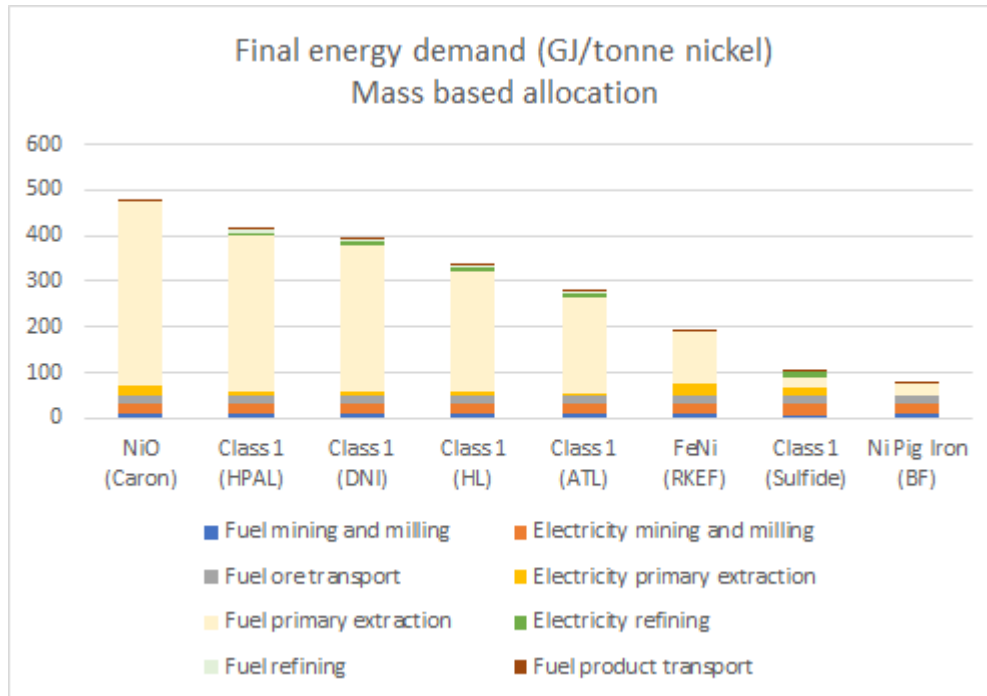


Figure 13: final energy demand for various processing methods broken down by energy type and processing stage. Mass based allocation was applied. An ore grade of 0.013 was assumed to determine the energy demand for mining. Product transport includes the transport of both intermediate products and refined products. Based on data from Eckelman (2010), Norgate & Jahanshahi (2011), Northey et al. (2014) and Khoo et al. (2017).

Appendix I1.4: Energy price

Future energy price is highly uncertain and difficult to model, especially due to the many changes that may occur to energy markets due to an increasing penetration of renewable energy. Because of this, Van der Linden (2020) assumed three broad scenarios for fuel price that are used in the model. One with an increasing average price (high price scenario), one with a decreasing average price (low price scenario) and one that varies in the middle (medium price scenario). These scenarios are shown in figure 14.

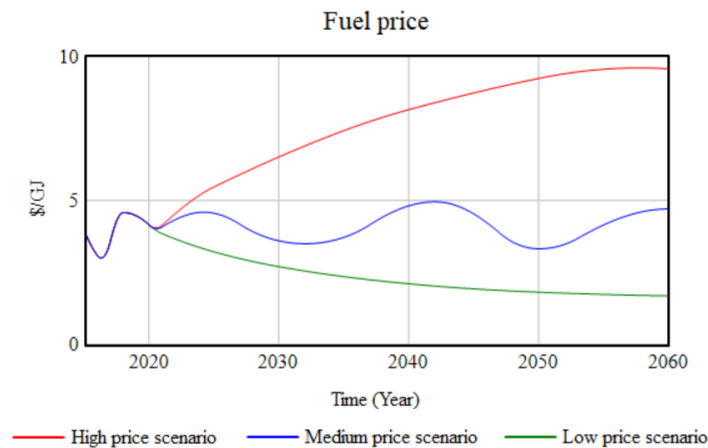


Figure 14: fuel price scenarios used in the model. Values are in 2005 \$. Data up to 2018 is based on BP (2019). The scenario shapes are based on Van der Linden (2020).

The initial fuel price was based on the average price for different types of coal, oil and natural gas covered by BP (2019). This was about 5 \$/GJ in 2015 (4 \$/GJ in 2005 \$). Electricity price was modelled linearly as a changing difference from the fuel price. In 2015, the average industrial electricity price in the USA was about 19 \$/GJ (15\$/GJ in 2005\$) (EIA, 2020b). Based on this the initial average difference between fuel and electricity prices was 11 2005\$/GJ.

It was assumed that as the share of renewable energy in the electricity mix increases (from about 22.8% in 2015 (REN21, 2015)), this difference will become increasingly smaller, until at a certain point fuel prices become more expensive than electricity prices because more fuel (such as hydrogen and synthetic fuels) is made from electricity than the other way around (Blok & Nieuwlaar, 2021). It was assumed that this point could happen at about 75% renewable energy share in the electricity mix.

The SSP database provides global data, but also a distinction between the following regions or categories: Asia, Latin America, Middle East and Africa, Organisation for Economic Cooperation and Development (OECD) and Reforming economies. Based on the SSP data, renewable energy shares in the electricity mix were determined for each region. For international waters, global averages were used. This data is shown in tables I4 - I7. Table I3 shows the nickel containing countries per SSP region.

Table I3: nickel containing countries per region as classified by IIASA (2018).

| Region | Countries |
|------------------------|---|
| Asia | PNG, Indonesia, Philippines, Myanmar, New Caledonia, China, Solomon Islands, India |
| Latin America | Argentina, Brazil, Guatemala, Colombia, Dominican Republic, Cuba |
| Middle East and Africa | Guinea, Côte d'Ivoire, Oman, Togo, Botswana, Zimbabwe, Zambia, Burundi, Tanzania, Malawi, Madagascar, Morocco, Cameroon, Ethiopia, South Africa |
| OECD | Australia, Canada, Puerto Rico, Turkey, Albania, Serbia, Kosovo, Poland, Finland, USA, Spain, Norway, Greece, Sweden |
| Reforming Economies | Russia, Kazakhstan |

Table I4: renewable energy shares for SSP1-19 per region.

| Renewable energy shares SSP1 RCP 1.9 | 2005 | 2010 | 2020 | 2030 | 2040 | 2050 | 2060 | 2070 | 2080 | 2090 | 2100 |
|--------------------------------------|-------|-------|-------|-------|-------|-------|-------|-------|-------|-------|-------|
| Asia | 0.143 | 0.163 | 0.234 | 0.334 | 0.763 | 0.815 | 0.786 | 0.721 | 0.758 | 0.821 | 0.866 |
| Latin America | 0.576 | 0.559 | 0.636 | 0.738 | 0.857 | 0.930 | 0.944 | 0.916 | 0.914 | 0.945 | 0.968 |
| Middle East and Africa | 0.101 | 0.087 | 0.146 | 0.301 | 0.721 | 0.856 | 0.881 | 0.889 | 0.913 | 0.914 | 0.920 |
| OECD | 0.159 | 0.189 | 0.303 | 0.424 | 0.715 | 0.917 | 0.909 | 0.867 | 0.867 | 0.936 | 0.939 |
| Reforming economies | 0.199 | 0.177 | 0.208 | 0.290 | 0.409 | 0.735 | 0.926 | 0.958 | 0.990 | 0.985 | 0.999 |
| Global | 0.180 | 0.196 | 0.281 | 0.394 | 0.737 | 0.858 | 0.855 | 0.817 | 0.841 | 0.887 | 0.909 |

Table I5: renewable energy shares for SSP2-19 per region.

| Renewable energy shares SSP2 RCP 1.9 | 2005 | 2010 | 2020 | 2030 | 2040 | 2050 | 2060 | 2070 | 2080 | 2090 | 2100 |
|--------------------------------------|-------|-------|-------|-------|-------|-------|-------|-------|-------|-------|-------|
| Asia | 0.145 | 0.174 | 0.285 | 0.592 | 0.662 | 0.641 | 0.574 | 0.594 | 0.617 | 0.683 | 0.785 |
| Latin America | 0.608 | 0.616 | 0.543 | 0.657 | 0.840 | 0.872 | 0.844 | 0.882 | 0.920 | 0.962 | 0.996 |
| Middle East and Africa | 0.123 | 0.120 | 0.108 | 0.306 | 0.427 | 0.514 | 0.579 | 0.617 | 0.717 | 0.808 | 0.865 |
| OECD | 0.155 | 0.203 | 0.263 | 0.396 | 0.567 | 0.603 | 0.624 | 0.679 | 0.725 | 0.751 | 0.839 |
| Reforming economies | 0.197 | 0.190 | 0.175 | 0.271 | 0.559 | 0.598 | 0.696 | 0.762 | 0.826 | 0.863 | 0.938 |
| Global | 0.179 | 0.211 | 0.270 | 0.480 | 0.615 | 0.631 | 0.618 | 0.654 | 0.701 | 0.762 | 0.846 |

Table I6: renewable energy shares for SSP5-19 per region.

| Renewable energy shares SSP5 RCP 1.9 | 2005 | 2010 | 2020 | 2030 | 2040 | 2050 | 2060 | 2070 | 2080 | 2090 | 2100 |
|--------------------------------------|-------|-------|-------|-------|-------|-------|-------|-------|-------|-------|-------|
| Asia | 0.143 | 0.130 | 0.126 | 0.189 | 0.421 | 0.609 | 0.715 | 0.769 | 0.808 | 0.826 | 0.826 |
| Latin America | 0.591 | 0.541 | 0.375 | 0.527 | 0.865 | 0.970 | 0.978 | 0.977 | 0.984 | 0.991 | 0.998 |
| Middle East and Africa | 0.142 | 0.127 | 0.089 | 0.193 | 0.600 | 0.767 | 0.793 | 0.822 | 0.871 | 0.920 | 0.959 |
| OECD | 0.148 | 0.180 | 0.209 | 0.305 | 0.571 | 0.732 | 0.802 | 0.836 | 0.861 | 0.877 | 0.892 |
| Reforming economies | 0.186 | 0.161 | 0.107 | 0.152 | 0.466 | 0.757 | 0.892 | 0.961 | 0.991 | 0.998 | 1.000 |
| Global | 0.176 | 0.182 | 0.174 | 0.251 | 0.525 | 0.703 | 0.779 | 0.820 | 0.857 | 0.883 | 0.901 |

Table 17: renewable energy shares for SSP2-baseline per region.

| Renewable energy shares SSP2 Baseline | 2005 | 2010 | 2020 | 2030 | 2040 | 2050 | 2060 | 2070 | 2080 | 2090 | 2100 |
|---------------------------------------|-------|-------|-------|-------|-------|-------|-------|-------|-------|-------|-------|
| Asia | 0.143 | 0.168 | 0.239 | 0.208 | 0.206 | 0.178 | 0.171 | 0.192 | 0.200 | 0.209 | 0.224 |
| Latin America | 0.608 | 0.616 | 0.503 | 0.445 | 0.441 | 0.444 | 0.420 | 0.465 | 0.505 | 0.502 | 0.562 |
| Middle East and Africa | 0.095 | 0.098 | 0.094 | 0.114 | 0.139 | 0.196 | 0.231 | 0.305 | 0.306 | 0.354 | 0.365 |
| OECD | 0.155 | 0.203 | 0.256 | 0.253 | 0.251 | 0.272 | 0.299 | 0.289 | 0.290 | 0.312 | 0.350 |
| Reforming economies | 0.196 | 0.189 | 0.169 | 0.159 | 0.165 | 0.185 | 0.195 | 0.204 | 0.236 | 0.304 | 0.353 |
| Global | 0.179 | 0.211 | 0.257 | 0.256 | 0.271 | 0.276 | 0.286 | 0.307 | 0.315 | 0.341 | 0.373 |

Appendix I1.5: Royalties and taxes

Royalties per country are shown in table I8. They influence the relative profitability of mines based on the country they are located in. Royalties could not be obtained for all countries, so for some, assumptions were made based on nearby countries. Royalties were assumed to remain static throughout the model.

Table I8: royalties per country as fraction of sales. For the countries in italics data for that specific country could not be found and the value of a nearby country was assumed. For international waters, 0 was assumed. The values in this table are quite uncertain and in future research, it would be beneficial to devote more attention to the royalties.

| Country | Royalty | Source | Country | Royalty | Source |
|----------------------|--------------|---|------------------------|-------------|--------------------------------------|
| Australia | 0.025 | Government of Western Australia (2013) | Zimbabwe | 0.02 | Manhando (2015) |
| PNG | 0.02 | EITI (2020) | <i>Zambia</i> | <i>0.02</i> | Assumption |
| Indonesia | 0.1 | The Insider Stories (2019) | <i>Burundi</i> | <i>0.02</i> | Assumption |
| Philippines | 0.05 | Republic of the Philippines (2018) | <i>Tanzania</i> | <i>0.02</i> | Assumption |
| Myanmar | 0.04 | Lexology (2019) | USA | 0 | Gentile (2019) |
| New Caledonia | 0.025 | Assumption | Spain | 0.1 | USSEC (2007) |
| <i>Argentina</i> | <i>0.02</i> | Assumption | Norway | 0.03 | USSEC (2018) |
| Brazil | 0.02 | AngloAmerican (2020) | <i>Malawi</i> | <i>0.02</i> | Assumption |
| <i>Guinea</i> | <i>0.02</i> | Assumption | <i>Solomon Islands</i> | <i>0.02</i> | Assumption |
| Canada | 0.13 | The Mining Association of Canada (2008) | Guatemala | 0.01 | Worstall (2019) |
| <i>Côte d'Ivoire</i> | <i>0.02</i> | Assumption | Colombia | 0.12 | Restrepo et al. (2015) |
| Russia | 0.08 | Government of Western Australia (2015) | Greece | 0.025 | Newman (2004) |
| <i>Puerto Rico</i> | <i>0</i> | Assumption | Dominican Rep. | 0.05 | World Bank (2006) |
| Turkey | 0.02 | Sakar & Clark (2013) | <i>Kazakhstan</i> | <i>0.08</i> | Assumption |
| Albania | 0.055 | Deloitte (2016) | Madagascar | 0.02 | Rabary (2019) |
| <i>Serbia</i> | <i>0.055</i> | Assumption | Cuba | 0.05 | Elias et al. (2019) |
| Kosovo | 0.05 | Republic of Kosovo (2012) | <i>India</i> | <i>0.04</i> | Assumption |
| <i>Oman</i> | <i>0.02</i> | Assumption | Morocco | 0.02 | Redstone exploration services (n.d.) |
| <i>Togo</i> | <i>0.02</i> | Assumption | <i>Cameroon</i> | <i>0.02</i> | Assumption |
| <i>Poland</i> | <i>0.055</i> | Assumption | <i>Ethiopia</i> | <i>0.02</i> | Assumption |
| Botswana | 0.03 | IDE-JETRO (n.d.) | <i>Sweden</i> | <i>0.03</i> | Assumption |
| Finland | 0 | Farooki et al. (2017) | South Africa | 0.0375 | Deloitte (2015b) |
| China | 0.04 | Wu et al. (2018) | <i>Int'l waters</i> | <i>0</i> | Assumption |

The royalty data was gathered from many different sources with varying degrees of accuracy and for different periods in time. Most royalties were as a fraction of sales, but in some cases, assumptions had to be made. The collected data probably contains inaccuracies and the values for countries for which no data was found are very rough estimates. Royalties may also change over time, which was not considered. Future research should be done to determine how to deal with royalties in a better fashion.

In addition to royalties, a tax on profit is also included in the model. This variable is a lot less important than the royalties because it does not determine the profitability (and thereby relative preference) of a certain mine. It only influences variables such as profit surplus and exploration efforts for that specific mine. Therefore, the same value of 30% is used for each mine (PWC, 2012).

Appendix I1.6: Reagents and other costs

In addition to the costs mentioned above, reagents and other costs also play an important role. However, no data was gathered for these costs. Instead, initial average total marginal costs were determined based on initial nickel price (see appendix I3.2), with an assumed initial nickel scarcity of 1 (demand = supply). The costs calculated above were then subtracted from this total cost and the remainder was assumed to be the cost for reagents and other costs.

However, because initial costs differ per run based on certain methodological assumptions and scenarios, some initial runs were first done (see figure I5) and the average of these runs was taken: 4750 \$/tonne. This value was assumed to remain constant throughout the model. In reality, these costs can vary and they are also different for each processing method and can be impacted by the carbon price and other economic dynamics. However, this is something that could be assessed further in future research.

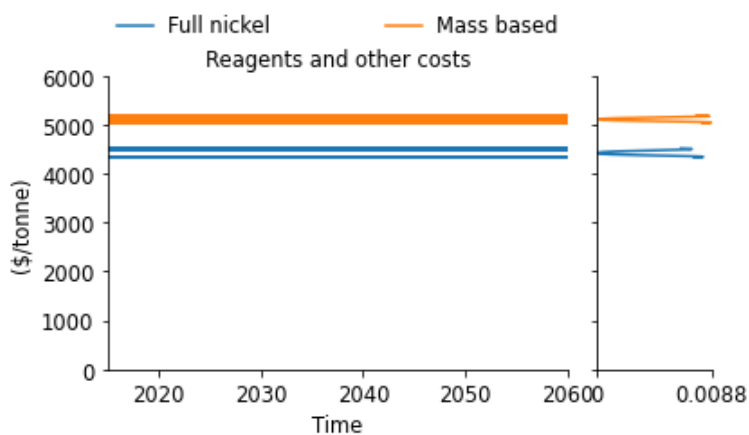


Figure I5: calculated costs for reagents and other per processing energy allocation method. The difference is relatively large between the two processing energy allocation methods, with smaller differences between SSPs. An average of 4750 \$/tonne was assumed

Appendix I1.7: Carbon price

A carbon price is included in the SSP scenarios with a target of 1.5 °C. This carbon price is shown in tables D2 – D5 and is the same for all regions in a certain scenario. It is assumed that the carbon price applies to all GHGs in terms of CO2-eq. Carbon costs are determined in the model by multiplying the carbon price with GHG emissions. These emissions are determined in the impact sub model, which is covered in appendix K.

Carbon costs for mining are currently fully allocated to nickel and don't impact by-product cost. This is something that could be changed in future adaptations of the model. However, an estimate of carbon costs for processing of by-products was included and so was an estimate of carbon costs for substitutes, based on the carbon costs for nickel. If more or less fuel was estimated to be required for the processing of a certain by-product, this was taken into account. However relative non-energy related emissions were not taken into account.

Appendix I2: By-products

Nickel mining has the following by-products, with in brackets the percentage of primary production of these metals originating from nickel mines: cobalt (~50%), palladium (~50%), platinum (~15%), osmium (~15%), rhodium (~15%), iridium (~5%), ruthenium (~5%), copper (~5%), gold (~5%), silver (undetermined) and selenium (undetermined) (Nassar et al., 2015). The database by Mudd (2020) includes a few more potential by-products, but excludes osmium, iridium, ruthenium and selenium, leading to a total of 19 by-products included in the model.

Of the elements for which the primary production from nickel mining is 15% or higher, cobalt, palladium and platinum are the most relevant for the energy system. Cobalt is mostly used in batteries and electric vehicles (van der Linden, 2020) and palladium and platinum are used in different types of vehicles and fuel cells (Manberger & Stenqvist, 2018). Different nickel deposits will become profitable at different times. This is partially because of the by-products that can be produced, but it also influences which by-products can be produced. So, nickel production is not only directly important for the energy system, it also influences the production of other metals that are important for the energy system.

Appendix I2.1: By-products in the model

By-products are treated in less detail in the model than nickel. Only a certain percentage of the production of each by-product is the result of nickel mining, so in reality most of the dynamics of by-products (with a low dependency on nickel) are determined by factors that are unrelated to nickel mining. Initial prices for each by-product are shown in table I9. Initial total by-product marginal costs were determined based on these prices in the same way as was done for nickel (see section I1.6).

Initial energy use for by-products was determined by using functions for the relationship between initial average ore grade and energy use for each by-product. This relationship is determined by a coefficient for by-product energy use and a power for by-product ore grade. Values for these variables, as well as for initial average by-product ore grade are shown in table I9.

General average energy costs were then determined based on the initial energy use, fuel price, electricity price and the fractions of electricity use for mining and for processing. Next, average other costs were determined based on the difference between average marginal costs (based on the initial marginal costs and the relative change in fuel price) and general average energy costs.

The average other costs were then combined with energy costs (based on energy use calculated with changing ore grades) and carbon costs to determine dynamic marginal costs for by-products. By converting this to marginal costs in terms of nickel and subtracting the energy costs for nickel mining, the potential additional costs for by-products could be calculated.

The whole structure is relatively complex and is probably easier to understand by engaging with the model. Part of the structure is included in the cost structure section of the model, part of it is included in the ore grade section of the model and part of it is included in the additional cost info section of the model. In future adaptations, this could be organised in a more logical way.

Table I9: by-product data. Non-price data was obtained from Valero et al. (2010), Valero et al. (2013), Valero & Valero (2014) and Valero et al. (2015). Where there were discrepancies between values, the data from the latest publication was used. NI = Nickel Institute.

| Element | Price (3 yr. avg. 2015 - 2017; \$/tonne)* | Inflation corrected price (2005 \$/tonne) | Average concentration in Earth's crust | Average ore grade | Average concentration in refined products** | Power for by-product ore grade** | Coefficient for energy use*** (GJ/tonne) | Sources for price data |
|--------------------|---|---|--|-------------------|---|----------------------------------|--|--------------------------|
| <i>By-products</i> | | | | | | | | |
| Cu | 5500 | 4097 | 6.6E-5 | 1.7E-02 | 0.81 | -0.35 | 23.8 | NI (2020) |
| Au | 39000000 | 29051100 | 1.3E-9 | 2.2E-06 | 0.00014 | -0.29 | 2645 | Bullion by Post (2020) |
| Ag | 600000 | 446940 | 1.2E-8 | 4.3E-06 | 0.9 | -0.5 | 24.7 | |
| U | 65692 | 48934 | 1.5E-6 | 3.2E-03 | 0.75 | -0.28 | 138.8 | Trading Economics (2020) |
| Mo | 18000 | 13408 | 1.8E-6 | 5.0E-04 | 0.92 | -0.5 | 23.6 | |
| W | 37890 | 28224 | 2.7E-6 | 8.9E-03 | 0.9 | -0.5 | 1.6 | Metalary (2020) |
| Pb | 1995 | 1486 | 6.7E-6 | 2.4E-02 | 0.64 | -0.5 | 3.6 | Trading Economics (2020) |
| Zn | 2320 | 1728 | 1.0E-4 | 6.1E-02 | 0.79 | -0.5 | 3.0 | |
| Co | 36000 | 26816 | 5.1E-9 | 1.9E-03 | 0.05 | -0.64 | 2.2 | NI (2020) |
| Pt | 32054000 | 23877025 | 5.0E-10 | 8.0E-07 | 0.9 | -0.5 | 20 | NI (2020) |
| Pd | 23334000 | 17381497 | 5.0E-10 | 8.0E-07 | 0.9 | -0.5 | 20 | NI (2020) |
| Rh | 29483000 | 21961887 | 5.0E-10 | 8.0E-07 | 0.9 | -0.5 | 20 | NI (2020) |
| Cr | 1175 | 875 | 2.0E-4 | 6.4E-01 | 0.81 | -0.5 | 11.8 | USGS (2020b) |
| Fe | 64 | 48 | 9.7E-4 | 7.3E-01 | 0.95 | -0.5 | 3.6 | Trading Economics (2020) |
| SiO ₂ | 45 | 34 | 2.3E-1 | 6.5E-01 | 0.98 | -0.5 | 4.0 | USGS (2020c) |
| Sc | 1600000 | 1191840 | 2.5E-5 | 6.0E-02 | 0.86 | -0.5 | 21.8 | Mudd (2020) |
| Re | 2280000 | 1698372 | 2.0E-10 | 2.2E-04 | 0.9 | -0.5 | 20 | USGS (2020d) |
| Mn | 1500 | 1117 | 4.9E-5 | 5.0E-01 | 0.67 | -0.5 | 20 | Mudd (2020) |
| Bi | 11557 | 8609 | 5.1E-8 | 2.5E-03 | 0.9 | -0.5 | 26.3 | USGS (2018) |
| <i>Nickel****</i> | | | | | | | | |
| Ni S | 11000 | 8194 | 5.8E-5 | 3.40E-02 | 0.47 | -0.67 | 17 | NI (2020) |
| Ni L | | | 4.1E-6 | 4.40E-02 | 0.08 | -0.5 | 2.1 | |

*The value for Cr is an average of 2014 and 2017. The values for Sc and Mn are 2018 averages.

** Valero et al. (2013) used 0.9 and -0.5 respectively when they lacked data. Here the same is done.

*** If no data could be found, a value of 20 (bold) was used. This is very arbitrary and likely to lead to inaccurate representations for these by-products. For gold, the coefficient of 135664 provided by Valero & Valero (2014) was adapted to accommodate an ore grade in t/t instead of an ore grade in g/t.

**** For nickel, different values than those provided by Valero et al. were used if more detailed information was available through the database by Mudd (2020).

A new by-product price was calculated based partially on the average marginal cost of that by-product based on the initial marginal costs and the relative change in fuel price, and partially on the average marginal cost based on the mining of the by-product from nickel deposits. The relative shares were based on the initial percentage of the production of a certain by-product due to nickel mining.

Another factor influencing by-product price is the degree of by-product scarcity. Keeping the scarcity at 1 would mean that if the ore grade of a by-product in a certain nickel deposit is equal to or greater than the overall average ore grade of the by-product, the price and therefore the revenue would always be higher than the costs due to the percentage cost on top of marginal cost. In reality this is not the case, because scarcity is an important driver of price.

However, without expanding the model to an unreasonable size, it is not possible to know what the dynamics around scarcity of by-products may be. Therefore, some assumptions were made. First it was assumed that as for nickel, scarcity would go up and down based on price dynamics. For by-products with a high dependency on nickel, such as cobalt and palladium, the scarcity was assumed to equal nickel scarcity. However, the lower the dependency of a by-product on nickel, the more out of sync its scarcity was assumed to be with nickel scarcity. This was done by relating the scarcity of these by-products to a delayed nickel scarcity.

Regardless of what choices are made regarding the scarcity of by-products, they will be arbitrary without expanding the model. Therefore, the choice for making the scarcities of the different metals out of sync was based on ameliorating hog cycles. In reality not all the scarcities of metals would be in sync and if they are or if they are assumed to be 1, the hog cycles would more frequently have higher peaks (and the peaks are already quite high). So, the reasoning for creating a by-product scarcity that is out of sync with nickel was to make the dynamics less extreme and less dependent on by-products.

It is important to keep in mind that because of the simplifications and arbitrary choices regarding by-products, the dynamics of the by-products are even more uncertain than the dynamics of nickel and the model should not be used to conclude anything meaningful about specific by-products, with the possible exception of cobalt and palladium because they are more dependent on nickel production.

By-products were deemed profitable if the additional revenue is greater than the additional costs. This can be because the by-product ore grade of a certain nickel project is higher than the average overall by-product ore grade and/or because modelled by-product scarcity drives up the price. In this case, the by-products are recovered and the additional costs for by-products are added to the total marginal cost of the deposit. For mines with platinum as a main product, the platinum is always recovered and the profitability of the platinum has a larger influence on whether a certain mine is profitable.

This marginal cost is used to determine the profitability of specific nickel mines. However, to determine the nickel price, only the costs allocated to nickel are relevant. There are different ways of allocating mining costs between nickel and its by-products. These are discussed in appendix I2.2.

The processing method can impact the recovery possibilities for by-products, but this is not considered. As a simplification, the same losses as the losses for nickel apply when relating the two to each other. This could be changed in future adaptations of the model.

Appendix I2.2: Mining energy cost allocation

When multiple minerals are mined from a certain deposit, there are different ways of allocating the mining costs between the by-products. Valero et al. (2015) discuss three methods: allocation based on mass, allocation based on prices and allocation based on ERC. The formulas for these allocation methods are shown in equations 3 - 5. Further information on how to calculate ERC can be found in Valero et al. (2015) and can be gathered from the model.

$$Mass_i[\%] = \frac{m_i}{\sum_i^n m_i} \quad (3)$$

$$Price_i[\%] = \frac{p_i m_i}{\sum_i^n p_i m_i} \quad (4)$$

$$ERC_i[\%] = \frac{B_i^* m_i}{\sum_i^n B_i^* m_i} \quad (5)$$

In which:

- m = annual production
- p = price
- B* = exergy replacement cost

Arguments can be made for or against each of these allocation methods. For example, an argument against mass-based allocation is that the fraction of gold in a certain deposit can be very small but it has high value and high mining costs, so it would be unfair to the other metals in the deposit to only attribute a small fraction of the costs to gold. In this case, price based-allocation is a better option and this is used as the main allocation method in this thesis.

Valero et al. (2015) argue that an even better allocation method is allocation based on ERCs, stating that it is a 'physical measure independent of monetary arbitrariness supported by the rigorous theory of Thermoconomics'. However, this method of allocation is much more complex and requires many more uncertain inputs.

Appendix I3: Nickel price and profit

In this appendix, the calculation methods for determining the nickel price and profit are discussed. However, first, the historic nickel price is shown in figure I6.

Appendix I3.1: Historic nickel price

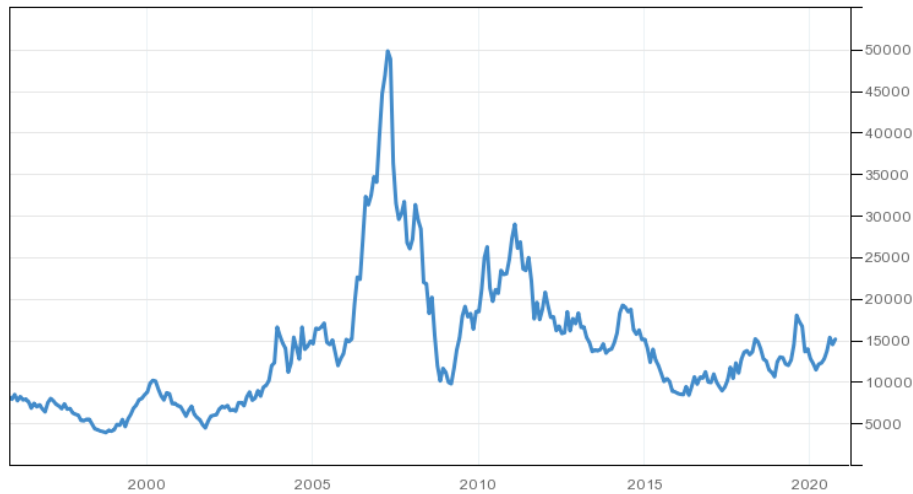


Figure I6: nickel price for the past 25 years in US\$/tonne (Trading Economics, 2020).

Appendix I3.2: Price calculation

Following van der Linden (2020), a switch for selecting between two different methods for calculating nickel price was included in the model. Both methods include a relationship with marginal cost and a relationship with scarcity. The first method, based on the days of demand in stock, is shown in equation 6 (Sverdrup et al., 2017). The second, based on availability and consumption, is shown in equation 7 (Usanov et al., 2013). This is the method that was also used to determine initial average total marginal costs, initial total by-product marginal costs and by-product price.

$$P = M * b \left(\frac{S}{Y} \right)^x \quad (6)$$

$$P = M * (1 + p) \left(\frac{A}{C} \right) \quad (7)$$

In which:

- P = price
- M = average marginal costs
- b = marginal cost bottom price relationship
- S = days of demand in stock
- Y = days in a year
- x = exponent nickel price curve
- p = percentage cost on top of marginal cost
- A = available supply
- C = forecasted consumption

Average marginal cost was based on existing mines, which includes operating mines and mines in C&M. This was done because including all mines would lead to unrealistically high costs, because unprofitable mines would also be included. In contrast, including only operating mines could potentially lead to 0 costs if no mines are operating at a certain point in time.

Appendix I3.3: Profit calculation

When looking at the price dynamics for individual mines, a distinction was made between current values, current potential values and future potential values. These different types of values are described in the main text (section 2.3.3). Details on their calculation are quite complex and can be understood best by engaging with the model.

Relative profit over investment was used to rank the different projects in terms of profitability. In future research, Net Present Value (NPV) and Internal Rate of Return (IRR) could be used instead. There are built in formulas for this in Vensim, but they are difficult to implement. Possibilities for implementation could be explored for future adaptations.

Appendix I4: Investment attractiveness

Profit is not the only factor that influences investment. To influence preferential investment in the model, an overall investment attractiveness index was researched. Investment attractiveness is influenced by a wide range of factors. The Fraser institute conducts the most elaborate survey-based analysis of mining company opinions in an attempt to rank the investment attractiveness of mining countries. However, the Fraser institute (2020) did not cover all the countries of interest in the model. Transparency International conducts an annual assessment of the Corruption Perception Index (CPI) of countries (see table I10). The countries included cover those of interest in the model. There is a decent correlation ($R^2 = 0.4$; figure I7) between the Fraser Investment attractiveness index and the CPI, so CPI was used as a proxy for investment attractiveness. In future adaptations of the model, other factors could be included.

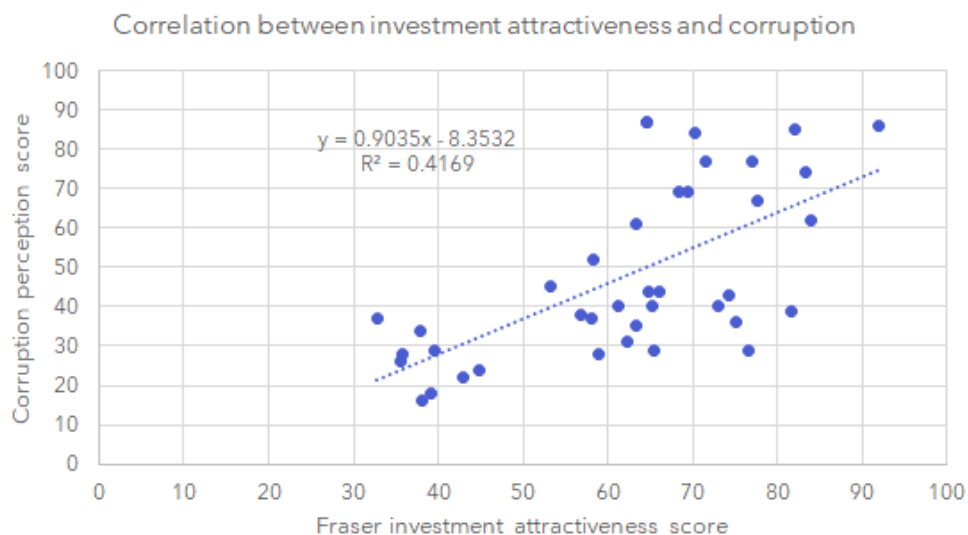


Figure I7: correlation between investment attractiveness and corruption (Fraser Institute, 2020; Transparency International, 2020)

Table I10: Fraser investment attractiveness score, corruption perception score and normalised corruption perception score per country in the model (Fraser Institute, 2020; Transparency International, 2020). For international waters, the lowest corruption perception score was assumed, simply to reflect the increased difficulty of DSM.

| Country | Fraser score | Corruption score | Normalised score | Country | Fraser score | Corruption score | Normalised score |
|---------------|--------------|------------------|------------------|-----------------|--------------|------------------|------------------|
| Australia | 77 | 77 | 0.87 | Zimbabwe | 45 | 24 | 0.09 |
| PNG | 59 | 28 | 0.15 | Zambia | 38 | 34 | 0.24 |
| Indonesia | 73 | 40 | 0.32 | Burundi | - | 19 | 0.01 |
| Philippines | - | 34 | 0.24 | Tanzania | 33 | 37 | 0.28 |
| Myanmar | - | 29 | 0.16 | USA | 69 | 69 | 0.75 |
| New Caledonia | - | 69 | 0.75 | Spain | - | 62 | 0.65 |
| Argentina | 53 | 45 | 0.40 | Norway | 70 | 84 | 0.97 |
| Brazil | 63 | 35 | 0.25 | Malawi | - | 31 | 0.19 |
| Guinea | 77 | 29 | 0.16 | Solomon Islands | - | 42 | 0.35 |
| Canada | 72 | 77 | 0.87 | Guatemala | 36 | 26 | 0.12 |
| Côte d'Ivoire | - | 35 | 0.25 | Colombia | 58 | 37 | 0.28 |
| Russia | - | 28 | 0.15 | Greece | - | 48 | 0.44 |
| Puerto Rico | - | 69 | 0.75 | Dominican Rep. | 36 | 28 | 0.15 |
| Turkey | 82 | 39 | 0.31 | Kazakhstan | - | 34 | 0.24 |
| Albania | - | 35 | 0.25 | Madagascar | - | 24 | 0.09 |
| Serbia | - | 39 | 0.31 | Cuba | - | 48 | 0.44 |
| Kosovo | - | 36 | 0.26 | India | - | 41 | 0.34 |
| Oman | - | 52 | 0.50 | Morocco | - | 44 | 0.38 |
| Togo | - | 29 | 0.16 | Cameroon | - | 25 | 0.10 |
| Poland | - | 58 | 0.59 | Ethiopia | - | 37 | 0.28 |
| Botswana | 63 | 61 | 0.63 | Sweden | 82 | 85 | 0.99 |
| Finland | 92 | 86 | 1.00 | South Africa | 65 | 44 | 0.38 |
| China | - | 41 | 0.34 | Int'l waters | - | 18 | 0.00 |

Appendix J: Price sub model input and data sources

Table J1: values and data sources used for the constants and lookups in the price sub model. A range is included and a row is highlighted yellow if uncertainty is assessed for a specific variable. Dmnl = dimensionless.

| Element | Unit | Type | Min | Max | Explanation/assumptions | Source |
|--|-------------------|----------|------------------------|-----|--|-------------------------|
| <i>Ore grade data</i> | | | | | | |
| Project ore type | Dmnl | Constant | Either a 1 or a 0 | | Indicates which ore type is used by a certain project | Mudd (2020) |
| Average nickel ore grade | Dmnl | Constant | Values in the database | | Ore grade was reported for reserves and for reserves and resources combined. The latter was assumed to apply to resources, which was assumed to work as a rough estimation but is not that accurate because it also contains the influence of the reserves. In future research this data could be manipulated in such a way that the ore grade for only resources is obtained, but this was not done here due to time constraints. | Mudd (2020) |
| Average by-product ore grade | | | | | | |
| Power for ore grades | Dmnl | Constant | 0.1 | 0.5 | Determines how quickly average ore grade declines. Van der Linden (2020) used a range between 0.38 and 0.42 | Assumption |
| <i>Cost data</i> | | | | | | |
| Fuel demand for mining, milling and beneficiation | GJ/ tonne ore | Constant | See table I1 | | Fuel or electricity demand for different mine types per tonne of ore. The lower the ore grade, the higher the energy demand | See table I1 |
| Fuel demand for ore transport | | | | | | |
| Electricity demand for mining, milling and beneficiation | | | | | | |
| Fuel demand for primary extraction | GJ/ tonne product | Constant | See table I1 | | Fuel or electricity demand for different processing methods per tonne of product. Depending on the processing energy allocation method this is equal to energy demand per tonne of nickel or it has to be divided by the nickel content of the product first. | See table I1 |
| Fuel demand for product transport | | | | | | |
| Electricity demand for primary extraction | | | | | | |
| Average nickel content of products | Dmnl | Constant | See table I2 | | Indicates the percentage of a certain product consisting of nickel. | See table I2 |
| Fuel demand for refining | GJ/ tonne | Constant | See table I1 | | Fuel or electricity demand for different refining methods per tonne of product. | See table I1 |
| Fuel demand for nickel transport | | | | | | |
| Electricity demand for refining | | | | | | |
| Autonomous specific energy consumption | Dmnl | Constant | 0.1 | | Efficiency improvements due to innovation. Rule of thumb value. In future research a more exact industry value can be found based on past developments. | Blok & Nieuwlaar (2021) |

| | | | | | | |
|---|----------------|----------|------------------------|---|--|------------|
| Initial fuel price | \$/GJ | Constant | 4 | Based on the average price for different types of coal, oil and natural gas covered by BP (2019). In 2005 \$. | BP (2019) | |
| Energy price scenario high | 1/Year | Lookup | See figure I4 | Three energy price scenarios, high, mid and low based on assumptions on how the energy price may change over time. Historic values up to 2018 from BP (2019). Behaviour adapted from Van der Linden (2020) | BP (2019); Van der Linden (2020) | |
| Energy price scenario mid | | | | | | |
| Energy price scenario low | | | | | | |
| Intercept electricity price function | \$/GJ | Constant | 15.805 | Linear formula based on a renewable energy share of 22.8% (REN21, 2015) and a difference of 11 \$/GJ between electricity and fuel price in 2015 (BP, 2019; EIA, 2020b) and a difference of 0 \$/GJ by the time the renewable energy share becomes 75% | Assumption | |
| Slope electricity price function | \$/GJ | Constant | -21.073 | | | |
| Royalty as a percentage of sales | Dmnl | Constant | See table I8 | Royalties were gathered from various data sources. When the type of royalty was unclear, it was assumed to be as a percentage of sales. Royalties for countries for which data could not be found were based on those of nearby countries. | See table I8 | |
| Override based on initial runs | \$/tonne | Constant | 4750 | Average value for reagents and other marginal costs based on initial runs. | See appendix I1.6 | |
| Carbon price | \$/tonne CO2eq | Lookup | Selected SSP scenarios | All included SSP scenarios have a certain carbon price (tax) except SSP2-baseline. | IIASA (2018) | |
| Regional renewable energy share | Dmnl | Lookup | Selected SSP scenarios | Based on the share of renewable energy in total electricity supply for the regions included in the SSP database | IIASA (2018) | |
| Coefficient capital costs | \$ | Constant | 41.238E6 | Variables used in the formula that relates capacity and capital costs for HPAL. Determined based on Dry (2013) | Dry (2013) | |
| Exponent capital costs | Dmnl | Constant | 1.0508 | | | |
| Additional expenses for DSM | Dmnl | Constant | 2 | 20 | DSM is assumed to be 2 - 20 times more expensive than ordinary mining. This is a highly uncertain assumption and more research is required to better represent DSM in the model. | Assumption |
| <i>Alternative energy calculation methods</i> | | | | | | |
| Power for nickel ore grade [sulfides] | Dmnl | Constant | -0.844; -0.67 | Variables used in the formulas that relate ore grade to energy use for the mining of sulfides and laterites. The first value is for Elshkaki et al. (2017), the second value is for Valero et al. (2013). For the formula by Elshkaki et al. (2017) uses a percentage as input for ore grade. The formula by Valero et al. (2013) was assumed to use a fraction as input for ore grade. | (Elshkaki et al., 2017; Valero et al., 2013) | |
| Power for nickel ore grade [laterites] | Dmnl | Constant | -0.607; -0.5 | | | |
| Coefficient for nickel energy use [sulfides] | GJ/tonne | Constant | 199.51; 17 | | | |
| Coefficient for nickel energy use [laterites] | GJ/tonne | Constant | 169.53; 2.1 | | | |

| | | | | | |
|---|---------------------|----------|-------------------|--|--------------------------------------|
| Processing fraction | Dmnl | Constant | 0.6 | Represents the fraction of the total energy use for mining and processing for processing. This is an assumption based on getting average final energy use close to calculation method 1. This variable is relevant when assessing mining and processing separately. However, it also influences the fraction of energy from electricity or from fuels based on the processing method. In reality the processing method would impact this fraction, but this is not included. | Assumption |
| <i>By-product and allocation data</i> | | | | | |
| Initial by-product price | \$/tonne by-product | Constant | See table I9 | Based on three-year average prices between 2015 and 2017. In 2005 \$. | See table I9 |
| Initial average ore grade by-products | Dmnl | Constant | See table I9 | Initial average ore grade of by-products | See table I9 |
| Power for by-product ore grades | Dmnl | Constant | See table I9 | Variables used in the formula that relates ore grade to energy use for the mining of different by-products | See table I9 |
| Coefficient for by-product energy use | Dmnl | Constant | See table I9 | | See table I9 |
| Average concentration by-products in Earth's crust | Dmnl | Constant | See table I9 | Average concentration of by-products in Earth's crust | See table I9 |
| Average concentration by-products in refined products | Dmnl | Constant | See table I9 | Average concentration of by-products in refined products | See table I9 |
| Average concentration nickel in Earth's crust | Dmnl | Constant | See table I9 | Average concentration of nickel in Earth's crust | See table I9 |
| Reference temperature | Kelvin | Constant | 298.15 | Reference temperature | Valero et al. (2015) |
| Universal gas constant | kJ/kmol Kelvin | Constant | 8.314 | Universal gas constant | |
| Projects with platinum as main product | Dmnl | Constant | Either a 1 or a 0 | Assumption, based on project name and/or company name in the database by Mudd (2020). | Mudd (2020) |
| <i>Nickel price data</i> | | | | | |
| Initial nickel price | \$/tonne | Constant | 8194 | Based on three-year average prices between 2015 and 2017. In 2005 \$. | Nickel Institute (2020) |
| Price averaging period | Year | Constant | 0.25 | Assumption by Van der Linden (2020) who used a range between 0.1 and 0.4. | Van der Linden (2020) |
| Percentage cost on top of marginal cost | Dmnl | Constant | 0.1 | Van der Linden (2020) used a range between 0.05 and 0.25 | Auping (2011); Van der Linden (2020) |

| | | | | | | |
|---|------|----------|---------------|--|--|------------|
| Exponent nickel price curve | Dmnl | Constant | -1 | Based on the model by Van der Linden (2020). In her thesis she mentions values between -0.85 and -0.65 and in her code, she mentions values between -0.95 and -0.85. However, -1 seems to lead to a reasonable price that is similar to the price calculated based on availability and consumption, so this is used. | Van der Linden (2020) | |
| Marginal cost bottom price relationship | Dmnl | Constant | 0.05 | Based on the model by Van der Linden (2020). In her thesis she mentions values between 0.3 and 0.36 and in her code, she mentions values between 0.08 and 0.12. However, 0.05 seems to lead to a reasonable price that is similar to the price calculated based on availability and consumption, so this is used. | Van der Linden (2020) | |
| Inflation | Dmnl | Constant | 1.3327 | Percentage increase of 2020 \$ compared to 2005 \$ | Inflation calculator | |
| <i>Profit data</i> | | | | | | |
| Long forecasting period | Year | Constant | 2 | Van der Linden (2020) assumed a value that is twice as much as the short forecasting period. | Auping (2011); Van der Linden (2020) | |
| Short forecasting period | Year | Constant | 1 | Van der Linden (2020) assumed a range between 0.5 and 2. | | |
| Averaging time | Year | Constant | 3 | The time over which the price is averaged to determine the investment price premise. | Assumption | |
| Nickel taxes | Dmnl | Constant | 0.3 | Tax on profit, applied equally to all countries. | PWC (2012) | |
| Minimum profit over investment | Dmnl | Constant | 1.2 | 2 | This variable determines the minimum profit over investment mining companies want to make to go forward with investment. | Assumption |
| Initial long-term profit forecast | Dmnl | Constant | 0; 0.5 | Van der Linden (2020) used 0. Here developing and operating mines were assumed to have a value of 0.5, because they had to have been profitable initially to be approved, and the rest were given a value of 0. | Assumption | |
| Long-term profit forecasting period | Year | Constant | 2 | See the model for its use. | Van der Linden (2020) | |
| <i>Investment attractiveness data</i> | | | | | | |
| Investment attractiveness | Dmnl | Constant | See table I10 | Normalised corruption perception score. | See table I10 | |
| Averaging period | Year | Constant | 1 | The time over which profit adjusted investment attractiveness is averaged to determine the final ranking. | Assumption | |

Appendix K: Background, assumptions & data: impacts

This appendix contains background information that can be consulted to provide some more context for the concepts related to the sustainability impacts discussed in the main text. Assumptions are also explained and values used in the model are shown.

Multiple nickel LCAs, including various impact categories, were assessed. Due to a lack of data for all processing methods from a single source, the same method as used for determining final fuel and electricity requirements was used for obtaining LCA estimates. Although different sources did cover multiple impact categories, there was only a consistent match between sources for Global Warming Potential (GWP) for all processing methods and electricity generation technologies. Therefore, only GWP was assessed in this thesis. However, once more detailed data becomes available for the other impact categories, this can be plugged into the model in the future.

Although life cycle emissions are not solely based on processing technology (there could also be country specific factors for example), processing technology is assumed to have the greatest contribution, and life cycle emissions are therefore distinguished based on this.

PED is also an impact category that is often assessed. However, in this thesis, only final energy use, excluding non-energy use, is included because this was easier to include for a dynamic energy mix. However, in future adaptations of the model, non-energy use can be included and final energy use could be converted into PED by adding (dynamic) conversion efficiencies for electricity generation technologies.

Appendix K1: Greenhouse gas emissions

The LCA by the Nickel Institute (2020) was used as the basis for determining GWP. They provided data for class I nickel and for ferronickel. Other sources that were used include Norgate & Jahanshahi (2011), Wang et al. (2015) and Khoo et al. (2017). Table K1 shows the GWP of the different processing methods included by these sources, as well as the estimated values used in this thesis.

This estimation was done as follows. First, the value of 45 kg CO₂eq/kg nickel for ferronickel production based on Nickel Institute (2020) was used for RKEF. Next, the value of 13 kg CO₂eq/kg nickel for class I nickel production based on Nickel Institute (2020) was converted to a value for HPAL (24 kg CO₂eq/kg nickel) and a value for PM sulfide production (9 kg CO₂eq/kg nickel) based on the statement by Nickel Institute (2020) that 27% of class I nickel came from HPAL in their calculations and the rest from PM sulfide production.

Wang et al. (2015) were the only source that included pig iron production and, since their value for RKEF was exactly the same as the value for Nickel Institute (2020), their value for pig iron production of 41 kg CO₂eq/kg nickel was used for BFs.

Norgate & Jahanshahi (2011) were the only source including the Caron process and HL. They used mass-based allocation. Assuming 77% nickel in the product created by the Caron process (see table I2), Caron was estimated to be about 2.5 times more CO₂ intensive than HPAL. HL was estimated to be about 0.78 times as CO₂ intensive as HPAL. Using the HPAL value determined based on Nickel Institute (2020), this led to estimated values of 19 kg CO₂eq/kg nickel for HL and 60 kg CO₂eq/kg nickel for Caron.

Norgate & Jahanshahi (2011) also reported a value for ATL that was 0.65 times as CO₂ intensive as HPAL and Wang et al. (2015) reported a value for ATL that was 0.4 times as CO₂ intensive as RKEF. On average this leads to a value for ATL of 16 kg CO₂eq/kg nickel.

Khoo et al. (2017) provided data for the GWP of stainless-steel production for HPAL, RKEF and DNI (1.09 times the value for HPAL). Even though this is for stainless steel, the relative values were assumed to be similar to relative values for nickel only, and based on this, a value of 26 kg CO₂eq/kg nickel was calculated for DNI.

Table K1: GWP of nickel processing technologies for the current electricity mix. In brackets, the relative GWP compared to one of the other processing technologies reported by a certain source is shown. These relative values are used to determine the final estimated values used in this thesis.

| Process | Nickel Institute (2020) | Norgate & Jahanshahi (2011) | Wang et al. (2015) | Khoo et al. (2017) | Estimated values |
|------------|--|--|--|--|--|
| | Kg CO ₂ eq./kg Ni (full allocation to nickel) | Kg CO ₂ eq./kg Ni (mass based allocation) | Kg CO ₂ eq./kg Ni (assumed full allocation to nickel) | Kg CO ₂ eq./kg Ni in stainless steel* | Kg CO ₂ eq./kg Ni (full allocation to nickel) |
| Class 1 | 13 (27% HPAL, 73% PM sulfide) | | | | |
| PM sulfide | | | | | 9 |
| HPAL | | 23 | | 79 (0.53 * RKEF) | 24 |
| HL | | 18 (0.78 x HPAL) | | | 19 |
| ATL | | 15 (0.65 x HPAL) | 18 (0.4 x RKEF) | | 16 |
| DNI | | | | 86 (1.09 x HPAL) | 26 |
| Caron | | 45** | | | 60 |
| RKEF*** | 45 (3.46 x Class 1) | 23** | 45 (2.5 x ATL) | 150 (1.89 x HPAL) | 45 |
| BF*** | | | 41 (0.91 x RKEF) | | 41 |

*Because this is in stainless steel the values are much higher than for just nickel.

**It is unclear what Norgate & Jahanshahi assumed as the percentage of nickel in the products from these processes. Based on the range of 15 - 45% for RKEF (see table I2) the value could be 51 - 153 kg CO₂eq/kg nickel. The lower end of this range is assumed. Based on 77% for Caron, the value could be 58 kg CO₂eq/kg nickel (2.5 x HPAL).

***Reported as ferronickel and pig iron for RKEF and BF respectively.

In this thesis, a distinction was made between LCA results for electricity generation and for other processes. This is because the other processes were assumed to remain relatively constant, but, because of the ET, the electricity generation mix will become significantly different in the future and so will its impacts. The fuel mix used on-site may also become different (by switching to more biofuels and hydrogen, etc.), however this was not fully considered. This is something that could be included in future adaptations of the model.

Nickel Institute (2020) indicated the percentage of the GWP caused by electricity generation. This includes electricity generation off-site and electricity generation on-site. Both were included as electricity generation, even though in the case of electricity generation on-site, the energy is delivered as a fuel. This was done to also partially reflect fuels becoming more renewable over time. However, this may have led to less consistency with other sources.

Table K2 shows the estimated contribution of electricity to GWP for the different processing methods and the final values used for GWP excluding electricity. These values were estimated as follows. First, the value of 47% for ferronickel production provided by Nickel Institute (2020) was used for RKEF. Next, the values for HPAL and PM sulfide production were determined based on the value of 32% for class I nickel provided by Nickel Institute (2020).

This was done by first taking the 13 kg CO₂eq/kg nickel from table K1 and multiplying it by 0.32 to obtain 4 kg CO₂eq/kg nickel that could be attributed to electricity and 9 kg CO₂eq/kg nickel that could be attributed to other factors. Then the 27% and 73% shares for HPAL and PM sulfide processing were used, in combination with a processing electricity use for PM sulfide processing that is 1.7 times the processing electricity use for HPAL, to determine that 2.65 kg CO₂eq/kg nickel could be attributed to electricity for HPAL and 4.5 kg CO₂eq/kg nickel could be attributed to PM sulfide processing, thereby leading to 11% and 50% contribution of electricity to GWP respectively, based on the estimated values in table K1.

Next, the values for HL, ATL and DNI were determined by relating the electricity use for these processes to the electricity use for HPAL. To illustrate for HL, the relative electricity use compared to HPAL (0.89) was multiplied by 2.65 kg CO₂eq/kg nickel and the subsequent value was divided by the estimated value for HL in table K1, leading to a 12% contribution of electricity to GWP.

The values for Caron and BF were determined by relating the electricity use for these processes to the electricity use for RKEF. The values for electricity use for these processes were first converted to values in terms of a full allocation to nickel by dividing the values obtained from table I1 by the values in table I2. The final values used for GWP excluding electricity were determined by multiplying the contribution of electricity to GWP by the estimated values in table I1 and then subtracting the subsequent values from the values in table I1.

Table K2: contribution of electricity to the GWP of nickel processing technologies and final values used for GWP (in kg CO₂ eq./kg Ni) excluding electricity in the model.

| Process | Contribution of electricity to GWP (Nickel Institute, 2020) | Electricity use (GJ/tonne Ni)* | Estimated Contribution of electricity to GWP | Final values used for GWP excl. electricity |
|------------|---|--------------------------------|--|---|
| Class 1 | 32% | | | |
| PM sulfide | | 31 (1.7x HPAL) | 50% | 5 |
| HPAL | | 18 | 11% | 21 |
| HL | | 16 (0.89 x HPAL) | 12% | 17 |
| ATL | | 14 (0.78 x HPAL) | 13% | 14 |
| DNI | | 17 (0.94 x HPAL) | 9% | 24 |
| Caron | | 29 (0.31 x RKEF) | 11% | 52 |
| RKEF*** | 47% | 93 | 47% | 24 |
| BF*** | | 40 (0.43 x RKEF) | 22% | 32 |

* Electricity use for smelting and refining (see table I1), as electricity use for mining was assumed to be equal for each processing method. Electricity use for HPAL, HL, ATL and DNI is very uncertain because it is based on relative PED compared to other processes and not specifically on relative electricity requirements

Table K3 shows the GWP for electricity generation technologies with and without CCS. The main sources used to determine these values are Hertwich et al. (2015) and Asdrubali et al. (2015), supplemented by Turconi et al. (2013) for oil and nuclear, Pehl et al. (2017) for biomass and Amponsah et al. (2014) for ocean energy. The value for oil + CCS was calculated as the average of coal + CCS and natural gas + CCS.

Table K3: GWP for electricity generation technologies. The cells containing the values that were used, are highlighted in yellow. In some cases, a single source was used, in other cases average values were used. Values are in kg CO₂eq/MWh except for the final column.

| Technology | Turconi et al. (2013) | Amponsah et al. (2014) | Hertwich et al. (2015) | Asdrubali et al. (2015) | Pehl et al. (2017) | Final value (tonne CO ₂ eq/GJ) |
|---------------|-----------------------|------------------------|------------------------|-------------------------|--------------------|---|
| Biomass | 51 | | | | 98 | 0.027 |
| Biomass + CCS | | | | | -312 | -0.087 |
| Coal | 924 | | 864 | 900 | | 0.24 |
| Coal + CCS | | | 233 | | 109 | 0.065 |
| Oil | 774 | | | | | 0.22 |
| Oil + CCS | | | | | | 0.067 |
| Natural gas | 533 | | 527 | 375 | | 0.15 |
| Gas + CCS | | | 247 | | 78 | 0.069 |
| Geothermal | | 32 | | 34 | | 0.0094 |
| Hydro | 8 | 25 | 42 | 12 | 97 | 0.0075 |
| Nuclear | 12 | | | | 4 | 0.0033 |
| Ocean | | 19 | | | | 0.0053 |
| Solar | 65 | 86 | 31 | 30 | 9 | 0.0086 |
| Wind | 18 | 17 | 10 | 9 | 4 | 0.0028 |

The GWP calculated in the model is the result cradle to gate life cycle emissions for nickel. It does not include any impacts of manufacturing stainless steel, batteries and other products, and also no emissions due to waste management.

To take into account innovation, a factor for carbon intensity improvement was also included in the model. The processing energy allocation method was also taken into account. In addition, a rough estimate for by-product processing emissions was based on the GWP for nickel and so was an estimate for the emissions for substitutes.

The estimated values in table K1 are based on the current average ore grade. However, as ore grade decreases, energy requirements and thereby GHG emissions increase. Because of this, some of the deposits in the database by Mudd (2020) lead to much higher GHG emissions, because of their lower ore grade. However, changing ore grade is only considered for the GWP due to electricity, even though this will likely also lead to increased fuel and reagent requirements, thereby impacting the GWP excluding electricity. This is something that could be improved in future adaptations of the model.

Appendix K2: SSP regional data

Tables K4 - K7 show the electricity mix for different regions per SSP (IIASA, 2018). The sums of the renewable energy technologies in these tables lead to the values in the tables in appendix I1.4. Unlike the global SSP data (appendix D1.1), totals were calculated instead of taken from the database to determine the shares, due to slight rounding discrepancies. This means the electricity mix share does not contain any geothermal or ocean energy in scenarios where there was no data for those, making it slightly different than what is indicated in appendix D1.1.

In the tables below, the fraction of an energy source + CCS refers to the fraction of that energy source, not the fraction of total electricity generation. To determine the fraction of oil with CCS, average values for biomass with CCS, coal with CCS and natural gas with CCS were used. For electricity generation, no distinction was made between PV and CSP in the database by IIASA (2018), so all solar energy was considered as PV.

Table K4: electricity mix per region for SSP1-19. Global is used for international waters.

| Electricity mix OECD SSP1 RCP 1.9 | 2005 | 2010 | 2020 | 2030 | 2040 | 2050 | 2060 | 2070 | 2080 | 2090 | 2100 |
|-----------------------------------|-------|-------|-------|-------|-------|-------|-------|-------|-------|-------|-------|
| Biomass share | 0.019 | 0.026 | 0.033 | 0.078 | 0.097 | 0.076 | 0.092 | 0.126 | 0.138 | 0.136 | 0.143 |
| Coal share | 0.381 | 0.346 | 0.255 | 0.036 | 0.031 | 0.015 | 0.014 | 0.017 | 0.016 | 0.012 | 0.011 |
| Oil share | 0.047 | 0.025 | 0.015 | 0.063 | 0.009 | 0.001 | 0.001 | 0.001 | 0.000 | 0.000 | 0.000 |
| Gas share | 0.190 | 0.227 | 0.209 | 0.214 | 0.090 | 0.044 | 0.067 | 0.111 | 0.115 | 0.050 | 0.049 |
| Geothermal share | 0.000 | 0.000 | 0.000 | 0.000 | 0.000 | 0.000 | 0.000 | 0.000 | 0.000 | 0.000 | 0.000 |
| Hydro share | 0.130 | 0.134 | 0.144 | 0.169 | 0.201 | 0.120 | 0.093 | 0.115 | 0.121 | 0.115 | 0.118 |
| Nuclear share | 0.222 | 0.213 | 0.218 | 0.263 | 0.154 | 0.022 | 0.009 | 0.005 | 0.001 | 0.001 | 0.001 |
| Ocean share | 0.000 | 0.000 | 0.000 | 0.000 | 0.000 | 0.000 | 0.000 | 0.000 | 0.000 | 0.000 | 0.000 |
| Solar share | 0.000 | 0.003 | 0.038 | 0.065 | 0.164 | 0.245 | 0.307 | 0.376 | 0.378 | 0.355 | 0.360 |
| Wind share | 0.009 | 0.026 | 0.088 | 0.112 | 0.254 | 0.477 | 0.417 | 0.250 | 0.230 | 0.330 | 0.318 |
| Fraction of bio + CCS | 0.000 | 0.000 | 0.000 | 0.088 | 0.915 | 0.969 | 0.996 | 1.000 | 1.000 | 1.000 | 1.000 |
| Fraction of coal + CCS | 0.000 | 0.000 | 0.000 | 0.009 | 0.164 | 0.745 | 0.998 | 1.000 | 1.000 | 1.000 | 1.000 |
| Fraction of gas + CCS | 0.000 | 0.000 | 0.013 | 0.034 | 0.326 | 0.875 | 0.990 | 0.952 | 0.907 | 0.936 | 0.750 |
| Fraction of oil + CCS | 0.000 | 0.000 | 0.004 | 0.044 | 0.468 | 0.863 | 0.995 | 0.984 | 0.969 | 0.979 | 0.917 |
| Total renewable share | 0.159 | 0.189 | 0.303 | 0.424 | 0.715 | 0.917 | 0.909 | 0.867 | 0.867 | 0.936 | 0.939 |
| Electricity mix REF SSP1 RCP 1.9 | 2005 | 2010 | 2020 | 2030 | 2040 | 2050 | 2060 | 2070 | 2080 | 2090 | 2100 |
| Biomass share | 0.002 | 0.002 | 0.012 | 0.071 | 0.135 | 0.354 | 0.597 | 0.681 | 0.723 | 0.681 | 0.769 |
| Coal share | 0.171 | 0.189 | 0.163 | 0.124 | 0.062 | 0.038 | 0.008 | 0.006 | 0.005 | 0.005 | 0.001 |
| Oil share | 0.027 | 0.013 | 0.023 | 0.008 | 0.004 | 0.004 | 0.000 | 0.000 | 0.000 | 0.000 | 0.000 |
| Gas share | 0.408 | 0.432 | 0.440 | 0.362 | 0.345 | 0.155 | 0.040 | 0.027 | 0.005 | 0.010 | 0.000 |
| Geothermal share | 0.000 | 0.000 | 0.000 | 0.000 | 0.000 | 0.000 | 0.000 | 0.000 | 0.000 | 0.000 | 0.000 |
| Hydro share | 0.197 | 0.175 | 0.188 | 0.203 | 0.216 | 0.310 | 0.273 | 0.254 | 0.259 | 0.301 | 0.225 |
| Nuclear share | 0.195 | 0.190 | 0.167 | 0.216 | 0.180 | 0.069 | 0.025 | 0.010 | 0.000 | 0.000 | 0.000 |
| Ocean share | 0.000 | 0.000 | 0.000 | 0.000 | 0.000 | 0.000 | 0.000 | 0.000 | 0.000 | 0.000 | 0.000 |
| Solar share | 0.000 | 0.000 | 0.002 | 0.005 | 0.013 | 0.025 | 0.031 | 0.020 | 0.007 | 0.001 | 0.001 |
| Wind share | 0.000 | 0.000 | 0.005 | 0.011 | 0.045 | 0.046 | 0.025 | 0.002 | 0.001 | 0.002 | 0.003 |
| Fraction of bio + CCS | 0.000 | 0.000 | 0.000 | 0.543 | 0.838 | 0.951 | 0.996 | 1.000 | 1.000 | 1.000 | 1.000 |
| Fraction of coal + CCS | 0.000 | 0.000 | 0.006 | 0.044 | 0.109 | 0.216 | 1.000 | 1.000 | 1.000 | 1.000 | 1.000 |
| Fraction of gas + CCS | 0.000 | 0.000 | 0.010 | 0.063 | 0.219 | 0.185 | 0.411 | 0.581 | 0.381 | 0.260 | 0.000 |
| Fraction of oil + CCS | 0.000 | 0.000 | 0.005 | 0.217 | 0.389 | 0.450 | 0.802 | 0.860 | 0.794 | 0.753 | 0.667 |
| Total renewable share | 0.199 | 0.177 | 0.208 | 0.290 | 0.409 | 0.735 | 0.926 | 0.958 | 0.990 | 0.985 | 0.999 |
| Electricity mix Asia SSP1 RCP 1.9 | 2005 | 2010 | 2020 | 2030 | 2040 | 2050 | 2060 | 2070 | 2080 | 2090 | 2100 |
| Biomass share | 0.004 | 0.009 | 0.018 | 0.054 | 0.059 | 0.050 | 0.051 | 0.062 | 0.069 | 0.074 | 0.099 |
| Coal share | 0.637 | 0.658 | 0.476 | 0.204 | 0.027 | 0.038 | 0.053 | 0.070 | 0.062 | 0.042 | 0.021 |
| Oil share | 0.051 | 0.025 | 0.008 | 0.029 | 0.001 | 0.000 | 0.000 | 0.000 | 0.001 | 0.001 | 0.000 |
| Gas share | 0.111 | 0.110 | 0.237 | 0.379 | 0.154 | 0.106 | 0.124 | 0.168 | 0.127 | 0.070 | 0.046 |
| Geothermal share | 0.000 | 0.000 | 0.000 | 0.000 | 0.000 | 0.000 | 0.000 | 0.000 | 0.000 | 0.000 | 0.000 |
| Hydro share | 0.138 | 0.144 | 0.169 | 0.198 | 0.182 | 0.139 | 0.123 | 0.115 | 0.112 | 0.116 | 0.123 |
| Nuclear share | 0.057 | 0.043 | 0.046 | 0.053 | 0.055 | 0.041 | 0.037 | 0.041 | 0.052 | 0.066 | 0.067 |
| Ocean share | 0.000 | 0.000 | 0.000 | 0.000 | 0.000 | 0.000 | 0.000 | 0.000 | 0.000 | 0.000 | 0.000 |
| Solar share | 0.000 | 0.000 | 0.011 | 0.030 | 0.395 | 0.478 | 0.485 | 0.449 | 0.473 | 0.523 | 0.541 |
| Wind share | 0.002 | 0.010 | 0.036 | 0.052 | 0.127 | 0.149 | 0.127 | 0.096 | 0.105 | 0.109 | 0.102 |
| Fraction of bio + CCS | 0.000 | 0.000 | 0.000 | 0.391 | 0.991 | 0.995 | 1.000 | 1.000 | 1.000 | 0.999 | 0.999 |
| Fraction of coal + CCS | 0.000 | 0.000 | 0.000 | 0.004 | 0.868 | 0.987 | 1.000 | 1.000 | 1.000 | 1.000 | 1.000 |
| Fraction of gas + CCS | 0.000 | 0.000 | 0.008 | 0.072 | 0.620 | 0.987 | 1.000 | 0.984 | 0.978 | 0.960 | 0.907 |
| Fraction of oil + CCS | 0.000 | 0.000 | 0.003 | 0.156 | 0.826 | 0.990 | 1.000 | 0.995 | 0.993 | 0.986 | 0.969 |
| Total renewable share | 0.143 | 0.163 | 0.234 | 0.334 | 0.763 | 0.815 | 0.786 | 0.721 | 0.758 | 0.821 | 0.866 |

| | | | | | | | | | | | |
|-------------------------------------|-------|-------|-------|-------|-------|-------|-------|-------|-------|-------|-------|
| Electricity mix MAF SSP1 RCP 1.9 | 2005 | 2010 | 2020 | 2030 | 2040 | 2050 | 2060 | 2070 | 2080 | 2090 | 2100 |
| Biomass share | 0.001 | 0.001 | 0.020 | 0.063 | 0.049 | 0.024 | 0.016 | 0.012 | 0.010 | 0.012 | 0.023 |
| Coal share | 0.239 | 0.190 | 0.175 | 0.023 | 0.004 | 0.002 | 0.002 | 0.001 | 0.001 | 0.001 | 0.000 |
| Oil share | 0.210 | 0.221 | 0.219 | 0.207 | 0.004 | 0.000 | 0.001 | 0.000 | 0.000 | 0.000 | 0.000 |
| Gas share | 0.440 | 0.494 | 0.446 | 0.450 | 0.256 | 0.135 | 0.112 | 0.106 | 0.084 | 0.084 | 0.079 |
| Geothermal share | 0.000 | 0.000 | 0.000 | 0.000 | 0.000 | 0.000 | 0.000 | 0.000 | 0.000 | 0.000 | 0.000 |
| Hydro share | 0.099 | 0.084 | 0.107 | 0.168 | 0.132 | 0.079 | 0.052 | 0.036 | 0.034 | 0.033 | 0.033 |
| Nuclear share | 0.010 | 0.008 | 0.014 | 0.019 | 0.016 | 0.007 | 0.004 | 0.003 | 0.002 | 0.001 | 0.001 |
| Ocean share | 0.000 | 0.000 | 0.000 | 0.000 | 0.000 | 0.000 | 0.000 | 0.000 | 0.000 | 0.000 | 0.000 |
| Solar share | 0.000 | 0.000 | 0.010 | 0.035 | 0.383 | 0.619 | 0.711 | 0.754 | 0.786 | 0.788 | 0.792 |
| Wind share | 0.001 | 0.002 | 0.010 | 0.036 | 0.156 | 0.134 | 0.103 | 0.087 | 0.083 | 0.081 | 0.072 |
| Fraction of bio + CCS | 0.000 | 0.000 | 0.000 | 0.568 | 0.998 | 1.000 | 1.000 | 1.000 | 1.000 | 1.000 | 1.000 |
| Fraction of coal + CCS | 0.000 | 0.000 | 0.000 | 0.006 | 0.925 | 1.000 | 1.000 | 1.000 | 1.000 | 1.000 | 1.000 |
| Fraction of gas + CCS | 0.000 | 0.000 | 0.003 | 0.078 | 0.697 | 0.976 | 0.995 | 0.984 | 0.977 | 0.946 | 0.867 |
| Fraction of oil + CCS | 0.000 | 0.000 | 0.001 | 0.218 | 0.873 | 0.992 | 0.998 | 0.995 | 0.992 | 0.982 | 0.956 |
| Total renewable share | 0.101 | 0.087 | 0.146 | 0.301 | 0.721 | 0.856 | 0.881 | 0.889 | 0.913 | 0.914 | 0.920 |
| Electricity mix LAM SSP1 RCP 1.9 | 2005 | 2010 | 2020 | 2030 | 2040 | 2050 | 2060 | 2070 | 2080 | 2090 | 2100 |
| Biomass share | 0.006 | 0.009 | 0.029 | 0.043 | 0.043 | 0.028 | 0.024 | 0.023 | 0.024 | 0.029 | 0.035 |
| Coal share | 0.047 | 0.049 | 0.106 | 0.002 | 0.008 | 0.002 | 0.006 | 0.008 | 0.009 | 0.006 | 0.003 |
| Oil share | 0.158 | 0.137 | 0.031 | 0.047 | 0.000 | 0.000 | 0.000 | 0.000 | 0.000 | 0.000 | 0.000 |
| Gas share | 0.195 | 0.234 | 0.208 | 0.196 | 0.123 | 0.063 | 0.048 | 0.074 | 0.076 | 0.048 | 0.029 |
| Geothermal share | 0.000 | 0.000 | 0.000 | 0.000 | 0.000 | 0.000 | 0.000 | 0.000 | 0.000 | 0.000 | 0.000 |
| Hydro share | 0.569 | 0.547 | 0.576 | 0.636 | 0.541 | 0.343 | 0.252 | 0.259 | 0.292 | 0.307 | 0.379 |
| Nuclear share | 0.024 | 0.021 | 0.019 | 0.017 | 0.012 | 0.004 | 0.002 | 0.001 | 0.001 | 0.001 | 0.000 |
| Ocean share | 0.000 | 0.000 | 0.000 | 0.000 | 0.000 | 0.000 | 0.000 | 0.000 | 0.000 | 0.000 | 0.000 |
| Solar share | 0.000 | 0.000 | 0.003 | 0.007 | 0.081 | 0.294 | 0.423 | 0.434 | 0.433 | 0.442 | 0.369 |
| Wind share | 0.000 | 0.004 | 0.028 | 0.052 | 0.192 | 0.265 | 0.244 | 0.201 | 0.165 | 0.168 | 0.185 |
| Fraction of bio + CCS | 0.000 | 0.000 | 0.034 | 0.273 | 0.997 | 1.000 | 1.000 | 1.000 | 1.000 | 1.000 | 1.000 |
| Fraction of coal + CCS | 0.000 | 0.000 | 0.000 | 0.000 | 0.169 | 1.000 | 1.000 | 1.000 | 1.000 | 1.000 | 1.000 |
| Fraction of gas + CCS | 0.000 | 0.000 | 0.032 | 0.125 | 0.443 | 0.778 | 0.881 | 0.927 | 0.888 | 0.893 | 0.897 |
| Fraction of oil + CCS | 0.000 | 0.000 | 0.022 | 0.133 | 0.536 | 0.926 | 0.960 | 0.976 | 0.963 | 0.964 | 0.966 |
| Total renewable share | 0.576 | 0.559 | 0.636 | 0.738 | 0.857 | 0.930 | 0.944 | 0.916 | 0.914 | 0.945 | 0.968 |
| Electricity mix Global SSP1 RCP 1.9 | 2005 | 2010 | 2020 | 2030 | 2040 | 2050 | 2060 | 2070 | 2080 | 2090 | 2100 |
| Biomass share | 0.012 | 0.016 | 0.025 | 0.064 | 0.071 | 0.061 | 0.068 | 0.080 | 0.083 | 0.083 | 0.097 |
| Coal share | 0.400 | 0.406 | 0.319 | 0.107 | 0.026 | 0.023 | 0.028 | 0.035 | 0.030 | 0.020 | 0.011 |
| Oil share | 0.065 | 0.046 | 0.030 | 0.057 | 0.004 | 0.001 | 0.000 | 0.000 | 0.000 | 0.000 | 0.000 |
| Gas share | 0.202 | 0.223 | 0.252 | 0.308 | 0.152 | 0.090 | 0.097 | 0.128 | 0.106 | 0.066 | 0.054 |
| Geothermal share | 0.000 | 0.000 | 0.000 | 0.000 | 0.000 | 0.000 | 0.000 | 0.000 | 0.000 | 0.000 | 0.000 |
| Hydro share | 0.162 | 0.162 | 0.183 | 0.220 | 0.217 | 0.151 | 0.120 | 0.115 | 0.114 | 0.113 | 0.116 |
| Nuclear share | 0.153 | 0.130 | 0.119 | 0.134 | 0.081 | 0.028 | 0.020 | 0.019 | 0.022 | 0.027 | 0.026 |
| Ocean share | 0.000 | 0.000 | 0.000 | 0.000 | 0.000 | 0.000 | 0.000 | 0.000 | 0.000 | 0.000 | 0.000 |
| Solar share | 0.000 | 0.002 | 0.021 | 0.040 | 0.281 | 0.400 | 0.459 | 0.483 | 0.512 | 0.535 | 0.548 |
| Wind share | 0.006 | 0.016 | 0.053 | 0.071 | 0.169 | 0.247 | 0.208 | 0.139 | 0.133 | 0.156 | 0.148 |
| Fraction of bio + CCS | 0.000 | 0.000 | 0.003 | 0.272 | 0.949 | 0.978 | 0.998 | 1.000 | 1.000 | 1.000 | 1.000 |
| Fraction of coal + CCS | 0.000 | 0.000 | 0.000 | 0.007 | 0.515 | 0.903 | 1.000 | 1.000 | 1.000 | 1.000 | 1.000 |
| Fraction of gas + CCS | 0.000 | 0.000 | 0.011 | 0.065 | 0.530 | 0.912 | 0.984 | 0.972 | 0.953 | 0.944 | 0.856 |
| Fraction of oil + CCS | 0.000 | 0.000 | 0.005 | 0.115 | 0.665 | 0.931 | 0.994 | 0.991 | 0.984 | 0.981 | 0.952 |
| Total renewable share | 0.180 | 0.196 | 0.281 | 0.394 | 0.737 | 0.858 | 0.855 | 0.817 | 0.841 | 0.887 | 0.909 |

Table K5: electricity mix per region for SSP2-19. Global is used for international waters.

| | | | | | | | | | | | |
|-----------------------------------|-------|-------|-------|-------|-------|-------|-------|-------|-------|-------|-------|
| Electricity mix OECD SSP2 RCP 1.9 | 2005 | 2010 | 2020 | 2030 | 2040 | 2050 | 2060 | 2070 | 2080 | 2090 | 2100 |
| Biomass share | 0.011 | 0.012 | 0.013 | 0.001 | 0.002 | 0.005 | 0.011 | 0.013 | 0.012 | 0.013 | 0.013 |
| Coal share | 0.394 | 0.358 | 0.242 | 0.028 | 0.015 | 0.009 | 0.002 | 0.000 | 0.000 | 0.000 | 0.000 |
| Oil share | 0.042 | 0.015 | 0.004 | 0.002 | 0.000 | 0.000 | 0.000 | 0.000 | 0.000 | 0.000 | 0.000 |
| Gas share | 0.186 | 0.209 | 0.277 | 0.353 | 0.233 | 0.164 | 0.083 | 0.035 | 0.001 | 0.000 | 0.000 |
| Geothermal share | 0.003 | 0.004 | 0.004 | 0.013 | 0.037 | 0.042 | 0.042 | 0.044 | 0.043 | 0.041 | 0.041 |
| Hydro share | 0.132 | 0.140 | 0.130 | 0.137 | 0.121 | 0.095 | 0.073 | 0.066 | 0.064 | 0.063 | 0.063 |
| Nuclear share | 0.223 | 0.215 | 0.213 | 0.221 | 0.185 | 0.224 | 0.291 | 0.286 | 0.275 | 0.249 | 0.161 |
| Ocean share | 0.000 | 0.000 | 0.000 | 0.000 | 0.000 | 0.000 | 0.000 | 0.000 | 0.000 | 0.000 | 0.000 |
| Solar share | 0.000 | 0.006 | 0.023 | 0.052 | 0.091 | 0.133 | 0.158 | 0.184 | 0.183 | 0.188 | 0.220 |
| Wind share | 0.009 | 0.040 | 0.094 | 0.193 | 0.316 | 0.329 | 0.340 | 0.372 | 0.422 | 0.446 | 0.502 |
| Fraction of bio + CCS | 0.000 | 0.000 | 0.000 | 0.433 | 0.636 | 0.962 | 0.926 | 0.960 | 0.998 | 1.000 | 1.000 |
| Fraction of coal + CCS | 0.000 | 0.000 | 0.000 | 0.564 | 0.992 | 0.990 | 1.000 | 1.000 | 1.000 | 1.000 | 1.000 |
| Fraction of gas + CCS | 0.000 | 0.000 | 0.000 | 0.122 | 0.619 | 0.882 | 0.850 | 0.850 | 0.852 | 1.000 | 0.000 |
| Fraction of oil + CCS | 0.000 | 0.000 | 0.000 | 0.373 | 0.749 | 0.944 | 0.925 | 0.937 | 0.950 | 1.000 | 0.667 |
| Total renewable share | 0.155 | 0.203 | 0.263 | 0.396 | 0.567 | 0.603 | 0.624 | 0.679 | 0.725 | 0.751 | 0.839 |

| | | | | | | | | | | | |
|-----------------------------------|-------|-------|-------|-------|-------|-------|-------|-------|-------|-------|-------|
| Electricity mix REF SSP2 RCP 1.9 | 2005 | 2010 | 2020 | 2030 | 2040 | 2050 | 2060 | 2070 | 2080 | 2090 | 2100 |
| Biomass share | 0.001 | 0.000 | 0.000 | 0.000 | 0.005 | 0.016 | 0.017 | 0.011 | 0.011 | 0.013 | 0.008 |
| Coal share | 0.189 | 0.221 | 0.190 | 0.001 | 0.003 | 0.005 | 0.003 | 0.000 | 0.000 | 0.000 | 0.000 |
| Oil share | 0.037 | 0.019 | 0.000 | 0.000 | 0.000 | 0.000 | 0.000 | 0.000 | 0.000 | 0.000 | 0.000 |
| Gas share | 0.423 | 0.408 | 0.438 | 0.522 | 0.171 | 0.065 | 0.035 | 0.000 | 0.000 | 0.000 | 0.000 |
| Geothermal share | 0.000 | 0.000 | 0.000 | 0.000 | 0.000 | 0.000 | 0.000 | 0.000 | 0.008 | 0.008 | 0.015 |
| Hydro share | 0.195 | 0.189 | 0.169 | 0.210 | 0.390 | 0.342 | 0.388 | 0.420 | 0.439 | 0.434 | 0.395 |
| Nuclear share | 0.155 | 0.163 | 0.197 | 0.206 | 0.267 | 0.332 | 0.266 | 0.238 | 0.174 | 0.137 | 0.062 |
| Ocean share | 0.000 | 0.000 | 0.000 | 0.000 | 0.000 | 0.000 | 0.000 | 0.000 | 0.000 | 0.000 | 0.000 |
| Solar share | 0.000 | 0.000 | 0.000 | 0.006 | 0.017 | 0.030 | 0.045 | 0.072 | 0.121 | 0.164 | 0.205 |
| Wind share | 0.000 | 0.000 | 0.006 | 0.055 | 0.148 | 0.210 | 0.246 | 0.259 | 0.247 | 0.245 | 0.314 |
| Fraction of bio + CCS | 0.000 | 0.000 | 0.000 | 1.000 | 0.733 | 0.844 | 0.936 | 1.000 | 1.000 | 1.000 | 1.000 |
| Fraction of coal + CCS | 0.000 | 0.000 | 0.000 | 1.000 | 1.000 | 1.000 | 1.000 | 1.000 | 0.000 | 0.000 | 0.000 |
| Fraction of gas + CCS | 0.000 | 0.000 | 0.000 | 0.130 | 0.918 | 0.850 | 0.851 | 0.000 | 0.000 | 0.000 | 0.000 |
| Fraction of oil + CCS | 0.000 | 0.000 | 0.000 | 0.710 | 0.884 | 0.898 | 0.929 | 0.667 | 0.333 | 0.333 | 0.000 |
| Total renewable share | 0.197 | 0.190 | 0.175 | 0.271 | 0.559 | 0.598 | 0.696 | 0.762 | 0.826 | 0.863 | 0.938 |
| Electricity mix Asia SSP2 RCP 1.9 | 2005 | 2010 | 2020 | 2030 | 2040 | 2050 | 2060 | 2070 | 2080 | 2090 | 2100 |
| Biomass share | 0.001 | 0.008 | 0.029 | 0.012 | 0.006 | 0.009 | 0.011 | 0.010 | 0.009 | 0.010 | 0.009 |
| Coal share | 0.639 | 0.659 | 0.531 | 0.072 | 0.016 | 0.004 | 0.003 | 0.002 | 0.000 | 0.000 | 0.000 |
| Oil share | 0.049 | 0.020 | 0.006 | 0.002 | 0.000 | 0.000 | 0.000 | 0.000 | 0.000 | 0.000 | 0.000 |
| Gas share | 0.109 | 0.105 | 0.104 | 0.177 | 0.090 | 0.038 | 0.019 | 0.002 | 0.000 | 0.000 | 0.000 |
| Geothermal share | 0.004 | 0.006 | 0.003 | 0.004 | 0.005 | 0.005 | 0.005 | 0.005 | 0.006 | 0.006 | 0.006 |
| Hydro share | 0.138 | 0.151 | 0.160 | 0.200 | 0.155 | 0.122 | 0.096 | 0.082 | 0.076 | 0.073 | 0.071 |
| Nuclear share | 0.058 | 0.043 | 0.075 | 0.157 | 0.232 | 0.318 | 0.404 | 0.402 | 0.382 | 0.317 | 0.215 |
| Ocean share | 0.000 | 0.000 | 0.000 | 0.000 | 0.000 | 0.000 | 0.000 | 0.000 | 0.000 | 0.000 | 0.000 |
| Solar share | 0.000 | 0.000 | 0.018 | 0.102 | 0.122 | 0.156 | 0.175 | 0.220 | 0.241 | 0.277 | 0.339 |
| Wind share | 0.002 | 0.008 | 0.074 | 0.274 | 0.375 | 0.349 | 0.287 | 0.277 | 0.285 | 0.318 | 0.360 |
| Fraction of bio + CCS | 0.000 | 0.000 | 0.000 | 0.057 | 0.692 | 0.844 | 0.906 | 1.000 | 1.000 | 1.000 | 1.000 |
| Fraction of coal + CCS | 0.000 | 0.000 | 0.000 | 0.215 | 1.000 | 1.000 | 1.000 | 1.000 | 1.000 | 1.000 | 0.000 |
| Fraction of gas + CCS | 0.000 | 0.000 | 0.000 | 0.165 | 0.915 | 0.861 | 0.850 | 0.851 | 0.000 | 0.000 | 0.000 |
| Fraction of oil + CCS | 0.000 | 0.000 | 0.000 | 0.146 | 0.869 | 0.902 | 0.919 | 0.950 | 0.667 | 0.667 | 0.333 |
| Total renewable share | 0.145 | 0.174 | 0.285 | 0.592 | 0.662 | 0.641 | 0.574 | 0.594 | 0.617 | 0.683 | 0.785 |
| Electricity mix MAF SSP2 RCP 1.9 | 2005 | 2010 | 2020 | 2030 | 2040 | 2050 | 2060 | 2070 | 2080 | 2090 | 2100 |
| Biomass share | 0.000 | 0.000 | 0.000 | 0.002 | 0.012 | 0.025 | 0.024 | 0.012 | 0.010 | 0.008 | 0.007 |
| Coal share | 0.000 | 0.000 | 0.000 | 0.002 | 0.003 | 0.001 | 0.001 | 0.001 | 0.000 | 0.000 | 0.000 |
| Oil share | 0.320 | 0.253 | 0.101 | 0.035 | 0.012 | 0.003 | 0.001 | 0.000 | 0.000 | 0.000 | 0.000 |
| Gas share | 0.544 | 0.618 | 0.788 | 0.603 | 0.445 | 0.307 | 0.171 | 0.093 | 0.030 | 0.000 | 0.000 |
| Geothermal share | 0.001 | 0.001 | 0.001 | 0.001 | 0.008 | 0.005 | 0.003 | 0.002 | 0.001 | 0.001 | 0.001 |
| Hydro share | 0.121 | 0.108 | 0.100 | 0.152 | 0.124 | 0.085 | 0.059 | 0.043 | 0.033 | 0.027 | 0.022 |
| Nuclear share | 0.012 | 0.009 | 0.002 | 0.053 | 0.113 | 0.175 | 0.249 | 0.289 | 0.253 | 0.192 | 0.135 |
| Ocean share | 0.000 | 0.000 | 0.000 | 0.000 | 0.000 | 0.000 | 0.000 | 0.000 | 0.000 | 0.000 | 0.000 |
| Solar share | 0.000 | 0.002 | 0.001 | 0.035 | 0.082 | 0.120 | 0.158 | 0.189 | 0.234 | 0.307 | 0.379 |
| Wind share | 0.002 | 0.008 | 0.006 | 0.116 | 0.201 | 0.279 | 0.334 | 0.371 | 0.438 | 0.463 | 0.457 |
| Fraction of bio + CCS | 0.000 | 0.000 | 0.000 | 0.250 | 0.619 | 0.779 | 0.805 | 0.928 | 1.000 | 1.000 | 1.000 |
| Fraction of coal + CCS | 0.000 | 0.000 | 0.000 | 0.500 | 0.500 | 0.500 | 0.500 | 0.500 | 0.000 | 0.000 | 0.000 |
| Fraction of gas + CCS | 0.000 | 0.000 | 0.000 | 0.135 | 0.490 | 0.906 | 0.850 | 0.850 | 0.850 | 0.000 | 0.000 |
| Fraction of oil + CCS | 0.000 | 0.000 | 0.000 | 0.295 | 0.536 | 0.728 | 0.718 | 0.759 | 0.617 | 0.333 | 0.333 |
| Total renewable share | 0.123 | 0.120 | 0.108 | 0.306 | 0.427 | 0.514 | 0.579 | 0.617 | 0.717 | 0.808 | 0.865 |
| Electricity mix LAM SSP2 RCP 1.9 | 2005 | 2010 | 2020 | 2030 | 2040 | 2050 | 2060 | 2070 | 2080 | 2090 | 2100 |
| Biomass share | 0.020 | 0.029 | 0.022 | 0.026 | 0.033 | 0.068 | 0.055 | 0.031 | 0.057 | 0.017 | 0.003 |
| Coal share | 0.053 | 0.053 | 0.009 | 0.002 | 0.001 | 0.000 | 0.000 | 0.000 | 0.000 | 0.000 | 0.000 |
| Oil share | 0.129 | 0.042 | 0.014 | 0.006 | 0.001 | 0.000 | 0.000 | 0.000 | 0.000 | 0.000 | 0.000 |
| Gas share | 0.185 | 0.268 | 0.423 | 0.294 | 0.092 | 0.021 | 0.012 | 0.000 | 0.000 | 0.000 | 0.000 |
| Geothermal share | 0.008 | 0.010 | 0.007 | 0.003 | 0.001 | 0.011 | 0.016 | 0.023 | 0.014 | 0.017 | 0.014 |
| Hydro share | 0.580 | 0.576 | 0.466 | 0.422 | 0.443 | 0.355 | 0.307 | 0.266 | 0.230 | 0.203 | 0.171 |
| Nuclear share | 0.025 | 0.021 | 0.012 | 0.041 | 0.067 | 0.107 | 0.144 | 0.118 | 0.080 | 0.038 | 0.004 |
| Ocean share | 0.000 | 0.000 | 0.000 | 0.000 | 0.000 | 0.000 | 0.000 | 0.000 | 0.000 | 0.000 | 0.000 |
| Solar share | 0.000 | 0.000 | 0.000 | 0.057 | 0.138 | 0.202 | 0.212 | 0.248 | 0.268 | 0.304 | 0.348 |
| Wind share | 0.000 | 0.000 | 0.047 | 0.148 | 0.224 | 0.236 | 0.255 | 0.313 | 0.351 | 0.421 | 0.460 |
| Fraction of bio + CCS | 0.000 | 0.000 | 0.000 | 0.090 | 0.622 | 0.724 | 0.666 | 0.613 | 0.910 | 0.743 | 0.000 |
| Fraction of coal + CCS | 0.000 | 0.000 | 0.000 | 0.615 | 1.000 | 0.000 | 0.000 | 0.000 | 0.000 | 0.000 | 0.000 |
| Fraction of gas + CCS | 0.000 | 0.000 | 0.000 | 0.189 | 0.874 | 0.850 | 0.850 | 0.857 | 0.000 | 0.000 | 0.000 |
| Fraction of oil + CCS | 0.000 | 0.000 | 0.000 | 0.298 | 0.832 | 0.525 | 0.505 | 0.490 | 0.303 | 0.248 | 0.000 |
| Total renewable share | 0.608 | 0.616 | 0.543 | 0.657 | 0.840 | 0.872 | 0.844 | 0.882 | 0.920 | 0.962 | 0.996 |

| Electricity mix Global SSP2 RCP 1.9 | 2005 | 2010 | 2020 | 2030 | 2040 | 2050 | 2060 | 2070 | 2080 | 2090 | 2100 |
|-------------------------------------|-------|-------|-------|-------|-------|-------|-------|-------|-------|-------|-------|
| Biomass share | 0.007 | 0.010 | 0.018 | 0.007 | 0.009 | 0.018 | 0.020 | 0.016 | 0.015 | 0.011 | 0.009 |
| Coal share | 0.404 | 0.411 | 0.325 | 0.041 | 0.012 | 0.004 | 0.002 | 0.001 | 0.000 | 0.000 | 0.000 |
| Oil share | 0.062 | 0.032 | 0.012 | 0.005 | 0.002 | 0.000 | 0.000 | 0.000 | 0.000 | 0.000 | 0.000 |
| Gas share | 0.204 | 0.216 | 0.264 | 0.309 | 0.177 | 0.109 | 0.059 | 0.026 | 0.006 | 0.000 | 0.000 |
| Geothermal share | 0.003 | 0.005 | 0.003 | 0.007 | 0.015 | 0.016 | 0.016 | 0.016 | 0.015 | 0.014 | 0.013 |
| Hydro share | 0.163 | 0.171 | 0.162 | 0.189 | 0.175 | 0.138 | 0.113 | 0.099 | 0.090 | 0.083 | 0.076 |
| Nuclear share | 0.151 | 0.129 | 0.129 | 0.165 | 0.194 | 0.255 | 0.320 | 0.320 | 0.292 | 0.238 | 0.154 |
| Ocean share | 0.000 | 0.000 | 0.000 | 0.000 | 0.000 | 0.000 | 0.000 | 0.000 | 0.000 | 0.000 | 0.000 |
| Solar share | 0.000 | 0.003 | 0.017 | 0.069 | 0.103 | 0.141 | 0.164 | 0.199 | 0.222 | 0.262 | 0.321 |
| Wind share | 0.006 | 0.022 | 0.070 | 0.208 | 0.313 | 0.318 | 0.306 | 0.324 | 0.360 | 0.393 | 0.428 |
| Fraction of bio + CCS | 0.000 | 0.000 | 0.000 | 0.077 | 0.558 | 0.829 | 0.834 | 0.895 | 0.963 | 0.967 | 0.970 |
| Fraction of coal + CCS | 0.000 | 0.000 | 0.000 | 0.293 | 0.997 | 0.994 | 1.000 | 1.000 | 1.000 | 1.000 | 1.000 |
| Fraction of gas + CCS | 0.000 | 0.000 | 0.000 | 0.142 | 0.684 | 0.883 | 0.850 | 0.850 | 0.850 | 1.000 | 1.000 |
| Fraction of oil + CCS | 0.000 | 0.000 | 0.000 | 0.171 | 0.746 | 0.902 | 0.895 | 0.915 | 0.938 | 0.989 | 0.990 |
| Total renewable share | 0.179 | 0.211 | 0.270 | 0.480 | 0.615 | 0.631 | 0.618 | 0.654 | 0.701 | 0.762 | 0.846 |

Table K6: electricity mix per region for SSP5-19. Global is used for international waters.

| Electricity mix OECD SSP5 RCP 1.9 | 2005 | 2010 | 2020 | 2030 | 2040 | 2050 | 2060 | 2070 | 2080 | 2090 | 2100 |
|-----------------------------------|-------|-------|-------|-------|-------|-------|-------|-------|-------|-------|-------|
| Biomass share | 0.009 | 0.012 | 0.012 | 0.025 | 0.101 | 0.113 | 0.095 | 0.084 | 0.071 | 0.055 | 0.045 |
| Coal share | 0.395 | 0.346 | 0.185 | 0.058 | 0.006 | 0.000 | 0.000 | 0.000 | 0.000 | 0.000 | 0.000 |
| Oil share | 0.037 | 0.030 | 0.013 | 0.003 | 0.000 | 0.000 | 0.000 | 0.000 | 0.000 | 0.000 | 0.000 |
| Gas share | 0.197 | 0.230 | 0.409 | 0.422 | 0.195 | 0.074 | 0.034 | 0.016 | 0.004 | 0.002 | 0.001 |
| Geothermal share | 0.003 | 0.004 | 0.005 | 0.010 | 0.008 | 0.006 | 0.004 | 0.003 | 0.003 | 0.002 | 0.002 |
| Hydro share | 0.127 | 0.125 | 0.106 | 0.122 | 0.149 | 0.118 | 0.089 | 0.071 | 0.059 | 0.050 | 0.045 |
| Nuclear share | 0.223 | 0.214 | 0.184 | 0.212 | 0.229 | 0.194 | 0.165 | 0.148 | 0.135 | 0.121 | 0.106 |
| Ocean share | 0.000 | 0.000 | 0.000 | 0.000 | 0.000 | 0.000 | 0.000 | 0.000 | 0.000 | 0.000 | 0.000 |
| Solar share | 0.000 | 0.005 | 0.024 | 0.039 | 0.120 | 0.259 | 0.367 | 0.434 | 0.485 | 0.524 | 0.565 |
| Wind share | 0.009 | 0.033 | 0.062 | 0.108 | 0.193 | 0.237 | 0.246 | 0.244 | 0.243 | 0.245 | 0.236 |
| Fraction of bio + CCS | 0.000 | 0.000 | 0.000 | 0.542 | 0.939 | 0.988 | 0.999 | 1.000 | 1.000 | 1.000 | 1.000 |
| Fraction of coal + CCS | 0.000 | 0.000 | 0.000 | 0.000 | 0.000 | 0.000 | 0.000 | 0.000 | 0.000 | 0.000 | 0.000 |
| Fraction of gas + CCS | 0.000 | 0.000 | 0.000 | 0.034 | 0.275 | 0.510 | 0.722 | 0.686 | 0.345 | 0.131 | 0.000 |
| Fraction of oil + CCS | 0.000 | 0.000 | 0.000 | 0.192 | 0.405 | 0.499 | 0.574 | 0.562 | 0.448 | 0.377 | 0.333 |
| Total renewable share | 0.148 | 0.180 | 0.209 | 0.305 | 0.571 | 0.732 | 0.802 | 0.836 | 0.861 | 0.877 | 0.892 |
| Electricity mix REF SSP5 RCP 1.9 | 2005 | 2010 | 2020 | 2030 | 2040 | 2050 | 2060 | 2070 | 2080 | 2090 | 2100 |
| Biomass share | 0.003 | 0.004 | 0.010 | 0.024 | 0.118 | 0.225 | 0.213 | 0.193 | 0.163 | 0.135 | 0.125 |
| Coal share | 0.169 | 0.110 | 0.041 | 0.009 | 0.000 | 0.000 | 0.000 | 0.000 | 0.000 | 0.000 | 0.000 |
| Oil share | 0.001 | 0.018 | 0.023 | 0.019 | 0.000 | 0.000 | 0.000 | 0.000 | 0.000 | 0.000 | 0.000 |
| Gas share | 0.486 | 0.517 | 0.570 | 0.543 | 0.325 | 0.130 | 0.073 | 0.038 | 0.009 | 0.002 | 0.000 |
| Geothermal share | 0.000 | 0.001 | 0.000 | 0.006 | 0.020 | 0.017 | 0.010 | 0.002 | 0.000 | 0.000 | 0.000 |
| Hydro share | 0.183 | 0.156 | 0.095 | 0.109 | 0.271 | 0.429 | 0.468 | 0.459 | 0.454 | 0.455 | 0.455 |
| Nuclear share | 0.158 | 0.194 | 0.259 | 0.278 | 0.209 | 0.112 | 0.035 | 0.000 | 0.000 | 0.000 | 0.000 |
| Ocean share | 0.000 | 0.000 | 0.000 | 0.000 | 0.000 | 0.000 | 0.000 | 0.000 | 0.000 | 0.000 | 0.000 |
| Solar share | 0.000 | 0.000 | 0.002 | 0.002 | 0.005 | 0.019 | 0.051 | 0.090 | 0.104 | 0.089 | 0.077 |
| Wind share | 0.000 | 0.000 | 0.000 | 0.010 | 0.052 | 0.068 | 0.151 | 0.217 | 0.270 | 0.319 | 0.342 |
| Fraction of bio + CCS | 0.000 | 0.000 | 0.000 | 0.447 | 0.909 | 0.973 | 0.988 | 1.000 | 1.000 | 1.000 | 1.000 |
| Fraction of coal + CCS | 0.000 | 0.000 | 0.000 | 0.000 | 0.000 | 0.000 | 0.000 | 0.000 | 0.000 | 0.000 | 0.000 |
| Fraction of gas + CCS | 0.000 | 0.000 | 0.000 | 0.024 | 0.225 | 0.474 | 0.611 | 0.581 | 0.236 | 0.000 | 0.000 |
| Fraction of oil + CCS | 0.000 | 0.000 | 0.000 | 0.157 | 0.378 | 0.482 | 0.533 | 0.527 | 0.412 | 0.333 | 0.000 |
| Total renewable share | 0.186 | 0.161 | 0.107 | 0.152 | 0.466 | 0.757 | 0.892 | 0.961 | 0.991 | 0.998 | 1.000 |
| Electricity mix Asia SSP5 RCP 1.9 | 2005 | 2010 | 2020 | 2030 | 2040 | 2050 | 2060 | 2070 | 2080 | 2090 | 2100 |
| Biomass share | 0.000 | 0.000 | 0.002 | 0.007 | 0.032 | 0.052 | 0.044 | 0.037 | 0.035 | 0.034 | 0.034 |
| Coal share | 0.633 | 0.646 | 0.500 | 0.213 | 0.036 | 0.000 | 0.000 | 0.000 | 0.000 | 0.000 | 0.000 |
| Oil share | 0.053 | 0.053 | 0.036 | 0.018 | 0.000 | 0.000 | 0.000 | 0.000 | 0.000 | 0.000 | 0.000 |
| Gas share | 0.112 | 0.128 | 0.272 | 0.401 | 0.188 | 0.051 | 0.010 | 0.002 | 0.000 | 0.000 | 0.000 |
| Geothermal share | 0.004 | 0.004 | 0.004 | 0.005 | 0.005 | 0.003 | 0.002 | 0.002 | 0.002 | 0.002 | 0.002 |
| Hydro share | 0.138 | 0.108 | 0.063 | 0.063 | 0.120 | 0.120 | 0.104 | 0.091 | 0.085 | 0.083 | 0.081 |
| Nuclear share | 0.059 | 0.042 | 0.066 | 0.179 | 0.354 | 0.340 | 0.275 | 0.230 | 0.192 | 0.174 | 0.174 |
| Ocean share | 0.000 | 0.000 | 0.000 | 0.000 | 0.000 | 0.000 | 0.000 | 0.000 | 0.000 | 0.000 | 0.000 |
| Solar share | 0.000 | 0.001 | 0.012 | 0.022 | 0.105 | 0.256 | 0.389 | 0.461 | 0.502 | 0.517 | 0.523 |
| Wind share | 0.001 | 0.017 | 0.046 | 0.091 | 0.160 | 0.177 | 0.176 | 0.177 | 0.184 | 0.190 | 0.186 |
| Fraction of bio + CCS | 0.000 | 0.000 | 0.000 | 0.724 | 0.958 | 0.986 | 0.994 | 0.998 | 0.998 | 0.998 | 0.999 |
| Fraction of coal + CCS | 0.000 | 0.000 | 0.000 | 0.000 | 0.000 | 0.000 | 0.000 | 0.000 | 0.000 | 0.000 | 0.000 |
| Fraction of gas + CCS | 0.000 | 0.000 | 0.000 | 0.002 | 0.005 | 0.013 | 0.033 | 0.032 | 0.000 | 0.000 | 0.000 |
| Fraction of oil + CCS | 0.000 | 0.000 | 0.000 | 0.242 | 0.321 | 0.333 | 0.342 | 0.343 | 0.333 | 0.333 | 0.333 |
| Total renewable share | 0.143 | 0.130 | 0.126 | 0.189 | 0.421 | 0.609 | 0.715 | 0.769 | 0.808 | 0.826 | 0.826 |

| | | | | | | | | | | | |
|-------------------------------------|-------|-------|-------|-------|-------|-------|-------|-------|-------|-------|-------|
| Electricity mix MAF SSP5 RCP 1.9 | 2005 | 2010 | 2020 | 2030 | 2040 | 2050 | 2060 | 2070 | 2080 | 2090 | 2100 |
| Biomass share | 0.000 | 0.000 | 0.000 | 0.007 | 0.053 | 0.086 | 0.075 | 0.065 | 0.065 | 0.063 | 0.055 |
| Coal share | 0.093 | 0.073 | 0.040 | 0.017 | 0.003 | 0.000 | 0.000 | 0.000 | 0.000 | 0.000 | 0.000 |
| Oil share | 0.262 | 0.173 | 0.056 | 0.011 | 0.000 | 0.000 | 0.000 | 0.000 | 0.000 | 0.000 | 0.000 |
| Gas share | 0.500 | 0.621 | 0.774 | 0.697 | 0.296 | 0.109 | 0.057 | 0.028 | 0.008 | 0.002 | 0.000 |
| Geothermal share | 0.001 | 0.001 | 0.001 | 0.013 | 0.014 | 0.006 | 0.004 | 0.002 | 0.002 | 0.001 | 0.001 |
| Hydro share | 0.141 | 0.123 | 0.076 | 0.110 | 0.246 | 0.195 | 0.124 | 0.090 | 0.072 | 0.059 | 0.052 |
| Nuclear share | 0.002 | 0.007 | 0.041 | 0.083 | 0.102 | 0.125 | 0.150 | 0.150 | 0.121 | 0.078 | 0.041 |
| Ocean share | 0.000 | 0.000 | 0.000 | 0.000 | 0.000 | 0.000 | 0.000 | 0.000 | 0.000 | 0.000 | 0.000 |
| Solar share | 0.000 | 0.001 | 0.010 | 0.037 | 0.189 | 0.334 | 0.431 | 0.508 | 0.584 | 0.654 | 0.716 |
| Wind share | 0.001 | 0.002 | 0.002 | 0.025 | 0.098 | 0.147 | 0.159 | 0.156 | 0.148 | 0.143 | 0.135 |
| Fraction of bio + CCS | 0.000 | 0.000 | 0.000 | 1.000 | 1.000 | 1.000 | 1.000 | 1.000 | 1.000 | 1.000 | 1.000 |
| Fraction of coal + CCS | 0.000 | 0.000 | 0.000 | 0.000 | 0.000 | 0.000 | 0.000 | 0.000 | 0.000 | 0.000 | 0.000 |
| Fraction of gas + CCS | 0.000 | 0.000 | 0.000 | 0.043 | 0.519 | 0.865 | 1.000 | 1.000 | 1.000 | 1.000 | 1.000 |
| Fraction of oil + CCS | 0.000 | 0.000 | 0.000 | 0.348 | 0.506 | 0.622 | 0.667 | 0.667 | 0.667 | 0.667 | 0.667 |
| Total renewable share | 0.142 | 0.127 | 0.089 | 0.193 | 0.600 | 0.767 | 0.793 | 0.822 | 0.871 | 0.920 | 0.959 |
| Electricity mix LAM SSP5 RCP 1.9 | 2005 | 2010 | 2020 | 2030 | 2040 | 2050 | 2060 | 2070 | 2080 | 2090 | 2100 |
| Biomass share | 0.000 | 0.001 | 0.003 | 0.023 | 0.158 | 0.174 | 0.152 | 0.144 | 0.140 | 0.129 | 0.128 |
| Coal share | 0.051 | 0.058 | 0.104 | 0.067 | 0.013 | 0.000 | 0.000 | 0.000 | 0.000 | 0.000 | 0.000 |
| Oil share | 0.146 | 0.102 | 0.031 | 0.006 | 0.000 | 0.000 | 0.000 | 0.000 | 0.000 | 0.000 | 0.000 |
| Gas share | 0.188 | 0.277 | 0.472 | 0.386 | 0.113 | 0.026 | 0.020 | 0.023 | 0.016 | 0.009 | 0.002 |
| Geothermal share | 0.009 | 0.011 | 0.007 | 0.012 | 0.009 | 0.006 | 0.004 | 0.004 | 0.003 | 0.003 | 0.002 |
| Hydro share | 0.582 | 0.524 | 0.341 | 0.381 | 0.432 | 0.364 | 0.282 | 0.231 | 0.197 | 0.176 | 0.165 |
| Nuclear share | 0.025 | 0.022 | 0.017 | 0.014 | 0.008 | 0.004 | 0.001 | 0.000 | 0.000 | 0.000 | 0.000 |
| Ocean share | 0.000 | 0.000 | 0.000 | 0.000 | 0.000 | 0.000 | 0.000 | 0.000 | 0.000 | 0.000 | 0.000 |
| Solar share | 0.000 | 0.001 | 0.004 | 0.017 | 0.083 | 0.213 | 0.319 | 0.382 | 0.431 | 0.475 | 0.505 |
| Wind share | 0.000 | 0.004 | 0.019 | 0.094 | 0.183 | 0.214 | 0.221 | 0.216 | 0.213 | 0.208 | 0.198 |
| Fraction of bio + CCS | 0.000 | 0.000 | 0.000 | 0.848 | 0.986 | 0.994 | 0.998 | 1.000 | 1.000 | 1.000 | 1.000 |
| Fraction of coal + CCS | 0.000 | 0.000 | 0.000 | 0.000 | 0.000 | 0.000 | 0.000 | 0.000 | 0.000 | 0.000 | 0.000 |
| Fraction of gas + CCS | 0.000 | 0.000 | 0.000 | 0.009 | 0.081 | 0.367 | 1.000 | 1.000 | 1.000 | 1.000 | 1.000 |
| Fraction of oil + CCS | 0.000 | 0.000 | 0.000 | 0.286 | 0.355 | 0.453 | 0.666 | 0.667 | 0.667 | 0.667 | 0.667 |
| Total renewable share | 0.591 | 0.541 | 0.375 | 0.527 | 0.865 | 0.970 | 0.978 | 0.977 | 0.984 | 0.991 | 0.998 |
| Electricity mix Global SSP5 RCP 1.9 | 2005 | 2010 | 2020 | 2030 | 2040 | 2050 | 2060 | 2070 | 2080 | 2090 | 2100 |
| Biomass share | 0.005 | 0.006 | 0.006 | 0.015 | 0.069 | 0.090 | 0.078 | 0.069 | 0.064 | 0.057 | 0.052 |
| Coal share | 0.403 | 0.395 | 0.291 | 0.128 | 0.020 | 0.000 | 0.000 | 0.000 | 0.000 | 0.000 | 0.000 |
| Oil share | 0.061 | 0.052 | 0.028 | 0.012 | 0.000 | 0.000 | 0.000 | 0.000 | 0.000 | 0.000 | 0.000 |
| Gas share | 0.207 | 0.239 | 0.392 | 0.434 | 0.199 | 0.067 | 0.028 | 0.014 | 0.004 | 0.002 | 0.001 |
| Geothermal share | 0.003 | 0.004 | 0.004 | 0.008 | 0.008 | 0.005 | 0.003 | 0.003 | 0.002 | 0.002 | 0.002 |
| Hydro share | 0.161 | 0.146 | 0.102 | 0.111 | 0.171 | 0.157 | 0.124 | 0.103 | 0.090 | 0.081 | 0.075 |
| Nuclear share | 0.153 | 0.131 | 0.116 | 0.175 | 0.256 | 0.230 | 0.192 | 0.166 | 0.139 | 0.115 | 0.098 |
| Ocean share | 0.000 | 0.000 | 0.000 | 0.000 | 0.000 | 0.000 | 0.000 | 0.000 | 0.000 | 0.000 | 0.000 |
| Solar share | 0.000 | 0.003 | 0.016 | 0.028 | 0.113 | 0.259 | 0.377 | 0.449 | 0.502 | 0.542 | 0.579 |
| Wind share | 0.006 | 0.022 | 0.046 | 0.089 | 0.163 | 0.192 | 0.198 | 0.197 | 0.198 | 0.201 | 0.193 |
| Fraction of bio + CCS | 0.000 | 0.000 | 0.000 | 0.626 | 0.954 | 0.989 | 0.997 | 1.000 | 1.000 | 1.000 | 1.000 |
| Fraction of coal + CCS | 0.000 | 0.000 | 0.000 | 0.000 | 0.000 | 0.071 | 0.167 | 0.500 | 0.500 | 0.500 | 0.500 |
| Fraction of gas + CCS | 0.000 | 0.000 | 0.000 | 0.019 | 0.183 | 0.426 | 0.730 | 0.823 | 0.787 | 0.674 | 0.234 |
| Fraction of oil + CCS | 0.000 | 0.000 | 0.000 | 0.215 | 0.379 | 0.495 | 0.631 | 0.774 | 0.762 | 0.725 | 0.578 |
| Total renewable share | 0.176 | 0.182 | 0.174 | 0.251 | 0.525 | 0.703 | 0.779 | 0.820 | 0.857 | 0.883 | 0.901 |

Table K7: electricity mix per region for SSP2-baseline. Global is used for international waters.

| | | | | | | | | | | | |
|------------------------------------|-------|-------|-------|-------|-------|-------|-------|-------|-------|-------|-------|
| Electricity mix OECD SSP2 Baseline | 2005 | 2010 | 2020 | 2030 | 2040 | 2050 | 2060 | 2070 | 2080 | 2090 | 2100 |
| Biomass share | 0.011 | 0.012 | 0.013 | 0.007 | 0.001 | 0.001 | 0.001 | 0.000 | 0.001 | 0.003 | 0.004 |
| Coal share | 0.394 | 0.358 | 0.250 | 0.141 | 0.122 | 0.112 | 0.114 | 0.138 | 0.190 | 0.174 | 0.095 |
| Oil share | 0.042 | 0.015 | 0.004 | 0.002 | 0.000 | 0.000 | 0.000 | 0.000 | 0.000 | 0.000 | 0.000 |
| Gas share | 0.186 | 0.209 | 0.277 | 0.433 | 0.539 | 0.597 | 0.571 | 0.547 | 0.469 | 0.445 | 0.441 |
| Geothermal share | 0.003 | 0.004 | 0.004 | 0.001 | 0.000 | 0.000 | 0.000 | 0.000 | 0.000 | 0.000 | 0.000 |
| Hydro share | 0.132 | 0.140 | 0.130 | 0.119 | 0.112 | 0.102 | 0.089 | 0.075 | 0.069 | 0.066 | 0.063 |
| Nuclear share | 0.223 | 0.215 | 0.213 | 0.171 | 0.087 | 0.019 | 0.016 | 0.027 | 0.051 | 0.068 | 0.114 |
| Ocean share | 0.000 | 0.000 | 0.000 | 0.000 | 0.000 | 0.000 | 0.000 | 0.000 | 0.000 | 0.000 | 0.000 |
| Solar share | 0.000 | 0.006 | 0.023 | 0.022 | 0.017 | 0.009 | 0.012 | 0.014 | 0.014 | 0.021 | 0.036 |
| Wind share | 0.009 | 0.040 | 0.087 | 0.104 | 0.122 | 0.160 | 0.197 | 0.199 | 0.205 | 0.222 | 0.247 |
| Fraction of bio + CCS | 0.000 | 0.000 | 0.000 | 0.000 | 0.000 | 0.000 | 0.000 | 0.000 | 0.000 | 0.000 | 0.000 |
| Fraction of coal + CCS | 0.000 | 0.000 | 0.000 | 0.000 | 0.000 | 0.000 | 0.000 | 0.000 | 0.000 | 0.000 | 0.000 |
| Fraction of gas + CCS | 0.000 | 0.000 | 0.000 | 0.000 | 0.000 | 0.000 | 0.000 | 0.000 | 0.000 | 0.000 | 0.000 |
| Fraction of oil + CCS | 0.000 | 0.000 | 0.000 | 0.000 | 0.000 | 0.000 | 0.000 | 0.000 | 0.000 | 0.000 | 0.000 |
| Total renewable share | 0.155 | 0.203 | 0.256 | 0.253 | 0.251 | 0.272 | 0.299 | 0.289 | 0.290 | 0.312 | 0.350 |

| | | | | | | | | | | | |
|------------------------------------|-------|-------|-------|-------|-------|-------|-------|-------|-------|-------|-------|
| Electricity mix REF SSP2 Baseline | 2005 | 2010 | 2020 | 2030 | 2040 | 2050 | 2060 | 2070 | 2080 | 2090 | 2100 |
| Biomass share | 0.001 | 0.000 | 0.000 | 0.000 | 0.000 | 0.001 | 0.001 | 0.001 | 0.001 | 0.001 | 0.001 |
| Coal share | 0.189 | 0.221 | 0.191 | 0.145 | 0.048 | 0.014 | 0.016 | 0.014 | 0.014 | 0.014 | 0.012 |
| Oil share | 0.037 | 0.019 | 0.000 | 0.000 | 0.000 | 0.000 | 0.000 | 0.000 | 0.000 | 0.000 | 0.000 |
| Gas share | 0.424 | 0.408 | 0.444 | 0.512 | 0.635 | 0.665 | 0.676 | 0.685 | 0.715 | 0.592 | 0.467 |
| Geothermal share | 0.000 | 0.000 | 0.000 | 0.000 | 0.000 | 0.000 | 0.000 | 0.000 | 0.000 | 0.000 | 0.000 |
| Hydro share | 0.194 | 0.189 | 0.168 | 0.151 | 0.140 | 0.129 | 0.109 | 0.092 | 0.085 | 0.091 | 0.091 |
| Nuclear share | 0.155 | 0.163 | 0.197 | 0.184 | 0.152 | 0.136 | 0.114 | 0.097 | 0.035 | 0.090 | 0.168 |
| Ocean share | 0.000 | 0.000 | 0.000 | 0.000 | 0.000 | 0.000 | 0.000 | 0.000 | 0.000 | 0.000 | 0.000 |
| Solar share | 0.000 | 0.000 | 0.000 | 0.000 | 0.000 | 0.000 | 0.000 | 0.000 | 0.000 | 0.003 | 0.011 |
| Wind share | 0.000 | 0.000 | 0.000 | 0.007 | 0.025 | 0.055 | 0.085 | 0.111 | 0.150 | 0.208 | 0.250 |
| Fraction of bio + CCS | 0.000 | 0.000 | 0.000 | 0.000 | 0.000 | 0.000 | 0.000 | 0.000 | 0.000 | 0.000 | 0.000 |
| Fraction of coal + CCS | 0.000 | 0.000 | 0.000 | 0.000 | 0.000 | 0.000 | 0.000 | 0.000 | 0.000 | 0.000 | 0.000 |
| Fraction of gas + CCS | 0.000 | 0.000 | 0.000 | 0.000 | 0.000 | 0.000 | 0.000 | 0.000 | 0.000 | 0.000 | 0.000 |
| Fraction of oil + CCS | 0.000 | 0.000 | 0.000 | 0.000 | 0.000 | 0.000 | 0.000 | 0.000 | 0.000 | 0.000 | 0.000 |
| Total renewable share | 0.196 | 0.189 | 0.169 | 0.159 | 0.165 | 0.185 | 0.195 | 0.204 | 0.236 | 0.304 | 0.353 |
| Electricity mix Asia SSP2 Baseline | 2005 | 2010 | 2020 | 2030 | 2040 | 2050 | 2060 | 2070 | 2080 | 2090 | 2100 |
| Biomass share | 0.001 | 0.009 | 0.031 | 0.021 | 0.015 | 0.025 | 0.019 | 0.009 | 0.008 | 0.014 | 0.015 |
| Coal share | 0.640 | 0.659 | 0.570 | 0.540 | 0.484 | 0.453 | 0.459 | 0.480 | 0.461 | 0.372 | 0.268 |
| Oil share | 0.049 | 0.020 | 0.006 | 0.002 | 0.000 | 0.000 | 0.000 | 0.000 | 0.000 | 0.000 | 0.000 |
| Gas share | 0.110 | 0.109 | 0.121 | 0.195 | 0.270 | 0.334 | 0.330 | 0.268 | 0.242 | 0.268 | 0.348 |
| Geothermal share | 0.004 | 0.006 | 0.004 | 0.002 | 0.000 | 0.000 | 0.000 | 0.000 | 0.000 | 0.000 | 0.000 |
| Hydro share | 0.138 | 0.152 | 0.166 | 0.155 | 0.166 | 0.142 | 0.125 | 0.123 | 0.124 | 0.116 | 0.111 |
| Nuclear share | 0.058 | 0.043 | 0.064 | 0.054 | 0.040 | 0.035 | 0.041 | 0.060 | 0.098 | 0.152 | 0.160 |
| Ocean share | 0.000 | 0.000 | 0.000 | 0.000 | 0.000 | 0.000 | 0.000 | 0.000 | 0.000 | 0.000 | 0.000 |
| Solar share | 0.000 | 0.000 | 0.019 | 0.015 | 0.013 | 0.006 | 0.014 | 0.030 | 0.034 | 0.040 | 0.049 |
| Wind share | 0.000 | 0.000 | 0.019 | 0.015 | 0.013 | 0.006 | 0.014 | 0.030 | 0.034 | 0.040 | 0.049 |
| Fraction of bio + CCS | 0.000 | 0.000 | 0.000 | 0.000 | 0.000 | 0.000 | 0.000 | 0.000 | 0.000 | 0.000 | 0.000 |
| Fraction of coal + CCS | 0.000 | 0.000 | 0.000 | 0.000 | 0.000 | 0.000 | 0.000 | 0.000 | 0.000 | 0.000 | 0.000 |
| Fraction of gas + CCS | 0.000 | 0.000 | 0.000 | 0.000 | 0.000 | 0.000 | 0.000 | 0.000 | 0.000 | 0.000 | 0.000 |
| Fraction of oil + CCS | 0.000 | 0.000 | 0.000 | 0.000 | 0.000 | 0.000 | 0.000 | 0.000 | 0.000 | 0.000 | 0.000 |
| Total renewable share | 0.143 | 0.168 | 0.239 | 0.208 | 0.206 | 0.178 | 0.171 | 0.192 | 0.200 | 0.209 | 0.224 |
| Electricity mix MAF SSP2 Baseline | 2005 | 2010 | 2020 | 2030 | 2040 | 2050 | 2060 | 2070 | 2080 | 2090 | 2100 |
| Biomass share | 0.000 | 0.000 | 0.000 | 0.000 | 0.000 | 0.000 | 0.000 | 0.004 | 0.008 | 0.012 | 0.009 |
| Coal share | 0.240 | 0.190 | 0.142 | 0.075 | 0.066 | 0.102 | 0.152 | 0.101 | 0.141 | 0.202 | 0.225 |
| Oil share | 0.243 | 0.205 | 0.087 | 0.035 | 0.013 | 0.003 | 0.001 | 0.000 | 0.000 | 0.000 | 0.000 |
| Gas share | 0.413 | 0.499 | 0.675 | 0.777 | 0.781 | 0.696 | 0.602 | 0.566 | 0.503 | 0.360 | 0.270 |
| Geothermal share | 0.001 | 0.001 | 0.001 | 0.000 | 0.000 | 0.000 | 0.000 | 0.000 | 0.000 | 0.000 | 0.000 |
| Hydro share | 0.092 | 0.087 | 0.086 | 0.072 | 0.058 | 0.043 | 0.032 | 0.029 | 0.030 | 0.033 | 0.027 |
| Nuclear share | 0.009 | 0.007 | 0.002 | 0.000 | 0.000 | 0.004 | 0.015 | 0.028 | 0.050 | 0.084 | 0.140 |
| Ocean share | 0.000 | 0.000 | 0.000 | 0.000 | 0.000 | 0.000 | 0.000 | 0.000 | 0.000 | 0.000 | 0.000 |
| Solar share | 0.000 | 0.002 | 0.001 | 0.001 | 0.001 | 0.007 | 0.017 | 0.028 | 0.043 | 0.061 | 0.082 |
| Wind share | 0.002 | 0.008 | 0.006 | 0.040 | 0.081 | 0.145 | 0.182 | 0.243 | 0.226 | 0.248 | 0.247 |
| Fraction of bio + CCS | 0.000 | 0.000 | 0.000 | 0.000 | 0.000 | 0.000 | 0.000 | 0.000 | 0.000 | 0.000 | 0.000 |
| Fraction of coal + CCS | 0.000 | 0.000 | 0.000 | 0.000 | 0.000 | 0.000 | 0.000 | 0.000 | 0.000 | 0.000 | 0.000 |
| Fraction of gas + CCS | 0.000 | 0.000 | 0.000 | 0.000 | 0.000 | 0.000 | 0.000 | 0.000 | 0.000 | 0.000 | 0.000 |
| Fraction of oil + CCS | 0.000 | 0.000 | 0.000 | 0.000 | 0.000 | 0.000 | 0.000 | 0.000 | 0.000 | 0.000 | 0.000 |
| Total renewable share | 0.095 | 0.098 | 0.094 | 0.114 | 0.139 | 0.196 | 0.231 | 0.305 | 0.306 | 0.354 | 0.365 |
| Electricity mix LAM SSP2 Baseline | 2005 | 2010 | 2020 | 2030 | 2040 | 2050 | 2060 | 2070 | 2080 | 2090 | 2100 |
| Biomass + CCS share | 0.020 | 0.029 | 0.023 | 0.001 | 0.000 | 0.001 | 0.002 | 0.035 | 0.074 | 0.058 | 0.083 |
| Coal + CCS share | 0.053 | 0.053 | 0.029 | 0.013 | 0.004 | 0.004 | 0.005 | 0.006 | 0.005 | 0.003 | 0.001 |
| Oil share | 0.129 | 0.042 | 0.014 | 0.006 | 0.002 | 0.000 | 0.000 | 0.000 | 0.000 | 0.000 | 0.000 |
| Gas + CCS share | 0.185 | 0.268 | 0.441 | 0.531 | 0.552 | 0.552 | 0.575 | 0.529 | 0.490 | 0.495 | 0.437 |
| Geothermal share | 0.008 | 0.010 | 0.007 | 0.002 | 0.000 | 0.000 | 0.000 | 0.000 | 0.000 | 0.000 | 0.000 |
| Hydro share | 0.580 | 0.576 | 0.457 | 0.381 | 0.316 | 0.256 | 0.193 | 0.152 | 0.132 | 0.116 | 0.104 |
| Nuclear share | 0.025 | 0.021 | 0.012 | 0.005 | 0.001 | 0.000 | 0.000 | 0.000 | 0.000 | 0.000 | 0.000 |
| Ocean share | 0.000 | 0.000 | 0.000 | 0.000 | 0.000 | 0.000 | 0.000 | 0.000 | 0.000 | 0.000 | 0.000 |
| Solar share | 0.000 | 0.000 | 0.000 | 0.000 | 0.000 | 0.000 | 0.005 | 0.029 | 0.050 | 0.079 | 0.125 |
| Wind share | 0.000 | 0.000 | 0.015 | 0.061 | 0.125 | 0.188 | 0.220 | 0.249 | 0.249 | 0.249 | 0.250 |
| Fraction of bio + CCS | 0.000 | 0.000 | 0.000 | 0.000 | 0.000 | 0.000 | 0.000 | 0.000 | 0.000 | 0.000 | 0.000 |
| Fraction of coal + CCS | 0.000 | 0.000 | 0.000 | 0.000 | 0.300 | 0.587 | 0.948 | 1.000 | 1.000 | 1.000 | 0.972 |
| Fraction of gas + CCS | 0.000 | 0.000 | 0.000 | 0.000 | 0.000 | 0.000 | 0.000 | 0.000 | 0.000 | 0.000 | 0.000 |
| Fraction of oil + CCS | 0.000 | 0.000 | 0.000 | 0.000 | 0.100 | 0.196 | 0.316 | 0.333 | 0.333 | 0.333 | 0.324 |
| Total renewable share | 0.608 | 0.616 | 0.503 | 0.445 | 0.441 | 0.444 | 0.420 | 0.465 | 0.505 | 0.502 | 0.562 |

| Electricity mix Global SSP2 Baseline | 2005 | 2010 | 2020 | 2030 | 2040 | 2050 | 2060 | 2070 | 2080 | 2090 | 2100 |
|--------------------------------------|-------|-------|-------|-------|-------|-------|-------|-------|-------|-------|-------|
| Biomass share | 0.007 | 0.010 | 0.018 | 0.010 | 0.006 | 0.010 | 0.007 | 0.007 | 0.011 | 0.014 | 0.016 |
| Coal share | 0.404 | 0.410 | 0.337 | 0.274 | 0.232 | 0.219 | 0.226 | 0.226 | 0.237 | 0.217 | 0.171 |
| Oil share | 0.061 | 0.032 | 0.012 | 0.005 | 0.002 | 0.001 | 0.000 | 0.000 | 0.000 | 0.000 | 0.000 |
| Gas share | 0.204 | 0.217 | 0.270 | 0.372 | 0.444 | 0.479 | 0.462 | 0.429 | 0.389 | 0.351 | 0.335 |
| Geothermal share | 0.003 | 0.005 | 0.003 | 0.001 | 0.000 | 0.000 | 0.000 | 0.000 | 0.000 | 0.000 | 0.000 |
| Hydro share | 0.163 | 0.171 | 0.161 | 0.143 | 0.135 | 0.115 | 0.096 | 0.086 | 0.081 | 0.076 | 0.068 |
| Nuclear share | 0.151 | 0.129 | 0.124 | 0.093 | 0.051 | 0.025 | 0.027 | 0.038 | 0.059 | 0.091 | 0.121 |
| Ocean share | 0.000 | 0.000 | 0.000 | 0.000 | 0.000 | 0.000 | 0.000 | 0.000 | 0.000 | 0.000 | 0.000 |
| Solar share | 0.000 | 0.003 | 0.017 | 0.014 | 0.010 | 0.006 | 0.012 | 0.023 | 0.029 | 0.041 | 0.059 |
| Wind share | 0.006 | 0.022 | 0.058 | 0.087 | 0.119 | 0.145 | 0.171 | 0.191 | 0.193 | 0.210 | 0.231 |
| Fraction of bio + CCS | 0.000 | 0.000 | 0.000 | 0.000 | 0.000 | 0.000 | 0.000 | 0.000 | 0.000 | 0.000 | 0.000 |
| Fraction of coal + CCS | 0.000 | 0.000 | 0.000 | 0.000 | 0.000 | 0.000 | 0.000 | 0.000 | 0.000 | 0.000 | 0.000 |
| Fraction of gas + CCS | 0.000 | 0.000 | 0.000 | 0.000 | 0.000 | 0.000 | 0.000 | 0.000 | 0.000 | 0.000 | 0.000 |
| Fraction of oil + CCS | 0.000 | 0.000 | 0.000 | 0.000 | 0.000 | 0.000 | 0.000 | 0.000 | 0.000 | 0.000 | 0.000 |
| Total renewable share | 0.179 | 0.211 | 0.257 | 0.256 | 0.271 | 0.276 | 0.286 | 0.307 | 0.315 | 0.341 | 0.373 |

Appendix L: Impacts sub model input and data sources

Table L1: values and data sources used for the constants and lookups in the impacts sub model. A range is included if uncertainty is assessed for a specific variable. Dmnl = dimensionless.

| Element | Unit | Type | Min | Max | Explanation/assumptions | Source |
|---|---------------------------------|----------|------------------------|-----|--|--|
| <i>Regional data</i> | | | | | | |
| Regional mix | Dmnl | Lookup | Selected SSP scenarios | | Electricity mix for the five regions included in the model | IIASA (2018) |
| Regional CCS fraction | Dmnl | Lookup | Selected SSP scenarios | | CCS fraction for the five regions included in the model | IIASA (2018) |
| Country regions | Dmnl | Constant | Either a 1 or a 0 | | Indicates which region a certain country belongs to | IIASA (2018) |
| <i>Project related data</i> | | | | | | |
| Project country | Dmnl | Constant | Either a 1 or a 0 | | Indicates which country a certain project is located in | Mudd (2020) |
| Project mine type | Dmnl | Constant | Either a 1 or a 0 | | Indicates which mine type is used by a certain project | Mudd (2020) |
| Project process | Dmnl | Constant | Either a 1 or a 0 | | Indicates which principal process is used by a certain project | Mudd (2020) |
| Process class | Dmnl | Constant | Either a 1 or a 0 | | Indicates whether a certain principal process leads to the production of class 1 or class 2 nickel. Most data was gathered from Schmidt et al. (2016). However, it was assumed that all HM laterite processing, including HL, ATL and DNI led to class 1 nickel. Because the frequency of these methods in the database by Mudd (2020) was low, this was assumed to not have a very large impact on the overall results. | Schmidt et al. (2016); assumption for HL, ATL and DNI. |
| <i>GHG emissions data</i> | | | | | | |
| GWP electricity generation technologies | Tonne CO ₂ eq /GJ | Constant | See table K3 | | GWP electricity generation technologies | See table K3 |
| GWP electricity generation technologies with CCS | Tonne CO ₂ eq /GJ | Constant | See table K3 | | GWP electricity generation technologies with CCS | See table K3 |
| Initial GHG emissions per process excluding electricity | Tonne CO ₂ eq /tonne | Constant | See table K2 | | Initial GHG emissions per process excluding electricity | See table K2 |
| Carbon intensity improvement | Dmnl | Constant | -0.001 | | Autonomous carbon intensity improvements due to innovation | Assumption |

Appendix M: Switches, base values and performance metrics

Table M1: switches included in the model, the number of options per switch and the base value. A&C = Availability and consumption.

| Switch | Options | Base | Elaboration |
|---|---------|---------------------|---|
| <i>Disruption scenario switches</i> | | | |
| <i>Energy transition switches</i> | | | |
| SSPs | 4 | 4 (BAU) | Three SSPs that comply with 1.5 °C (which can be seen as the disruption scenarios) and one BAU scenario. This switch influences electricity generation capacity, electricity demand, electricity mix, VRE share, population, GDP and carbon price |
| Transport scenario | 2 | 1 (electrification) | Electrification and hydrogen scenario. A further distinction is made between BAU and the ET based on the SSPs Influences vehicle mix. |
| Flexibility scenario | 3 | 2 (mid) | Three flexibility scenarios that determine storage requirement. |
| Energy price scenario | 3 | 2 (mid) | Low price scenario, medium price scenario and high price scenario. Influences the energy costs for mining and processing, by-product costs and substitute costs. |
| <i>Other disruption scenario switches</i> | | | |
| Supply disruption | 2 | 1 (off) | When this switch is turned on, a supply disruption occurs for 1 year starting in 2030 and in 2045. The disruption affects the country that at that time has the largest share of nickel mining and it shuts down all mines in that country for a year. |
| Radical innovation | 2 | 1 (off) | When this switch is turned on, a radical new battery technology is discovered that does not require nickel. It occurs in 2035 and in 2050 and the effect in 2035 is that the substitution threshold for batteries is halved. The effect in 2050 is that the substitution threshold is halved again. |
| <i>Structural uncertainty switches</i> | | | |
| Paradigm switch | 2 | 2 (OCP) | FSP & OCP. The main paradigm used in this thesis is the OCP. This switch influences intensity changes, price elasticity changes, substitution and exploration. |
| Processing method energy allocation | 2 | 2 (full) | Mass based allocation and full allocation to nickel. Influences the percentage of energy costs for processing attributed to nickel. This switch also influences GHG emissions. |
| Mining energy allocation | 3 | 2 (price) | Mass based allocation, price-based allocation and ERC based allocation. Influences the percentage of mining energy costs attributed to nickel. |
| By-product inclusion | 2 | 1 (incl.) | Option to include or exclude by-products in determining costs and profit of the mines. |
| Price calculation | 2 | 2 (A&C) | Calculation based on days of demand in stock and calculation based on availability and consumption. The parameters contributing to these two methods were set in such a way that they lead to very similar results. Therefore, only one of the methods is used in the model, the calculation based on availability and consumption. |
| Option to mine resources | 2 | 1 (off) | Option to mine resources when no profit is being made, but the mine has not been mothballed yet. |

| <i>Sustainability policy switches</i> | | | |
|--|---|----------|---|
| EoL management of batteries | 4 | 2 (same) | Four EoL waste management strategies. One where the EoL waste management of batteries is worse than traditional uses of class 1 nickel, one where it is the same, one where it is better and one where there is further increased effort in managing battery waste. |
| Improved EV battery lifetime | 2 | 1 (off) | When this switch is turned on the EV battery lifetime doubles from 8 years to 16 years, the assumed lifetime of the vehicles. |
| Forward supply chain loss reduction | 2 | 1 (off) | When this switch is turned on, all losses occurring in the forward supply chain are halved. |
| <i>Unused switches (not included in the experimental set up, but potentially interesting to explore in future adaptations)</i> | | | |
| Energy calculation method | 3 | 1 | In addition to the main energy calculation method described in section I1.1, an additional method is included in the form of two different formulas (see section I1.2). |
| Vehicle calculation | 2 | 1 | This switch changes between two alternative methods for determining the number of vehicles. |
| Stockpiling inclusion | 2 | 1 (off) | This switch allows the inclusion of stockpiling. Further research is required how it can best be implemented. |

Table M2: key uncertainties in the model, their range and their base values. These variables are highlighted in yellow in tables F1, H1, J1 and L1. *Additional runs were done with values between 0.01 and 0.3.

| Uncertainty | Minimum | Maximum | Base value |
|--|----------------|----------------|-------------------|
| <i>Demand sub model</i> | | | |
| Substitution threshold batteries | 2.5 | 5 | 3.75 |
| Administration postponed demand | 0.5 | 2 | 1 |
| <i>Supply sub model</i> | | | |
| Power for price-based exploration | 0.5 | 1 | 0.75 |
| Opportunity check frequency | 2 | 3 | 2.5 |
| Global maximum capacity increase percentage* | 0.1 | 0.5 | 0.25 |
| Maximum capacity | 1E5 | 1E6 | 5.5E5 |
| Average mine operation plan | 10 | 20 | 15 |
| Average maximum profit deficit as percentage of investment | 0.03 | 0.08 | 0.05 |
| Average minimum profit surplus as percentage of investment | 0.03 | 0.08 | 0.05 |
| Average maximum mothball time | 10 | 30 | 20 |
| <i>Price sub model</i> | | | |
| Power for ore grades | 0.1 | 0.5 | 0.3 |
| Additional expenses for DSM | 2 | 20 | 10 |
| Minimum profit over investment | 1.2 | 2 | 1.6 |

Table M3: performance metrics assessed in the results.

| Performance metric | Unit | Elaboration |
|---|------------|---|
| <i>Main demand indicators</i> | | |
| Final nickel demand | Tonne/year | Annual nickel demand including price effects but excluding postponed demand |
| Cumulative final demand | Tonne | Total final nickel demand between 2015 and 2060 |
| <i>Additional demand indicators</i> | | |
| Total functional nickel demand | Tonne/year | Annual nickel demand excluding price effects and postponed demand. |
| Total substitution | Tonne/year | Substitution for all demand categories |
| Substitution of batteries | Tonne/year | Substitution for only batteries |
| Demand changes due to price elasticity | Tonne/year | Increase or reduction in demand due to price elasticity |
| Demand request | Tonne/year | Annual nickel demand including price effects and postponed demand |
| Postponed demand | Tonne/year | Demand that has not been fulfilled in the year that it occurred and is to be fulfilled at a later time |
| Nickel demand for vehicle batteries | Tonne/year | Nickel demand for batteries in EVs |
| Nickel demand for electricity generation | Tonne/year | Nickel demand for stainless steel in electricity generation technologies |
| Nickel demand for stationary batteries | Tonne/year | Nickel demand for batteries for stationary purposes |
| Nickel demand for the RoE | Tonne/year | Nickel demand for stainless steel and other applications in the RoE |
| <i>Main supply indicators</i> | | |
| Nickel mining | Tonne/year | Annual nickel mining, excluding mining losses. |
| Cumulative mined nickel | Tonne | Total mined nickel between 2015 and 2060 |
| <i>Additional supply indicators</i> | | |
| Nickel processing | Tonne/year | Annual nickel processing, excluding processing losses. |
| Cumulative mined cobalt | Tonne | Total mined cobalt between 2015 and 2060 |
| Cumulative mined palladium | Tonne | Total mined palladium between 2015 and 2060 |
| Fraction of mines per mine type | Dmnl | Fraction of mines that are OC |
| Fraction of mines per ore type | Dmnl | Fraction of mines that are laterite mines |
| Depletion of original resources | Tonne | Cumulative mined nickel and cumulative mining losses subtracted from the original resource total in the database by Mudd (2020) |
| Total operating mining capacity utilisation | Dmnl | Share of the operating mining capacity that is being used at a certain point in time |
| Total exploration | Tonne/year | Indicates the total exploration done by the different mines in the model. |
| <i>Main economic indicator</i> | | |
| Average periodic nickel price | \$/tonne | Average nickel price per quarter |
| <i>Additional economic indicators</i> | | |
| Degree of nickel scarcity | Dmnl | Annual consumption over availability |
| Average nickel marginal costs | \$/tonne | Annual average marginal costs for nickel |

| | | |
|---|--------------------------------|---|
| Average nickel royalties | \$/tonne | Annual average royalties for nickel |
| Reagents and other marginal costs | \$/tonne | Annual average costs for reagents and other costs. Set at 4750 \$/tonne, but included here anyway so all costs are represented. |
| Average credits for by-products | \$/tonne | Annual average costs allocated to by-products |
| Average marginal costs deposits | \$/tonne | Annual average marginal costs for the whole deposits, including both nickel and by-products. |
| Average energy costs | \$/tonne | Total annual average marginal costs for energy use |
| Average energy costs mining | \$/tonne | Annual average marginal costs for energy use for mining |
| Average energy costs smelting & refining | \$/tonne | Annual average marginal costs for energy use for smelting and refining |
| Average carbon costs | \$/tonne | Annual average costs for GHG emissions |
| Average electricity price | \$/GJ | Annual average electricity price |
| <i>Main sustainability indicators</i> | | |
| Average final energy use | GJ/tonne | Total average final energy use |
| Average ore grade of existing mines | Dmnl | Average ore grade of operating and mothballed mines |
| Average ore grade of known deposits | Dmnl | Average ore grade of all deposits in the database by Mudd (2020) |
| Cumulative GHG emissions | Tonne CO ₂ -eq | Total GHG emissions between 2015 and 2060 |
| Total EoL RR | Dmnl | Average EoL RR of class 2 and class 1 nickel combined |
| <i>Additional sustainability indicators</i> | | |
| Average final energy use mining | GJ/tonne | Average final energy use for mining |
| Average final energy use processing | GJ/tonne | Average final energy use for processing. This does not include refining |
| Total final energy use | GJ/year | Total annual final energy use of all mines combined |
| Total GHG emissions | Tonne CO ₂ -eq/year | Total annual final GHG emissions of all mines combined |
| Total recycling | Tonne/year | Total annual secondary production of nickel |
| Recycling input rate | Dmnl | Share of total nickel consumption from recycled nickel |

Appendix N: Additional results

This appendix includes some results that were not deemed relevant enough to be included in the main text but could nevertheless be interesting. The order of the results presented here is the same order as the results presented in the main text.

Appendix N1: Additional demand projections

Figure N1 shows the impact of the selection of the electrification or hydrogen transportation scenario on final nickel demand and substitution. On average, the nickel demand in the hydrogen scenario is higher. This is partially because there is more substitution in the electrification scenario, but mostly due to a highly uncertain assumption of the nickel intensity of hydrogen tanks based on Tokimatsu et al. (2018). Therefore, until further research is done on the nickel requirements of hydrogen infrastructure, this result should be treated with caution and all other figures are based solely on the electrification scenario.

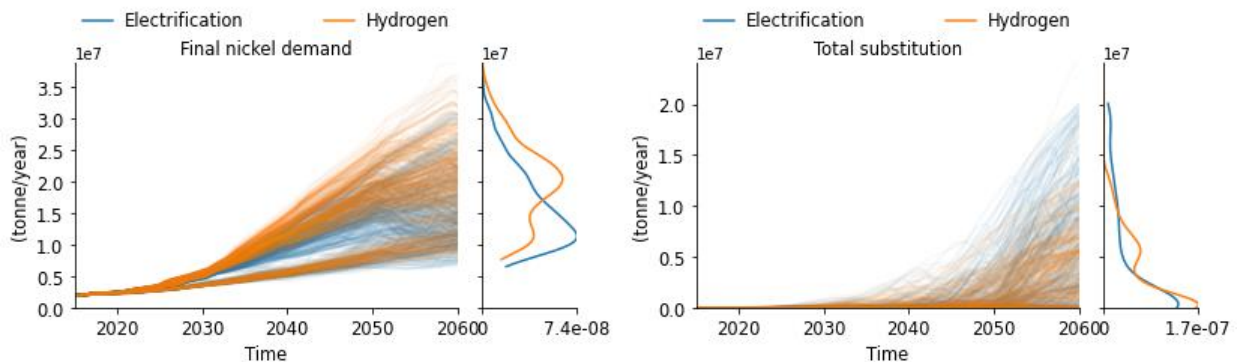


Figure N1: impact of the transport scenario on final demand and substitution.

Figure N2 shows demand change due to price elasticity and battery substitution, which both increase as total functional demand increases. Figure N3 shows demand request and postponed demand for both the OCP and the FSP. In the FSP, postponed demand and the demand request become very high because supply is not able to fulfil demand and price effects like substitution don't occur. The impact of postponed demand can be seen by comparing final demand with demand request.

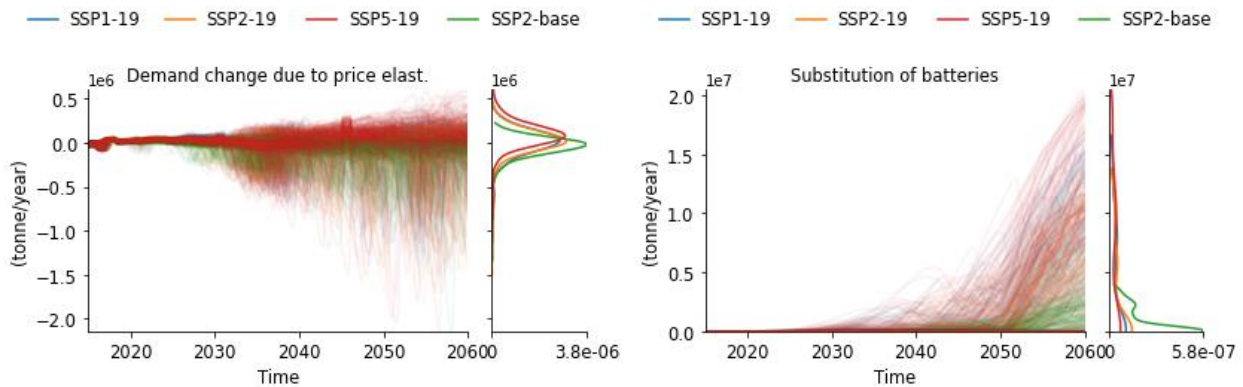


Figure N2: demand change due to price elasticity and battery substitution per assessed SSP.

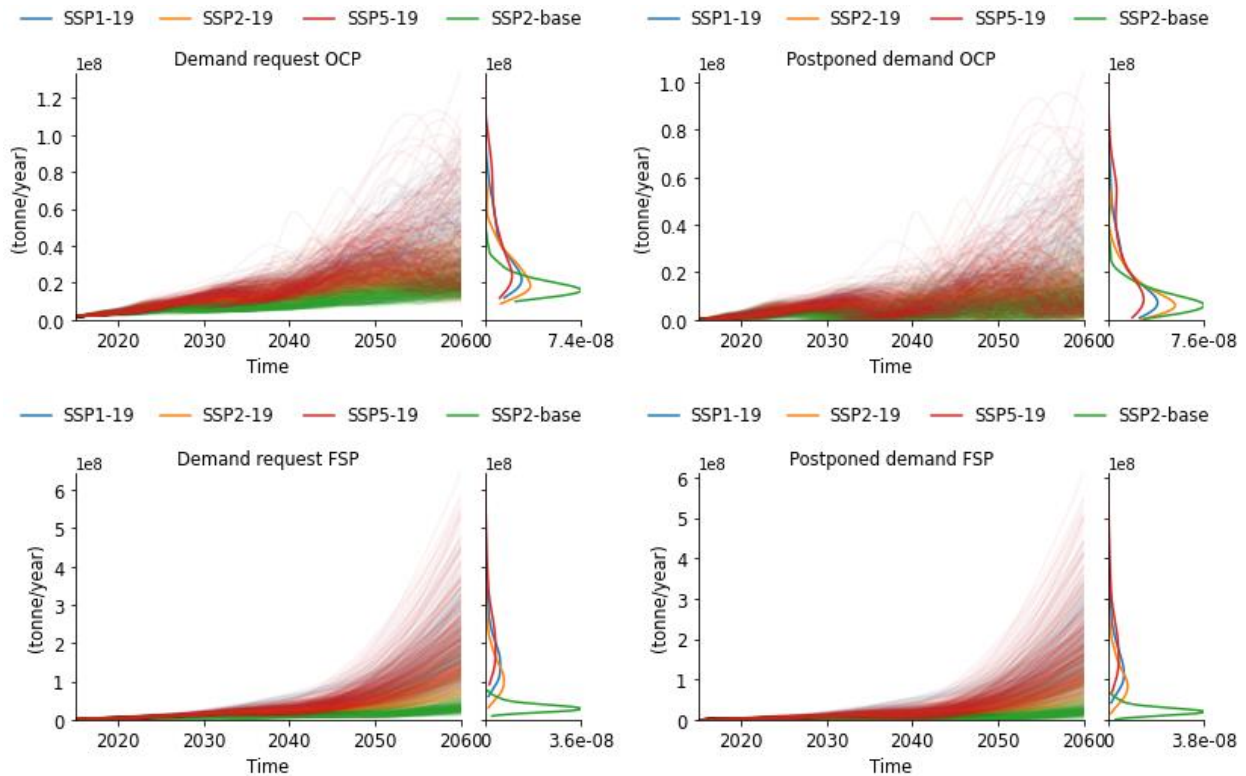


Figure N3: demand request and postponed demand for the OCP (top) and the FSP (bottom).

Figure N4 shows the relative impact of electricity generation capacity and SBS to total nickel demand. The fluctuation in the nickel demand for electricity generation capacity is caused by the discrete implementation. This is something that could potentially be adapted in future versions of the model, but it does not have a large impact on the overall results.

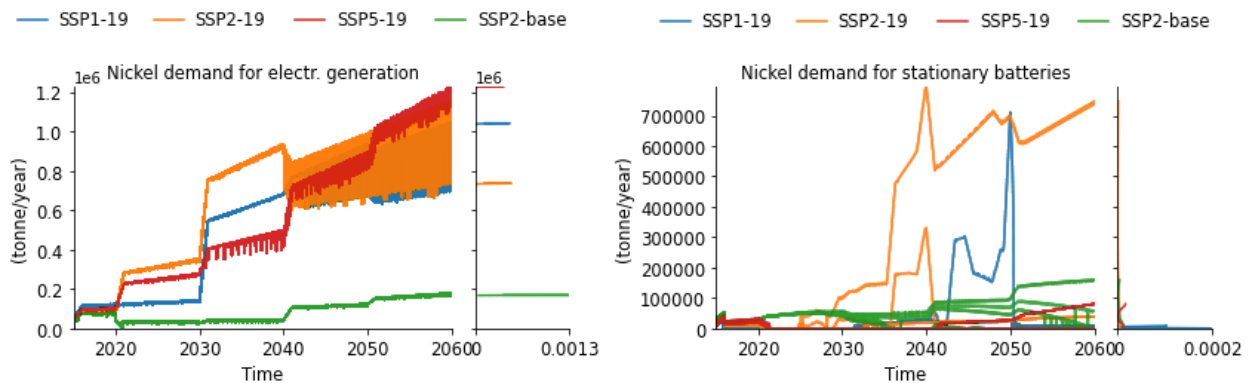


Figure N4: nickel demand for electricity generation capacity and SBS per SSP.

Most nickel is required for SBS in the SSP2 scenarios because of the lower GDP per capita in these scenarios, which means a lower number of vehicles is projected, including EVs that can be used for V2G storage and battery repurposing. SSP2-19 has a higher share of EVs than SSP2-baseline in earlier years, which is why SSP2-baseline requires the most nickel for stationary storage initially. Then, because SSP2-19 has a slightly lower GDP per capita than SSP2-baseline and a higher VRE share, most nickel for new SBS is required for SSP2-19.

In all scenarios, SBS contributes to a relatively small share of the total nickel demand. This is because most storage is covered by PHS, CSP TES, V2G and battery repurposing. When the hydrogen scenario is included, the electrification transportation scenario leads to slightly lower SBS requirements, because there is more V2G. Storage requirements are also avoided through other flexibility measures.

The impact of the flexibility scenarios is shown in figure N5. The choice of flexibility scenario makes a difference for SBS requirements. For the ET scenarios, nickel is only required for new SBS in the low flexibility scenario. However, because this storage is not much, the choice of flexibility scenario is negligible for the final nickel demand. Figure N5 also shows that when EV batteries have a shorter lifetime, less SBS is required due to the repurposing of EV batteries. However, this leads to a relatively small additional nickel demand compared to the savings obtained when increasing EV battery lifetime.

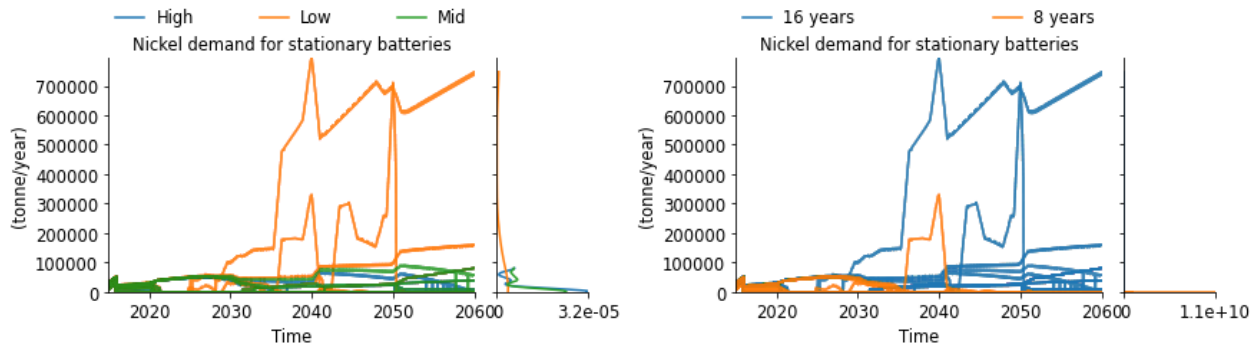


Figure N5: nickel demand for SBS per flexibility scenario and for EV battery lifetime.

Appendix N2: Additional BAU single run results

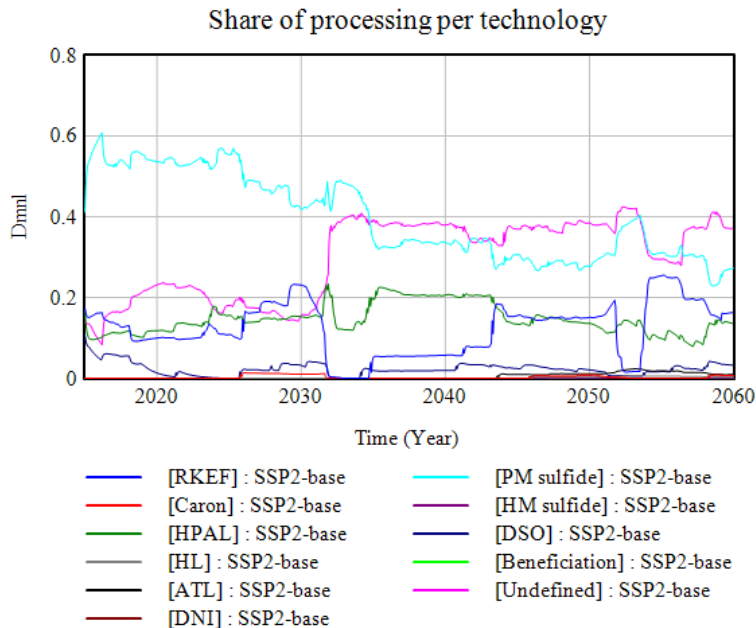


Figure N6: share of processing per technology for a single run with base settings. Shares differ per run. Assumptions: DSO = BF, beneficiation = PM sulfide, undefined = HPAL.

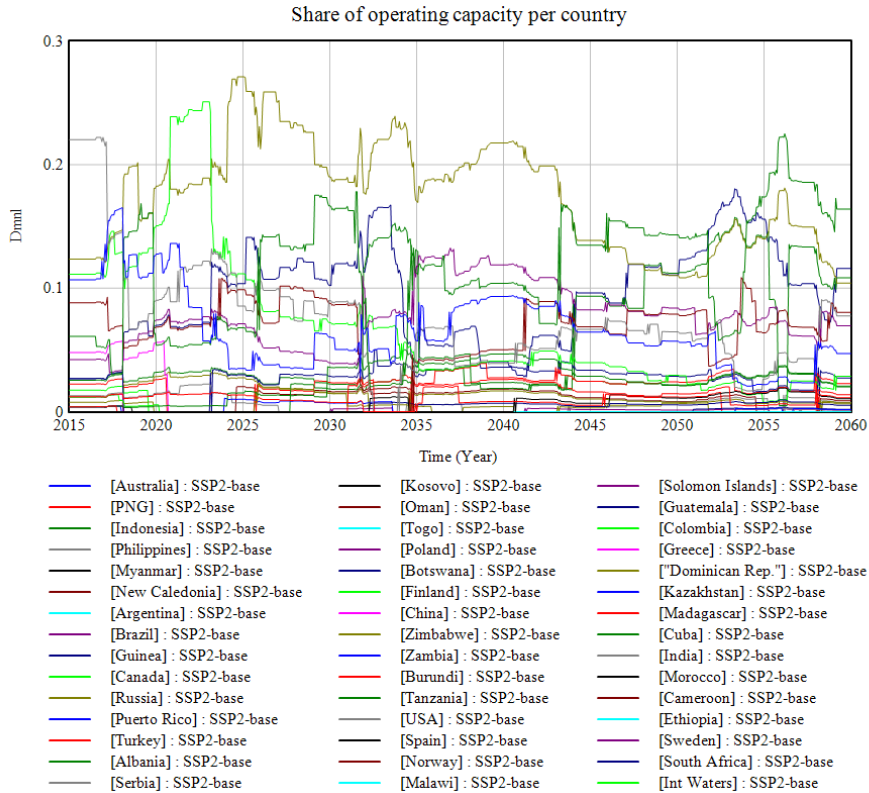


Figure N7: share of operating capacity per country for a single run with base settings. Shares differ per run. Because multiple colours are repeated, it is not always clear which country a certain line refers to. However, this figure is meant for illustrative purposes. Further information can be obtained by running the model.

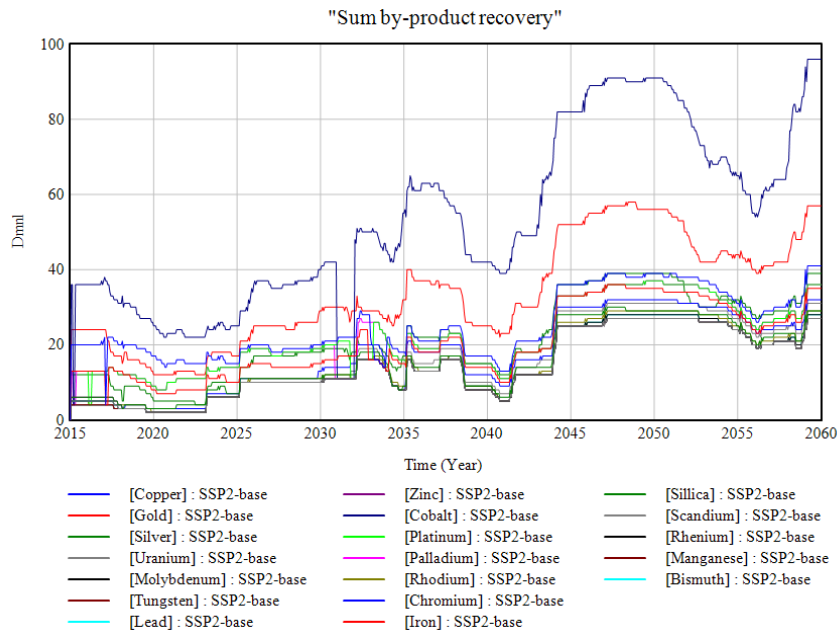


Figure N8: number of mines from which certain by-products are recovered for a single run with base settings. Values differ per run. Because multiple colours are repeated, it is not always clear which by-product a certain line refers to. However, this figure is meant for illustrative purposes. Further information can be obtained by running the model.

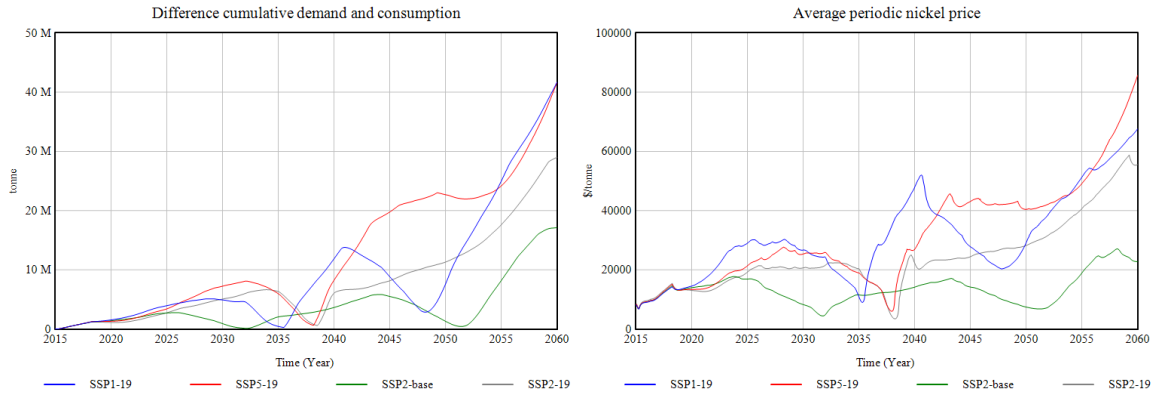


Figure N9: resilience for the four assessed SSPs for single runs with base settings (only varying the SSPs). On the left, the difference between cumulative demand and consumption is shown in tonne. On the right, the average periodic nickel price is shown in \$/tonne. Behaviour differs per run, however, in general, the resilience is higher for the BAU scenario (SSP2-baseline) than for the ET scenarios.

Appendix N3: Additional energy transition results

Figure N10 shows the average marginal costs for royalties and for reagents and other costs. Royalties fluctuate with price as they are a certain fraction of the price. This fraction changes as the nickel share from certain countries changes, but this effect is less visible. Reagents and other costs were assumed to remain constant at 4750 \$/tonne.

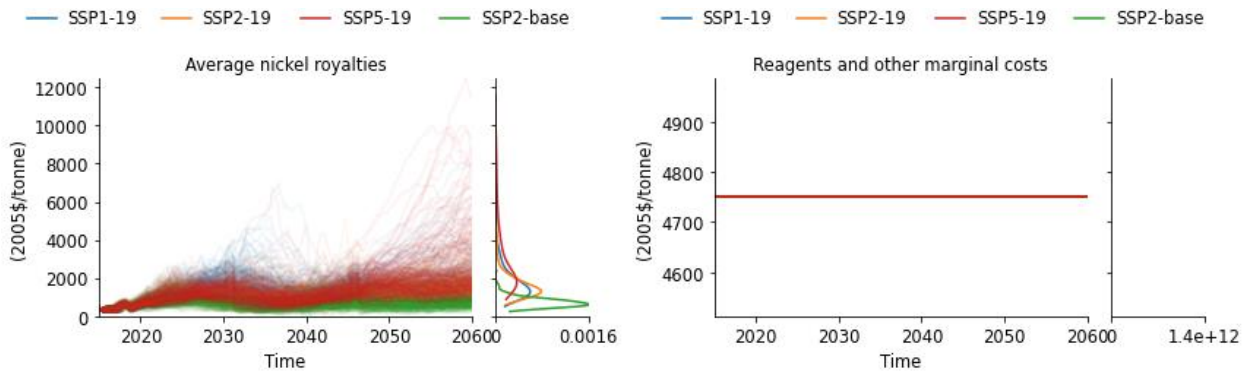


Figure N10: average marginal costs for royalties and reagents and other costs.

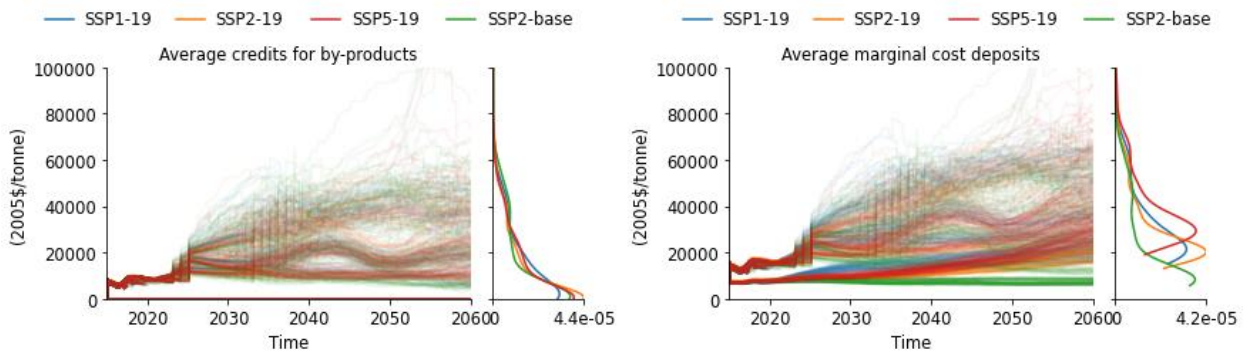


Figure N11: by-product credits and average marginal costs for deposits. Values go up to about 250000 2005\$/tonne for both figures, but they were cut off at 100000 2005\$/tonne for better clarity.

Figure N11 shows by-product credits and the average marginal costs for deposits. The average marginal costs for nickel shown in figure 3.7 (main text) equal the average marginal costs for deposits minus the average credits for by-products. The height of this credit is based on the by-product composition and on mining energy allocation. In figure N11, there are two distinct pathways for average marginal costs for deposits. This is based on the choice to include or exclude by-products in the model.

Figure N12 shows average final energy use for mining and processing. For mining, final energy use is determined by mine type, ore grade and efficiency improvements. For processing, it is determined by efficiency improvements, the processing energy allocation method, and the processing method (which depends i.a. on ore type). Single run results for the fraction of each processing method were shown in figure N6. This shows that the share of more energy intensive processing methods increases over time.

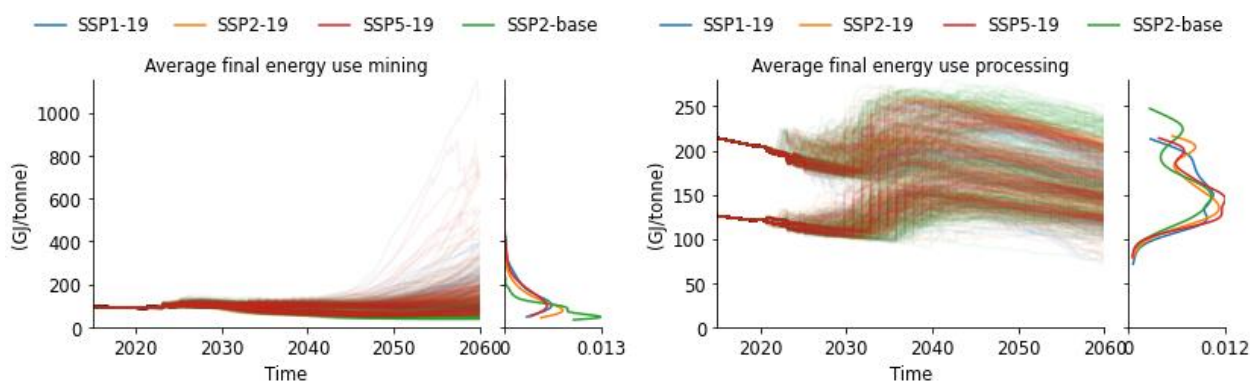


Figure N12: average final energy use for mining and processing (this does not include refining).

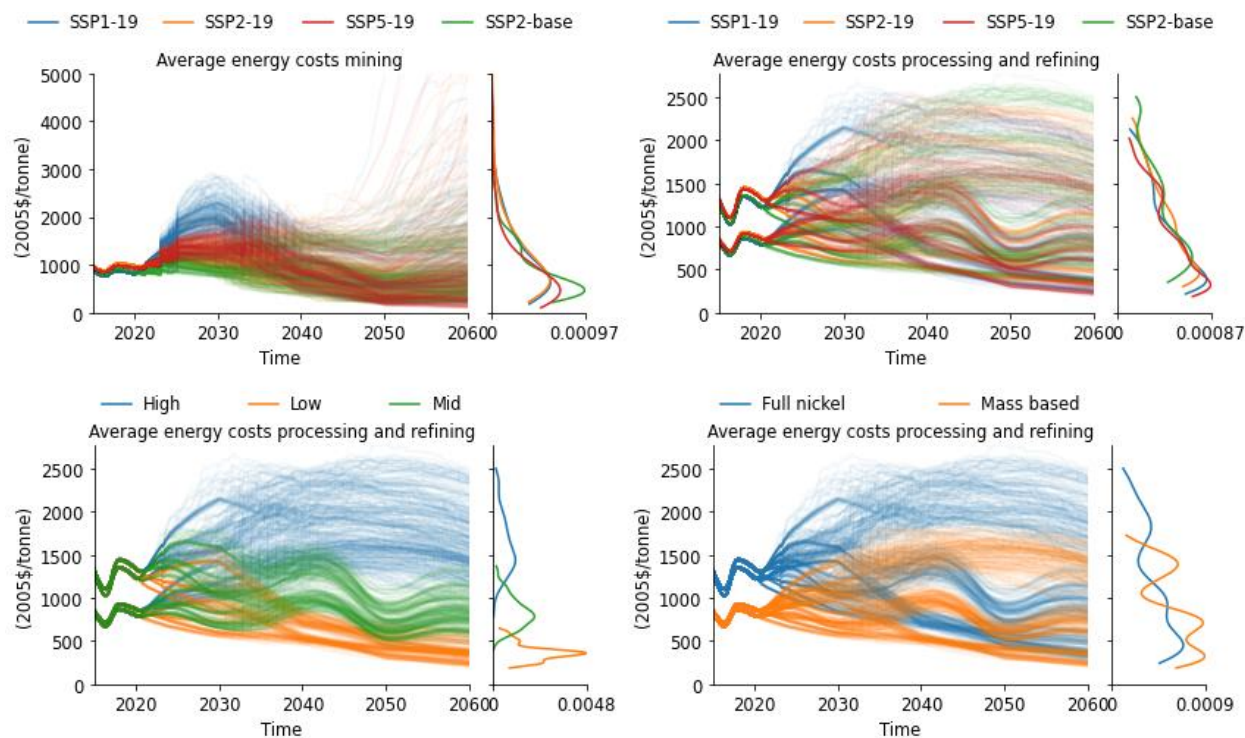


Figure N13: average energy costs for mining (up to 14000 2005\$/tonne, but cut off for clarity) per SSP (top left) and average energy costs for processing & refining per SSP (top right), per fuel price scenario (bottom left) and per processing energy allocation method (bottom right).

Figure N13 shows average energy costs for mining, processing and refining. For mining, costs increase first in the ET scenarios (mostly due to carbon price), after which they gradually decrease in most runs (due to efficiency improvements and a reduction in carbon emissions), but increase rapidly in some (due to decreasing ore grades). In the BAU scenario, the influence of the fuel price (appendix I1.3) is visible.

The three fuel price scenarios are also visible in the average energy costs for processing and refining, and so are energy efficiency improvements as a downward trend is visible over time. The rest of the differences are determined by the mix of processing methods which depends on the deposit types of the existing mines at a certain time. The processing energy allocation method also has a large impact.

Figure N14 shows the total annual final energy use and total annual GHG emissions of all mines combined. The total final energy use by 2060 ranges between about 0.2 PJ/year and 30 EJ/year, with the values for most runs between 0.5 and 5 EJ. The annual total GHG emissions by 2060 range between about 1E4 and 5.5E8, with the values for most runs between 2E7 and 3E8 tonne CO₂eq/year. Due to the large annual fluctuations in the model, the extremes are deemed less relevant than the values with the highest density. The total GHG emissions of the ET scenarios first increase and then become lower over time due to the increasing share of renewable energy.

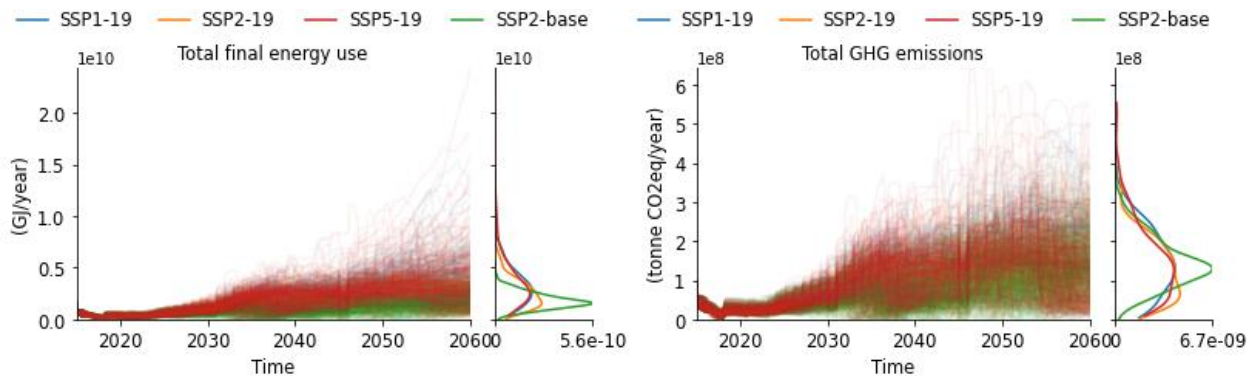


Figure N14: total annual final energy use and total annual GHG emissions of all mines combined.

Figure N15 shows the results for multiple runs for mine type (OC) share and ore type (laterite) share. This figure shows that over time a higher share of laterites is being mined, which leads to higher energy costs for processing. However, because most laterites have OC mines, the share of OC mining increases which leads to lower energy costs for mining.

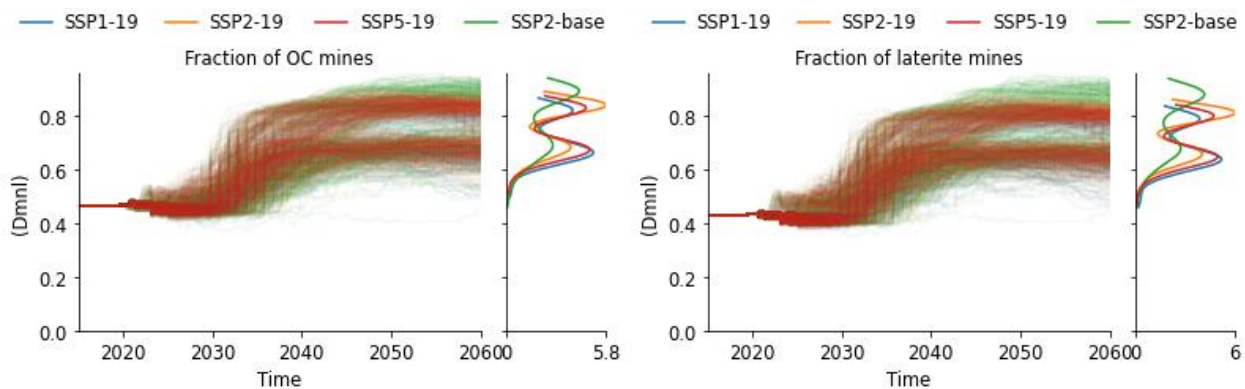


Figure N15: fraction of existing mines per mine type and per ore type.

Appendix N4: Additional results for other disruptions

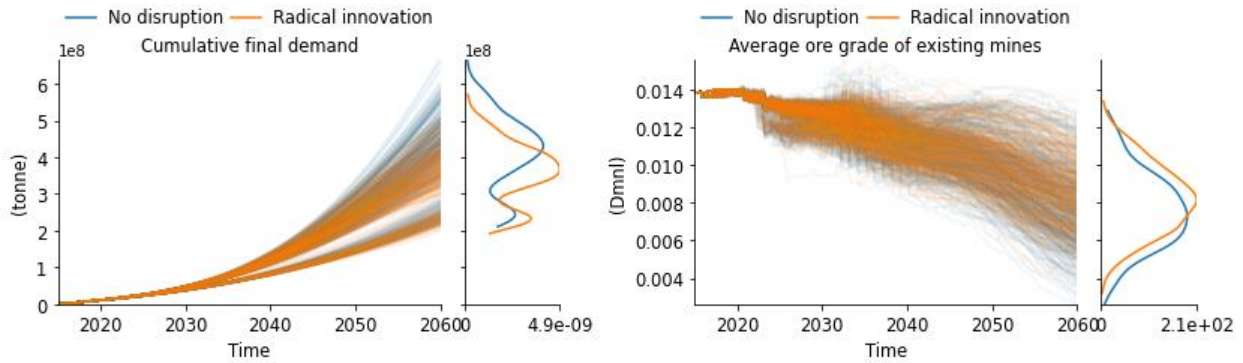


Figure N16: additional results for the radical battery innovation disruption.

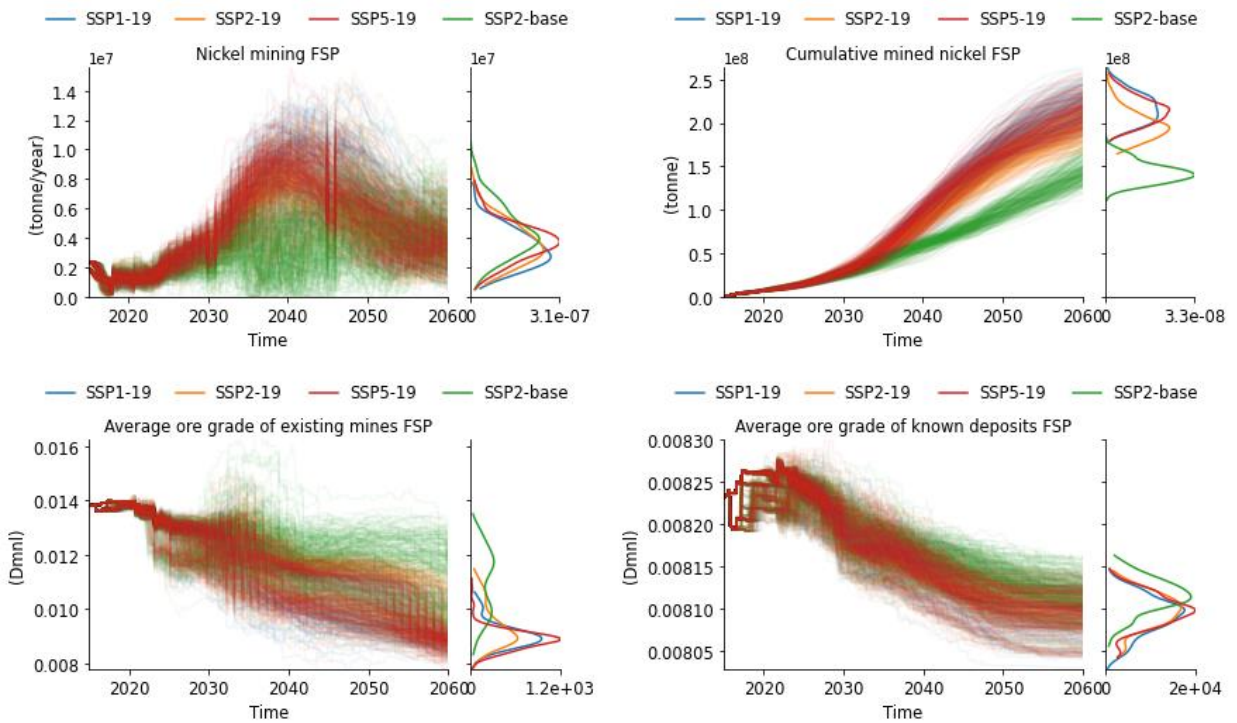


Figure N17: additional results for the FSP. As more resources are depleted, less can be mined and cumulative mined nickel levels off. The results for ore grade are based purely on what was included in the database by Mudd (2020) and the order in which specific mines are commissioned and decommissioned.

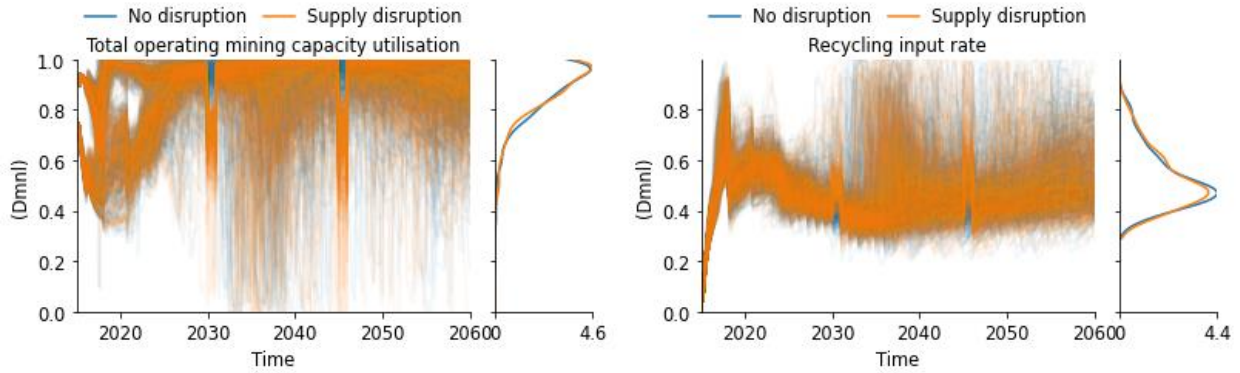


Figure N18: additional results for the influence of a 1-year supply disruption in 2030 and 2045, where mining stopped in the country with the largest share of supply at those times. The supply disruption is visible in the total operating mining capacity utilisation, as certain mines stop producing without necessarily being mothballed, and in the recycling input rate, where the share of recycled nickel in final nickel availability increases as less primary nickel is available.

Appendix N5: Additional sustainability policy results

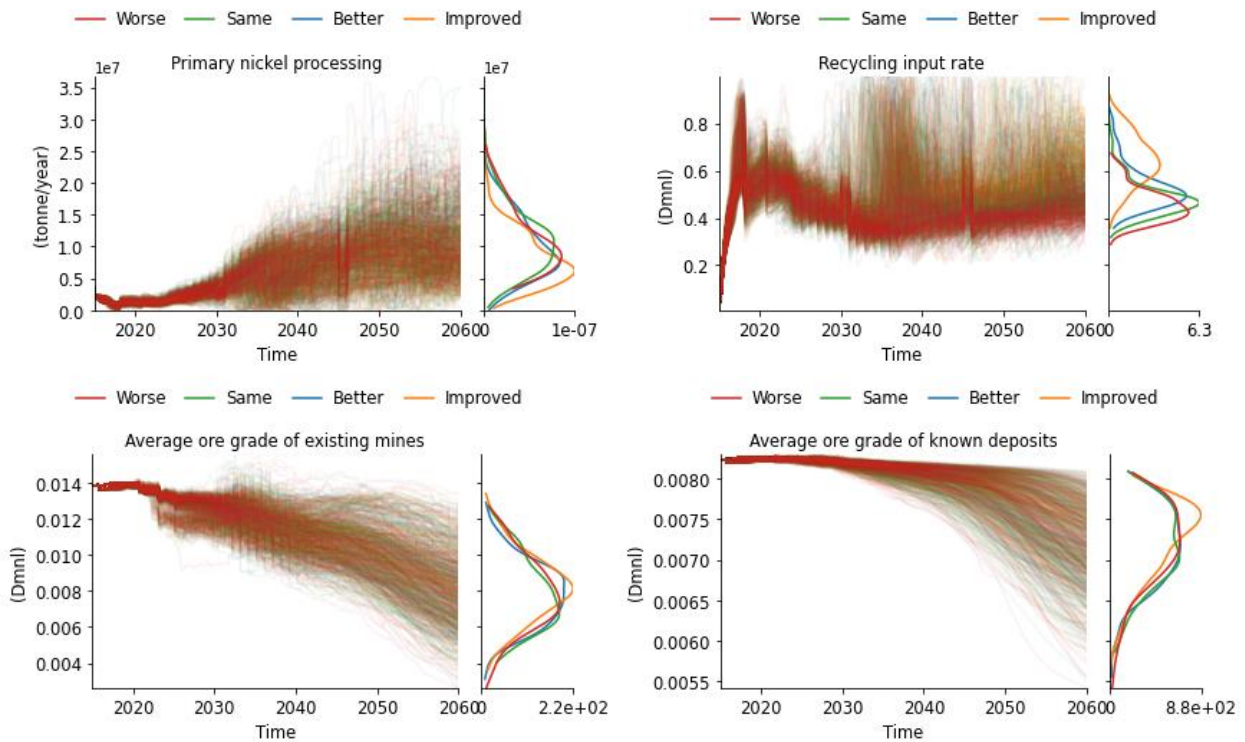


Figure N19: additional results for EoL waste management.

Figure N20 shows total recycling per EoL waste management strategy and per SSP. It logically follows that a better recycling strategy with a higher EoL RR also leads to more recycling. In addition, there is more recycling in the ET scenarios than in the BAU scenarios. This is likely because there is more demand in the ET scenarios and therefore also more waste, and because the share of batteries is larger and batteries have a much shorter lifetime than stainless steel, thereby ending up in scrap faster.

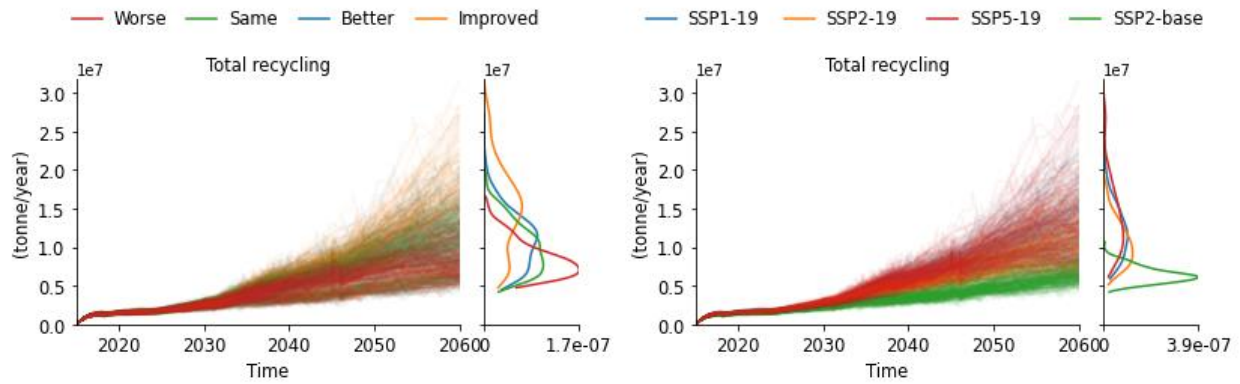


Figure N20: total recycling per EoL waste management strategy and per SSP.

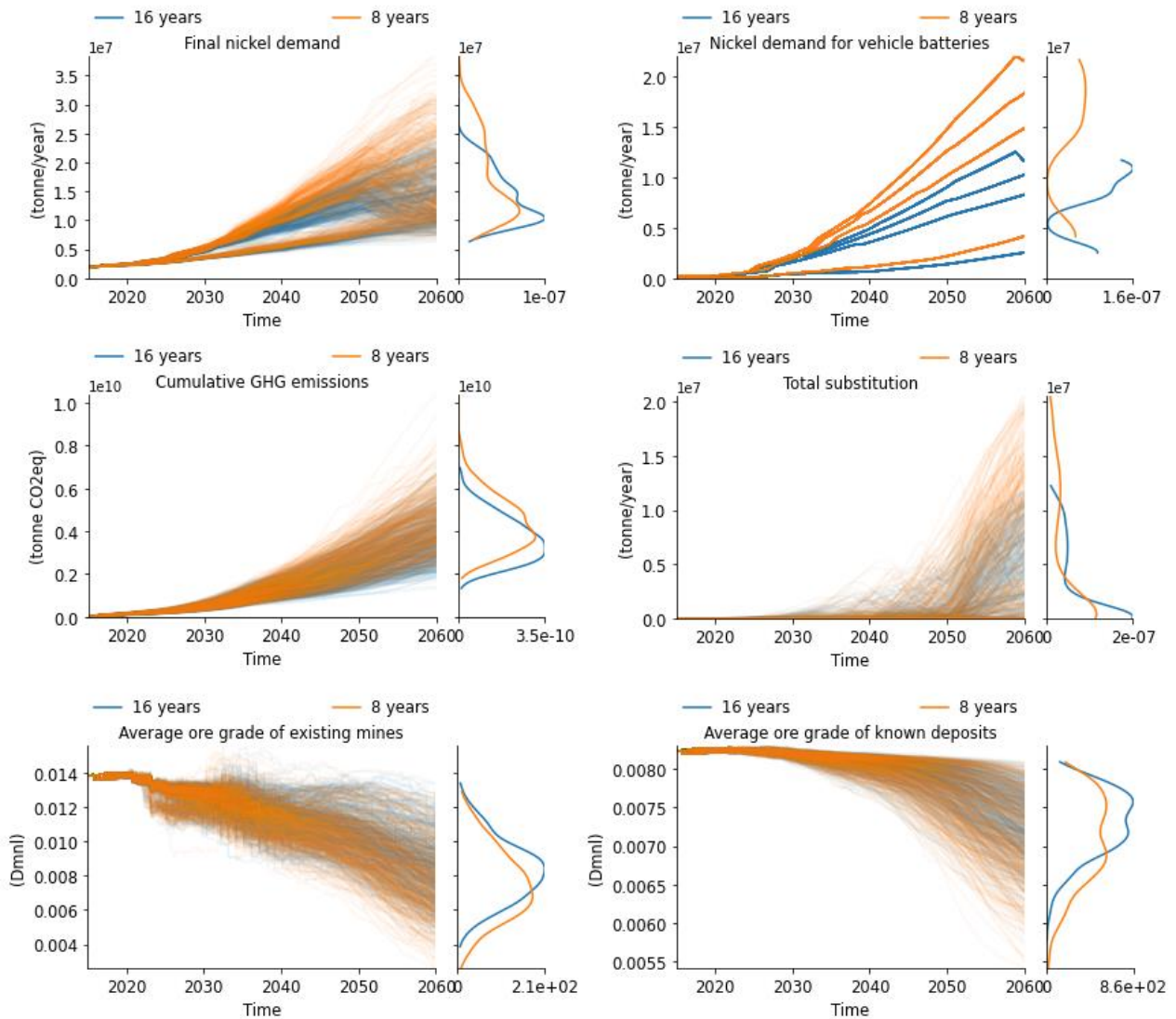


Figure N21: additional results for EV battery lifetime increase.

Appendix N6: Additional structural uncertainty results

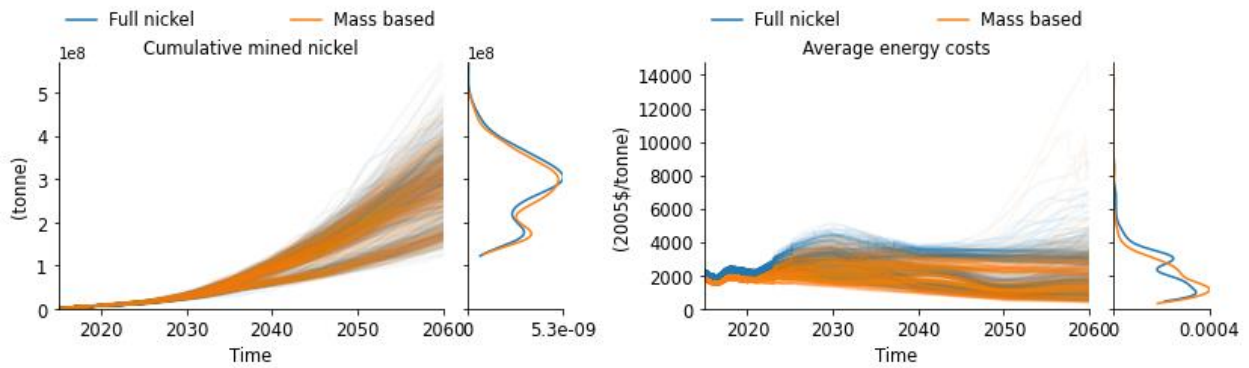


Figure N22: additional results for processing energy allocation method.

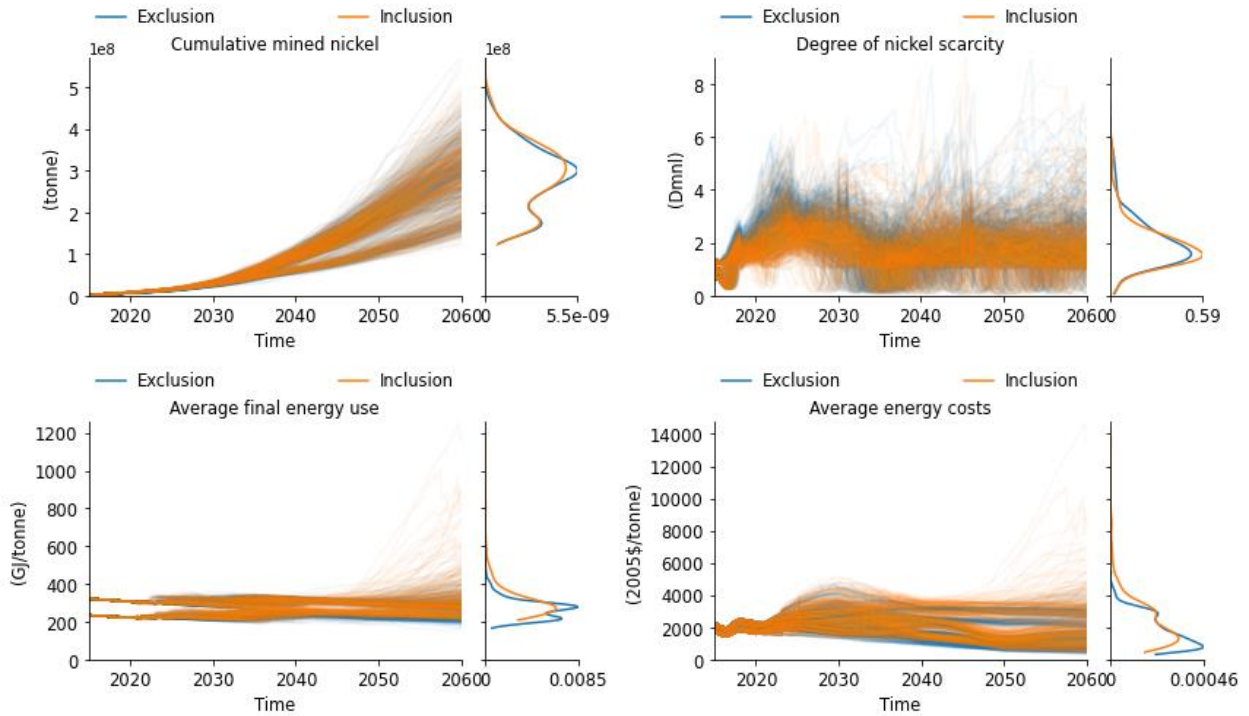


Figure N23: additional results for by-product inclusion.

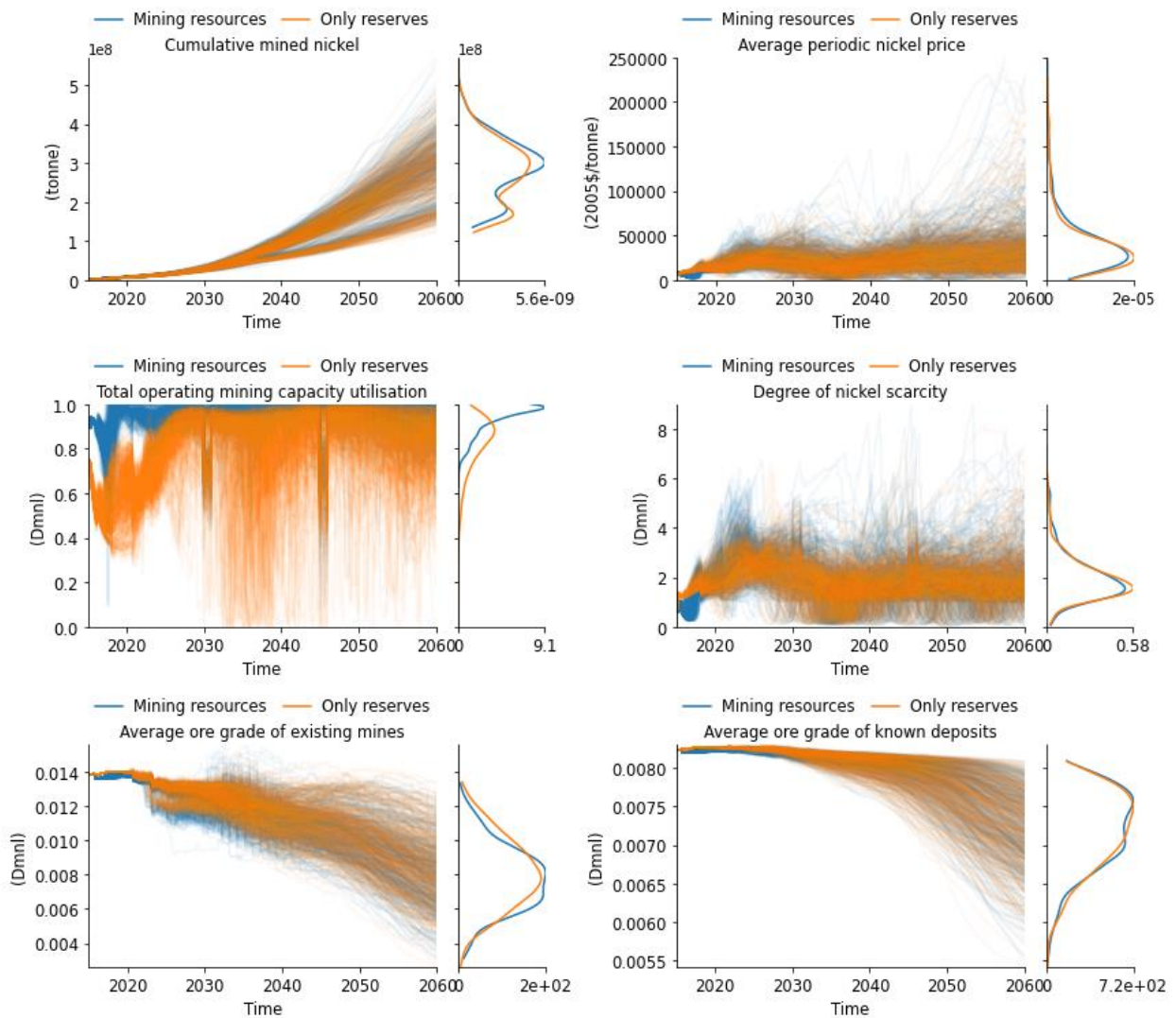


Figure N24: results for the option to mine resources just before a mine is potentially mothballed. This leads to a much higher and more realistic operating mining capacity utilisation, as well as to more cumulative mined nickel and different points in time for the peaks and troughs of the cycles in average periodic nickel price.

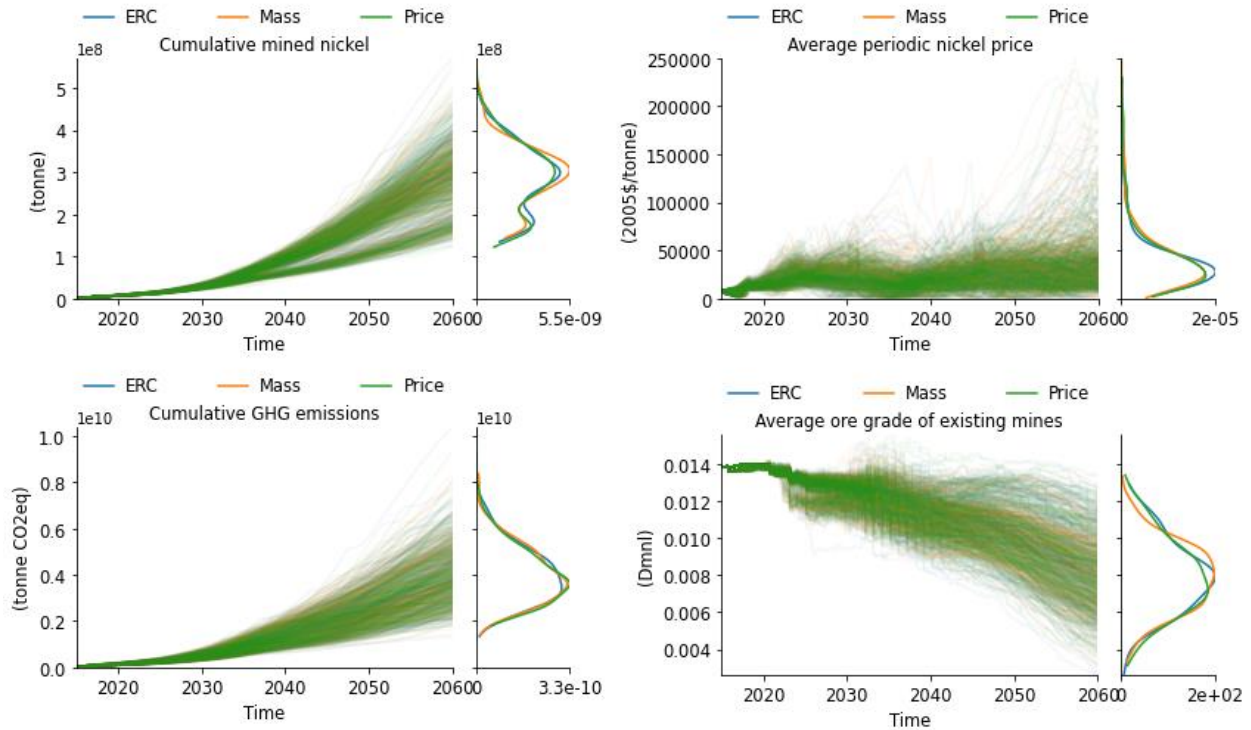


Figure N25: results for the mining energy allocation method.

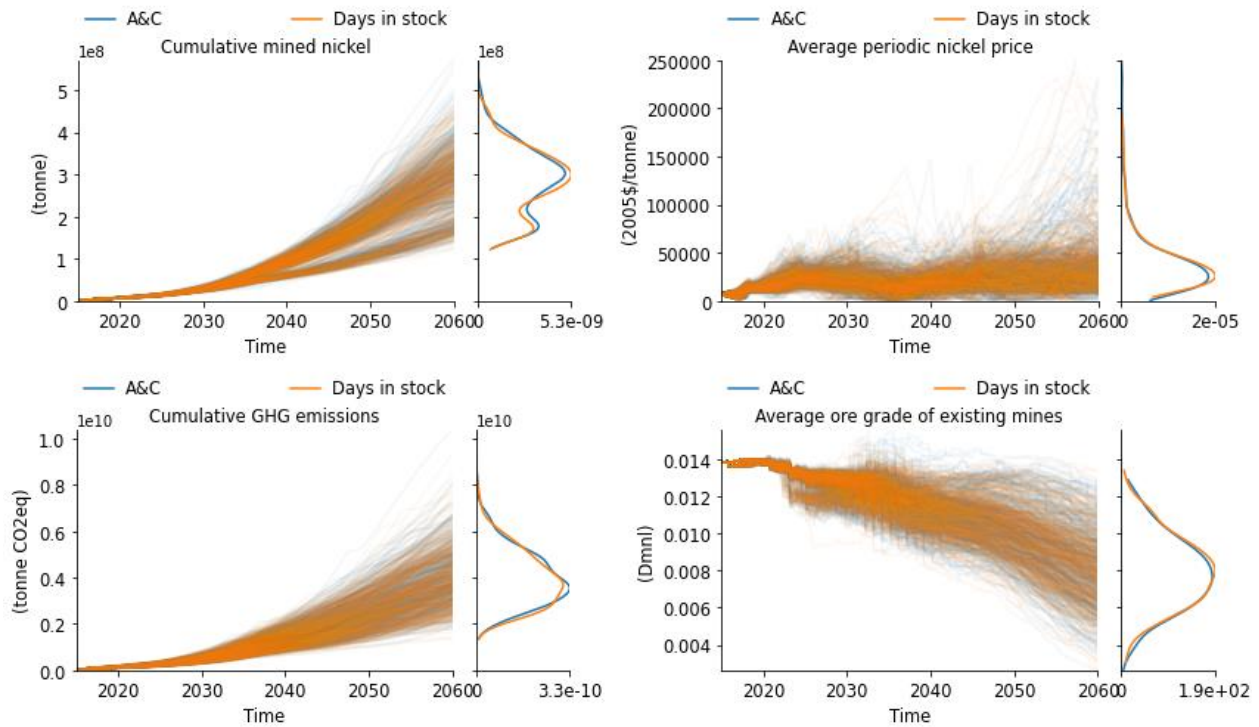


Figure N26: results for the price method. A&C = availability and consumption.

Appendix N7: Identification of influential parameters

The graphs below are usually generated with a much larger number of runs than 1000, so they should be considered as crude results. However, they were simply used for further exploration of certain influential parameters. Further results can be generated for all these figures, but the focus in the current work was on average periodic nickel price as an indicator for resilience, and average final energy because of the interest in the material-energy nexus. In future research other performance metrics could be assessed in more detail and more runs could be done to create more robust versions of the figures below.

Average periodic nickel price

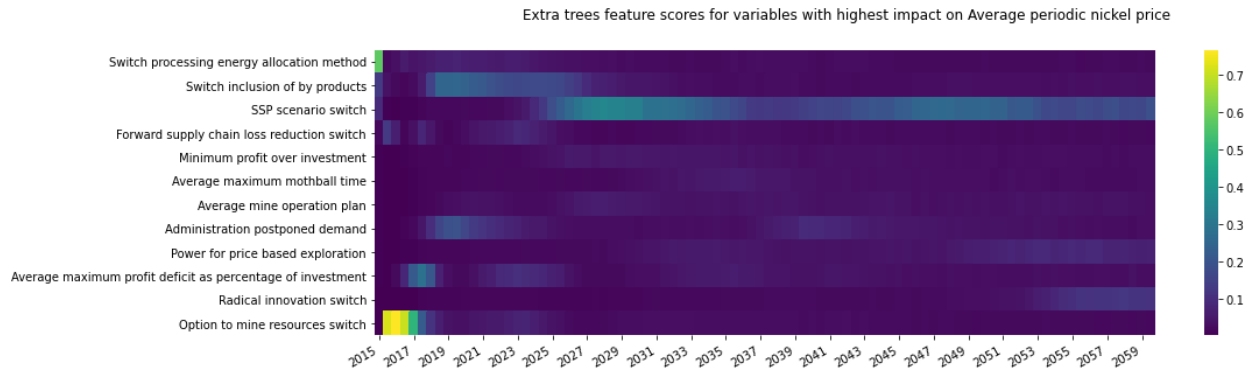


Figure N27: variables with the highest impact on average periodic nickel price at different points in time. Average periodic nickel price is impacted most by the SSPs in later years. At the start, the option to mine resources, the inclusion of by-products and the processing energy allocation method play an important role. The impacts of radical innovation are also visible. Parameters that have a large impact are average maximum profit deficit as percentage of investment, administration of postponed demand and power for price-based exploration.

Average final energy use

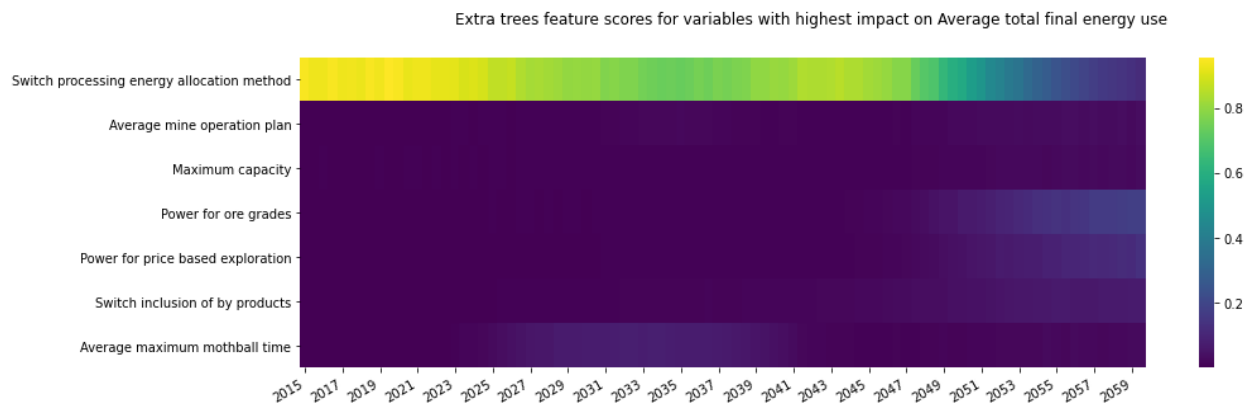


Figure N28: variables with the highest impact on average final energy use at different points in time. The processing energy allocation method switch has the largest impact by far. The parameter with the largest impact in intermediate years is average maximum mothball time. The parameter with the largest impact in later years, where, in some cases, average final energy use shoots up, is the power for ore grades. The power for price-based exploration also has an impact in later years.

Final nickel demand

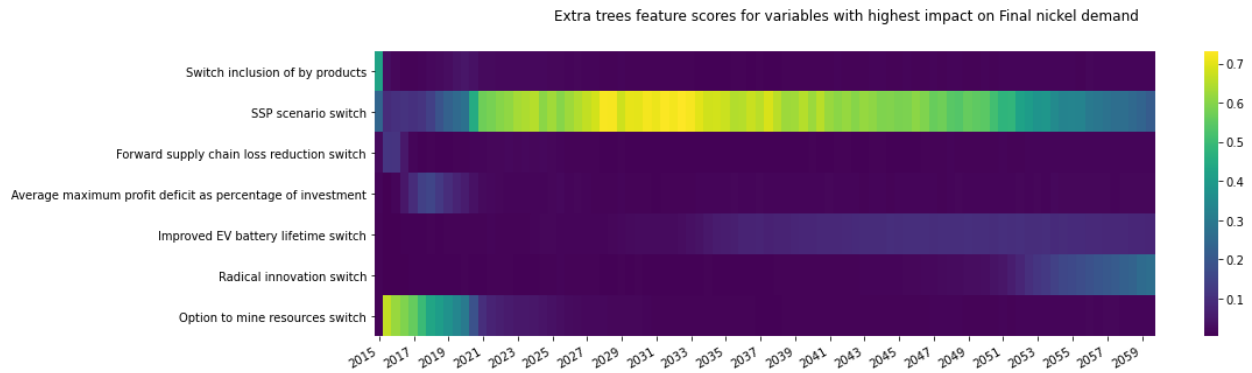


Figure N29: variables with the highest impact on final nickel demand at different points in time.

Nickel mining

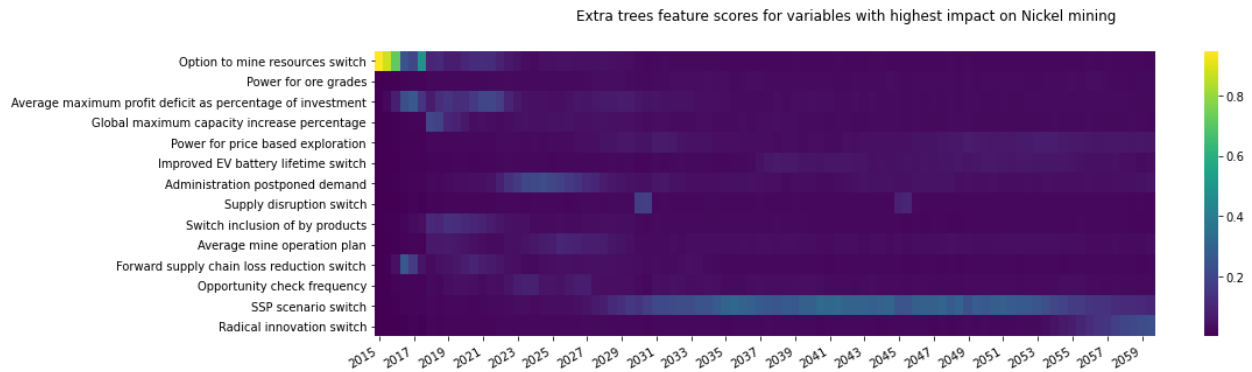


Figure N20: variables with the highest impact on nickel mining at different points in time.

Average ore grade of existing mines

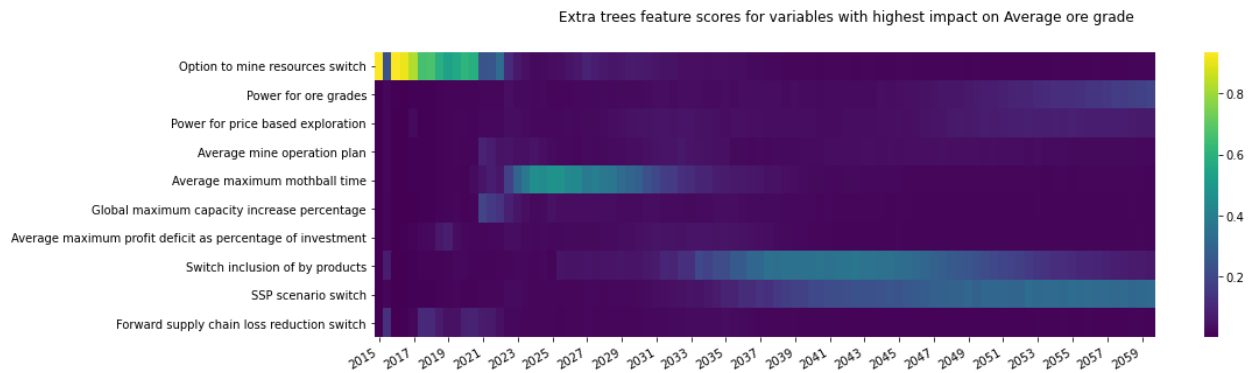


Figure N31: variables with the highest impact on average ore grade of existing mines at different points in time.

Average ore grade of all deposits

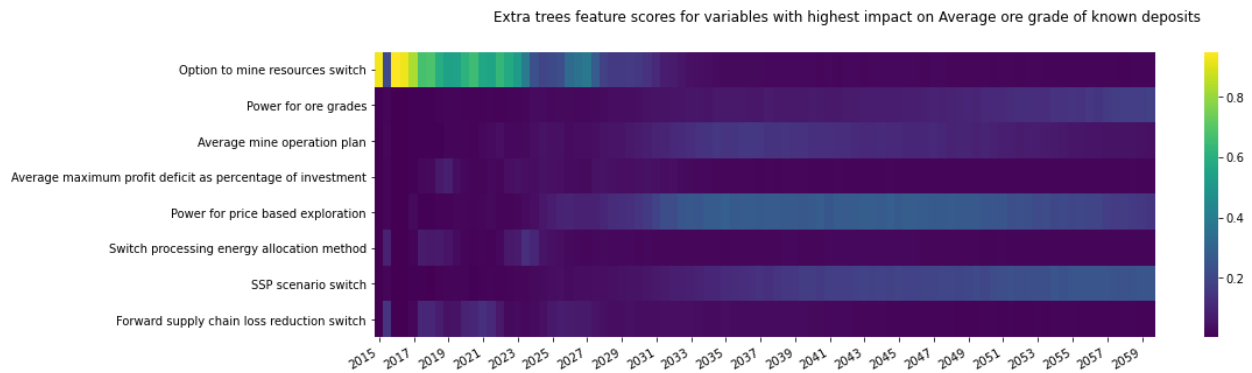


Figure N32: variables with the highest impact on average ore grade of all deposits at different points in time.

Cumulative GHG emissions

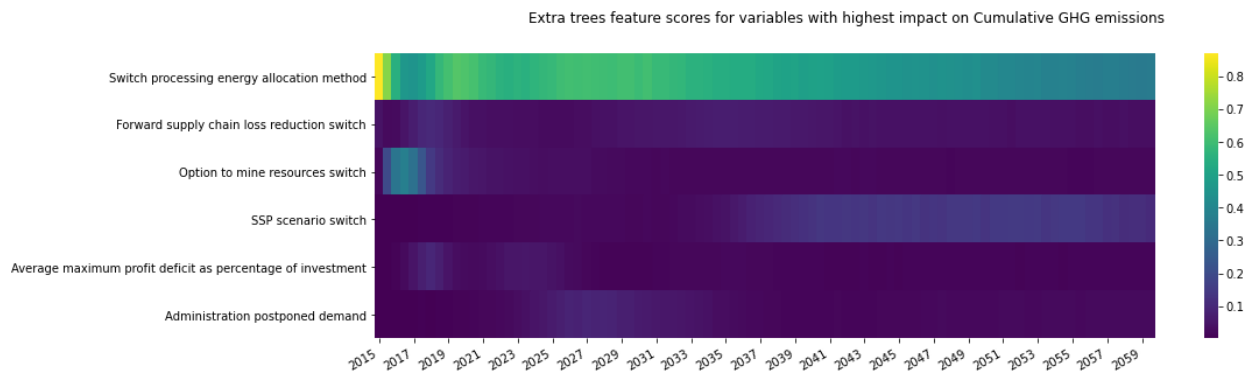


Figure N33: variables with the highest impact on cumulative GHG emissions at different points in time.

EoL RR

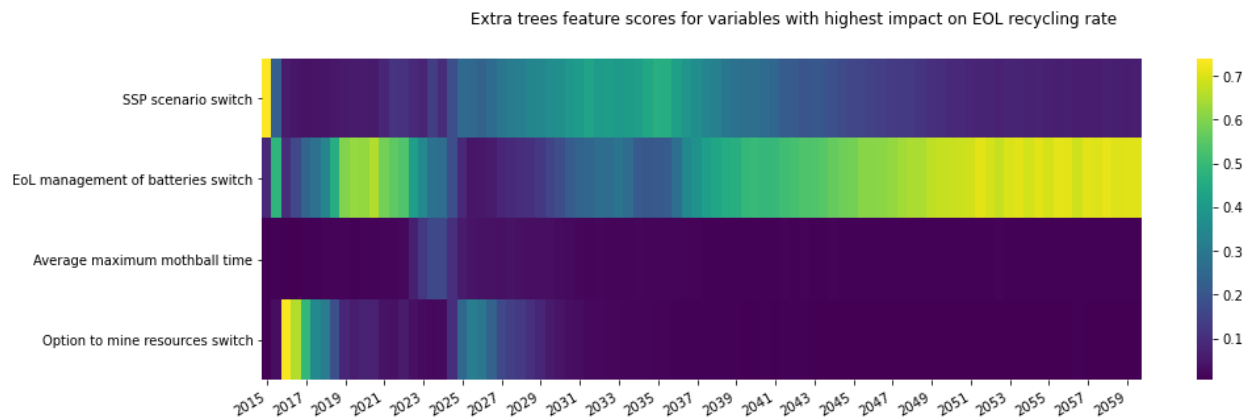


Figure N34: variables with the highest impact on EoL RR at different points in time.

Appendix N8: Additional parametric uncertainty results

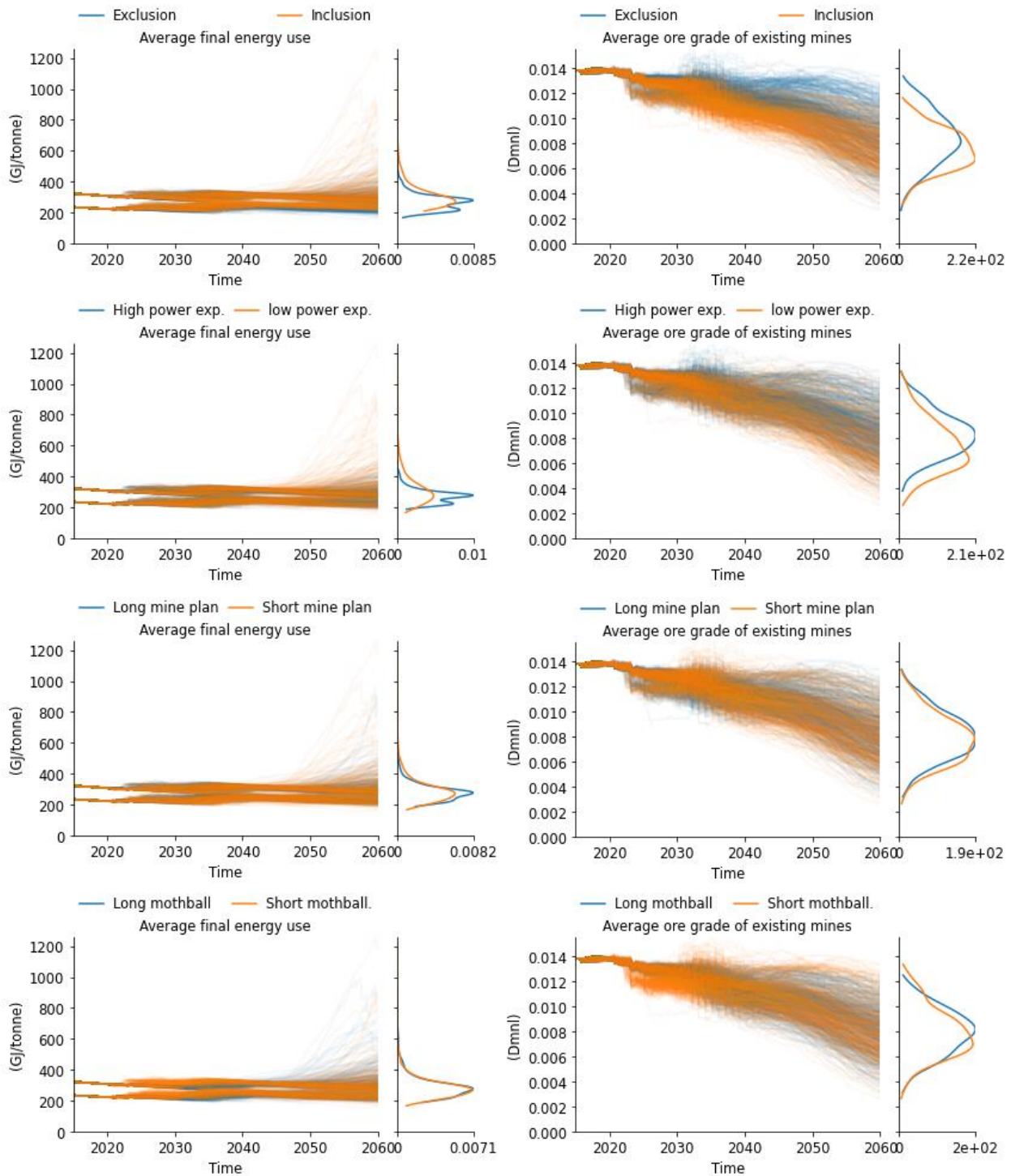


Figure N35: average final energy use and average ore grade of existing mines for the inclusion of by-products switch, power for price-based exploration ($\leq 0.7 = \text{low}$, $> 0.7 = \text{high}$), average mine operation plan ($\leq 15 \text{ years} = \text{short}$, $> 15 \text{ years} = \text{long}$) and average maximum mothball time ($\leq 20 \text{ years} = \text{short}$, $> 20 \text{ years} = \text{long}$).

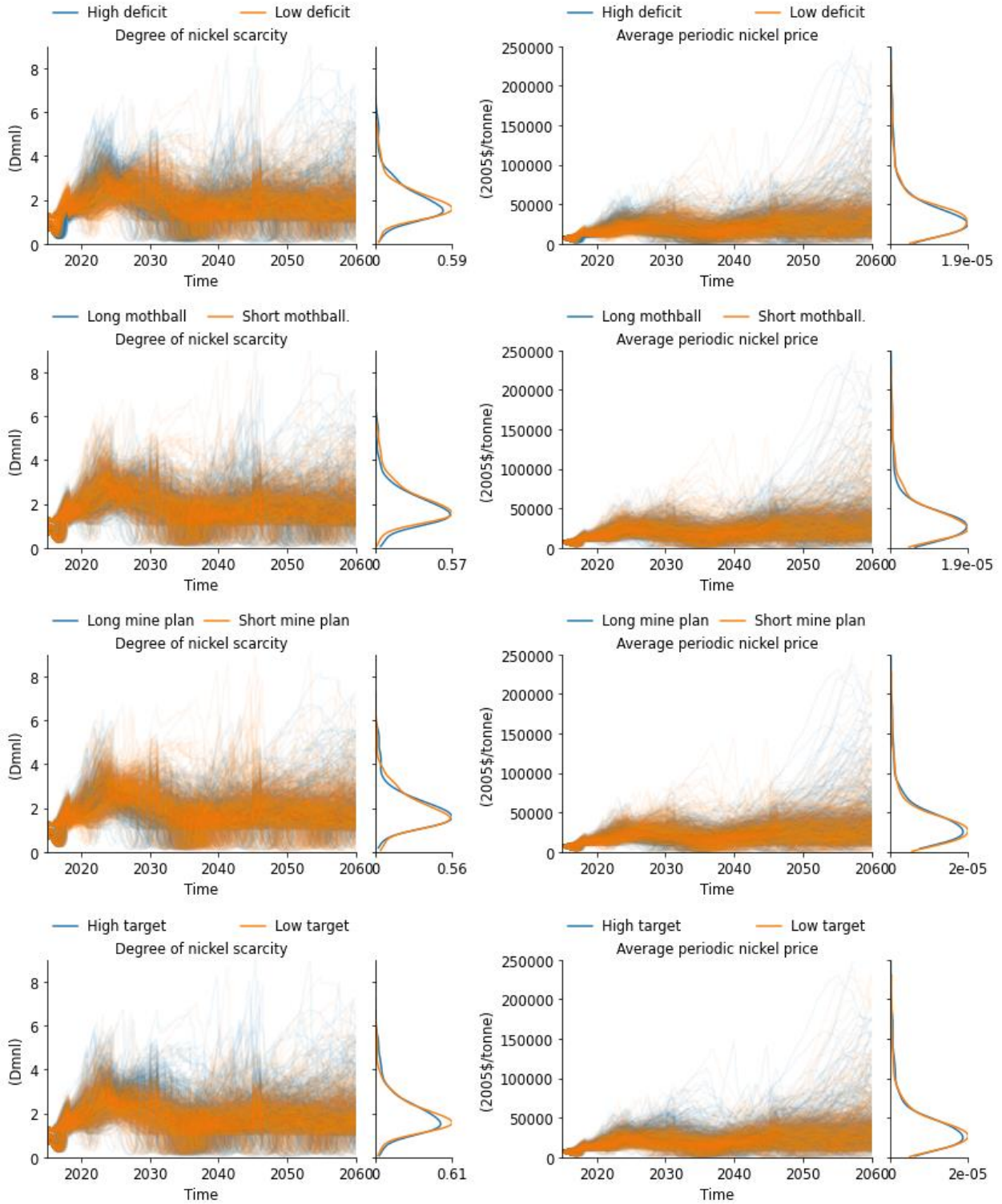


Figure N36: degree of nickel scarcity and the average periodic nickel price for average maximum profit deficit as percentage of investment (≤ 0.055 = low, > 0.055 = high; note: these values are fractions), average maximum mothball time (≤ 20 years = short, > 20 years = long), average mine operation plan (≤ 15 years = short, > 15 years = long) and a minimum profit over investment target (≤ 1.6 = low, > 1.6 = high).

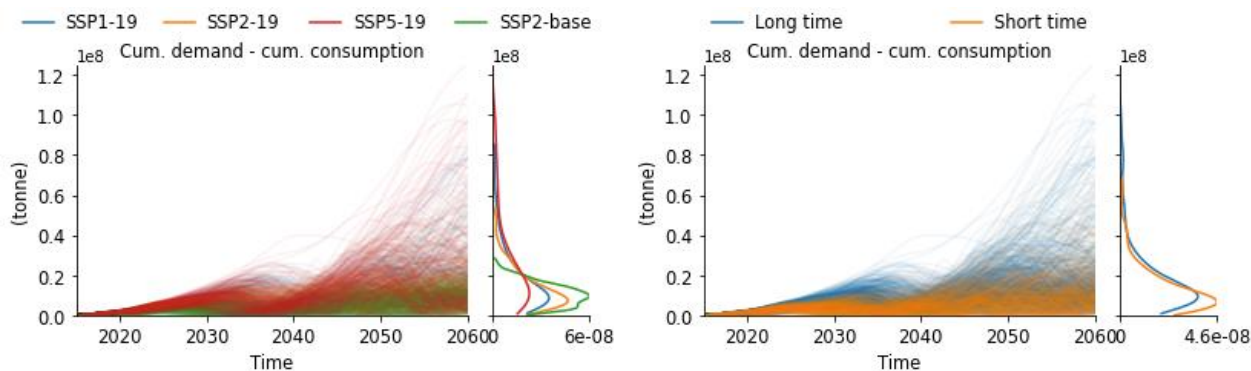


Figure N37: difference between cumulative demand and consumption per SSP and for lower values for administration of postponed demand (≤ 1 year) and higher values (> 1 year). This can be used as an indicator for resilience in addition to price (also see figure N9).

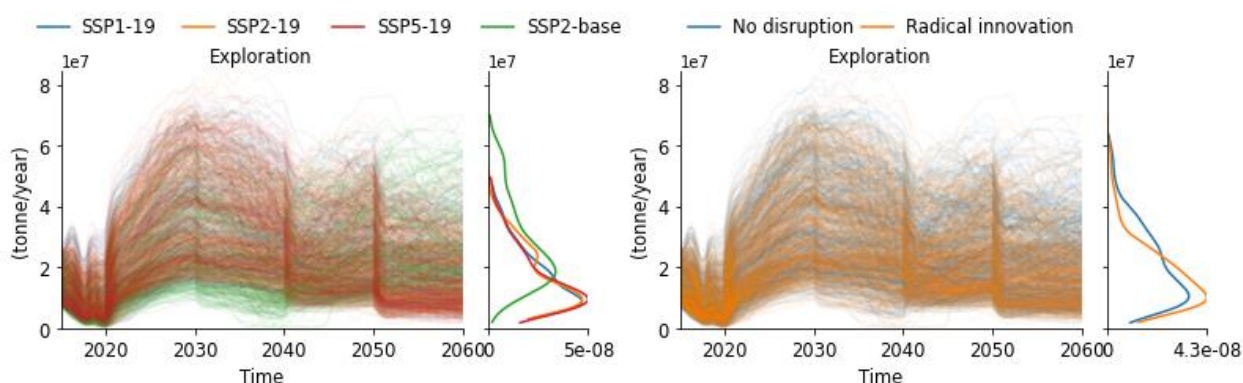


Figure N38: additional results for exploration. The thick lines every 10 years are caused by the discrete implementation of new vehicle mix. The changes in new vehicle mix are used to determine the expectations of the ET, which impacts exploration in the model. In the ET scenarios, the expectations of the ET are initially high, which leads to a large amount of exploration between 2020 and 2040. Then, as a large part of the transition has occurred, expectations decrease again. In the BAU scenario, the expectations of the ET transition are initially low, but after 2040 they start to increase as the BAU starts to catch up with the ET. The radical innovation disruption leads to a lower nickel demand, which means less nickel is required and there is generally also slightly less exploration.

Appendix N9: Results for a reduced global capacity increase

This appendix shows results for a global maximum capacity increase percentage between 1% and 30% instead of between 10% and 50%. In contrast with figure N27, the global maximum capacity increase percentage has a large impact on nickel price in figure N39. Administration of postponed demand remains important, but power for price-based exploration is not included here, because only the top two largest impacts at any point in time are included and it is overshadowed by the SSPs and the global maximum capacity increase percentage.

The results in figure N40 show a lower nickel availability for a lower global maximum capacity increase percentage, leading to more substitution and thereby a lower demand and lower GHG emissions. The average ore grade of known deposits also remains higher.

Average periodic nickel price

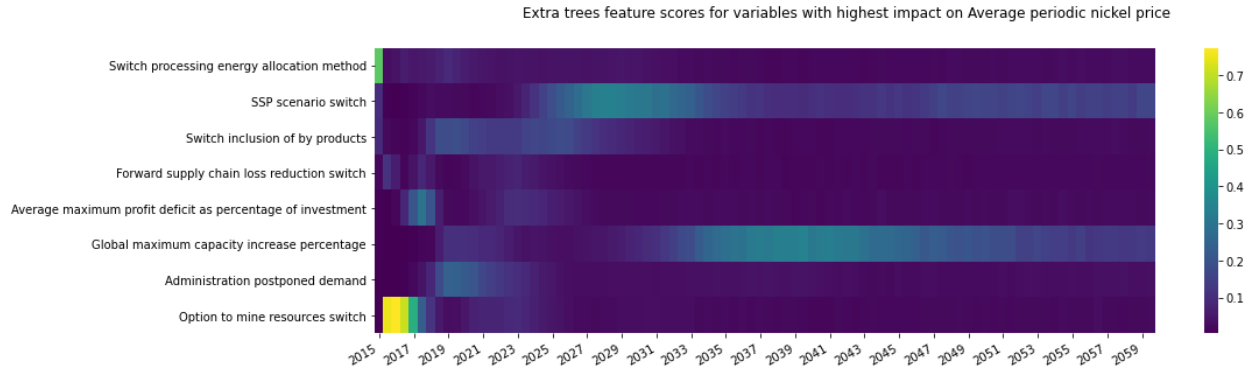


Figure N39: variables with the highest impact on average periodic nickel price at different points in time for a global maximum capacity increase percentage between 1% and 30%.

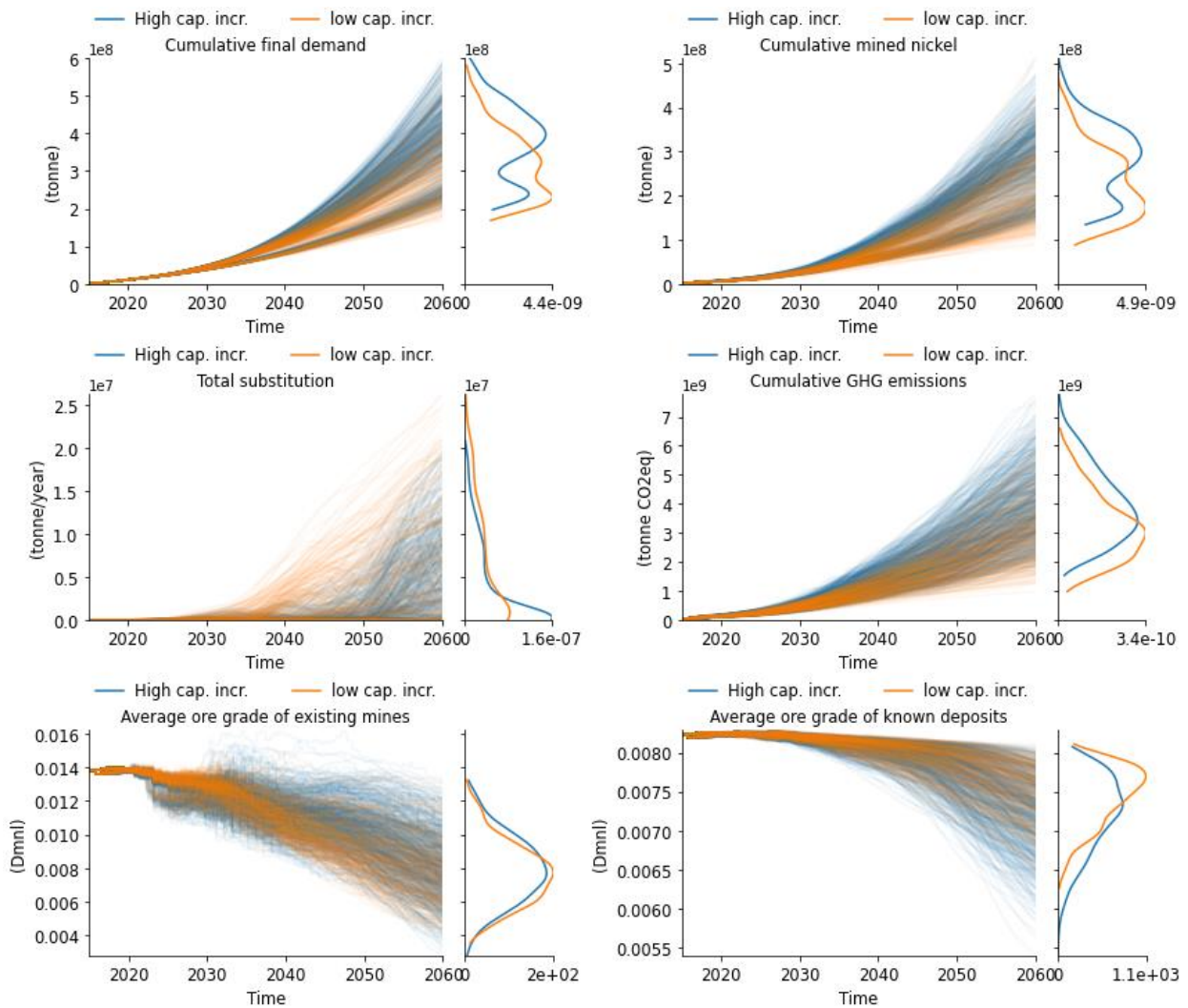


Figure N40: results for performance metrics for global maximum capacity increase (≤ 0.10 = low, > 0.10 = high).

Appendix N10: Focus on ore grade

In this appendix, additional attention is paid to ore grade because of its interesting behaviour in the current model. Figure N41 shows average ore grade of existing mines and average ore grade of known deposits based on values for certain influential parameters (also see figure N31 and figure N32) for the OCP. Values for the same parameters are very similar for the FSP at the start. However, for the FSP, the values are zoomed in more, because ore grade changes less, as can be seen in figure N42. This allows the inspection of additional details that are not visible in Figure N41. Different parameters were chosen in figure N42 (because of the similarity between the FSP and the OCP at the start) to show additional explanations for the differences in behaviour between runs at a higher resolution.

Figure N41 shows that the SSPs have a large impact on the development of the ore grade. The ore grade decreases more for the ET scenarios than for the BAU scenario because of the higher nickel demand and subsequent supply. Of the BAU runs that are clearly visible for existing mines, most runs also exclude by-products, which also generally leads to higher average ore grades for existing mines. This is because when by-products are not considered, the mines with the highest nickel ore grade are most attractive. The impact of the inclusion of by-products on average ore grade of known deposits is lower, as mining takes place regardless of which mine this occurs in, thereby generally reducing average ore grade.

There are some exceptions to the general reduction of average ore grade of known deposits (which can be seen in figure N42), where ore grade sometimes increases slightly over time. This is because, in some cases, the average ore grade reported in the database by Mudd (2020) was higher for the resources of a certain deposit than for the reserves. It is assumed that in these cases different factors than ore grade have a larger influence in determining the profitability of part of a certain deposit. Another case where the average ore grade of known deposits could increase, is if new deposits are discovered. However, this was not included in the current model. It was assumed that over time it becomes less likely to find new deposits with higher ore grades, so the general trend of a reducing ore grade over time is a decent representation of reality.

Figure N41 also shows that a higher power for ore grade leads to a sharper decrease in ore grade for both existing mines and known deposits. This is in line with equation 2 (appendix I1.1). A higher power for price-based exploration leads to a less sharp decrease in ore grade, because this leads to lower exploration and thereby less mining. This is in line with equation 1 (appendix G1.1).

Figure N42 shows some more similarities between certain runs where the ore grade of existing mines increases over time around 2030. In addition to excluding by-products, many of these runs allow the mining of resources, have reduced losses, a short average maximum mothball time and a high global maximum capacity increase percentage.

Figure N42 also shows that when the switch for mining resources is turned on, average ore grade initially decreases faster. The same applies to runs where loss reduction is included. However, in general the differences in the FSP runs are very minor and don't have a large impact on the overall results.

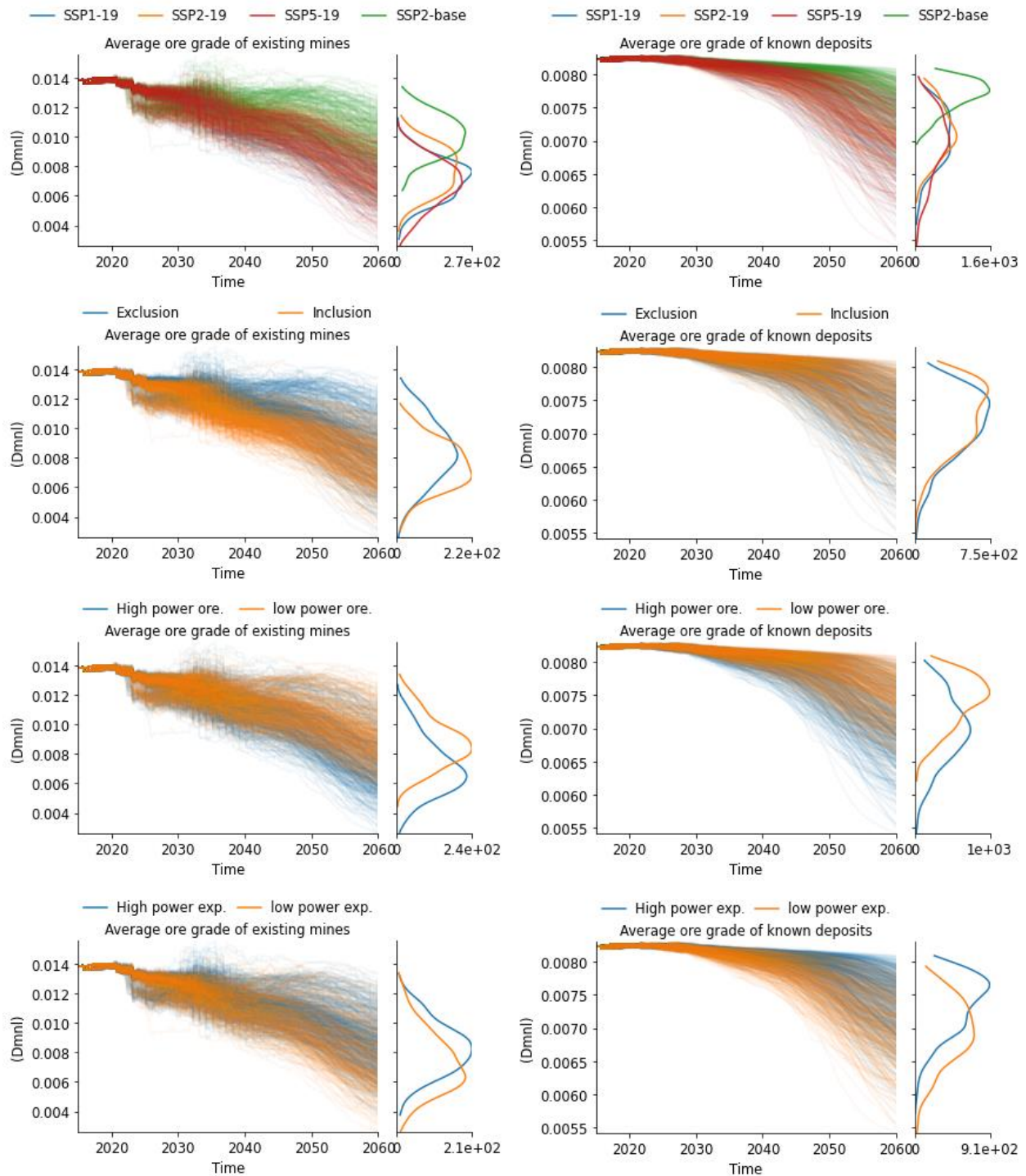


Figure N41: from top to bottom, the impact of SSP, by-product inclusion, power for ore grade (high > 0.3; low <= 0.3) and power for price-based exploration (high > 0.7; low <= 0.7) on average ore grade of existing mines and average ore grade of known deposits for the OCP.

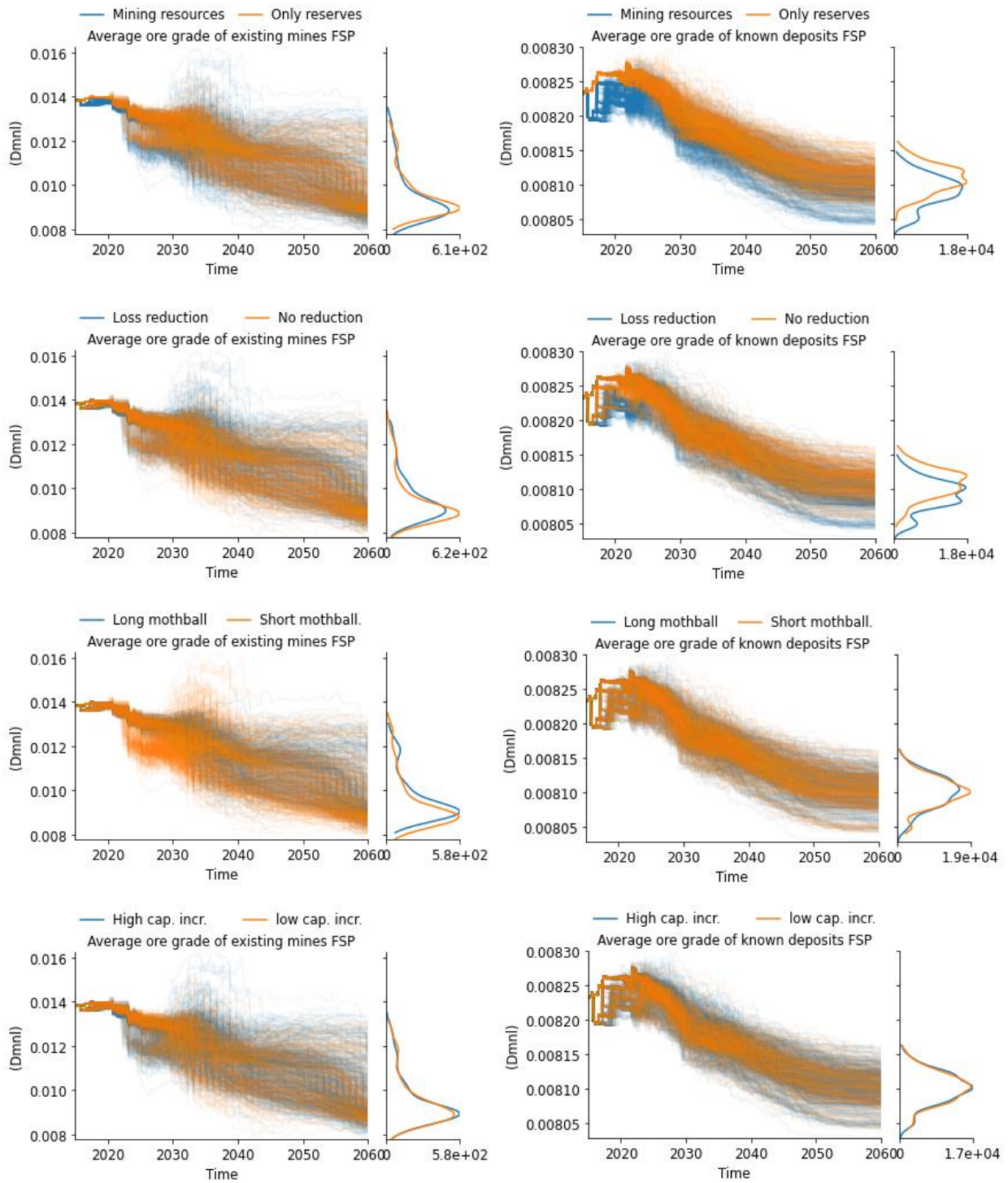


Figure N42: from top to bottom, the impact of mining resources, loss reduction, average maximum mothball time (long >20 years; short <= 20 years) and global maximum capacity increase (high > 0.25; low <= 0.25) on average ore grade of existing mines and average ore grade of known deposits for the FSP.

Appendix N11: Results for top supplying countries

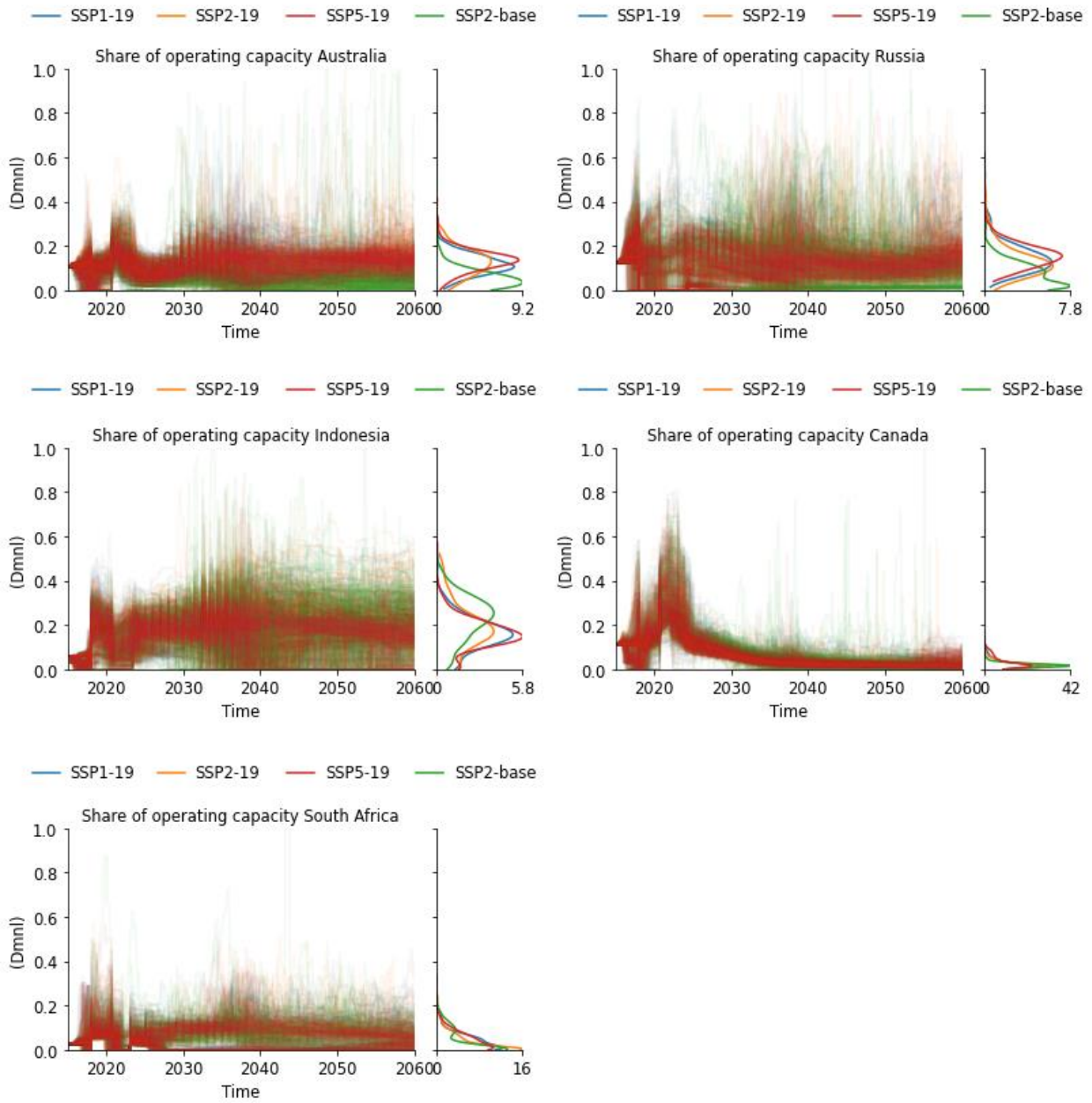


Figure N43: share of operating capacity for top supplying countries per SSP.

Appendix N12: Class I vs class II nickel

As stated in section 2.3.2 and appendix G3.1, nickel products can be divided into class I (used in various products, including batteries) and class II (used in stainless steel) nickel. Class I products contain more nickel and class II products could potentially be processed further to produce more class I products if there is an oversupply of class II and an undersupply of class I. This is illustrated in figure N44.

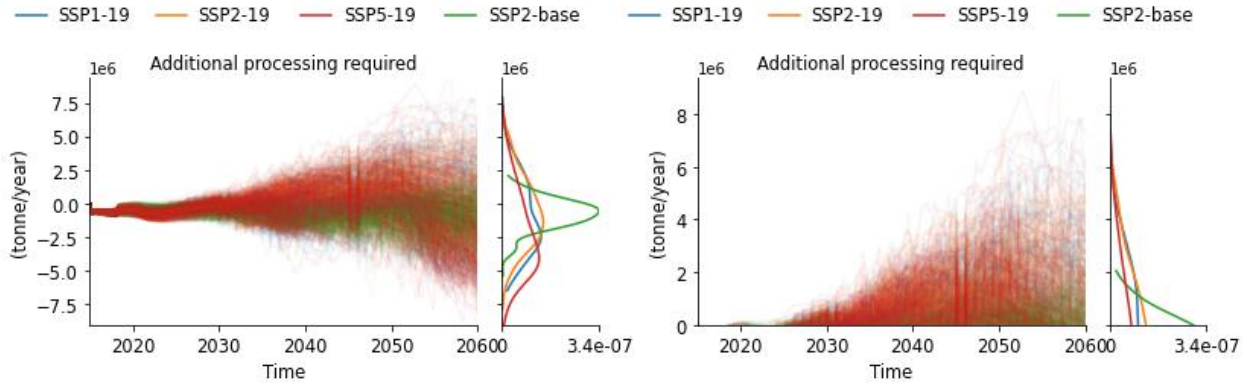


Figure N44: additional processing required when less class I nickel is produced than required and more class II is produced than required (right). The figure on the left shows there are also situations (when the value is negative) where there is not enough class II nickel to fulfil class II demand and/or there may be more class I nickel than required. Note: the way this was calculated ($\text{MIN}(\text{Class based demand}[\text{Class 1}] - \text{Initial consumption per class}[\text{Class 1}], \text{Initial consumption per class}[\text{Class 2}] - \text{Class based demand}[\text{Class 2}])$) means that for the positive values there may still be more class I required if the values in this figure are limited by the availability of a surplus of class II nickel.

Appendix O: Comparison with previous research

In this appendix, the results and assumptions of the current research are compared with previous research in further detail. Table O1 contains a comparison with the work by Van der Linden (2020) and below this table a comparison with other work is made.

Table O1: differences in the assumptions used for factors determining the amount of nickel in EV batteries and in the RoE for Van der Linden (2020) and the current study. The yellow highlighted cells indicate the assumptions that lead to higher nickel requirements. If the assumptions lead to similar demand no cell is highlighted.

| Factor | Van der Linden (2020) | Current study |
|---|---|--|
| <i>Nickel in EV batteries</i> | | |
| Method for projecting number of vehicles | Based on a relationship between GDP and number of vehicles for cars and trucks and a relationship between population and number of vehicles for buses. This led to about 1.2E9 - 2.3E9 vehicles by 2050, with 1.5E9 for SSP2-baseline | Based on a relationship between GDP/capita and number of vehicles (Our World in Data, 2014). This led to about 2.1E9 - 2.8E9 vehicles, with 2.2E9 for SSP2-baseline. |
| Lifetime of vehicles | 20 years for cars, 30 years for buses, 18 years for trucks | 16 years for all types |
| Lifetime EV batteries | Not included (equal to vehicle lifetime) | 8 years (16 years for the improved EV battery lifetime policy) |
| EV share of new vehicles | Extrapolated from BNEF (2019) | Extrapolated from BNEF (2019) and Van der Linden (2020). For the electrification scenario and the ET scenarios the values are the same as for Van der Linden (2020) up to 2050. For BAU, these values were based on the IEA RTS. |
| Battery market share | Projected a larger share of NMC811 batteries with 72% nickel and 9% cobalt and did not consider NCA+ | Projected a larger share of NCA+ batteries with 82% nickel and 5% cobalt because these batteries have a higher energy density. |
| Battery capacity of vehicles | Included an uncertainty range of 20 - 120 kWh/BEV | 71 kWh/BEV |
| <i>Nickel in the RoE</i> | | |
| Nickel per dollar GDP | Used a value of 5.43E-6 lb/\$ (= 2.46E-9 tonne/\$). It is unclear where this figure comes from. It is also unclear whether the demand modelled in a bottom-up way was subtracted from this. | Base year demand RoE/base year GDP (= 21.38E-9 tonne/\$ for SSP2-baseline). The base year demand modelled in a bottom-up way was subtracted from the total nickel demand in the base year to obtain the RoE base year demand. |
| <i>Other differences</i> | | |
| Nickel in electricity generation capacity | Not considered as a separate category, considered as part of the RoE | Considered as a separate category due to the large changes expected in the ET. |
| Nickel in consumer electronics | Included as a separate category, considered to increase based on population. | Not considered as a separate category, considered as part of the RoE because less extreme changes are expected for this category |
| Nickel for stationary storage | Based on an increase in demand and a slowing of this increase over time. | Based on behind the meter requirements and grid requirements not covered by PHS, CSP TES, V2G and repurposed vehicle batteries |

Below a comparison is made between assumptions in the current study and those in other studies. The data for Wood Mackenzie (n.d.) could not be accessed, so this study was excluded from the comparison.

- **Consideration of EVs:** three of the studies in figure 3.28 (main text) did not consider (or barely considered) nickel demand for EV batteries. Elshkaki et al. (2017) did not focus on the ET and their analysis did not contain any EVs. Rietveld et al. (2019), who have similar values for the RoE and electricity generation capacity compared to the current analysis, also barely considered EVs. De Koning et al. (2018) did consider EVs, but did not consider nickel demand for EVs, instead focussing on other materials.
- **Projected vehicle stock:** in the current study, the projected number of motor vehicles (including passenger vehicles, trucks and buses) is between 2.1 billion and 2.8 billion by 2050 for the different SSPs (2.2 billion for SSP2-baseline). This matches reasonably well with projections by WEC (2011), IEA (2017a), IEA (2017b) and EIA (2019a), who combined project about 2 billion - 2.5 billion passenger vehicles and trucks by 2050 and with projections by Watari et al. (2018) who based on IEA (2017a) projected 1.9 - 2.3 billion light duty vehicles (passenger vehicles and light trucks). However, the value for SSP2-baseline in the current analysis is about 700 million more than the number projected by Van der Linden (2020) for SSP2-baseline, and the number projected by Valero et al. (2018a), who only considered passenger vehicles.
- **Projected EV share of new vehicles:** the projected EV share of new vehicles also differs per study. The relative shares of the different types of EVs also make a difference. In the current study, the EV share of new vehicles for the ET is the same as the projection by Van der Linden (2020), which comes close to the B2DS share used by Watari et al. (2018) based on IEA (2017a). The BAU EV share of new vehicles by Valero et al. (2018) also comes close to this. The BAU EV share of new vehicles in the current study is the same as the RTS share used by Watari et al. (2018) based on IEA (2017a).
- **Battery type:** in the current study a larger share of NCA+ (82% nickel) is projected, compared to a larger share of NMC811 (72% nickel) projected by Van der Linden (2020) and a nickel intensity of 0.6 kg/kWh, equivalent to a 100% share of NMC622 (54% nickel) used by Manberger & Stenqvist (2018).
- **Battery capacity:** Similar values for battery capacity were used in the current study, the study by Van der Linden (2020) and the study by Manberger & Stenqvist (2018). Valero et al. (2018a) and Watari et al. (2018) didn't consider battery capacity and type. Instead, they assumed a certain nickel intensity per vehicle, 58 and 47 kg/vehicle for BEVs and 18 and 19 kg/vehicle for PHEVs respectively. This is close to the nickel intensity calculated in the current study.
- **Lifetime assumptions:** in the current study, a vehicle lifetime of 16 years was assumed. This is similar to the 15 years assumed by Watari et al. (2018). Manberger and Stenqvist (2018) assumed 15 years for passenger vehicles, 10 - 15 years for buses and 20 years for trucks. Van der Linden et al. (2020) assumed 20 years for passenger vehicles, 18 years for trucks and 30 years for buses. It is unclear what lifetime was used by Valero et al. (2018a). However, something that was considered in the current study that none of the other studies included (Manberger & Stenqvist (2018) did consider it, but only applied it to lithium), is that EV batteries generally don't last as long as the vehicles they are used in. EV batteries need to be replaced every 8 years (Walker et al., 2015; Assuncao et al., 2016; De Rousseau et al., 2017 White et al., 2020).
- **Other considerations:** regarding the RoE, nickel demand in the current study was calculated by dividing the base year demand for the RoE (total base year demand - base year demand for the energy system) by the base year GDP. This led to a similar RoE demand compared to Rietveld et al. (2019). However, the value for nickel per dollar GDP is 10 times larger than the value used by Van der Linden (2020). It is unclear where Van der Linden (2020) obtained her value. Valero et al. (2018a) also project lower demand for the RoE because they assume a constant demand. Regarding electricity generation, Watari et al. (2018) did not consider nickel for electricity generation capacity.

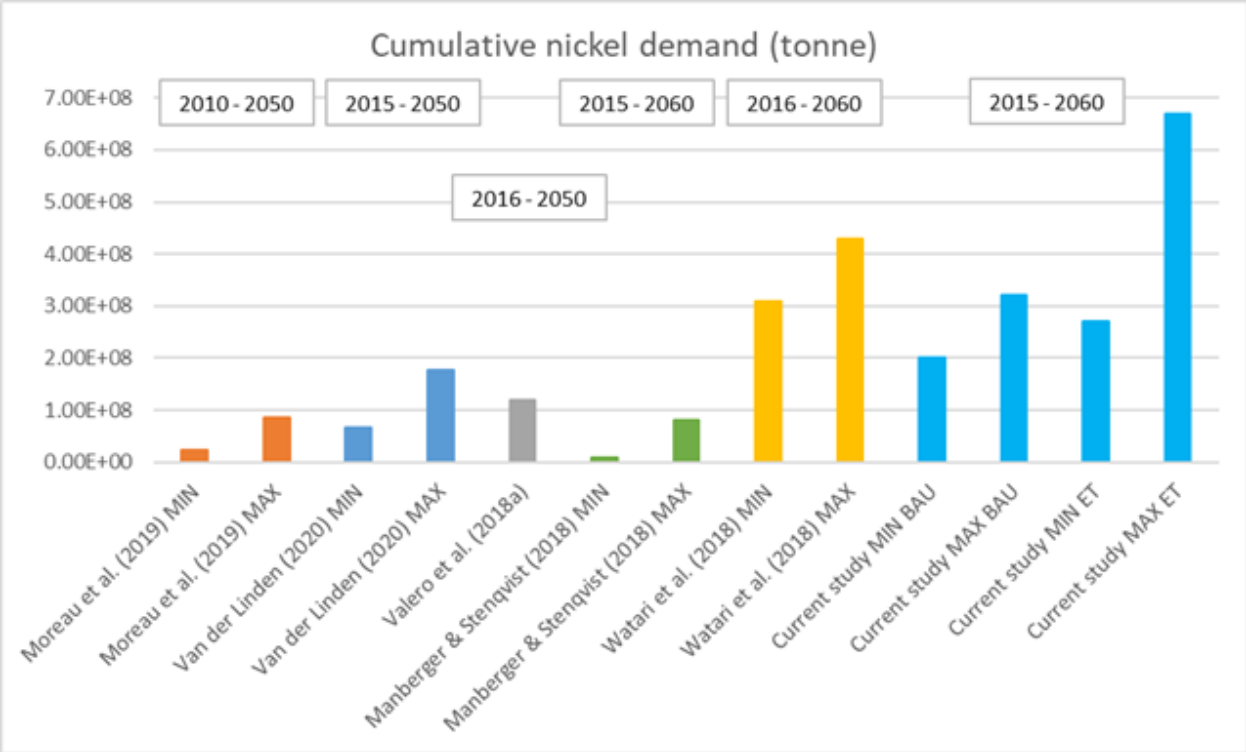


Figure O1: cumulative nickel demand reported in previous research and in the current study for both the BAU scenario and the ET scenarios. It is important to keep in mind the different time scales for proper comparison. The best comparison can be made with the work by Manberger & Stenqvist (2018) and the work by Watari et al. (2018), who calculated cumulative nickel demand for a similar time frame compared to the current study. The data for the nickel projections by Van der Linden (2020) was not obtained from her report directly, as she mainly reported on cobalt. Instead, it was obtained by adding a variable for cumulative demand to her model, subtracting the years before 2015 and running her model using the code she provided. The data for Manberger & Stenqvist likely only refers to nickel for the ET and does not include nickel for BAU.

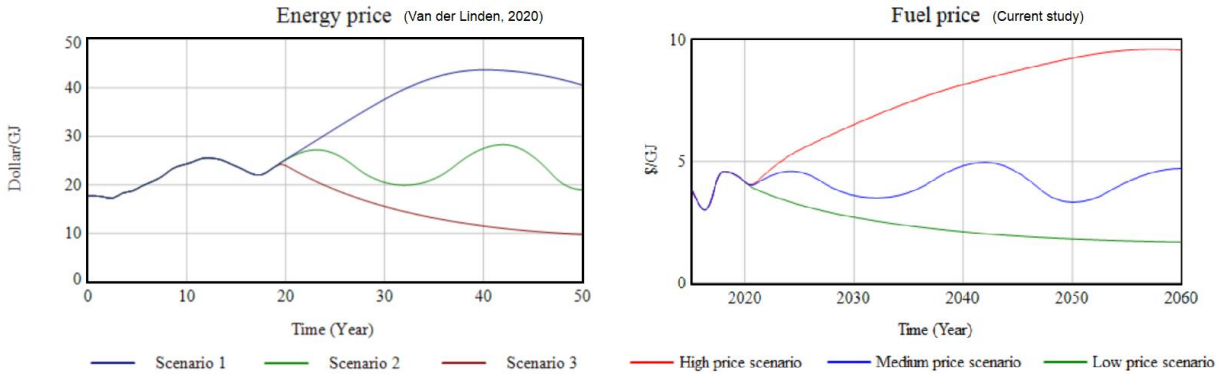


Figure O2: difference in fuel price (referred to by Van der Linden (2020) as energy price) in the model by Van der Linden (2020) and the current model. Van der Linden (2020) states in her model that her initial energy price is based on the oil price in 2000. It is therefore assumed that her values are in 2000\$. The values in the current study are in 2005\$. A total inflation of 13.41% occurred in the period between 2000 and 2005. The initial energy price in the current model was based on a mixture of crude oil, natural gas and coal prices reported by BP (2019).

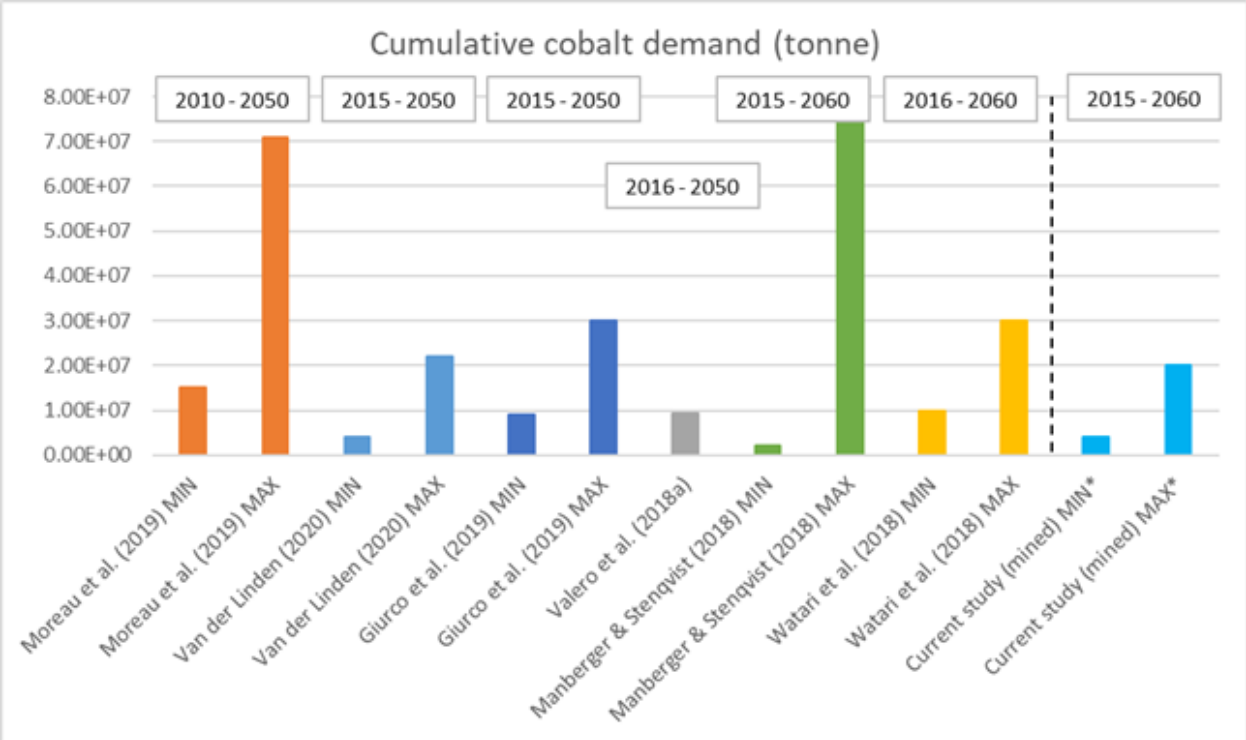


Figure O3: cumulative cobalt demand reported in previous research and cumulative mined cobalt in the current study. The * indicates that the values for the current study refer to cobalt mined as a by-product of nickel production and not cobalt demand.

References appendices

Achkari, O., & El Fadar, A. (2020). Latest developments on TES and CSP Technologies–Energy and environmental issues, applications and research trends. *Applied Thermal Engineering*, 167, 114806.

Alonso, E., Sherman, A. M., Wallington, T. J., Everson, M. P., Field, F. R., Roth, R., & Kirchain, R. E. (2012). Evaluating rare earth element availability: A case with revolutionary demand from clean technologies. *Environmental science & technology*, 46(6), 3406-3414.

Amponsah, N. Y., Troldborg, M., Kington, B., Aalders, I., & Hough, R. L. (2014). Greenhouse gas emissions from renewable energy sources: A review of lifecycle considerations. *Renewable and Sustainable Energy Reviews*, 39, 461-475.

AngloAmerican (2020). *US geological survey minerals year book 2013*. Retrieved from <https://www.angloamerican.com/-/media/Files/A/Anglo-American-PLC-V2/documents/tax-fact-sheets/brazil-fact-sheet-final-2014.pdf>

Asdrubali, F., Baldinelli, G., D'Alessandro, F., & Scrucca, F. (2015). Life cycle assessment of electricity production from renewable energies: Review and results harmonization. *Renewable and Sustainable Energy Reviews*, 42, 1113-1122.

Ashby, A. D., Van Etten, E. J. B., & Lund, M. A. (2016). Pitfalls of gold mine sites in care and maintenance. *Proceedings of the 11th International Conference on Mine Closure* (pp. 313-324). Australian Centre for Geomechanics Perth. https://doi.org/10.36487/ACG_rep/1608_22_Ashby

Assuncao, A., Moura, P.S., & de Almeida, A. (2016). Technical and economic assessment of the secondary use of repurposed electric vehicle batteries in the residential sector to support solar energy. *Applied Energy* 181, 120-131. doi:[10.1016/j.apenergy.2016.08.056](https://doi.org/10.1016/j.apenergy.2016.08.056)

Auping, W. L. (2011). *The Uncertain Future of Copper: An Exploratory System Dynamics Model and Analysis of the Global Copper System in the Next 40 Years* (Delft University of Technology). Retrieved from <https://repository.tudelft.nl/islandora/object/uuid%3A4998f817-848d-4879-9d5f-2c0bd9ee4c81>

Auping, W. L., & Pruyt, E. (2013). (Un)desired Tantalum? *In Proceedings of the 31st international conference of the system dynamics society*.

Bleiwas, D.I. (1984). Nickel Availability – Market Economy countries: A mineral Availability Program Appraisal. Information Circular, Bureau of Mines, United States.

Blok, K., & Nieuwlaar, E. (2021). *Introduction to energy analysis* (3rd edition), London and New York: Routledge, Taylor & Francis Group.

BNEF (2016). *Used Electric Car Batteries Get Second Life as Home Storage*. Retrieved from <https://www.bloomberg.com/news/articles/2016-08-25/used-electric-car-batteries-will-get-second-life-as-home-storage>

BNEF (2019). *2H 2019 Battery Metals Outlook: Demand Realities*. Bloomberg finance L.P.

BP (2019). *BP Statistical Review of World Energy 2019. 68th edition*. Retrieved from <https://www.bp.com/content/dam/bp/business-sites/en/global/corporate/pdfs/energy-economics/statistical-review/bp-stats-review-2019-full-report.pdf>.

Brown, T., Schlachtberger, D., Kies, A., Schramm, S., & Greiner, M. (2018). Synergies of sector coupling and transmission reinforcement in a cost-optimised, highly renewable European energy system. *Energy*, 160, 720-739.

Buchholz, P., & Brandenburg, T. (2018). Demand, Supply, and Price Trends for Mineral Raw Materials Relevant to the Renewable Energy Transition. Wind Energy, Solar Photovoltaic Energy and Energy Storage. *Chemie Ingenieur Technik*, 90(1-2), 141-153.

Budinis, S., Krevor, S., Mac Dowell, N., Brandon, N., & Hawkes, A. (2018). An assessment of CCS costs, barriers and potential. *Energy strategy reviews*, 22, 61-81.

Bullion by Post (2020). *Gold Price in USD per Kilogram for Last 10 Years*. Retrieved from <https://www.bullionbypost.eu/gold-price/10year/kilograms/USD/>

Capellán-Pérez, I., de Castro, C., & González, L. J. M. (2019). Dynamic Energy Return on Energy Investment (EROI) and material requirements in scenarios of global transition to renewable energies. *Energy Strategy Reviews*, 26, 100399.

Castillo, E., & Eggert, R. (2019). *Reconciling Diverging Views on Mineral Depletion: A modified Cumulative Availability Curve Applied to Copper Resources* (wp201902). Colorado School of Mines, Division and Business.

Dagnachew, A. G., Hof, A. F., Lucas, P. L., & van Vuuren, D. P. (2019). *Insight into Energy Scenarios: A comparison of key transition indicators of 2° C scenarios*. The Hague, The Netherlands: PBL Netherlands Environmental Assessment Agency.

Deetman, S., Pauliuk, S., Van Vuuren, D. P., Van Der Voet, E., & Tukker, A. (2018). Scenarios for demand growth of metals in electricity generation technologies, cars, and electronic appliances. *Environmental science & technology*, 52(8), 4950-4959.

De Koning, A., Kleijn, R., Huppes, G., Sprecher, B., van Engelen, G., & Tukker, A. (2018). Metal supply constraints for a low-carbon economy? *Resources, Conservation and Recycling*, 129, 202-208.

Deloitte (2015a). *Energy storage: Tracking the technologies that will transform the power sector*. Retrieved from: <https://www2.deloitte.com/content/dam/Deloitte/no/Documents/energy-resources/energy-storage-tracking-technologies-transform-power-sector.pdf>

Deloitte (2015b). *State of Mining in Africa: in the spotlight*. Retrieved from https://www2.deloitte.com/content/dam/Deloitte/za/Documents/energy-resources/za_state_of_mining_africa_09022015.pdf

Deloitte (2016). *Extractive Industries Transparency Initiative in Albania Report for the year 2016*. Retrieved from https://eiti.org/files/documents/2016_albania_eiti_report.pdf

De Rousseau, M., Gully, B., Taylor, C., Apelian, D., & Wang, Y. (2017). Repurposing used electric car batteries: a review of options. *Jom*, 69(9), 1575-1582.

Dry, M. (2013). Early evaluation of metal extraction projects. *Alta Nickel-Cobalt-Copper Conference*. Perth, Australia. Retrieved from: <https://www.researchgate.net/publication/290390996> EARLY EVALUATION OF METAL EXTRACTIO
N PROJECTS

- Dunn, J.B., Gaines, L., Barnes, M., Sullivan, J., & Wang, M (2012). *Material and Energy Flows in the Material Production, Assembly, and End-of life Stages of the Automotive Lithium-ion Battery Life Cycle*. Argonne National Laboratory. <https://doi.org/10.2172/1177517>
- Eckelman, M. J. (2010). Facility-level energy and greenhouse gas life-cycle assessment of the global nickel industry. *Resources, conservation and recycling*, 54(4), 256-266.
- Energy Information Administration (EIA, 2019a). *International Energy Outlook 2019: With projections to 2050*. Retrieved from <https://www.eia.gov/outlooks/ieo/pdf/ieo2019.pdf>
- Energy Information Administration (EIA, 2019b). *Electric Power Monthly*. Capacity factors for utility scale generators primarily using fossils fuels. Retrieved on 25 November 2020 from https://www.eia.gov/electricity/monthly/epm_table_grapher.php?t=epmt_6_07_a
- Energy Information Administration (EIA, 2019c). *Electric Power Monthly*. Capacity factors for utility scale generators primarily using non-fossils fuels. Retrieved on 25 November 2020 from https://www.eia.gov/electricity/monthly/epm_table_grapher.php?t=epmt_6_07_b
- Energy Information Administration (EIA, 2020a). *Capital Cost and Performance Characteristic Estimates for Utility Scale Electric Power Generating Technologies*. Retrieved from: https://www.eia.gov/analysis/studies/powerplants/capitalcost/pdf/capital_cost_AEO2020.pdf
- Energy Information Administration (EIA, 2020b). *Electric Power Monthly. Average Price of Electricity to Ultimate Customers*. Retrieved from: https://www.eia.gov/electricity/monthly/epm_table_grapher.php?t=epmt_5_3
- Elias, M., O'Callaghan, P., Vargas, A.M., & Buban, K. (2019). *Moa Nickel Project, Cuba (NI 43-101)*. CSA Global Pty Ltd. Retrieved from <https://www.csaglobal.com/moa-iv/>
- Elshkaki, A., & Graedel, T. E. (2013). Dynamic analysis of the global metals flows and stocks in electricity generation technologies. *Journal of Cleaner Production*, 59, 260-273.
- Elshkaki, A., Reck, B. K., & Graedel, T. E. (2017). Anthropogenic nickel supply, demand, and associated energy and water use. *Resources, Conservation and Recycling*, 125, 300-307.
- Emdadi, A., Vuille, F., Moreau, V., & Faurat, D. (2017). *Material Constraints for a 100% Global Renewable Energy System*. 30th International Conference on Efficiency, Cost, Optimization Simulation and Environmental Impact of Energy Systems, ECOS 2017 (2-6 July 2017). International Measurement Confederation (MEKO).
- Ercan, T., Noori, M., Zhao, Y., & Tatari, O. (2016). On the front lines of a sustainable transportation fleet: applications of vehicle-to-grid technology for transit and school buses. *Energies*, 9(4), 230.
- EuRIC (2020). Metal Recycling Fact Sheet [brochure]. Retrieved from <https://www.euric-aisbl.eu/position-papers/item/335-euric-unveils-metal-recycling-brochure>
- European Automobile Manufacturers Association (ACEA, 2020). *Average vehicle age*. Statista Research Department. Retrieved from <https://www.acea.be/statistics/tag/category/average-vehicle-age>
- Extractives Hub (n.d.). *Mining Industry Overview*. Centre for Energy, Petroleum and Mineral Law & Policy, University of Dundee. Retrieved from: <https://www.extractiveshub.org/topic/view/id/21/chapterId/268>
- Extractive Industries Transparency Initiative (EITI, 2020). *Papua New Guinea: an overview*. Retrieved from https://eiti.org/fr/implementing_country/46#tax-and-legal-framework-

Farooki, M., Webb, a., & Hinde, C. (2017). *The Competitiveness of the European Union's Mining Sector* (689364). Strategic Dialogue on Sustainable Raw Materials for Europe. Retrieved from https://www.stradeproject.eu/fileadmin/user_upload/pdf/STRADE_Rpt_D2-01_EU-MiningIndustry-Competitiveness_Apr2017_FINAL.pdf

Fizaine, F., & Court, V. 2015. Renewable electricity producing technologies and metal depletion: A sensitivity analysis using the EROI. *Ecological Economics*, *Elsevier*, 110(C), 106-118. doi: 10.1016/j.ecolecon.2014.12.001

Fraser Institute (2020). *Survey of Mining Companies 2019*. Retrieved from <https://www.fraserinstitute.org/studies/annual-survey-of-mining-companies-2019>

Fuel Cells and Hydrogen (FCH, 2010). *A portfolio of power-trains for Europe: a fact-based analysis. The role of battery Electric vehicles, plug-in hybrids and fuel cell electric vehicles*. FCH JU publications. Retrieved from: https://www.fch.europa.eu/sites/default/files/documents/Power_trains_for_Europe.pdf

García-Olivares, A., Ballabrera-Poy, J., García-Ladona, E., & Turiel, A. (2012). A global renewable mix with proven technologies and common materials. *Energy Policy*, 41, 561-574.

Gentile, N. (2019). Multinational Mining Corporations are exploiting U.S. Taxpayers: Outdated Mining Laws Allow Foreign Companies to Mine U.S. Public Lands for Free. Centre for American Progress. Retrieved from <https://www.americanprogress.org/issues/green/reports/2019/11/21/477569/multinational-mining-corporations-exploiting-u-s-taxpayers/>

Gigametals Corporation (2019). *Battery metals for a clean energy future*. Retrieved from: https://www.gigametals.com/site/assets/files/4910/giga_metals_presentation_4sep19.pdf

Giurco, D., Dominish, E., Florin, N., Watari, T., & McLellan, B. (2019). Requirements for minerals and metals for 100% renewable scenarios. In *Achieving the Paris Climate Agreement Goals* (pp. 437-457). Springer, Cham.

Glöser, S., Soulier, M., & Tercero Espinoza, L. A. (2013). Dynamic analysis of global copper flows. Global stocks, postconsumer material flows, recycling indicators, and uncertainty evaluation. *Environmental Science & Technology*, 47(12), 6564-6572. doi:10.1021/es400069b

Government of Western Australia, Department of State Development (2013). *Mineral royalty rate analysis stakeholder consultation paper - West Australian Department of Mines and Petroleum*. Retrieved from: https://www.jtsi.wa.gov.au/docs/default-source/default-document-library/mrra_stakeholder_consultation_paper_2013.pdf?sfvrsn=3c746b1c_5

Government of Western Australia, Department of State Development (2015). *Mineral Royalty Rate Analysis: Final report 2015*. Retrieved from: https://www.jtsi.wa.gov.au/docs/default-source/default-document-library/mineral-royalty-rate-analysis-final-report-0315.pdf?sfvrsn=76076e1c_6

Grandell, Leena, Antti Lehtilä, Mari Kivinen, Tiina Koljonen, Susanna Kihlman, and Laura S. Lauri. "Role of critical metals in the future markets of clean energy technologies." *Renewable Energy* 95 (2016): 53-62.

Grand View Research (GVR, 2019). *Concentrated Solar Power Market Analysis, By Technology (Parabolic Trough, Linear Fresnel, Dish, Power Tower), By Region (North America, Europe, Asia Pacific, South & Central America, MEA), And Segment Forecast, 2018 – 2025*. Retrieved from: <https://www.grandviewresearch.com/industry-analysis/concentrated-solar-power-csp-market>

Habib, K., & Wenzel, H. (2014). Exploring rare earths supply constraints for the emerging clean energy technologies and the role of recycling. *Journal of Cleaner Production*, 84, 348-359.

Hadjipaschalis, I., Poullikkas, A., & Efthimiou, V. (2009). Overview of current and future energy storage technologies for electric power applications. *Renewable and sustainable energy reviews*, 13(6-7), 1513-1522.

Harris, J.M., & Roach, B. (2018). The Theory of Environmental Externalities. *Environmental and Natural Resource Economics: A Contemporary Approach* (4th edition, p.74). New York: Taylor & Francis.

Hausfather, Z. (2018): *Explainer: How 'Shared Socioeconomic Pathways explore future climate change. Carbon brief*. Retrieved from: <https://www.carbonbrief.org/explainer-how-shared-socioeconomic-pathways-explore-future-climate-change>

Henckens, M., van Ierland, E.C., Driessen, P.P.J., & E. Worrella, E. (2016). Mineral resources: Geological scarcity, market price trends, and future generations. *Resources Policy*, 49, 102-111. doi: 10.1016/j.resourpol.2016.04.012.

Hertwich, E. G., Gibon, T., Bouman, E. A., Arvesen, A., Suh, S., Heath, G. A., ... & Shi, L. (2015). Integrated life-cycle assessment of electricity-supply scenarios confirms global environmental benefit of low-carbon technologies. *Proceedings of the National Academy of Sciences*, 112(20), 6277-6282.

Hydrogen Council (HC, 2017). Hydrogen Scaling up. Retrieved from: <https://hydrogencouncil.com/wp-content/uploads/2017/11/Hydrogen-scaling-up-Hydrogen-Council.pdf>

Ilika Technologies Ltd. (Ilika, 2019). *Solid-state battery technology: Capital markets Day December 2019*. <https://www.ilika.com/images/uploads/downloads/Ilika-Capital-Markets-Day-Presentation-Dec-2019.pdf>

InsideEVs (2020). *Compare Electric Cars: EV Range, Specs, Pricing & More*. Retrieved on 4 August 2020 on <https://insideevs.com/reviews/344001/compare-evs/>

Institute of Developing Economies -Japan External Trade Organisation (IDE-JETRO, n.d.). *Norilsk Nickel*. Retrieved from https://www.ide.go.jp/English/Data/Africa_file/Company/botsuwana01.html

International Copper Association (ICA, n.d.). *Copper Recycling*. Retrieved from: <https://copperalliance.org/wp-content/uploads/2017/03/ica-copper-recycling-201712-A4-HR2.pdf>

International Institute for Applied Systems Analysis (IIASA, 2018). *SSP Database: Shared Socioeconomic Pathways – version 2.0, December 2019*. Retrieved from: <https://tntcat.iiasa.ac.at/SspDb/dsd?Action=htmlpage&page=about>

International Energy Agency (IEA, 2017a). *Energy Technology Perspectives 2017: Catalysing Energy Technology Transformations*. Retrieved from https://webstore.iea.org/download/direct/1058?fileName=Energy_Technology_Perspectives_2017-PDF.pdf

International Energy Agency (IEA, 2017b). *The Future of Trucks: implications for energy and the environment*. Retrieved from <https://webstore.iea.org/download/direct/288>

International Energy Agency (IEA, 2019): *Material efficiency in clean energy transitions*. Retrieved from <https://webstore.iea.org/download/direct/2454>

International Energy Agency: Photovoltaic Power Systems Programme (IEA PVPS, 2019). *Trends in Photovoltaic Applications*. Retrieved on 25 November 2020 from <https://iea-pvps.org/wp-content/uploads/2020/02/5319-iea-pvps-report-2019-08-lr.pdf>

International Energy Agency (IEA, 2020b): *Innovation in batteries and electricity storage*. Retrieved from: [http://documents.epo.org/projects/babylon/eponet.nsf/0/969395F58EB07213C12585E7002C7046/\\$FILE/battery_study_en.pdf](http://documents.epo.org/projects/babylon/eponet.nsf/0/969395F58EB07213C12585E7002C7046/$FILE/battery_study_en.pdf)

International Hydropower Association (IHA, 2016). *2016 Hydropower Status Report*. Retrieved from: https://www.hydropower.org/sites/default/files/publications-docs/2016%20Hydropower%20Status%20Report_1.pdf

International Hydropower Association (IHA, 2017). *2017 Hydropower Status Report*. Retrieved from: <https://www.hydropower.org/sites/default/files/publications-docs/2017%20Hydropower%20Status%20Report.pdf>

International Hydropower Association (IHA, 2018). *2018 Hydropower Status Report*. Retrieved from: <https://www.hydropower.org/publications/2018-hydropower-status-report#:~:text=Worldwide%20hydropower%20installed%20capacity%20rose,153%20GW%20of%20pumped%20storage>.

International Hydropower Association (IHA, 2019). *2019 Hydropower Status Report*. Retrieved from: https://www.hydropower.org/sites/default/files/publications-docs/2019_hydropower_status_report_0.pdf

International Hydropower Association (IHA, 2020). *2020 Hydropower Status Report*. Retrieved from: https://www.hydropower.org/sites/default/files/publications-docs/2020_hydropower_status_report.pdf

International Renewable Energy Agency (IRENA (2017). *Electricity Storage and Renewables: Costs and markets to 2030*. Retrieved from: https://www.irena.org/DocumentDownloads/Publications/IRENA_Electricity_Storage_Costs_2017.pdf

International Renewable Energy Agency (IRENA, 2018). *Hydrogen from Renewable Power: Technology outlook for the energy transition*. Retrieved from: <https://www.irena.org/publications/2018/Sep/Hydrogen-from-renewable-power>

International Stainless-Steel Forum (ISSF, 2021). *Recycling*. Retrieved 6 February 2021 from <https://www.worldstainless.org/about-stainless/environment/recycling/>

Johnson, J., Reck, B. K., Wang, T., & Graedel, T. E. (2008). The energy benefit of stainless-steel recycling. *Energy policy*, 36(1), 181-192.

Khoo, J. Z., Haque, N., Woodbridge, G., McDonald, R., & Bhattacharya, S. (2017). A life cycle assessment of a new laterite processing technology. *Journal of Cleaner Production*, 142, 1765-1777.

Kis, Z., Pandya, N., & Koppelaar, R. H. (2018). Electricity generation technologies: Comparison of materials use, energy return on investment, jobs creation and CO2 emissions reduction. *Energy Policy*, 120, 144-157.

Kleijn, R., & Van der Voet, E. (2010). Resource constraints in a hydrogen economy based on renewable energy sources: An exploration. *Renewable and sustainable energy reviews*, 14(9), 2784-2795.

Kleijn, R., Van der Voet, E., Kramer, G. J., Van Oers, L., & Van der Giesen, C. (2011). Metal requirements of low-carbon power generation. *Energy*, 36(9), 5640-5648.

Kyle, J. (2010) Nickel laterite processing technologies – where to next? *In ALTA 2010 Nickel/Cobalt/Copper Conference, 24 - 27 May, Perth, Western Australia*. <https://researchrepository.murdoch.edu.au/id/eprint/4340/>

- Lexology (2019). *Mining duties, royalties and taxes in Myanmar*. Retrieved from <https://www.lexology.com/library/detail.aspx?q=9c8c4d35-718a-4bc7-a063-bbd8f6e2d4eb>
- Månberger, A., & Stenqvist, B. (2018). Global metal flows in the renewable energy transition: Exploring the effects of substitutes, technological mix and development. *Energy policy*, 119, 226-241.
- Manhando, B. (2018) *Overview of the Zimbabwe Mining Sector* [presentation] Chamber of Mines of Zimbabwe. Retrieved from <http://www.mineafrika.com/documents/Zimbabwe's%20Mining%20Sector%20-%20Chamber%20of%20Mines.pdf>
- McLellan, B., Yamasue, E., Tezuka, T., Corder, G., Golev, A., & Giurco, D. (2016). Critical minerals and energy—impacts and limitations of moving to unconventional resources. *Resources*, 5(2), 19.
- Meshram, P., Abhilash, & Pandey, B.D. (2018). Advanced Review on Extraction of Nickel from Primary and Secondary Sources, *Mineral Processing and Extractive Metallurgy Review*, 40(3), 157-193. DOI: [10.1080/08827508.2018.1514300](https://doi.org/10.1080/08827508.2018.1514300)
- Metalary (2020). *Tungsten Price*. Retrieved from: <https://www.metalary.com/tungsten-price/>
- Mocker, M., Aigner, J., Kroop, S., Lohmeyer, R., & Franke, M. (2015). Raw Materials for Renewable Energy Technologies—Availability and Ecological Aspects. *Chemie Ingenieur Technik*, 87(4), 439-448.
- Moreau, V., Dos Reis, P. C., & Vuille, F. (2019). Enough Metals? Resource Constraints to Supply a Fully Renewable Energy System. *Resources*, 8(1), 29.
- Moss, R. L., Tzimas, E., Kara, H., Willis, P., Kooroshy, J. (2011). *Critical Metals in Strategic Energy Technologies - Assessing Rare Metals as Supply-Chain Bottlenecks in Low-Carbon Energy Technologies* (report no. JRC65592). JRC-scientific Strategy reports, European Commission. doi: 10.2790/35600 10.2790/35716
- Moss, R.L., Tzimas, E.; Willis, P., Arendorf, J., (2013a). *Critical Metals in the Path towards the Decarbonisation of the EU Energy Sector. Assessing rare metals as supply-chain bottlenecks in low-carbon energy technologies*. (report no. JRC82322). Joint Research Centre. European Commission. https://doi.org/10.2790/46338_
- Moss, R. L., Tzimas, E., Kara, H., Willis, P., & Kooroshy, J. (2013b). The potential risks from metals bottlenecks to the deployment of Strategic Energy Technologies. *Energy Policy*, 55, 556-564.
- Mudd, G. M. (2010). Global trends and environmental issues in nickel mining: Sulfides versus laterites. *Ore Geology Reviews*, 38(1-2), 9-26.
- Mudd, G. (2020). *Nickel Resources Database* [personal communication, 10 November, 2020]
- Murakami, S., Kawamoto, T., Masuda, A., & Daigo, I. (2015). Metal demand to meet SDG energy-related goals. *Glob. Env. Res*, 19, 181-186.
- Nansai, K., Nakajima, K., Kagawa, S., Kondo, Y., Suh, S., Shigetomi, Y., & Oshita, Y. (2014). Global flows of critical metals necessary for low-carbon technologies: the case of neodymium, cobalt, and platinum. *Environmental science & technology*, 48(3), 1391-1400.
- Nassar, N. T., Graedel, T. E., & Harper, E. M. (2015). By-product metals are technologically essential but have problematic supply. *Science advances*, 1(3)

Newman, H.R. (2004). *The Mineral Industry of Greece. U.S. Geological Survey Minerals Yearbook 2004*. Retrieved from <https://s3-us-west-2.amazonaws.com/prd-wret/assets/palladium/production/mineral-pubs/country/2004/grmyb04.pdf>

Nickel institute (n.d.). *About Nickel*. Retrieved from: <https://nickelinstitute.org/about-nickel/>

Nickel Institute (2016). *Nickel Recycling*. Retrieved from: https://www.nickelinstitute.org/media/2273/nickel_recycling_2709_final_nobleed.pdf

Nickel institute (2018). *Nickel Energizing Batteries*. Retrieved from: https://nickelinstitute.org/media/2318/nickel_battery_infographic-finalen2.pdf

Nickel Institute (2020). *Life Cycle Assessment of Nickel Products: Reference year 2017*. Final Report.

Nordelöf, A., Romare, M., & Tivander, J. (2019). Life cycle assessment of city buses powered by electricity, hydrogenated vegetable oil or diesel. *Transportation Research Part D: Transport and Environment*, 75, 211-222.

Norgate, T., & Jahanshahi, S. (2011). Assessing the energy and greenhouse gas footprints of nickel laterite processing. *Minerals Engineering*, 24(7), 698-707.

Northey, S. A., Haque, N., Lovel, R., & Cooksey, M. A. (2014). Evaluating the application of water footprint methods to primary metal production systems. *Minerals Engineering*, 69, 65-80.

Oldenbroek, V., Verhoef, L. A., & Van Wijk, A. J. (2017). Fuel cell electric vehicle as a power plant: Fully renewable integrated transport and energy system design and analysis for smart city areas. *International Journal of Hydrogen Energy*, 42(12), 8166-8196.

Olivetti, E.A., Ceder, G., Gaustad, G.G., & Fu, X. (2017). Lithium-Ion Battery Supply Chain Considerations: Analysis of Potential Bottlenecks in Critical Metals. *Joule*, 1(2). Doi: 10.1016/j.joule.2017.08.

Olson, D., Bakken, B. E. (2019): *Utility-scale solar PV from big to biggest: How lowest costs will power the growth of big solar – everywhere*. DNV GL Group. <https://www.dnvgl.com/feature/utility-scale-solar.html>

O'Neill, B. C., Kriegler, E., Ebi, K. L., Kemp-Benedict, E., Riahi, K., Rothman, D. S., ... & Solecki, W. (2017). The roads ahead: Narratives for shared socioeconomic pathways describing world futures in the 21st century. *Global Environmental Change*, 42, 169-180.

Our World in Data (2014): *Motor vehicles per 1000 inhabitants vs GDP per capita, 2014*. Retrieved on 25 November 2020 from <https://ourworldindata.org/grapher/road-vehicles-per-1000-inhabitants-vs-gdp-per-capita?country=MOZ+NER>

Pehl, M., Arvesen, A., Humpenöder, F., Popp, A., Hertwich, E. G., & Luderer, G. (2017). Understanding future emissions from low-carbon power systems by integration of life-cycle assessment and integrated energy modelling. *Nature Energy*, 2(12), 939-945.

Pihl, E., Kushnir, D., Sandén, B., & Johnsson, F. (2012). Material constraints for concentrating solar thermal power. *Energy*, 44(1), 944-954.

Prasetyo, P. (2018). The effect of entry into force of the mining law 2009 began January 2014 in the production of NPI (Nickel Pig Iron) in China. In *IOP Conference Series: Materials Science and Engineering*, 285(1), 012015. IOP Publishing.

PWC (2012): *Corporate income taxes, mining royalties and other mining taxes: A summary of rates and rules in selected countries*. Retrieved from <https://www.pwc.com/gx/en/energy-utilities-mining/publications/pdf/pwc-gx-mining-taxes-and-royalties.pdf>

Rabary, L. (2019). *Update 2-Madagascar to raise minerals taxes, take 20% stake in mining projects*. Thomson Reuters. Retrieved from <https://uk.reuters.com/article/madagascar-mining/update-2-madagascar-to-raise-minerals-taxes-take-20-stake-in-mining-projects-idUKL8N28K3I6>

Radoia, P. (2019). *European Market Outlook*. Retrieved on 26 November from <https://www.solarpowersummit.org/wp-content/uploads/2019/03/Day-1-European-Market-Outlook.pdf>

Raugei, M., & Leccisi, E. (2016). A comprehensive assessment of the energy performance of the full range of electricity generation technologies deployed in the United Kingdom. *Energy Policy*, 90, 46-59.

Redstone Exploration Services (n.d.). *Morocco*. Retrieved from <http://redstone-exploration.com/country-profiles/morocco/>

REN21 (2015). *Renewables 2015 Global Status Report*. Retrieved from <https://www.ren21.net/wp-content/uploads/2019/05/GSR2015-Full-Report-English.pdf>

Republic of Kosovo (2012). *Mining Strategy of the Republic of Kosovo 2012 – 2025*. Ministry of Economic Development. Retrieved from <https://kryeministri-ks.net/wp-content/uploads/docs/Mining-Strategy-of-the-Republic-of-Kosovo-2012-2025.pdf>

Republic of the Philippines (2018). *Nickel industry projects lower production in 2019*. Philippine News Agency. Retrieved from <https://www.pna.gov.ph/articles/1055926>

Restrepo, J.C., Velez Gomez, L.D., Ramirez Canedo, J.C., & Duque, E. (2015). *Mining in Colombia: A review of the calculation of government take*. Retrieved from <https://www.researchgate.net/publication/281650586-Mining-in-Colombia-A-review-of-the-calculation-of-government-take/link/5da0e310299bf116fe9ed034/download>

Riahi, K., Van Vuuren, D. P., Kriegler, E., Edmonds, J., O'Neill, B. C., Fujimori, S., ... & Lutz, W. (2017). The shared socioeconomic pathways and their energy, land use, and greenhouse gas emissions implications: an overview. *Global Environmental Change*, 42, 153-168.

Rietveld, E., Boonman, H., van Harmelen, T., Hauck, M., Bastein, T. (2019). *Global Energy Transition and Metal Demand - An Introduction and Circular Economy Perspectives*. TNO. Doi: 10.13140/RG.2.2.25790.54086

Sakar, G.E., & Clark, D. (2013). *Turkey: Mining Sector and Mining Law*. Mondaq. Retrieved from <https://www.mondaq.com/turkey/mining/217158/mining-sector-and-mining-law>

Schmidt, T., Buchert, M., & Schebek, L. (2016). Investigation of the primary production routes of nickel and cobalt products used for Li-ion batteries. *Resources, Conservation and Recycling*, 112, 107-122.

Sinn, H.W. (2017). Buffering volatility: A study on the limits of Germany's energy revolution. *European Economic Review*, 99, 130-150. doi: [10.1016/j.euroecorev.2017.05.007](https://doi.org/10.1016/j.euroecorev.2017.05.007)

Speirs, J., Contestabile, M., Houari, Y., & Gross, R. (2014). The future of lithium availability for electric vehicle batteries. *Renewable and Sustainable Energy Reviews*, 35, 183-193.

Sprecher, B., Daigo, I., Murakami, S., Kleijn, R., Vos, M., & Kramer, G. J. (2015). Framework for resilience in material supply chains, with a case study from the 2010 rare earth crisis. *Environmental science & technology*, 49(11), 6740-6750.

Statista (2018a). *Number of passenger cars and commercial vehicles in use worldwide from 2006-2015*. Retrieved on from: <https://www.statista.com/statistics/281134/number-of-vehicles-in-use-worldwide/#:~:text=In%202015%2C%20around%20947%20million,vehicles%20were%20in%20operation%20worldwide.>

Statista (2018b). *Nickel demand worldwide from 2015-2018*. Retrieved on 25 November from <https://www.statista.com/statistics/273653/global-demand-for-nickel-since-2007/>

Statista (2020). *Average service life of trucks in Japan from fiscal year 2010-2019*. Retrieved from: <https://www.statista.com/statistics/679750/japan-truck-average-lifespan/>

Strategic Dialogue on Sustainable Raw Materials for Europe (STRADE, 2016). *European Policy Brief: The Cost Competitiveness of Mining Operations in the European Union*. No.08/2016. Retrieved from: <https://st6.ning.com/topology/rest/1.0/file/get/3410397167?profile=original>

Sullivan, J. L., Clark, C. E., Han, J., & Wang, M. (2010). *Life-cycle analysis results of geothermal systems in comparison to other power systems* (No. ANL/ESD/10-5). Argonne National Lab. (ANL), Argonne, IL, United States. Doi: 10.2172/993694

Sumitomo Metal Mining Col, Ltd (SMM, n.d.). *Producing High-Quality Products from Low-Grade Nickel Oxide Ore*. Retrieved from: https://www.smm.co.jp/E/csr/activity_highlights/persistence/highlights1.html

Sverdrup, H. U., Ragnarsdottir, K. V., & Koca, D. (2017). Integrated Modelling of the Global Cobalt Extraction, Supply, Price and Depletion of Extractable Resources Using the WORLD6 Model. *BioPhysical Economics and Resource Quality*, 2(4). doi:10.1007/s41247-017-0017-0

Sverdrup, H. U., & Olafsdottir, A. H. (2019). Assessing the long-term global sustainability of the production and supply for stainless steel. *Biophysical Economics and Resource Quality*, 4(2), 8.

The Insider Stories (2019). *Indonesia Raises Nickel Royalty from 5% to 10%*. Retrieved from <https://theinsiderstories.com/indonesia-raises-nickel-royalty-from-5-to-10/>

The Mining Association of Canada (2008). *Comparative review of the rate of royalty in the Canada mining regulation, as relates to National and International Competitiveness*. Retrieved from <https://mining.ca/wp-content/uploads/2019/03/ComparativeReviewoftheRateofRoyalty.pdf>

Tidball, R., Bluestein, J., Rodriguez, N., & Knoke, S. (2010). *Cost and performance assumptions for modeling electricity generation technologies* (No. NREL/SR-6A20-48595). National Renewable Energy Lab. (NREL), Golden, CO, United States. Doi: 10.2172/993653

Tokimatsu, K., Wachtmeister, H., McLellan, B., Davidsson, S., Murakami, S., Höök, M., ... & Nishio, M. (2017). Energy modeling approach to the global energy-mineral nexus: A first look at metal requirements and the 2 C target. *Applied energy*, 207, 494-509.

Tokimatsu, K., Höök, M., McLellan, B., Wachtmeister, H., Murakami, S., Yasuoka, R., & Nishio, M. (2018). Energy modeling approach to the global energy-mineral nexus: Exploring metal requirements and the well-below 2° C target with 100 percent renewable energy. *Applied energy*, 225, 1158-1175.

Trading Economics. (2020). *Commodities*. Retrieved from: <https://tradingeconomics.com/commodities>

Transparency International (2020). *Corruption Perception Index 2019*. Retrieved from <https://www.transparency.org/en/cpi/2019/index/nzl>

Turconi, R., Boldrin, A., & Astrup, T. (2013). Life cycle assessment (LCA) of electricity generation technologies: Overview, comparability and limitations. *Renewable and sustainable energy reviews*, 28, 555-565.

United Nations Environment Programme (UNEP, 2011). *Recycling rates of metals*. Retrieved from https://wedocs.unep.org/bitstream/handle/20.500.11822/8702/Recycling_Metals.pdf?sequence=1&isAllowed=y

United States Department of Energy (USDOE, 2011). *Critical Materials Strategy*. https://www.energy.gov/sites/prod/files/DOE_CMS2011_FINAL_Full.pdf

United States Geological Survey (USGS, 2018). *Mineral Commodities Summaries: Bismuth*. Retrieved from: <https://s3-us-west-2.amazonaws.com/prd-wret/assets/palladium/production/mineral-pubs/bismuth/mcs-2018-bismu.pdf>

United States Geological Survey (USGS, 2020a). *National Minerals Information Centre: Nickel Statistics and Information*. Retrieved from: <https://www.usgs.gov/centers/nmic/nickel-statistics-and-information>

United States Geological Survey (USGS, 2020b). *Commodity Statistics and Information: Chromium Statistics and Information*. Retrieved from: <https://www.usgs.gov/centers/nmic/chromium-statistics-and-information>

United States Geological Survey (USGS, 2020c). *National Minerals Information Centre: Silica statistics and Information*. Retrieved from: <https://www.usgs.gov/centers/nmic/silica-statistics-and-information>

United States Geological Survey (USGS, 2020d). *National Minerals Information Centre: Rhenium Statistics and Information*. Retrieved from: <https://www.usgs.gov/centers/nmic/rhenium-statistics-and-information>

Usanov, A., Ridder, M., Auping, W. L., & Lingemann, S. (2013). *Coltan, Congo and Conflict* (Rapport No 21 05 13). Retrieved from https://hcss.nl/sites/default/files/files/reports/HCSS_21_05_13_Coltan_Congo_Conflict_web.pdf

U.S. Securities and Exchange Commission (USSEC, 2007). *Annual Report 2007: Lunding Mining Corporation*. Retrieved from <https://www.sec.gov/Archives/edgar/data/1377085/000120445908001228/lundinexh991.htm>

U.S. Securities and Exchange Commissions (USSEC, 2018). *EMX Royalty Corporation (formerly Eurasian Minerals Inc.) Management Discussion and Analysis three and six months ended June 30, 2018*. Retrieved from <https://www.sec.gov/Archives/edgar/data/1285786/000106299318003448/exhibit99-2.htm>

Valero, A., Valero, A., & Martínez, A. (2010). Inventory of the exergy resources on earth including its mineral capital. *Energy*, 35(2), 989-995.

Valero, A., Valero, A., & Domínguez, A. (2013). Exergy replacement cost of mineral resources. *Journal of environmental accounting and management*, 1(1), 147-148.

- Valero, A., & Valero, A. (2014). *Thanatia: The Destiny of the Earth's Mineral Resources: a Thermodynamic Cradle-to-cradle Assessment* (1st edition). Singapore: World Scientific.
- Valero, A., Domínguez, A., & Valero, A. (2015). Exergy cost allocation of by-products in the mining and metallurgical industry. *Resources, Conservation and Recycling*, 102, 128-142.
- Valero, A., Valero, A., Calvo, G., & Ortego, A. (2018a). Material bottlenecks in the future development of green technologies. *Renewable and Sustainable Energy Reviews*, 93, 178-200.
- Valero, A., Valero, A., Calvo, G., Ortego, A., Ascaso, S., & Palacios, J. L. (2018b). Global material requirements for the energy transition. An exergy flow analysis of decarbonisation pathways. *Energy*, 159, 1175-1184.
- Van der Linden (2020). Exploration of the Cobalt System: Scenarios for a critical material for the energy system. *Delft University of Technology*. <https://repository.tudelft.nl/islandora/object/uuid%3Ae51dbb87-09f7-4c33-a956-226874a1e7b7?collection=education>
- Van der Voet, E., Van Oers, L., Verboon, M., & Kuipers, K. (2019). Environmental implications of future demand scenarios for metals: methodology and application to the case of seven major metals. *Journal of Industrial Ecology*, 23(1), 141-155.
- Vidal, O., Le Boulzec, H., & François, C. (2018). Modelling the material and energy costs of the transition to low-carbon energy. *EPJ Web of Conferences*, 189 (00018). EDP Sciences. <https://doi.org/10.1051/epiconf/201818900018>
- Walker S, Young S, Fowler M. (2015). Repurposing electric vehicle batteries for energy storage to support the smart grid. *IEEE Canadian Review*, 20-23. Retrieved on 26 November from [http://canrev.ieee.ca/cr73/Repurposing Electric Vehicle Batteries for Energy Storage to Support the Smart Grid.pdf](http://canrev.ieee.ca/cr73/Repurposing%20Electric%20Vehicle%20Batteries%20for%20Energy%20Storage%20to%20Support%20the%20Smart%20Grid.pdf)
- Wang, S., Li, H., Li, C., Hao, X., Bao, Q., & Zhang, L. (2015). LCA Evaluation for Different Treatment Processes of Nickel Laterite Ore. In *Energy Technology 2015* (93-103). Springer, Cham. https://doi.org/10.1007/978-3-319-48220-0_11
- Watari, T., McLellan, B., Ogata, S., & Tezuka, T. (2018). Analysis of potential for critical metal resource constraints in the international energy agency's long-term low-carbon energy scenarios. *Minerals*, 8(4), 156.
- Watari, T., McLellan, B. C., Giurco, D., Dominish, E., Yamasue, E., & Nansai, K. (2019). Total material requirement for the global energy transition to 2050: A focus on transport and electricity. *Resources, Conservation and Recycling*, 148, 91-103.
- WBMS (2018) *Nickel Workbook June 2018* [personal communication, 12 May, 2020]
- World Energy Council (WEC, 2011). *Global Transport Scenarios 2050*. Retrieved from: https://www.worldenergy.org/assets/downloads/wec_transport_scenarios_2050.pdf
- Wentker, M., Greenwood, M., & Leker, J. (2019). A bottom-up approach to lithium-ion battery cost modeling with a focus on cathode active materials. *Energies*, 12(3), 504.
- White, C., Thompson, B., & Swan, L. G. (2020). Repurposed electric vehicle battery performance in second-life electricity grid frequency regulation service. *Journal of Energy Storage*, 28, 101278.

Wood Mackenzie (n.d.): Figure in Els, F. (2018). *Electric vehicle demand will double nickel price – as soon as 2022*. Retrieved from: <http://www.mining.com/electric-vehicle-demand-will-double-nickel-price-soon-2022>

World Bank (2006). *Mining Royalties A Global Study of Their Impact on Investors, Government, and Civil Society* (37258). Retrieved from <http://documents1.worldbank.org/curated/en/103171468161636902/pdf/372580Mining0r101OFFICIAL0U SE0ONLY1.pdf>

World Bank (2017). *The growing role of minerals and metals for a low carbon future*. Washington, D.C. <https://doi.org/10.1596/28312>

Worstell, T. (2019). *Guatemalan Nickel Royalties – If Only The Guardian Understood Basic Economics*. Continental Telegraph. Retrieved from <https://www.continentaltelegraph.com/2019/06/guatemalan-nickel-royalties-if-only-the-guardian-understood-basic-economics/>

Wu, G., Li, Y., & Tongda, J. (2018). *Mining in China: overview*. Thomson Reuters. Retrieved from [https://uk.practicallaw.thomsonreuters.com/w-011-1348?transitionType=Default&contextData=\(sc.Default\)&firstPage=true&bhcp=1](https://uk.practicallaw.thomsonreuters.com/w-011-1348?transitionType=Default&contextData=(sc.Default)&firstPage=true&bhcp=1)

Zerrahn, A., Schill, W. P., & Kempfert, C. (2018). On the economics of electrical storage for variable renewable energy sources. *European Economic Review*, 108, 259-279.

Zhou, T., Roorda, M. J., MacLean, H. L., & Luk, J. (2017). Life cycle GHG emissions and lifetime costs of medium-duty diesel and battery electric trucks in Toronto, Canada. *Transportation Research Part D: Transport and Environment*, 55, 91-98.